ALKALINE MAGMATISM IN CENTRAL-EASTERN PARAGUAY

Relationships with coeval magmatism in Brazil

Piero Comin-Chiaramonti
Celso de Barros Gomes
Editors

edusp

FAPESP

Dados Internacionais de Catalogação na Publicação (CIP)
(Câmara Brasileira do Livro, SP, Brasil)

P. Comin-Chiaramonti and C. B. Gomes

Alkaline Magmatism in Central-eastern Paraguay: Relationships with Coeval Magmatism in Brazil / P. Comin-Chiaramonti and C. B. Gomes (editors). – São Paulo: Editora da Universidade de São Paulo, 1996

ISBN: 85-314-0326-6

1. Geofísica - Paraguai 2. Geomorfologia - Paraguai 3. Magmatismo - Paraguai 4. Rochas ígneas alcalinas - Paraguai I. Comin-Chiaramonti, P. II. Gomes, C. B.

96-3359 CDD-551.1309892

Índices para catálogo sistemático:

1. Paraguai: Magmatismo alcalino: Geologia
551.1309892

Edusp – Editora da Universidade de São Paulo
Av. Prof. Luciano Gualberto, Travessa J, 374
6º andar – Ed. da Antiga Reitoria – Cidade Universitária
05508-900 – São Paulo – SP – Brasil Fax (011) 211-6988
Tel. (011) 813-8837 r. 216

Printed in Brazil 1995

Foi feito o depósito legal

CONTENTS

LIST OF CONTRIBUTORS

BARBIERI, M.	Dipartimento di Scienze della Terra, Università "La Sapienza", Piazzale Aldo Moro 5, 00185 Rome, Italy
BELLIENI, G.	Dipartimento di Mineralogia e Petrologia, Università di Padova, Corso Garibaldi 37, 35100 Padova, Italy
BERROCAL, J.	Instituto Astronômico e Geofísico, Universidade de São Paulo, Caixa Postal 30627, 01051 São Paulo, Brazil
CAPALDI, G.	Dipartimento di Geofisica e Vulcanologia, Università Federico II, Largo S. Marcelino 10, 80138 Naples, Italy
CARBONIN, S.	Dipartimento di Mineralogia e Petrologia, Università di Padova, Corso Garibaldi 37, 35100 Padova, Italy
CASTILLO, A.M.C.	Instituto de Ciências Básicas, Universidad Nacional de Asunción, Departamento de Geologia, Ciudad Universitaria, San Lorenzo, C.C. 1039-1804, Asunción, Paraguay
CASTORINA, F.	Dipartimento di Scienze della Terra, Università "La Sapienza"', Piazzale Aldo Moro 5, 00185 Rome, Italy
CENSI, P.	Istituto di Mineralogia, Petrografia e Geochimica, Università di Palermo, Via Archirafi 36, 90100 Palermo, Italy
COMIN-CHIARAMONTI, P.	Dipartimento di Ingegneria Chimica, dell'Ambiente e delle Materie Prime, Università di Trieste, Piazzale Europa 1, 34100 Trieste, Italy
CUNDARI, A.	Dipartimento di Geofisica e Vulcanologia, Università Federico II, Largo S. Marcellino 10, 80138 Naples, Italy
DE MIN, A.	Dipartimento di Scienze della Terra, Università di Trieste, Via E. Weiss 8, 34127 Trieste, Italy
DUDDY, I.R.	Geotrack International Pty Ltd, P.O. Box 4120, Melbourne University, Victoria 3052, Australia
ERNESTO, M.	Instituto Astronômico e Geofísico, Universidade de São Paulo, Caixa Postal 30627, 01051 São Paulo, Brazil
FERNANDES, C.	Instituto Astronômico e Geofísico, Universidade de São Paulo, Caixa Postal 30627, 11051 São Paulo, Brazil

FÚLFARO, V.J.	Instituto de Geociências e Ciências Exatas, Universidade Estadual Paulista, Caixa Postal 178, 13500 Rio Claro, Brazil
GOMES, C.B.	Instituto de Geociências, Universidade de São Paulo, Caixa Postal 11348, 05422-970 São Paulo, Brazil
GREEN, P.F.	Geotrack International Pty Ltd, P.O. Box 4120, Melbourne University, Victoria 3052, Australia
HEGARTY, K.A.	Geotrack International Pty Ltd, P.O. Box 4120, Melbourne University, Victoria 3052, Australia
LAURENZI, M.A.	Istituto di Geocronologia e Geochimica Isotopica (CNR), Via Cardinale Maffi 36, 56100 Pisa, Italy
MARZOLI, A.	Dipartimento di Scienze della Terra, Università di Trieste, Via E. Weiss 8, 34127 Trieste, Italy
MORBIDELLI, L.	Dipartimento di Scienze della Terra, Università "La Sapienza", Piazzale Aldo Moro 5, 00185 Rome, Italy
ORUÉ, D.	Instituto de Ciências Básicas, Universidad Nacional de Asunción, Departamento de Geologia, Ciudad Universitaria, San Lorenzo, C.C. 1039-1804, Asunción, Paraguay
PARDINI, G.	Istituto di Geocronologia e Geochimica Isotopica (CNR), Via Cardinale Maffi 36, 56100 Pisa, Italy
PETRINI, R.	Dipartimento di Scienze della Terra, Università di Trieste, Via E. Weiss 8, 34127 Trieste, Italy
PICCIRILLO, E.M.	Dipartimento di Scienze della Terra, Università di Trieste, Via E. Weiss 8, 34127 Trieste, Italy
PRINCIVALLE, F.	Dipartimento di Scienze della Terra, Università di Trieste, Via E. Weiss 8, 34127 Trieste, Italy
RUBERTI, E.	Instituto de Geociências, Universidade de São Paulo, Caixa Postal 11348, 05422-970 São Paulo, Brazil
SABELLI, D.	Dipartimento di Scienze della Terra, Università di Trieste, Via E. Weiss 8, 34127 Trieste, Italy
TIRONE, M.	Dipartimento di Scienze della Terra, Università di Trieste, Via E. Weiss 8, 34127 Trieste, Italy
VELÁZQUEZ, J.C.	Instituto de Ciências Básicas, Universidad Nacional de Asunción, Departamento de Geologia, Ciudad Universitaria, San Lorenzo, C.C 1039-1804, Asunción, Paraguay
VELÁZQUEZ, V.F.	Instituto de Geociências-Curso de Pós-Graduação, Universidade de São Paulo, Caixa Postal 11348, 05422-970 São Paulo, Brazil

PREFACE

Breve violencia de aguacero y viento:
el oro del lapacho se ha borrado.
En malmomento había aparecido.
En maltiempo florece, para muchos,
la primavera: esteril despertar.
Queda el lago del alma con su herida
-estela plateada- de añoranza.

Lady Noemi Ferrari de Nagy, poetess, who spent her life teaching human sciences to generations of Paraguayan peoples.

The main aim of the present volume is that of making available to the scientific community a large new data set on the Mesozoic to Tertiary alkaline magmatism of Eastern Paraguay, at the central-western side of the Paraná Basin in South America. The papers include the results of a ten year investigation on the magmatic rocks. The project was developed through multidisciplinary studies involving geology, petrology, mineralogy, isotope geochemistry and palaeomagnetism which also allow an attempt at comparing all the Mesozoic alkaline occurrences along the northern margins of the Paraná Basin.

The research has been carried out mainly by scientists from Brazilian (São Paulo and Rio Claro), Paraguayan (Asunción), Australian (Melbourne) and Italian (Trieste, Naples, Padova, Palermo and Rome) Universities and CNR (Consiglio Nazionale delle Ricerche) Centers (Padova, Pisa and Rome), besides several graduate students both in Brazil and in Italy.

A great many other people from Paraguay, both public officials and private citizens, farmers and cowboys, gave freely of their time, knowledge and hospitality.

Finally, we acknowledge our debts to our wifes Paola and Maria Conceição (P.C.C. and C.B.G., respectively) who patiently took care of everything else while we were involved with this task.

Piero Comin-Chiaramonti
and
Celso de Barros Gomes

ACKNOWLEDGEMENTS

The preparation and edition of this book was possible only by means of the continuous financial support provided by CNPq (Conselho Nacional de Desenvolvimento Científico e Tecnológico), CNR (Consiglio Nazionale delle Ricerche), FAPESP (Fundação de Amparo à Pesquisa do Estado de São Paulo), FINEP (Financiadora de Estudos e Projetos), MURST (Ministero dell'Università e della Ricerca Scientifica e Tecnologica) and São Paulo (USP) and Trieste Universities.

The following Institutions are acknowledged for their analytical support, laboratory facilities and collaboration:

1) CEPA, Palermo, Italy (director R. Alaimo);
2) GEOTRACK, Melbourne, Australia (director K. A. Hegarty);
3) Istituto di Mineralogia e Petrografia, Trieste University, Italy (director E.M. Piccirillo);
4) Istituto di Geocronologia e Geochimica Isotopica, CNR, Pisa, Italy (director G. Ferrara);
5) Centro Studi Orogeno Alpi Orientali, CNR, Padova, Italy (director F.P. Sassi);
6) Centro di Studio per il Quaternario e l'Evoluzione Ambientale, CNR, Rome (director G. Cavarreta), Mr. F.Filippi, L. Furlan and R. Zettin (Trieste University), Dr. A. Giaretta and Mr. R. Carampin (CNR Center, Padova), Dr. G. Montana (Palermo University), Mrs. R.C. Lemos and K.R.B. Vancini, I. Kroehne and F.J.P. Almeida Filho (USP) are sincerely thanked for their valuable technical support.

FOREWORD

In compiling during the 1980's a brief, general account of the alkaline rocks of Paraguay, and undertaking a short field trip, I learned not only that a most interesting province existed in the country, but that the available data were characterized principally by their paucity. Although I may have been ignorant up to that time of the extent and potential interest of the Paraguayan alkaline rocks, others were not, and in 1987 an international team of Brazilian, Italian, Paraguayan and Australian geologists initiated a cooperative programme to make a thorough investigation of the province. Several papers have already resulted from the cooperation, but the bulk of the work is now published in this extensive monograph, under the enthusiastic editorships of Piero Comin-Chiaramonti and Celso B.Gomes.

The alkaline rocks and carbonatites of Paraguay are important, I would suggest, for three principal reasons. Firstly, the study of all the approximately contemporaneous igneous rocks within a limited spatial and tectonic area, that is within a single province, must be one of the most important approaches to solving petrogenetic problems, and this monograph will thus make one more province readily available for comparative studies. Secondly, the exceptionally broad range of rock-types represented in the Paraguayan alkaline province has an intrinsic interest including as it does picrite basalt-basanite-trachyphonolite-phonolite, nephelinite, leucitite, rhyolite, gabbro-essexite-tephrite-phonolite, ijolite-nepheline syenite, carbonatite and fenite. Thirdly, the Paraguayan alkaline province is one part of the exceptionally extensive alkaline volcanism that affected the southern and eastern parts of South America in Jurassic to Tertiary times, notably in southern and central Brazil, so that the Paraguayan section of this "super-province" should be considered in any major synthesis. This aspect is addressed in several chapters and underlined by the subtitle to the book.

There is potentially a further aspect to regional considerations of the alkaline rocks of Paraguay, and this is their relationship to the alkaline rocks that are scattered along a north-south line across western Argentina. As far as I am aware the Argentinian rocks have not been considered in detail in a regional context, and they are not the concern of the present monograph. However, the wealth of information now available on the Paraguayan rocks contrasts even more starkly with the lack of detail on the alkaline rocks of Argentina, whilst an even more frustrating situation is provided by the alkaline rocks of southern Uruguay, of which very little is known.

Most aspects of the alkaline magmatism of central and eastern Paraguay are covered in the present volume - geology, geophysics, geochronology, petrography, petrochemistry, petrology and mineralogy. The wealth of data herein now make this one of the more fully described of the world's alkaline provinces, and to have all this information within a single volume is a great convenience. The Editors and the many contributors are to be congratulated and thanked for their efforts in bringing this major project to such a successful conclusion.

Alan R.Woolley

GEOLOGY OF EASTERN PARAGUAY

V.J.Fúlfaro

Alkaline Magmatism in Central-Eastern Paraguay. Relationships with Coeval Magmatism in Brazil. Comin-Chiaramonti, P. & Gomes, C. B. (eds.), 1996, Edusp/Fapesp, São Paulo, pp. 17-29.

ABSTRACT

Eastern Paraguay is located on the former western margin of Gondwana, which includes the western limit of the Paraná Basin. The geological framework of Eastern Paraguay includes two Precambrian basement crystalline highs, the Caapucú to the south and the Apa High to the north, which are divided by a large downfaulted block, an aulacogen, here named the Bajo de San Pedro. In its central part, this aulacogen is filled with sedimentary rocks ranging in age from possibly Cambrian to Lower Mesozoic. The presence between two major cratons, the northern end of the Rio de La Plata Craton (the Caapacú High) and the southern end of the Amazon Craton (the Apa High), of an aulacogen with more than 5,000 m of sedimentary deposits (the Bajo de San Pedro) plus the proximity of the Andean chain makes Eastern Paraguay an important region to study in its own right and also to understand the Paraná Basin better. The distribution of the Paleozoic-Mesozoic deposits of Paraguay has been greatly influenced by two major events - the separation of South America from Africa and the Andean orogeny. Evidence for this comes from study of the outcrop pattern, the structural framework of central-eastern Paraguay and the identification of major breaks in the stratigraphic record.

INTRODUCTION

The Republic of Paraguay in central South American has an area of 406,752 km^2 and is divided by the Paraguay river into two large parts traditionally named Occidental Paraguay (Gran Chaco) to the west and Oriental Paraguay to the east, each with totally different geomorphology, geology, soils, vegetation and climate. This paper deals with the geology of Eastern Paraguay, which includes the western limit of the Paraná Basin, a 1,200,000 km^2 cratonic basin occupying part of Brazil, Uruguay and Paraguay. In Paraguay alone the Basin covers an area of 110,000 km^2.

The area reported herein with about 160,000 km^2, is limited by the Paraguay river to the west, the Apa river to the north and the Paraná river to the east and south (Fig. 1). The Paraná and Paraguay rivers are classified among the 15 largest rivers of the world. The eastern part of Paraguay was originally mostly covered by forests of subtropical vegetation in contrast to the lowlands covered by bush and open "cerrado" type of veg-

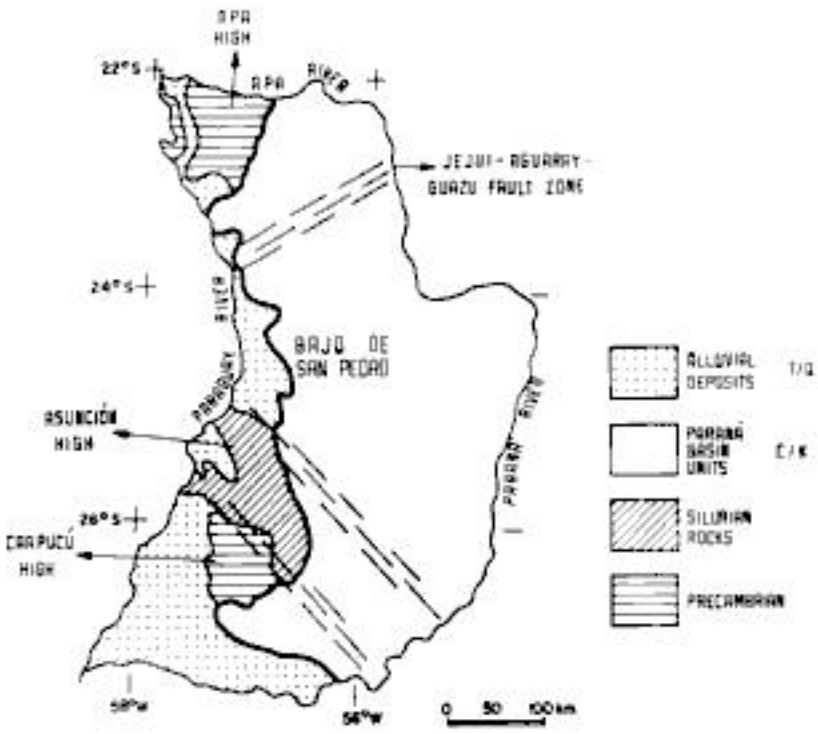

Figure 1 - Geological and geotectonic features of Eastern Paraguay.

etation of the usually dry climate of the Gran Chaco. Due to intensive human occupation, modern cities as Concepción and Pedro Juan Caballero to the north, Coronel Oviedo and Villarrica in the centre, Ciudad del Leste to the east and Encarnación to the south are rapidly developing

(Fig. 2). Even so, a large part of Eastern Paraguay still consists mostly of farmland and great areas are predominantly rural.

The first notice about this country was brought to Europe by Ulrich Schmidl, who explored the Paraguay river in 1564. Later the jesuit father Sepp (1697) commented on the geography of the region. Charlevoix (1747) made the first geographical observations about the country. Also in the same century Azara (1790) provided a geographical description of Paraguay. The pioneer works about the geology and mineralogy of Paraguay were done by Mersay (1860), Du Graty (1865), Hisbsch (1891), Milch (1895), but only in the last half of the twentieth century have regional geological studies in Paraguay began (Carnier, 1911; Goldschlag, 1913; Harrington, 1950, 1956; Eckel, 1959; Putzer, 1962).

Until 1982 all the papers dealing with the geology of Eastern Paraguay were based mostly on outcrop observations even through in great areas of the country outcrops are not abundant. The majority of these publications relate

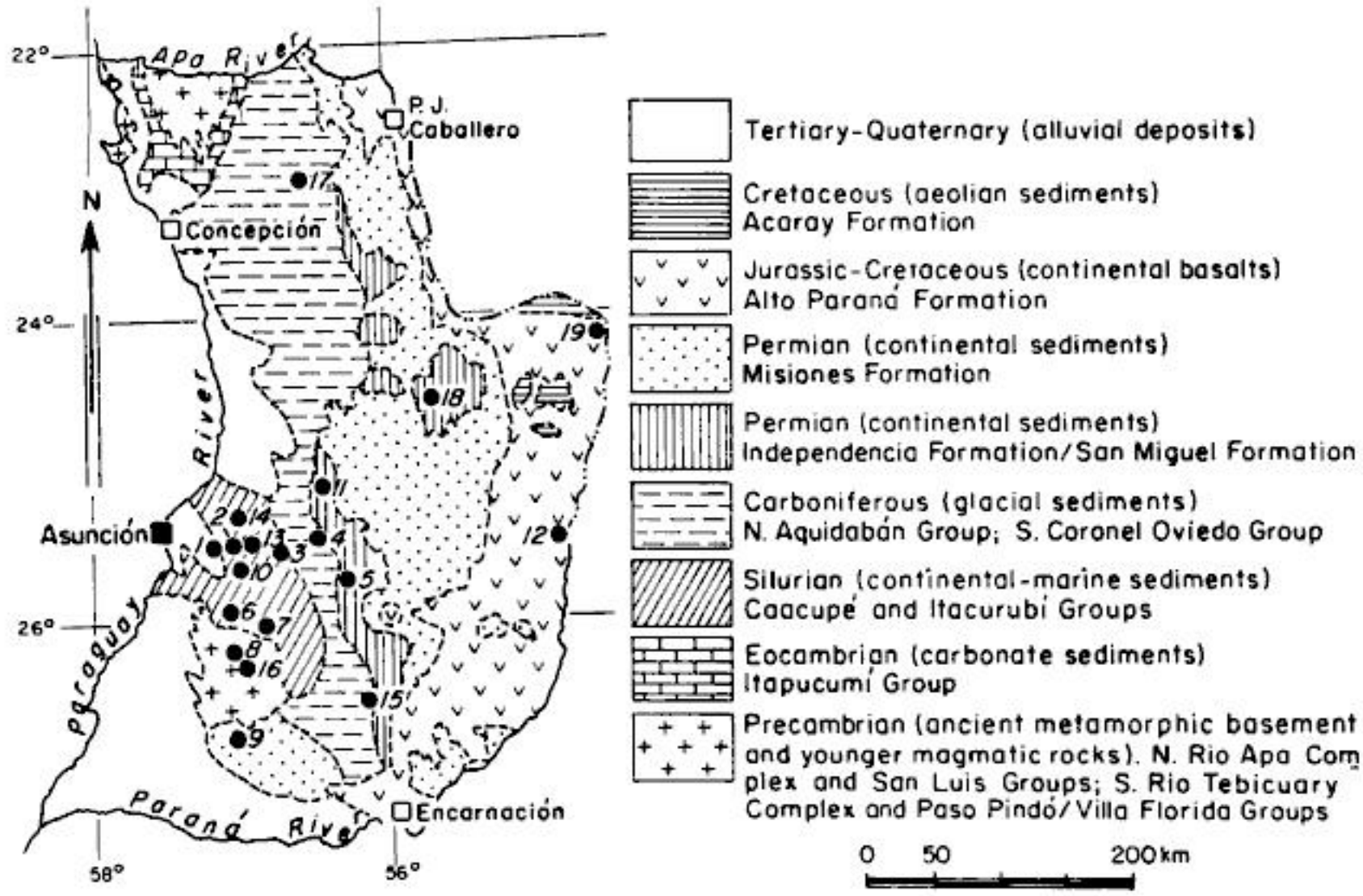

Figure 2 - Geological sketch map of Eastern Paraguay (simplified after Proyecto PAR 83/005, 1986, and Occidental Company, 1987). Localities as follow: 1. Ypacaraí-Itauguá; 2. Caacupé; 3. Itacurubí; 4. Coronel Oviedo; 5. Villarrica; 6. Quiindy; 7. Quyquyó; 8. Caapucú; 9. San Juan Bautista; 10. Paraguarí; 11. Carayaó; 12. Ciudad del Leste; 13. Eusebio Ayala; 14. Tobati; 15. Yuty; 16. Villa Florida; 17. Yby Jahú; 18. Curuguaty; 19. Salto del Guairá.

to the hilly region of central-eastern Paraguay with its fair to good outcrops. In all Eastern Paraguay there are only two deep wells (Asunción n 1 and n 2, with depths of 3,223 m and 2,985 m, respectively), which have added greatly to our knowledge. These were both drilled in the years 1981/1982 by Pecten-Occidental-Trend with latitude 24°04'12.55"S and longitude 56°27'12.42"W (Asunción nº 1) and latitude 23°41'47.96"S and longitude 56°35'2.38"W (Asunción nº 2).

The geological description presented herein is based on both the literature and my own experience as a result of several research trips to Paraguay, leading to the publication of the 1:1,000,000 scale Geological Map of Paraguay (1986), sponsored by the United Nations Development Programme (UNDP) and the Paraguayan government (Proyecto PAR-83/005).

The main literature about Eastern Paraguay includes: Eckel (1959) and therein references; Wolfart (1961); Putzer (1962); Fúlfaro & Landim (1971); Comte & Hasui (1971); Palmieri (1973); OEA (1975); Stormer et al. (1975); Wiens (1982); Palmieri & Velázquez (1983) and therein references; Petri & Fúlfaro (1983) and therein references; Almeida & Hasui (1984) and therein references; Ramos (1984); Bellieni et al. (1986); Gomez Duarte (1986); Zalán et al., (1987); Bitschene & Lippolt (1986); Bitschene (1987); Kanzler (1987); Comin-Chiaramonti et al. (1992) and therein references; Velázquez (1992).

TECTONIC FRAMEWORK AND EVOLUTION

The geology of Eastern Paraguay is best understood by relating its stratigraphic sequences and outcrop patterns to its Palaeozoic and Mesozoic tectonic evolution.

The Precambrian-Early Paleozoic crystalline rocks of Eastern Paraguay occur in two structural highs, one to the south named Caapucú and the other to the north, the Apa High (Fig. 1). Isolated and smaller outcrops of these rocks are also present in the Ypacaraí and Acahay valleys in the centre of the country and along the Paraguay river from Asunción to the northern limit of the country in the valley of the Apa river.

The Caapucú High, previously named "Saliente del Pilar" or "Précambrico Sur", has an area of 4,000 km^2 and is exposed in a NW-SE band between the cities of Quiindy and San Juan Bautista. It is considered to be the most northwestern exposure of the Rio de La Plata Craton. Its topography is very subdued with numerous swampy areas locally called "esteros". The highest topographic points are low hills of porphyritic granitic rocks. Kanzler (1987) divided these rocks into three zones from south to north.

The southern zone mainly consists of orto- and paragneisses, migmatites, amphibolites, talc schists and rhyolite dykes grouped into the Rio Tebicuary Complex. These are thought to have a Lower Proterozoic or even older age. The central zone includes the Paso Pindó and Villa Florida Groups. The rocks of the Paso Pindó Group consist of interfingering conglomerates, sandstones and siltstones, all being slightly metamorphosed. The Villa Florida Group, of magmatic and metamorphic origin, is made up of granites, rhyolites, granodiorites, quartzites, gneisses, amphibolites and marbles and serpentinites in smaller proportions. Both groups are considered to be Middle Proterozoic in age. The northern zone of the Caapucú High exposes the Caapucú Group of Upper Proterozoic age with granites, rhyolites and some associated pyroclastic rocks. This area went through an important magmatic event during Early Cambrian-Early Ordovician (576 to 480 Ma, Brasiliano Cycle, cf. Almeida & Hasui, 1984).

The Apa High outcrops are distributed from the Apa River (Fig. 2) southward to the 22°50'S parallel and show a roughly triangular shape. They include Precambrian crystalline rocks covered by metamorphosed limestones of Vendian age (near the Proterozoic/Phanerozoic boundary). The most ancient stratigrahic unit is the Apa Basal Complex consisting of mafic gneisses, granites, metasediments and granitoid-pegmatitic intrusives. The age of this unit is considered to be Lower Proterozoic (Proyecto PAR-83/005). Unconformably above the Basal Complex the San Luis Group is found, which includes the former Estrella and Centurión Groups of Middle Proterozoic age. It begins with a basal conglomerate. The group is chiefly a volcano-sedimentary sequence with low grade metamorphism and

some degree of deformation. Its metasediments correspond to arkosic sandstones, sandstones, conglomerates and phyllites, being the magmatic rock-types represented by aphanitic granites, locally porphyritic, biotite-muscovite granites and pyroclastic effusives, rhyodacites and metavolcanics. The San Luis Group was strongly affected by the Cretaceous intrusions that also had caused a generalized tilt to the east.

The Itapucumí Group of Vendian age rests on the previous units with strong angular unconformity. The base of this group has a basal conglomerate that passes upward into the arkosic sandstone. Neverthless, it is predominantly composed of limestones with intercalated oolitic and shaly beds and also probably intercalated stromatolitic beds; it may also contain bodies of marble (Fig. 2). The Itapucumí Group has an exposure area of 2,075 km^2 in Eastern Paraguay plus 45 km^2 in the adjacent Gran Chaco. It is correlated with the Corumbá Group that crops out in continuity in neighbouring Brazil. Intrusions of granites, diorites, monzonites, and contact metamorphic rocks such as hornfels and rhyolites, rhyodacites and dacitic effusives of Upper Proterozoic age occur in the Centurión region. These rocks have been included in the San Ramón Group, although their relationships with the Itapucumí Group are not well stablished.

The Apa High, probably the most southern tip of the Central Brazilian Shield (Amazon Craton), has a geomorphology basically dominated by its local lithologies. The meta-volcanics and metasedimentary rocks of its northwestern part form low but distinct hills with difference levels of 150 to 200 m. These hills have a semi-circular pattern and open to the west. To the southwest the limestones underlie a low "plateau" dipping gently to the west-southwest. Its eastern limit is defined by a 50 to 100 m escarpment of the limestone "plateau". The crystalline rocks in the northern area of the Apa High define a monotonous topography with wide, open, low hills. With the exception of the higher elevations of the Centurión region to the northwest, the whole area is lowland and has "cerrado" type of vegetation.

The Phanerozoic of Eastern Paraguay has two major basins - Ordovician/Silurian and Devonian sediments in the Lower and Middle Paleozoic were deposited on a convergent margin with the paleo-Pacific plate being subducted under the Gondwana Continent (Fúlfaro et al., 1982; Gohrbandt, 1992), whereas the Carboniferous-Permian units of the Paraná Basin were deposited in a cratonic basin.

The Paleozoic-Mesozoic section in those basins has a great range of thickness from perhaps less than 100 m in outcrop on the structural highs to almost 6,000 m in the Bajo of San Pedro (Figs. 1 and 4). This Phanerozoic section consists almost entirely of sandstones and shales mainly because the region was at high paleolatitudes. Sandstones may be two to three times more abundant than shales.

STRATIGRAPHIC EVOLUTION

The Precambrian outcrops are separated into two parts by the Bajo of San Pedro, which seems to be part of a major lineament that crosses southern South America. Litherland & Bloomfield (1981) named this lineament the Chiquitos lineament in Bolívia and in the Paraná Basin it is called the Yguazú lineament (Fúlfaro et al., 1982). The Phanerozoic stratigraphic record of Eastern Paraguay begins with Upper Ordovician-Silurian deposits (Fig. 3).

South of the Asunción High the contact of Ordovician-Silurian deposits with the Precambrian basement crops out in the Quiindy-Quyquyhó and La Colmena-Acahay areas, the northern margin of the Caapucú High (Fig. 2). Silurian deposits indicate a sea connection with the western proto-Pacific ocean with the sea crossing the Chaco area and reaching Eastern Paraguay through an aulacogen limited, in this part of the country, by the Apa High to the north and the Caapucú High to the south. The remnant of this ancient aulacogen is now represented by the San Pedro downfaulted block, the so-called Bajo de San Pedro. Thus, the main tectonic framework of Eastern Paraguay includes five elements: Caapucú High, Asunción High with the Ypacaraí rift valley, the Bajo de San Pedro and the Apa High. These were formed and were active at different times. Collectivelly, these tectonic elements control the present outcrop pattern and have greatly influenced past sedimentation.

The rigid tectonic control of these units in the

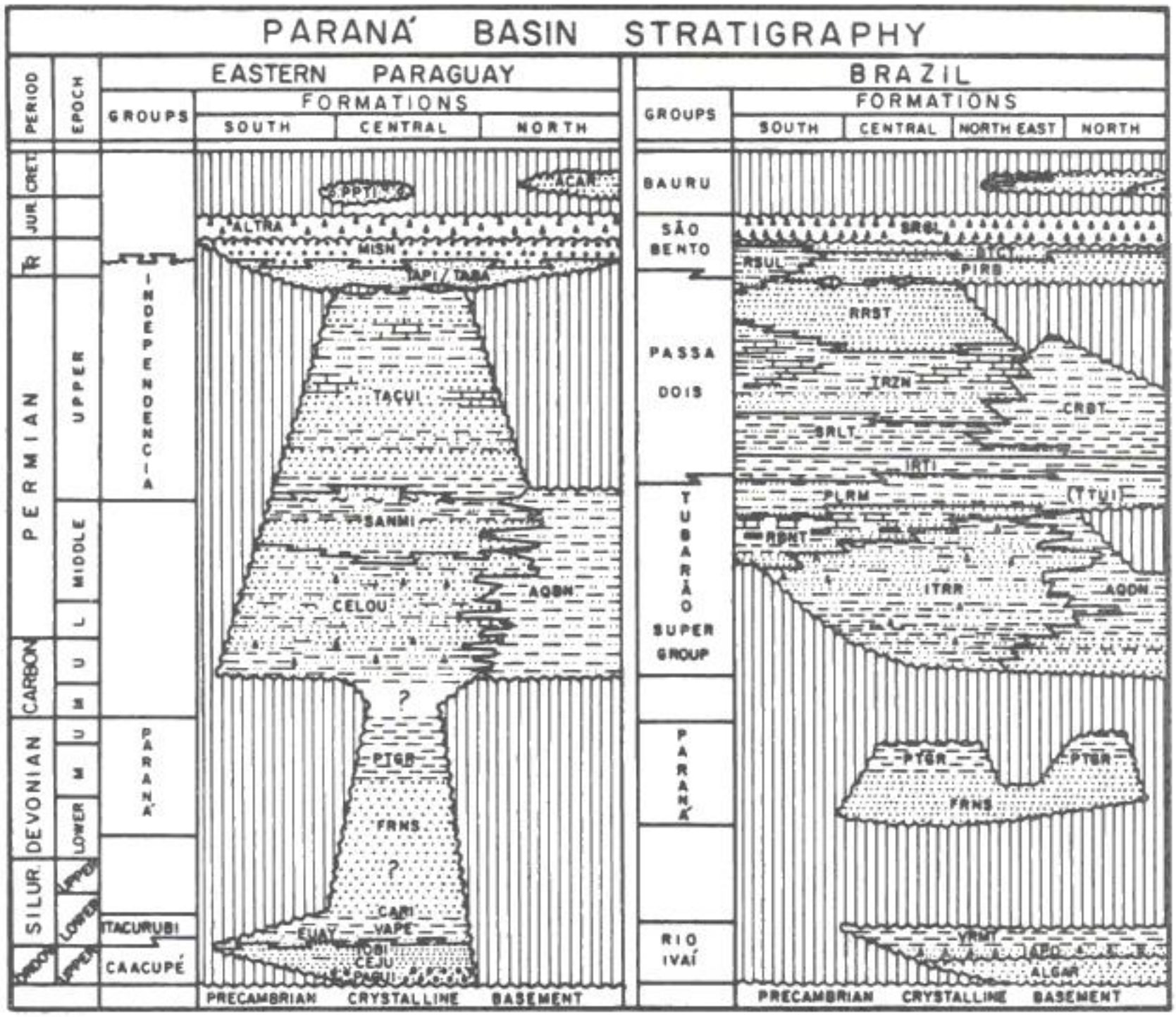

Figure 3 - Paraná Basin lithostratigraphic column. *Eastern Paraguay*: PAGUI (Paraguarí Fm.), CEJU (Cerro Jhú Fm.), TOBI (Tobati Fm.), EUAY (Eusebio Ayala Fm.), VAPE (Vargas Peña Fm.), CARI (Cariy Fm.), CELOV (Coronel Oviedo Fm.), AQBN (Aquidabán Fm.), SANMI (San Miguel Fm.), TACUI (Tacuary Fm.), TAPI (Tapytá Fm.), TABA (Tabacuá Fm.), MISN (Misiones Fm.), ALTRA (Alto Paraná Fm.), PATI (Patiño Fm.), ACAR (Acaray Fm.); cf. Proyecto PAR 83/005. *Brazil*: IAPO (Iapó Fm.), VRM (Vila Maria Fm.), ALGAR (Alto Graças Fm.), FRNS (Furnas Fm.), PTGR (Ponta Grossa Fm.), AQDN (Aquidauana Fm.), ITRR (Itararé Group or Subgroup), RBNT (Rio Bonito Fm.), PLRM (Palermo Fm.), ITUI (Tatuí Fm.), IRTI (Iratí Fm.), SRLT (Serra Alta Fm.), CRBT (Corumbataí Fm.), TRZN (Terezina Fm.), RRST (Rio do Rasto Fm.), RSUL (Rosário do Sul Fm.), PIRB (Pirambóia Fm.), BTCT (Botucatu Fm.), SRGL (Serra Geral Fm.), modified from Stevaux & Perinotto (1989).

outcropping areas (Fig. 1) is an expression of ancient structural lines that were reactivated several times during the Phanerozoic. As clearly demonstrated by paleogeographic interpretations, one of the most important tectonic feature of Paraguay, the Asunción Arch, a badly defined cratonic structure, did not exist until Silurian times.

The Ordovician-Silurian deposits belong to the Caacupé and Itacurubí Groups (Figs. 2 and 3). The Caacupé and Itacurubi Groups together form a section of about 1,000 m. At the top of this seemingly continous section a convincing Llandoverian (Lower Silurian) fauna occurs in the Vargas Peña shales (Wolfart, 1961). The age of the sedimentary rocks below is uncertain, but its lower parts have been considered Upper Ordovician (Aceñolaza & Baldis, 1987). In the following text these two groups are simply referred to as Silurian. The basal Caacupé Group is divided into the Paraguarí, Cerro Jhú and Tobati Formations. From base to top the Paraguarí fanglomerates, cross-bedded coarse sandstones and arkoses represent the classical terrigenous clastic wedge stage of the initial filling of an aulacogen. The following sagging stage is represented by the Cerro Jhú and Tobati Formations

all nearshore, shallow water, marine sandstones. The continental crossbedded sandstones of the Cerro Jhú Formation have a transitional contact with rocks of the Paraguarí Formation, and pass upward into the well sorted sandstones of the Tobati Formation, that were called the "saccaroid" sands by Eckel (1959). The three units of the Caacupé Group represent the basal clastic sequence of the Ordovician-Silurian marine transgression. The upper transitional contact of the Caacupé Group with the Itacurubí Group shows that the upper Caacupé sequence is the basal part of a marine transgression.

The Itacurubí Group includes the marine fossiliferous Eusebio Ayala, Vargas Peña and Caryi Formations. The Eusebio Ayala unit is transitional with the underlying "saccaroid" Tobati Sandstones and consists mainly of rhytmic layers of fine micaceous sandstones and shales with intercalated beds of conglomeratic sandstones and with finning-upward beds of conglomerate representing, probably, the final stages of distant marginal fan deltas. A shallow marine environment is inferred for this unit.

The shales of the Vargas Peña unit have restricted outcrops. In their type locality near the city of Itauguá to the west of the Ypacaraí valley, weathered white to yellowish micaceous shale is dominant. The Vargas Peña has a transitional contact with the underlying Eusebio Ayala Formation, which has an abundant Lower Silurian faunal assemblage consisting of brachiopds, mollusca, graptolites, trilobites, etc. (DeGraff, 1981). This assemblage indicates a shallow marine environment.

The uppermost part of the Itacurubí Group, the marine fossiliferous sediments of the Caryi Formation, is represented by fine to medium sandstones, with cross-bedded layers intercalated with horizontal layers of fine, micaceous sandstones and shales. The faunal assemblage of this unit suggests a shallow marine water environment of gulfs and protected bays, an environment with strong continental influence. Commonly considered as the beginning of the Silurian regression, the Caryi Formation may indeed represent only an oscillatory stage of the Silurian transgression. In Cerro Loma Caryi, near the city of Itacurubí de la Cordillera, the lithologies of Caryi and Eusebio Ayala Formations interfinger. Also along the Emboscada-Arroyos y Esteros route, 8 km from the Piribebuy river, an outcrop shows lateral transition from the Caryi sandstones to the shales of the Vargas Peña Formation.

The extension of the Silurian rocks of Paraguay to the eastern part of the Paraná Basin in subsurface is a matter of controversy. Deposits of the same age occur in the northern part of the Paraná Basin in Goiás State, where they are called the Vila Maria Formation. Zalán et al. (1987) have made a basinwide correlation of the Silurian units through drill holes and proposed a correlation between the Paraguayan beds and the Vila Maria beds in subsurface. Rocks of similar age occur in Bolivia and Peru in the Andean mobile belt. On the South American craton similar beds of Silurian age also occur in the Parnaíba and the Amazon basins with an indication of a former connection to the paleo-Tethys boreal sea. Thus, it seems likely that there was a sea that connected Eastern Paraguay to Bolivia and Peru. However, the eastern extent of this sea into Brazil is uncertain. Milani (1992) presented a tentative paleogeography for the Paraná Basin in the Ordovician-Silurian time. Nevertheless his interpretation is quite different from that of this paper.

Harrington (1950) assigned the Itacurubí deposits to the Devonian based on a correlation to the Devonian beds of the eastern part of the Paraná Basin. This misinterpretation was corrected by Wolfart (1961), who identified the faunal assemblage as being of Lower Silurian (Llandoverian) age. Since the publication of Wolfart's paper and the work of Putzer (1962), the general belief is that there were no Devonian rocks in Eastern Paraguay and in the whole western margin of the Paraná Basin.

Oil exploration efforts made in Eastern Paraguay in the last decade have lead to a discovery of Devonian sediments north of the Asunción High (Fig. 4), between the Ypané and Jejui-Aguaray Guazú rivers. The Asunción drill holes n° 1 and n° 2 (Pecten-Occidental-Trend) have encountered 370 and 265 m, respectively, of Devonian beds in the San Pedro downfaulted block. The correlation of these sediments with the Furnas and Ponta Grossa units of the Paraná Basin seems well stablished.

In the first drill hole, the Furnas Formation

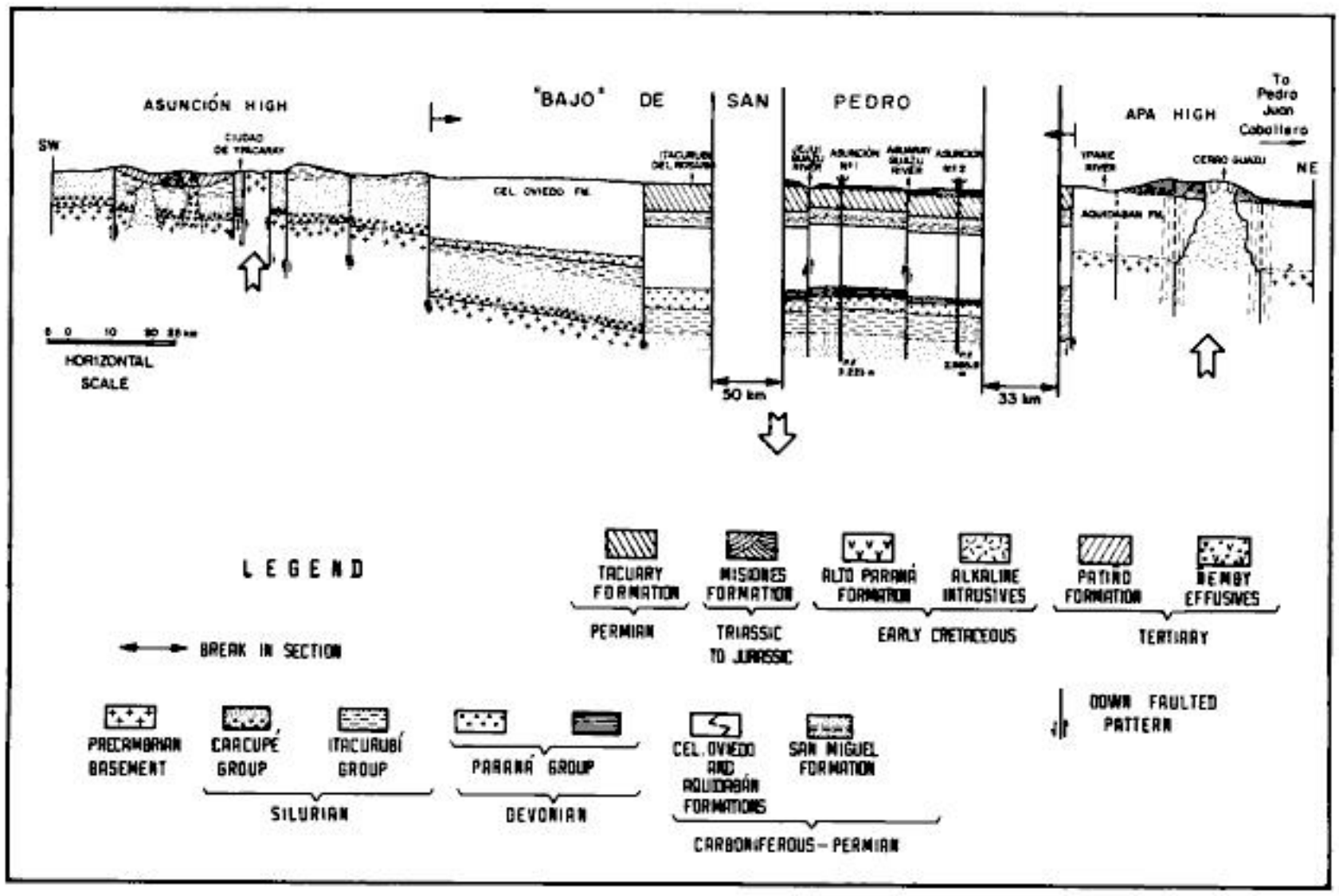

Figure 4 - SW-NE geological cross-section of Eastern Paraguay.

is present from to 2,050 to 2,240 m and is represented by conglomeratic sandstones, arkoses and shale beds cut at several levels by intrusive rocks. The Ponta Grossa Formation is present from 1,870 to 2,050 m and consists of shales with some beds of sandstones up to 5 m thick. In the Asunción n° 2 drill hole the Furnas occurs between the 2,077 to 2,275 m and its lithology is somewhat different from that of the n° 1 well. The Ponta Grossa Formation occurs from 2,000 to 2,077 m.

The presence of Devonian beds in these two wells links the widespread Devonian deposits of Peru and Bolivia across Paraguay to the Devonian deposits of the Paraná Basin. Also, the existence of Devonian strata in the Bajo de San Pedro shows that sedimentation extended well beyond its presently preserved limits. Later activity of the Asunción Arch lead to the erosion of much of these Devonian deposits which are today preserved only in downfaulted blocks. The good correlation of the Devonian sediments preserved in the San Pedro block shows that they were part of a much larger basin and not deposited as isolated graben fill.

In Western Paraguay (Chaco area), Devonian sediments crop out in the Cerro León region over an area of 2,000 km^2 near Lake Palmar de las Islas. These Devonian beds of the Chaco area are referred to as San Alfredo Formation. The micaceous sandstones of the San Alfredo are at least 2,000 m thick. These outcrops, according to Gomez Duarte (1986), are part of the Central High or Cerro León uplift of Cretaceous age. Strong tectonic block faulting occurred in Paraguay during the Cretaceous and is related to the initial rifting and later drift of South America from Africa.

The contact of the Silurian outcrops with the succeeding Carboniferous section in Eastern Paraguay occurs in a fault zone (Figs. 1 and 4). An important feature is the strong difference between the NW structural trend presented by the Silurian outcrop units map and the almost N-S orientation of the Late Paleozoic beds of the Paraná Basin. The N-S strike of the Late Paleozoic beds, their eastern dip and the correlation with the rest of the Paraná Basin indicates that the Asunción Arch was an effective barrier at this time between the Paraná Basin and the Chaco region. A new basin configuration seems to have been stablished at this time.

In Eastern Paraguay the Carboniferous-Per-

mian beds lie unconformably on the Precambrian, Silurian and Devonian. Fúlfaro et al. (1982) described a long erosion period after a Lower Carboniferous uplift. Outside of the Bajo de San Pedro block, this period of erosion caused the erosion of all Devonian deposits.

The main unit of the so-denominated Carboniferous rocks in Paraguay is the Coronel Oviedo Formation in the central part of the country. To the north, in the Apa High region, this unit interfingers with the Aquidabán Formation (Figs. 2 and 3). There is no practical evidence that these rocks are truly Carboniferous in age even through it is suggested by the older literature. Today, the Coronel Oviedo Formation is believed to correlate with the Itararé Formation in Brazil of Upper Carboniferous (Stephanian) Permian age.

The Coronel Oviedo Formation crops out in central-eastern Paraguay south of the Jejui-Aguaray-Guazú fault and extends to the northern limit of the Caapucú High. It has a 5 to 35 km W-E outcrop belt commonly obscured by Quaternary deposits. To the north of this fault zone the typical lithologies of the Coronel Oviedo and Aquidabán Formations interfinger.

The Coronel Oviedo Formation contains diamictites, commonly referred as tillites, sandstones and thin intercalations of argillaceous beds. Outcrops are poor and scarce. In eastern Paraguay extensive swampy plains, the "esteros", occur in the outcrop belt of this formation. These swampy areas are a combination of an argillaceous substrat and Quaternary tectonic reactivation, which has produced the mosaic block faulting of eastern Paraguay.

In addition to the previous mentioned tillites and sandstones, varved shales are also present. Twelve kilometers north of the city of Coronel Oviedo in the region of Carayaó, supra-glacial tills are present. The interpretation of possible depositional environments of this formation is always complicated by the intense tectonism within these areas and the widespread cover of Quaternary sediments.

To the north, the Aquidabán Formation covers an outcrop area of 12,097 km^2. The formation lies above an unconformity with the Upper Precambrian (Vendian) limestones of the Itapucumí Formation; its upper contact is also unconformable with the Triassic-Jurassic sandstones of the Misiones Formation. The main characteristic of the Aquidabán sandstones is their reddish color.

The Coronel Oviedo and Aquidabán Formations contain diamictites and striated pebbles and, thus, indicating its glacial origin. Nevertheless, evidence of fluvial deposition are numerous and suggest outwash or marginal reworking of glacial deposits. Other evidence of reworking near the front of a glacier are mud flow deposits.

In Western Paraguay in the Chaco, Carboniferous sedimentary rocks are present in the Carandayti and Curupayti basins. Here they carry the name Palmar de las Islas Group and are divided in to the San José and Cabrera Formations. These two units, with different names, extend into Bolivia.

The Permian Independencia Group (Figs. 2 and 3) consists of the San Miguel and Tacuary Formations. The name Independencia Series was given by Harrington (1956). Eckel (1959) considered these deposits in Paraguay as belonging to the Santa Catarina System. Following the earlier work of White (1908), who first stablished a stratigraphic sequence for the Paraná Basin in Brazil, Putzer (1962) adopted the Brazilian Passa Dois Series for the unit. In the description of the MOPC 41 sheet, it was called the Ybytyruzú Series. Wiens (1982) had proposed the following division for the Permic succession: San Miguel, Tacuary, Tapytá and Cabacuá. During the stratigraphic revision of Proyecto PAR 83/005, the later two units were dropped and the San Miguel and Tacuary Formations were grouped into the Independencia Group.

The San Miguel Formation crops out from the Carayaó region in the north to the Yuti area to the south. It is not present to the north of the Jejui-Aguaray Guazú fault zone. The formation consists of sandstones, argillaceous beds and diamictites in transitional contact with the underlying Coronel Oviedo Formation. Hutchinson et al. (1979) described beds of conglomerate at its base which are followed by an alternation of sandstones and shales, all deposited in fluvial, lacustrine, deltaic and shallow marine environments. Fossil wood is a characteristic of this unit not only in Paraguay but also in the rest of the Paraná Basin.

The upper contact of the San Miguel unit with the Tacuary Formation is very difficult to

observe, but it seems to be transitional. The Tacuary Formation is formed by a rhythmic succession of siltstones, shales, fine sandstones and some carbonates, which are in general oolitic. One of its characteristics in outcrop is given by its great variety of colors. The faunal assemblage of this unit mainly consists of molluscs, ostracodes and crustaceans. Deposition occurred in a shallow Permian sea. This assemblage permits its correlation to the Terezina Formation in the Brazilian part of the Paraná Basin.

The Tacuary Formation, as is true to all the previous Paleozoic units, has its northern limit in the Jejui-Aguaray Guazú fault zone that is also the northern border of the Bajo de San Pedro. North of this fault zone only the reddish sandstone of the Aquidabán Formation are present. The removal of post-Aquidabán beds probably occurred in the Triassic. Thus, a strong erosional unconformity seem to separate Mesozoic Formations from Paleozoic ones.

Aeolian sandstones of the Misiones Formation (Fig. 2), which are correlated to the Botucatu sandstones found in Brazil, rest on Silurian, Carboniferous and Permian sediments and, thus, show that most of the uplift in central-eastern Paraguay was prior to its deposition. These relations are best shown in the region of the Asunción High (Fig. 4). The Misiones Formation has two different interfingering depositional facies, a fluvial sandstone with interstial clay, and an overlying predominantly well sorted, eolian sandstones. The fluvial sequence was divided by Wiens (1982) into the Tapytá and Cabacuá Formations. These units should be discarded. Conglomeratic layers are intercalated within these sandstones and frequently the pebbles show wind action and are interpreted as true ventifacts. In the area from Cerro Yaguarón to Paraguarí these sandstones are cut by alkaline intrusives belonging to the Sapucai Formation (Early Cretaceous).

The extensive lava flows of Early Cretaceous age present in the Paraná Basin are also well represented in Paraguay, where they carry the denomination Alto Paraná Formation (Fig. 2). This formation crops out in a strait band from Pedro Juan Caballero to the north, southward to the Jejui-Aguaray Guazú fault zone. From this point to the south the outcrop area enlarges in the Bajo de San Pedro area, becoming strait again south of the Caapucú High in direction to Encarnación. Thus, its larger area of exposure in the downfaulted block of San Pedro suggests a later post-Cretaceous subsidence of the rift.

Above the basalts of the Alto Paraná Formation the geological map of Paraguay indicates some small outcrops of deposits correlative to the Upper Cretaceous Bauru Group in Brazil. Nevertheless is very difficult to find these deposits in field work and such mapped areas may be due to remote sensing interpretation. This sequence is named Acaray Formation (Fig. 2).

The Cenozoic in Paraguay is marked by a strong uplift as shown by the presence of fanglomerates and volcanic rocks in Eastern Paraguay. The final configuration of the so-called Chaco Basin, which started at the end of the Cretaceous, developed at this time. Near Asunción city and in all the Ypacaraí rift valley, fanglomerates of the Patiño Formation were widely deposited. In the type locality at Cerro Patiño, graded, finning-upward conglomeratic beds start with pebbles as large as 40 cm. Such conglomerates contain a suite of all the regional underlying rocks. The Patiño Formation is cut by volcanic rocks of the Ñemby Formation, which are related to the last movement in the Asunción High. The final establishment of the Ypacaraí rift valley system occurred at this time in the Tertiary.

Extensive Quaternary sedimentation is related to the Paraguay river (Fig. 2), being in the Asunción city area its deposits are named San Antonio Formation. These deposits include also fine sediments of natural leaves and alluvial plains that contain fragments of Quaternary mammal fossil bones. Impressive is the big deltaic fluvial plain in the southern part of the country, where the Paraná river meets the Paraguay river.

DISCUSSION AND CONCLUDING REMARKS

The regression of the Late Proterozoic Itapucumí sea (Fig. 5) was followed by a general uplift and consequent erosion. Probably in the Cambro-Ordovician time the Chiquitos lineament formed an aulacogen that cut Paraguay. Into this aulacogen the continental sedimentation of the Caacupé Group with the fluvial conglomerates of

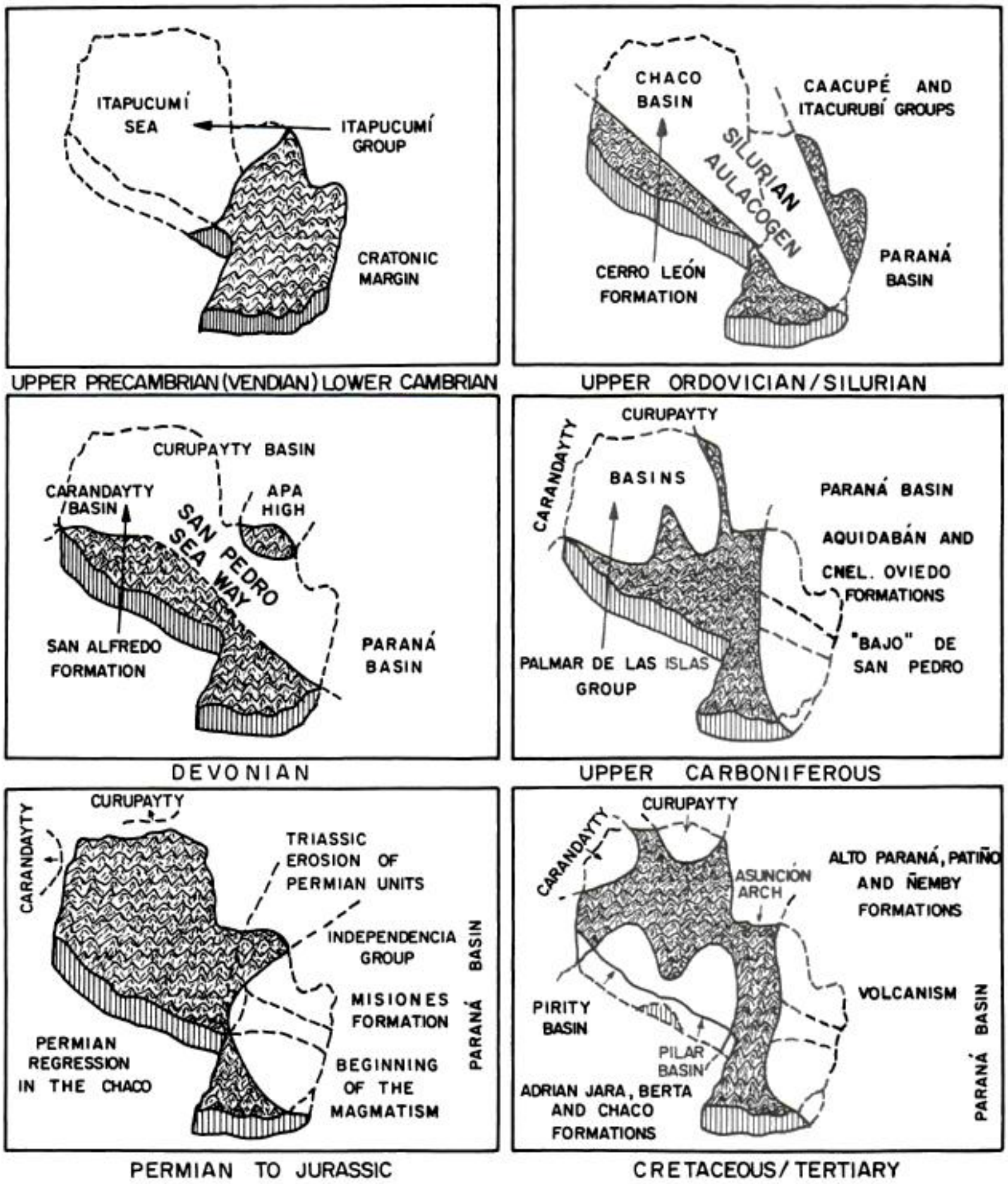

Figure 5 - Phanerozoic tectonic and paleogeographic evolution of Paraguay.

the Paraguarí Formation began in the Upper Ordovician (Fig. 4).

The depositional sequence that had started in the Upper Ordovician continued into the Silurian, filled the aulacogen and buried its margins. The preserved thickness of the Silurian sequence is about 1,000 m and the thin basal fluvial conglomerates (20 m) changed rapidly first to marine sandstones followed by the fossiliferous shales of Llandoverian age.

The original northern limits of the Silurian sea probably did not extend far from the limits of the aulacogen. Evidence for this comes from two factors - probable continuous Silurian-Devonian sedimentation in the aulacogen whereas beyond the aulacogen Devonian deposits rests directly on the basement. The original southern limits of the Silurian sea were probably close to those of the present southern limit of the conglomerates of the Paraguarí Formation.

The distribution of Devonian sediments in Paraguay has long been a problem. Until recently Devonian rocks were not recognized in Eastern Paraguay and the general belief was that Devonian sediments were restricted to Western Paraguay and present only in the Carandayti and Curupayti basins (Fig. 5). First, these deposits were miscorrelated with the Silurian. Later they were restricted to Western Paraguay even through isopachs of Devonian sediments in Brazil suggested that they should be present in Eastern Paraguay. The discovery of Devonian rocks in the subsurface (Asunción wells n° 1 and nº 2) clarified this problem, because it showed that the western Devonian connects to the Devonian of the Paraná Basin through the buried San Pedro seaway (Fig. 5).

After Devonian sedimentation, there was an interval of erosion in the Lower Carboniferous. Upper Carboniferous beds of the Coronel Oviedo Formation lie unconformably on the Devonian. This interval of erosion may be related to the initial stages of the later collision between the Patagonian craton with the South American craton. The Coronel Oviedo Formation represents the beginning of cratonic sedimentation on this part of Gondwana. Because this part of Gondwana was at low latitude, it has widely distributed glacial deposits, most of which consist of rain out diamictons deposited in a shallow sea. After these glacial events, there was isostatic uplift in marginal areas, which lead to deltaic deposition in Permian time, the San Miguel Formation.

In latest Permian time, Eastern Paraguay was uplifted, unlike the Brazilian part of the Paraná Basin, where the Upper Permian Palermo Formation was deposited. The uplift of the southern Andes may have been responsible for this and also for the alkaline intrusions of the Alto Paraguay Province of Permo-Triassic age (Gomes et al., 1993). This uplifted area expanded in the Triassic as shown by the widespread presence of the eolian Misiones sandstones across all the Paraná Basin even well beyond the limits of the Permian deposits.

In the Lower Cretaceous, extensive alkaline intrusives occurred in preferencial zones of weakness in the Asunción and Apa Highs and along the margins of the San Pedro downfaulted block. These alkaline intrusives are contemporaneous with the Cretaceous basalts of the Alto Paraná Formation in Paraguay and the Serra Geral Formation in Brazil. Related to this event in the Asunción area, a great uplift occurred and produced the Ypacaraí rift valley, which was filled with conglomerates (Patiño Formation) derived from Silurian and Triassic-Jurassic deposits. In the Tertiary, olivine-rich volcanics ranging in age from 39 to 61 Ma were locally extruded (Ñemby Formation). These volcanic rocks show derivation from subcrustal lithosphere and demonstrate that the Ypacaraí rift is a major cratonic rift.

The present geomorphology of Paraguay is largely inherited from Cretaceous-Tertiary tectonic events outlined above.

ACKNOWLEDGEMENTS

The author wants to express thanks for the critical review of this paper made by Professor Paul Edwin Potter of Cincinnati University and presently Visiting Professor of the Instituto de Geociências e Ciências Exatas of the State University of São Paulo (UNESP).

REFERENCES

ACEÑOLAZA, F.G. & BALDIS, B. (1987) The Ordovician system of South America, correlation charts and explanatory notes. Episodes 22:1-68.

ALMEIDA, F.F.M. & HASUI, Y. (1984) O Pré-Cambriano do Brasil. Editora Edgard Blücher Ltda. São Paulo, 378p.

AZARA, F. (1790) Geografía física y esférica de las provincias del Paraguay y Misiones Guaranies. Anales Mus. Nac. Montevideo, V.1, 655p.

BELLIENI, G.; COMIN-CHIARAMONTI, P.; MARQUES, L.M.; MARTINEZ, L.A.; MELFI, A.J.; NARDY, A.J.R.; PICCIRILLO, E.M.; STOLFA, D. (1986) Continental flood basalts from the central-western regions of the Paraná plateau (Paraguay and Argentina): petrology and petrogenetic aspects. Neues Jb. Miner. Abh., *154*:111-139.

BITSCHENE, P.R. (1987) Mesozoicher und Kanozoicher magmatism in OstParaguay: Arbeinteznur Geologie und Petrologie zweier Alkaliprovinzen. Ph.D. Thesis, Heildelberg University, 317p.

BITSCHENE, P.R. & LIPPOLT, J.H. (1986) Acid magmatites of the Brazilian cycle in East Paraguay. Zbl. Geol. Paläont., Teil I, 9/*10*:1457-1468.

CARNIER, K. (1911) Paraguay, Versuch zu einer morphologischen Betrachtung der Landschaftformer. Mitt. Geog. Gesell., *29*:1-50

CHARLEVOIX, P.F.X. (1747) Histoire du Paraguay. Paris, 2608.

COMIN-CHIARAMONTI, P.; CUNDARI, A.; GOMES, C.B.; PICCIRILLO, E.M.; CENSI, P.; DE MIN, A.; BELLIENI, G.; VELÁZQUEZ, V.F.; ORUÉ, D. (1992) Potassic dyke swarm in the Sapucai Graben, eastern Paraguay: petrographical, mineralogical and geochemical outlines, Lithos, *28*:283-301.

COMTE, D. & HASUI, Y. (1971) Geochronology of Eastern Paraguay by potassium-argon method. Rev. Bras. Geoc., *1*:33-43.

DeGRAFF, J.M.; FRANCO, R.; ORUÉ, D. (1981) Interpretación geofísica y geologica del Valle de Ypacaraí (Paraguay) y su formación. Rev. Assoc. Geol.Arg., *36*:240-256.

DU GRATY (1865) La Republique du Paraguay, 2d. ed. C. Murquardt, Brussels, 407p.

ECKEL, E.B. (1959) Geology and mineral resources of Paraguay - A reconnaissance. U.S. Geol. Surv. Prof. Paper, *327*:110p.

FÚLFARO, V.J. & LANDIM, P.M.B. (1971) A seqüência gondwânica ocidental: República do Paraguai. An. XXV Congr. Bras. Geol., *2*:241-246.

FÚLFARO, V.F.; SAAD, A.R.; SANTOS, M.V.; VIANNA, R.B. (1982) Compartimentação e evolução tectônica da Bacia do Paraná. Rev. Bras. Geoc., *12*:590-610.

GOHRBANDT, K.H.A. (1992) Paleozoic paleogeographic and depositional developments on the central proto-Pacific margin of Gondwana: their importance to hydrocarbon accumulation. J. South Amer. Earth Sci., *6*:267-287.

GOLDSCHLAG, M. (1913) Zur Petrographie Paraguay und Mato Grosso. Mitt. Geog. Gesell., *8*:293-301.

GOMES, C.B.; COMIN-CHIARAMONTI, P.; DE MIN, A.; ROTOLO, S.G. and VELÁZQUEZ, V.F. (1993) Província Alcalina do Alto Paraguai (Mato Grosso do Sul e Paraguai): características geoquímicas. 4° Congr. Bras. Geoq., Anais, p.55-58.

GOMEZ DUARTE, G. (1986) Contribución al conocimiento de la geologia del norte del Chaco paraguayo, Lagerenza, MOPC, Paraguay.

HARRINGTON, H.J. (1950) Geologia del Paraguay Oriental. Fac. Ci. Ex., Fis. Mat., Contr. Cient., Ser. E., Geologia, *1*:1-88.

HARRINGTON, H.J. (1956) Paraguay. In: Handbook of South American Geology. Geol. Soc. Amer. Mem., *65*:99-114.

HIBSCH, J.E. (1891) Einige Gesteine aus Paraguay, Tscherm. Miner. Petr. Mitt., *12*:253-255.

HUTCHINSON, D.S. (1979) Geology of the Apa High. T.A.C. (int. rep.), Asunción, 46p.

KANZLER, A. (1987) The southern Precambrian in Paraguay. Geological inventory and age relation. ZBl. Geol. Paläont., Teil. I, *7/8*:753-765.

LITHERLAND, M. & BLOOMFIELD, K. (1981) The Proterozoic history of Eastern Bolivia. Precambrian Reserch, *15*:157-179.

MERSAY, A. (1860) Histoire physique, economique et politique du Paraguay et des établissements des Jesuits. Librairie L. Hochette & Cie., Paris, 486p.

MILANI, E.J. (1992) Intraplate tectonics and the evolution of the Paraná Basin, SE Brazil. Inversion tectonics of the Cape Fold Belt, Karoo and Cretaceous Basins of Southern Africa. In: M. Wit & I. Ransome (eds.). A.A. Balkema, p.101-108.

MILCH, L. (1895) Über Gesteine aus Paraguay. Tscherm. Miner. Petr. Mitt., *14*:383-394.

OCCIDENTAL COMPANY (1987) Generalized geological map of Paraguay and adjacent areas. Asunción, Paraguay.

ORGANIZACIÓN DE LOS ESTADOS AMERICANOS - O.E.A. (1975) Cuenca del Plata, Republica del Paraguay - Proyecto Aquidabán. Desarrollo de la región nororiental. Washington, 197p.

PALMIERI, J.H. (1973) El complejo alcalino de Sapukai (Paraguay Oriental), Ph.D. Thesis, University of Salamanca, 298p.

PALMIERI, J.H. & VELÁZQUEZ, J.C. (1982) Geologia del Paraguay. Colección Apoyo a Catedra. Serie Ciencias Naturales, Ed. NAPA, Asunción, 65p.

PETRI, S. & FÚLFARO, V.J. (1983) Geologia do Brasil. Fanerozóico T.A. Queiroz/EDUSP, São Paulo, 631p.

PROYECTO PAR 83/005 (1986) Mapa geológico del Paraguay. Comisión Nacional de Desarrollo Regional - Ministério de Defensa Nacional, Asunción, 270p.

PUTZER, H. (1962) Die geologie von Paraguay. Beitr. Reg. Geol. Erde, *2*:1-182.

RAMOS, V.A. (1984) Patagonia: uin continente paleozoico a la deriva? Congr. Geol. Argentino, 9, Actas, *2*:311-325.

SEPP, P.A. (1697) Reisebeschreibung nach Paraguay. Nürnberg, 820p.

STEVAUX, J.C. & PERINOTTO, J.A.J. (1989) O Subgrupo Guatá: XI Congr. Bras. Paleont., Anais, *5*:26-33.

STORMER, J.C.; GOMES, C.B.; TORQUATO, R.F. (1975) Spinel lherzolite nodules in basanite lavas from Asunción, Paraguay. Rev. Bras. Geoc, *5*:176-185.

VELÁZQUEZ, V.F. (1992) Província Alcalina Central, Paraguai Oriental: aspectos petrográficos, tectônicos e geocronológicos. Ms.D. Dissertation, University of São Paulo, 119p.

WHITE, I.C. (1968) Relatório final da Comissão de Estudos das Minas de Carvão de Pedra no Brasil, Parte I, p.1-204.

WIENS, F. (1982) Mapa geologico de la región oriental. Republica del Paraguay, escala 1:500.000. Simp. Rec. Natur. Paraguay, Asunción, 9p.

WOLFART, T.R. (1961) Stratigraphie und fauna der alteren Paleozoikum (Silur-Devon) in Paraguay. Geologie JB, *78*:29-102.

ZALÁN, V.P.; WOLFF, S.; CONCEIÇÃO, J.C.J.; SANTOS VIEIRA, I.; MENDONÇA STOLFI, M.A.; APPI, V.T.; ZANOTTO, O.A. (1987) A divisão tripartite do Siluriano da Bacia do Paraná. Rev. Bras. Geoc., *17*: 242-252.

ALKALINE MAGMATISM IN PARAGUAY: A REVIEW

C.B.Gomes, P.Comin-Chiaramonti, V.F.Velázquez, D.Orué

Alkaline Magmatism in Central-Eastern Paraguay. Relationships with Coeval Magmatism in Brazil. Comin-Chiaramonti, P. & Gomes, C. B. (eds.), 1996, Edusp/Fapesp, São Paulo, pp. 31-56.

ABSTRACT

This paper reviews general aspects regarding the occurrences of alkaline rocks found concentrated in three major regions of Paraguay: northern, northeastern and central-eastern. Knowledge on those rocks, mainly emphasizing the historical background and their geologic, tectonic and geochronological features, has been updated to July, 1992. Radiometric determinations (dominantly by K/Ar method) place the rocks into three well-defined age groups. The older one, about 240 Ma, is found restricted to the northern area of Paraguay (Alto Paraguay Province). The second age group clusters around 130 Ma and comprises the larger number of occurrences; outcrops are distributed over the northeastern (Amambay Province) and central-eastern (Central Province) sections of the country. The younger group, only consisting of occurrences from the Central Province, shows a large age span, two episodes of magmatic activity being clearly distinguished (60-70 Ma, Na-rich phonolites; 39-61 Ma, Asunción nephelinites).

INTRODUCTION

Scanty references on alkaline rocks from Paraguay may be found among older geological description of its eastern region (DuGraty, 1865; Pöhlmann, 1886; Derby, 1887, 1898; Hibsch, 1891; Evans, 1894; Milch, 1895, 1905; Lisboa, 1909; Carnier, 1911, 1913; Goldschlag, 1913; Willmann, 1915). A more complete account only appeared for the first time in literature of the fifties as part of Harrington's (1950, 1956) summaries of Paraguayan geology. These were followed by the excellent, especially considering the hitherto widely scattered published information, monograph by Eckel (1959), which includes a locality map of some already known occurrences of alkaline rocks in northern and central Paraguay. Additional information is in Putzer's (1962) extensive geological investigation of Paraguay, and in Putzer & van dem Boom (1962). Thereafter, this topic remained almost totally neglected in the literature for two decades.

At the beginning of the seventies, the alkaline rocks of Paraguay attracted new attention due to their economic importance as potential minerals, in particular phosphates and uranium, as well as their petrological and age significance (Comte & Hasui, 1971). Related to the former aspect are the

contributions by Berbert & Triguis (1973) and Palmieri et al. (1974), dealing with some carbonatite complexes in northeastern Paraguay. Palmieri (1973), Palmieri & Arribas (1975) and Stormer et al. (1975) stimulated research towards a better understanding of these rocks. The paper by Vera Morinigo & Penayo (1967) represents a summary of unpublished material from various local sources. Of great importance are the reports by OEA (1975) and Mariano (1978) describing the geology and petrography of several alkaline bodies.

The last decade brought considerable improvement in the knowledge of alkaline magmatism in Paraguay, basically as a result of a seven-year mineral exploration programme conducted in the whole country by Anschutz Corporation of Denver, Colorado, U.S.A.. After four years of work, a geological map at the scale of 1:500,000 (TAC, 1981; Wiens, 1982) was made available, showing new occurrences and providing more data on the characterization and distribution of alkaline rocks in Paraguay. Meantime, useful internal reports were produced (Hutchinson, 1979, 1980; Hales, 1980; Druecker, 1981; Sanders, 1981; Blair, 1982). Aspects of the geology of these rocks have been discussed in several papers, i.e. tectonic control (DeGraff et al., 1981; Almeida, 1983; DeGraff, 1985; Bitschene et al., 1985, 1986; Druecker & Gay, 1987), geochronology (Ulbrich & Gomes, 1981; Eby & Mariano, 1986; Bitschene, 1987; Sonoki & Garda, 1988), petrology and geochemistry (Bitschene & Lippolt, 1984; Comin-Chiaramonti et al., 1986; De Vito, 1987; De Min, 1988; Demarchi et al., 1988; Gallo, 1988; Bitschene & Báez Presser, 1989; Censi et al., 1989; Gomes et al., 1989), and general geology (Premoli & Velázquez, 1981; Palmieri & Velázquez, 1982; Wiens, 1986; Proyecto PAR 83/005, 1986; Livieres & Quade, 1987; Woolley, 1987).

The investigation of Paraguayan alkaline rocks was strongly intensified by the end of the last decade, due to the launching in September 1987 of an international cooperative programme involving university researchers from Australia, Brazil, Italy and Paraguay. Several papers have been already published, mostly on the petrology and geochemistry (Comin-Chiaramonti et al., 1990a,b; Censi et al., 1991; Comin-Chiaramonti et al., 1991a,b,c,d; Marzoli, 1991; Comin-Chiaramonti et al., 1992a,b,c). Other papers addressed geochronology (Ulbrich et al., 1990; Velázquez et al., 1990a,b; Green et al., 1991a,b; Velázquez, 1992; Velázquez et al., 1992) and palaeomagnetism (Ernesto et al., 1990).

GEOLOGICAL ASPECTS

Paraguay, one of the two land-locked countries in South America, lies between latitudes 19 and 28S and longitudes 54° and 63°W (Fig. 1) and covers a total area of 406,752 km^2. The country is bounded by Argentina, Bolivia and Brazil, and is bisected by the Paraguay river along a north-south line. The geology of Paraguay is characterized by two large sedimentary basins, the Andean to the west and the Paraná to the east. Only the geology of the area east of the Paraguay river (also referred to as Eastern Paraguay) and extending over about 150,000 km^2 will be discussed in this book. The boundary between these two basins is formed by the so-called Central

Figure 1 - Index map showing the location of Paraguay and the contour lines (dots) of the Paraná Basin (Petri & Fúlfaro, 1983, modified after Northfleet et al., 1969).

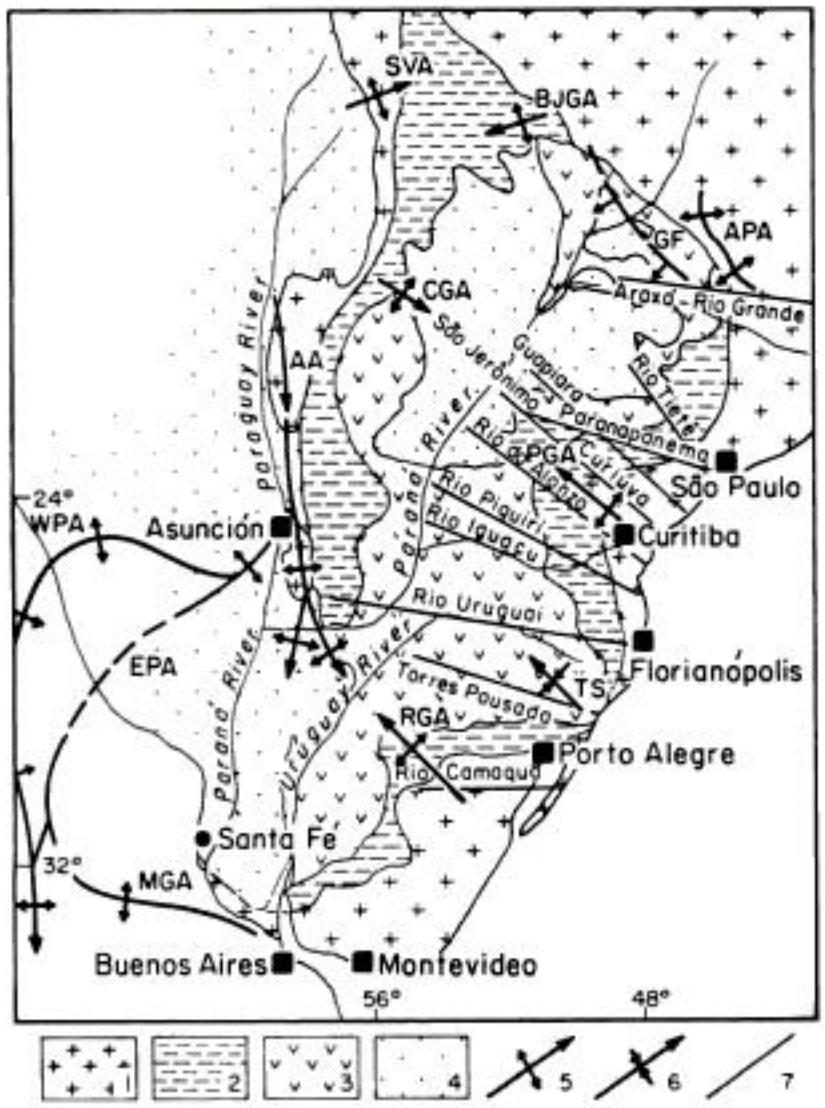

Figure 2 - Geological sketch map of the Paraná Basin (simplified after Melfi et al., 1988): 1. pre-Devonian crystalline basement; 2. pre-volcanic sediments (mainly Paleozoic); 3. flood volcanics of the Serra Geral Formation (Lower Cretaceous); 4. post-volcanic sediments (mainly Upper Cretaceous); 5. arch-type structure; 6. syncline-type lineament; 7. tectonic and/or magnetic lineament.

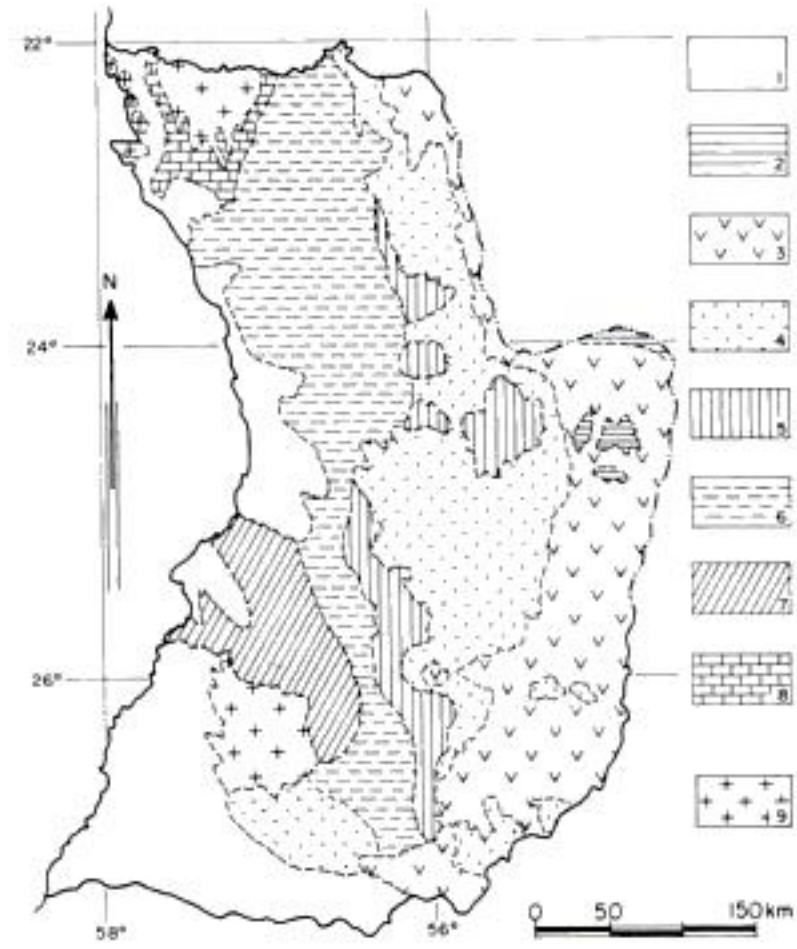

Figure 3 - Geological sketch map of Eastern Paraguay (simplified and modified after Proyecto PAR 83/005, 1986, and Occidental Company, 1987). Legends: 1. Tertiary-Quaternary (alluvial deposits); 2. Cretaceous (eolian sediments) - Acaray Formation; 3. Jurassic-Cretaceous (continental basalts) - Alto Paraná Formation; 4. Triassic-Jurassic (continental sediments) - Misiones Formation; 5. Permian (continental sediments) - Independencia Group; 6. Carboniferous (glacial sediments) - N.Aquidabán Group, S.Coronel Oviedo Formation; 7. Silurian (continental-marine sediments) - Caacupé and Itacurubí Groups; 8. Eocambrian (carbonate sediments) - Itapucumí Group; 9. Precambrian (ancient metamorphic basement and younger magmatic rocks) - N.Rio Apa Complex and San Luis Group, S.Rio Tebicuary Complex and Paso Pindó/Villa Florida Groups. For Tertiary-Cretaceous (Ñemby Formation) and Mesozoic (Sapucai Formation) alkaline occurrences see Fig. 5.

Paraguay Anticline (Putzer, 1962; Asunción Arch, cf. Northfleet et al., 1969, and Almeida, 1983) which also represents the western structural lineament associated with the Paraná Basin (Fig. 2). The west side comprises the Paraguayan part of the Gran Chaco, a vast aggrading alluvial plain, most of continental origin, consisting of unconsolidated clay and fine sand of Tertiary and Quaternary age.

In Eastern Paraguay, the outcropping rocks can be subdivided roughly into five major assemblages, depending on age and mode of origin. The oldest one comprises magmatic and metamorphic rocks of Precambrian age. They are exposed at the surface in few places, two major areas being recognized and corresponding to the structural highs of Apa, to the north, and Caapucú, to the south (Fig. 3). At the northern end, an old metamorphic basal complex is represented by gneisses, migmatites, granulites, amphibolites, meta-quartzites, meta-arkoses and pegmatitic intrusions (Wiens, 1982, 1986). Comte & Hasui (1971) reported minimum K/Ar ages of 1056 and 1250 Ma for amphibolites and pegmatites, respectively, occurring in the Apa river region, suggesting that these rocks may extend into Almeida's (1965) Guaporé Craton within Paraguayan territory. The basement sequence is overlain by the Upper Precambrian San Luis Group, consisting of metasedimentary and granitic rocks and also of acid volcanics (rhyolites) related to the Centurión Suite, which is a member of the San Luis Series (Wiens, 1986). To the south, older metamorphic rocks (quartzites, biotite schists, talc schists, granitic pegmatites

and aplites of the Rio Tebicuary Complex; Wiens, 1984) occur between the localities of Villa Florida and San Juan Bautista. Overlying the basement complex are gneisses, metasedimentary rocks and amphibolites belonging to the Paso Pindó and Villa Florida Groups (Wiens, 1984), which are correlated with the San Luis Series to the north. Younger igneous associations comprise granites and related granodiorites with small bodies of aplite and pegmatite, rhyolites (quartz porphyries) and rhyolitic dykes of the Caapucú Group (Wiens, 1984). K/Ar and $^{40}Ar/^{39}Ar$ age determinations (Comte & Hasui, 1971; Bitschene & Lippolt, 1986; Kanzler, 1987) for various rock-types from different localities (San Bernardino, Ypacaraí, Caapucú, Villa Florida) indicate that acid magmatism in the region is associated in time with the Brasiliano orogenic cycle (1000-450 Ma, Almeida & Hasui, 1984). For this magmatic event, Bitschene & Lippolt (1986) suggested a time span ranging from 573 up to 536 Ma.

The following subdivision consists of marine and continental sedimentary rocks varying in age from Cambrian to Upper Silurian (Early Devonian ?), with a taphrogenetic event of Ordovician age.

Cambrian (Upper Proterozoic to Early Cambrian; Zaire & Fairchild, 1985) exposures are limited to the northern portion of Paraguay, where they surround Precambrian rocks south of the Apa and east of the Paraguay river (Fig. 3). The outcropping rocks, which are about 300-400 m thick (Harrington, 1950), include limestones and dolostones with intercalations of claystone, sandstone, arkose and conglomerate of the Itapucumí Group. Following Almeida (1965), the Itapucumí rocks seem to correspond to the Cerradinho Formation at the base of the Corumbá Group, which represents the pelitic-carbonate sequence of the Paraguay-Araguai belt in the adjacent Brazilian state of South Mato Grosso.

Marine and continental Silurian sediments cover large area in central-southwestern of Eastern Paraguay (Fig. 3) and are subdivided into the major Caacupé and Itacurubí groups. The Caacupé Group (Harrington, 1950) is essentially made up of early Silurian (Upper Ordovician; Harrington, 1972) cross-bedded arkosic sandstones with a basal conglomerate and clay/shale intercalations. The environment is dominantly continental (fluvial), with a WNW-trending current drift (Bigarella & Comte, 1969). Deep exploratory drilling indicated a total thickness of approximately 300 m for this sequence (Wiens, 1982). It grades transitionally into the Itacurubí Group (Harrington, 1950), which is composed of fossiliferous marine sandstones, argillaceous sandstones and siltstones, the total thickness of which is estimated at 150 m (Wiens, 1982). According to Petri & Fúlfaro (1983), the occurrence of Silurian sediments in Eastern Paraguay is indicative of a marine transgression event, related to the Andean Geosyncline, which overflowed the area of the future Asunción Arch.

The third major subdivision is represented by sediments, mostly of continental origin, which range in age from Carboniferous to Cretaceous, and are associated with Mesozoic intrusive complexes and lava sequences. The Carboniferous formations, up to 670 m thick (Wiens, 1982), occupy two vast areas (Fig. 3) and comprise sandstones, tillites and varved shales, largely of glacial and fluvioglacial origin and unconformably rest on Silurian material. Following a suggestion by OEA (1975), PAR 83/005 (1986) have proposed the subdivision of the Carboniferous rocks into the Coronel Oviedo and Aquidabán Formations. The latter occurs mainly in northern Paraguay, and seems to correlate with the lower part of the Tubarão Group (Aquidauana Subgroup) in the Brazilian states of South Mato Grosso, Mato Grosso and Goiás.

Permian lacustrine, arkosic sandstones and argillaceous sandstones with interbedded silstones, up to 500 m thick, form the Independencia Group (Harrington, 1950; Putzer, 1962; Wiens, 1982), cropping out in two areas in the central region of Eastern Paraguay (Fig. 3). Palaeontological evidence points to a late Permian age and sedimentary features allow correlation of these formations with the Brazilian Passa Dois Group (Estrada Nova Formation and, possibly in part, with the Rio do Rastro Formation, according to Petri & Fúlfaro, 1983).

Triassic sediments mainly consist of massive, sometimes cross-bedded red sandstones with intercalations of red shale, all of continental origin (fluvial and/or desert environments). They are widespread through the eastern parts of Paraguay, the largest outcrop area being represented by an

almost continuous southward-trending band extending from the Apa to the Paraná rivers (Fig. 3). The thickness of the sequence can reach up to 320 m (Wiens, 1982). The sediments, included in the Misiones Formation (Harrington, 1950), are directly correlated with the Botucatu sandstones of southeastern Brazil (conforming to the Pirambóia and Botucatu Formations of Petri & Fúlfaro, 1983).

On the basis of preliminary K/Ar age determinations (Amaral et al., 1967; Comte & Hasui, 1971), the Triassic period in Paraguay appears to correspond to the onset of alkaline magmatic activity. Notably, the alkaline complex of Pão de Açúcar, mostly cropping out on the Brazilian side of the Paraguay river, just north of Porto Murtinho, Brazil (Fig. 5, see ahead), yielded, according to the latter authors, an Early Triassic age. It is noteworthy that this occurrence is the oldest known magmatic episode at the margins of the Paraná Basin.

Jurassic to Cretaceous rocks are represented by the stratoid tholeiitic volcanics of the Serra Geral Formation, by alkaline complexes, and also by sediments of the Acaray Formation (Fig. 3).

In Eastern Paraguay, lava flows of the Alto Paraná Formation cover an area of about 40,000 km^2 and constitute the westerly fringe of the great basalt field of the Paraná Basin (Bellieni et al., 1986). The thickness of the whole sequence exceeds 360 m, and it is possible to distinguish more than twenty different flows. Sills are widespread but outcropping dykes are less common. Radiometric determinations gave K/Ar ages of 127 Ma and 130 Ma (Comte & Hasui, 1971, and Bitschene, 1987, respectively).

Alkaline rocks of the Sapucai Formation (Palmieri & Velázquez, 1982) include intrusive and extrusive rock-types, mainly occurring as small stocks, plugs, volcanic domes, dykes and lava flows, are located in northeastern and central-eastern Paraguay. Older data (Comte & Hasui, 1971; Palmieri, 1973; Palmieri & Arribas, 1975) indicated K/Ar ages ranging from 180 to 100 Ma.

The Acaray Formation is composed of cross-bedded aeolian sandstones up to 100 m thick. These sediments, covering small areas, are restricted to the eastern boundaries of Paraguay and extend far into Brazil. They probably correspond to the Brazilian Caiuá Formation, at the base of the Bauru Group, and unconformably rest on the Serra Geral basalts (Soares et al., 1980).

The fourth major subdivision is essentially made up of small plugs, flows and dykes of nephelinites, and subordinately of ankaratrites (Ñemby Formation, Palmieri & Velázquez, 1982), cropping out in the neighborhood of Asunción. They usually bear variable amounts of crustal (sedimentary, metamorphic and volcanic rock-types) and mantle (spinel peridotite) xenoliths, and yielded K/Ar ages from 61 up to 39 Ma (Comte & Hasui, 1971; Stormer et al., 1975; Bitschene, 1987; Comin-Chiaramonti et al., 1991c).

The final subdivision includes recent sediments of Tertiary and Quaternary age essentially occurring as alluvial deposits. In general they are made up of unconsolidated clay, silt and fine sand, and are widespread in all terranes along the broad, nearly level valleys of the major streams, e.g. the Paraguay river.

TECTONIC FEATURES

The major structural feature of Paraguay is a northward-trending, anticlinal flexure parallel to and only a short distance east of the Paraguay river, which separates the two great syneclises of the Gran Chaco of Paraguay, Bolivia and Argentina to the west, and the Paraná of southern Brazil to the east. Available data indicate that the western limb of the anticline is much steeper than the eastern one (Eckel, 1959). Sedimentary rocks and overlying Serra Geral basalts on the eastern limb dip generally at angles of 2-3 E-NE toward the centre of the basin (Harrington, 1950; DeGraff et al., 1981). The anticlinal crest (Central Paraguay Anticline or Asunción Arch) is thought to have been in evidence since early Palaeozoic time. In Upper Jurassic this structure was subjected to intense reactivation, which produced chiefly N and NW-trending faults and associated magmatic activity of tholeiitic and alkaline affinities (Almeida, 1983). However, the existence of a continuous, NS-trending structure is still a matter of controversy. An alternative interpretation by Thomas (1976) proposed a more complex model consisting of two NW-trending

anticlines (Asunción and Apa, to the north), a synclinal unit (San Pedro), also NW-trendind and lying between the antiforms, and abundant faults and minor fractures (Fig. 4). NW-SE structures in Eastern Paraguay are ubiquitous as evidenced from faults, lineaments and dykes (Druecker & Gay, 1987; Gomes et al., 1989).

Another important tectonic direction in Eastern Paraguay is represented by NE-SW alignments, essentially reflecting Precambrian structural features reactivated in the Mesozoic (Petri & Fúlfaro, 1983). Some NE-trending lineaments shown in Figure 4 include the prominent anticlinal structures of Ponta Porã, Capitán Bado, Igatimí and Caaguazú.

Wiens (1982) drew attention to two additional structural directions, N-S and E-W, both reflecting control by old Precambrian lineaments, while the latter may be associated with some local intrusions of basic and ultra-basic bodies.

Aeromagnetic, ground magnetic and gravimetric surveys and interpretation of Landsat images indicate that the western edge of the Paraná Basin in Paraguay experienced NE-SW crustal extension during late Mesozoic time (DeGraff et al., 1981; DeGraff, 1985; Mariano & Druecker, 1985; Druecker & Gay, 1987; Livieres & Quade, 1987). This extensional tectonic regime, genetically related to the continental breakup of the Western Gondwana-land and associated with the opening of the South Atlantic, is responsible for the generation of NW-SE- trending structures which have arches (e.g. Ponta Grossa, Fig. 2, extending over Brazilian territory for about 600 km), faults and lineaments as their most impressive geologic expressions. According to Fúlfaro et al. (1982), the formation of the NW arches started in the Devonian but reached its maximum development in Triassic-Jurassic time. Major zones of normal faulting in Eastern Paraguay trend north- westerly, on average, and at least two NW-trending zones of tectonic subsidence are recognized (DeGraff, 1985). The complex graben structure in the Asunción-Sapucai region (Ypacaraí valley), 25-40 km wide and 200 km long, filled by up to 2,500 m of sedimentary rocks, is the most important of these rifting zones and is the site of intense magmatic activity of alkaline affinity.

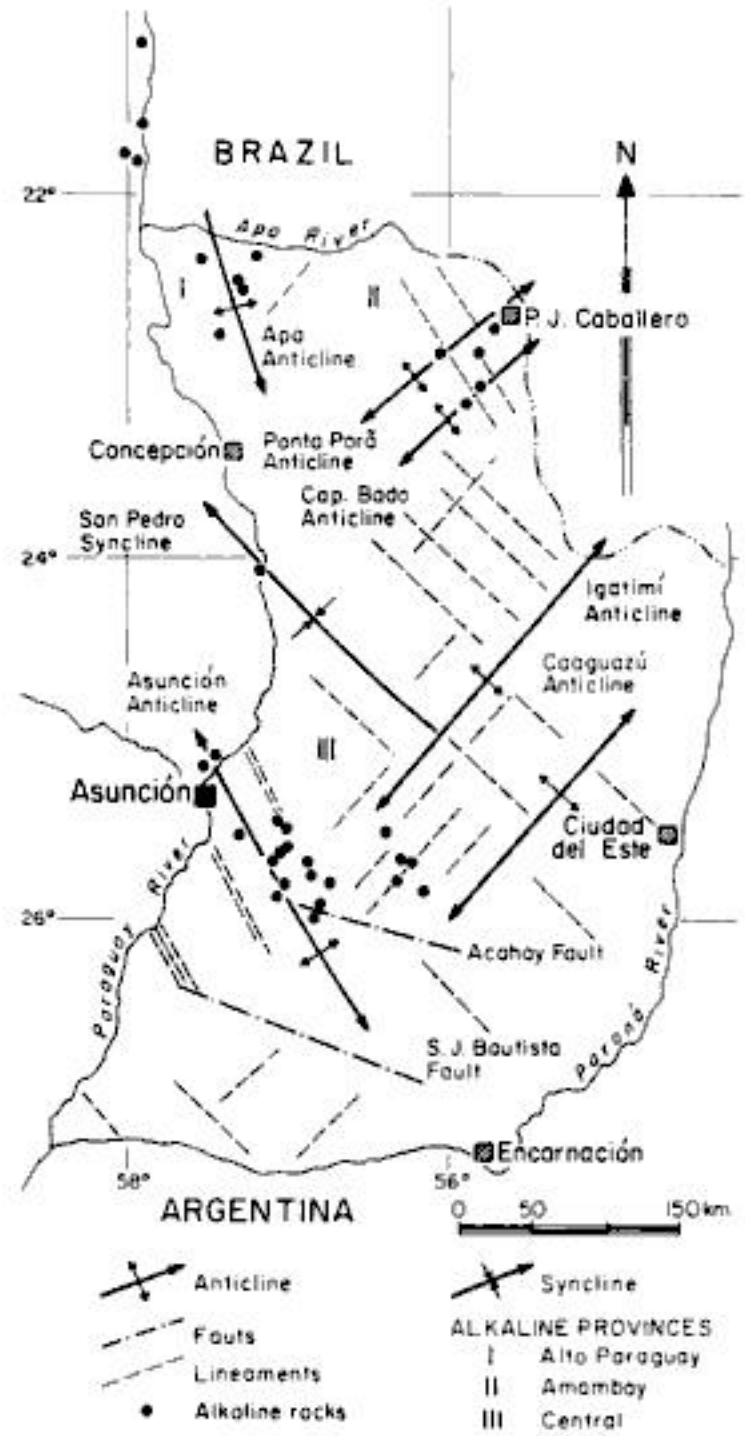

Figure 4 - Geographical distribution and tectonic setting of alkaline rocks of Paraguay (Livieres & Quade, 1987).

ALKALINE MAGMATISM

Alkaline rocks in Paraguayan territory have been known for a long time, but, in general, only a few occurrences have been as yet investigated in detail. Thus, for most cases, only preliminary data, chiefly based on petrographic descriptions of some rock-types, are available at present. However, several theses, submitted to various universities (Palmieri, 1973; Bitschene, 1987; De Vito, 1987; De Min, 1988; Gallo, 1988; Marzoli, 1991; Velázquez, 1992) are also available.

General distribution

Alkaline rocks can be found concentrated in three major regions of Paraguay: northern, northeastern and central-eastern. Regarding its stratigraphy, all have been included in the Sapucai Formation of Cretaceous age by Palmieri &

Velázquez (1982). Recently, a new outcrop area has been discovered at the most southerly tip of the country, near the localities of San Juan Bautista and San Ignacio (Comin-Chiaramonti et al., 1992c).

The first attempt to address the Paraguayan rocks as a whole was made by Almeida (1983) who distinguished central and northern geographical concentrations, both tectonically related to the Asunción Arch. Livieres & Quade (1987), on the basis of petrological and chemical characteristics, geographical distribution and tectonic association, proposed grouping the 32 alkaline occurrences then known into the three provinces of Alto Paraguay, Amambay and Central (Fig. 4). Excluding the new bodies to the south, this classification can be directly correlated with the geographical distribution shown in Figure 5; thus, for convenience, the Livieres & Quade's (1987) terminology will be adopted here.

Alto Paraguay Province

Alkaline rocks occurring in this province are tectonically linked with the NW-SE-trending antiform structure of Apa (Livieres & Quade, 1987). In general, they lie between latitudes 21°04' and 22°22'S and longitudes 57°20' and 58°03'W, being the largest exposures found along the two major rivers draining the region, the Paraguay and Apa (Fig. 5). A total of seven occurrences is listed by these authors: San Carlos (22°14'S, 57°21'W), Buena Vista (22°21'S, 57°27'W), Santa Maria (22°42'S, 57°31'W) and Centurión (22°42'S, 57°31'W) in Eastern Paraguay; Fuerte Olimpo (21°05'S, 57°54'W), Cerro Boggiani (21°34'S, 58°00'W) and Puerto Guaraní (21°32'S, 58°02'W) in the Chaco Basin. The small bodies near Puerto Guaraní (Tres Hermanos hills, Carnier, 1913) may indeed represent the continuation of the Brazilian complex of Pão de Açúcar (Eckel, 1959; Livieres & Quade, 1987).

The geology of these complexes is poorly known. Scarce data deal with petrographic descriptions of samples collected during geologic expeditions carried out at or before the end of the last century and the beginning of the present one (DuGraty, 1865; Pöhlmann, 1886; Evans, 1894; Lisboa, 1909; Carnier, 1911, 1913; Goldschlag, 1913; Willmann, 1915). Additional information comes from regional geological investigations by a few researchers in the Apa river area and on the banks of the Paraguay river (Eckel, 1959; Putzer, 1962; Putzer & van den Boom, 1962; OEA, 1975; Hutchinson, 1979, 1980; Wiens, 1986).

As a result of earlier studies, dykes of phonolite and porphyritic syenite have been identified in the vicinity of the Apa river, 2-3 km SW of the village of Centurión, intruding muscovite schists and quartzites (Carnier, 1911; Goldschlag, 1913). Pöhlmann (1886) described dykes of nepheline basalt associated with limestones at the locality of Colonia Santa María del Apa.

Regarding the occurrences of the Paraguay river, only a few comments are available on the presence of porphyritic dykes at Fuerte Olimpo (DuGraty, 1865; Carnier, 1913) and of syenitic rocks at Puerto Guaraní (Carnier, 1913).

Dominantly lying on the Brazilian side of the Paraguay river, just north of Porto Murtinho, Brazil, Pão de Açúcar (occasionally also referred to as Fecho dos Morros) represents the most prominent alkaline complex in the area. This is included here because small bodies of rock that seem to be related to it occur in Paraguay. The intrusion, reaching about 5 km of diameter, rises abruptly from the river's edge and is described as made up principally of nepheline syenites (foyaites) with lesser amounts of fine-grained rocks, black phonolites and "bostonites" displaying fluidal and trachytic textures, respectively (Lisboa, 1909; Carnier, 1911, 1913; Eckel, 1959).

More recent literature on the Alto Paraguay occurrences includes papers by Putzer (1962), Putzer & van den Boom (1962) and Wiens (1986) as well as the articles of OEA (1975) and Hutchinson (1979), focussing on the Buena Vista and San Carlos bodies, respectively. Related to both occurrences, Wiens (1986) described the presence of aphanitic and porphyritic rocks near Fuerte San Carlos, showing occasionally fluidal structure and ranging in composition from trachytes to phonolites; they form dykes intruded into Precambrian rocks. In Buena Vista, he reported the occurrence of trachytic-phonolitic rocks associated with metasediments of the San Luis Group. On the basis of petrographic evidence, the country rocks (meta-sandstones) are

considered to have been affected by fenitization. Putzer & van den Boom (1962) provided petrographic data and chemical analyses for rocks from the Cerro Boggiani and Puerto Guaraní intrusions. For the latter, two outcrop areas occur, a low hill at the western margin of the Paraguay river and a small island. Cerro Boggiani consists of two small hills, 80-100 m high, lying a short distance from the mouth of the Boggiani stream. Both Cerro Boggiani and Puerto Guaraní include saturated to undersaturated syenites as their main rock-types as well as tinguaites. However, at Cerro Boggiani the syenitic rocks appear to be slightly richer in feldspathoids (sodalite and lesser nepheline).

During the second semester of 1992, after this article had been written, our team conducted two expeditions to the area, work being concentrated on the alkaline occurrences lying along the Paraguay river. The data currently available indicate the necessity of an additional review of the Alto Paraguay Province, which will be undertaken in a farther paper.

Amambay Province

In the northeastern sector of Paraguay, alkaline rocks are distributed over an area about 140 km long and 70 km wide, having the Apa river and the Brazilian border as northern and eastern limits; its other boundaries roughly corresponding to the parallel 23°30'S and the meridian 56°20'W. As emphasized by Livieres & Quade (1987), the emplacement of the intrusions is tectonically controlled by NE-trending structures, the Ponta Porã and Capitán Bado antiforms (Fig. 4). As also shown on Landsat images, the Ponta Porã structure is the most conspicuous linear feature in the area, extending over a long distance: from the Paraguay river, in the SW, to the city of Pedro Juan Caballero, near the Brazilian border. On the basis of aeromagnatic maps, Hales (1980) distinguished major NW-trending fracture zones, which appear to have played a role in the geological setting of the alkaline complexes.

Although still insufficient, the recent literature available on the Amambay Province, is considerably more than on Alto Paraguay Province. At least five occurrences are known (Livieres & Quade, 1987): Cerro Chiriguelo (22°37'S, 55°57'W), Cerro Sarambí (22°45'S, 56°14'W; which also includes two small bodies, Cerro Apuá and Cerro Peró), Cerro Guazú (23°05'S, 56°02'W), Cerro Tayay (23°00'S, 55°53'W) and Ypané (22°48'S, 55°54'W). The first two complexes are clearly associated with the Ponta Porã antiform; while the Cerro Guazú and Tayay intrusions seem to be controlled by the Capitán Bado structure; Ypané lies between both antiforms. In the Amambay Province, alkaline rocks occur as annular complexes, stocks, dykes, and also as ring and radial dykes. In spite of the small number of occurrences, the geological knowledge available of these rocks is not, however, uniform. For economical reasons, since their rock associations are bearing carbonatites, Cerro Chiriguelo and Cerro Sarambí have been more intensively investigated and, additionally, submitted to a drilling programme (Grossi-Sad, 1972) and geophysical surveys (Druecker, 1981).

The Cerro Chiriguelo (Cerro Corá, Pedro Juan Caballero) complex is intruded into Precambrian metasediments and forms an approximately circular structure about 7.5 km in diameter. The surrounding ridges of country rocks are strongly updomed on the west, northwest and northern rims, but the southern and eastern rims are covered by late Paraná basalt flows (Haggerty & Mariano, 1983). According to Censi et al. (1989), the complex is made up of carbonatites, breccias with abundant xenoliths of Precambrian basement and massive fenites, which partially surround the brecciated area. The main carbonatite body is a sövite of elliptical shape trending NE-SW and about 600 x 300 m, cropping out at the centre of the intrusion. Alvikites, ferrocarbonatites and fenitic dykes are scattered over the whole area. At least three stages of carbonatitic rocks are distinguished: C1, sövite; C2, alvikite; C3, ferrocarbonatite. A C4 stage is proposed on the basis of late formation of barite, quartz and uranium minerals. Magmatic rocks associated with the carbonatites are fenitic trachytes with strong potassic affinities.

Other contributions to the better geological knowledge of the complex are those of Grossi-Sad (1972), Berbert & Triguis (1973), OEA (1975), Mariano (1978), Druecker (1981), Premoli & Velázquez (1981), Almeida (1983), Eby & Mariano (1986) and Livieres & Quade (1986). Mariano (1978) reported the occurrence

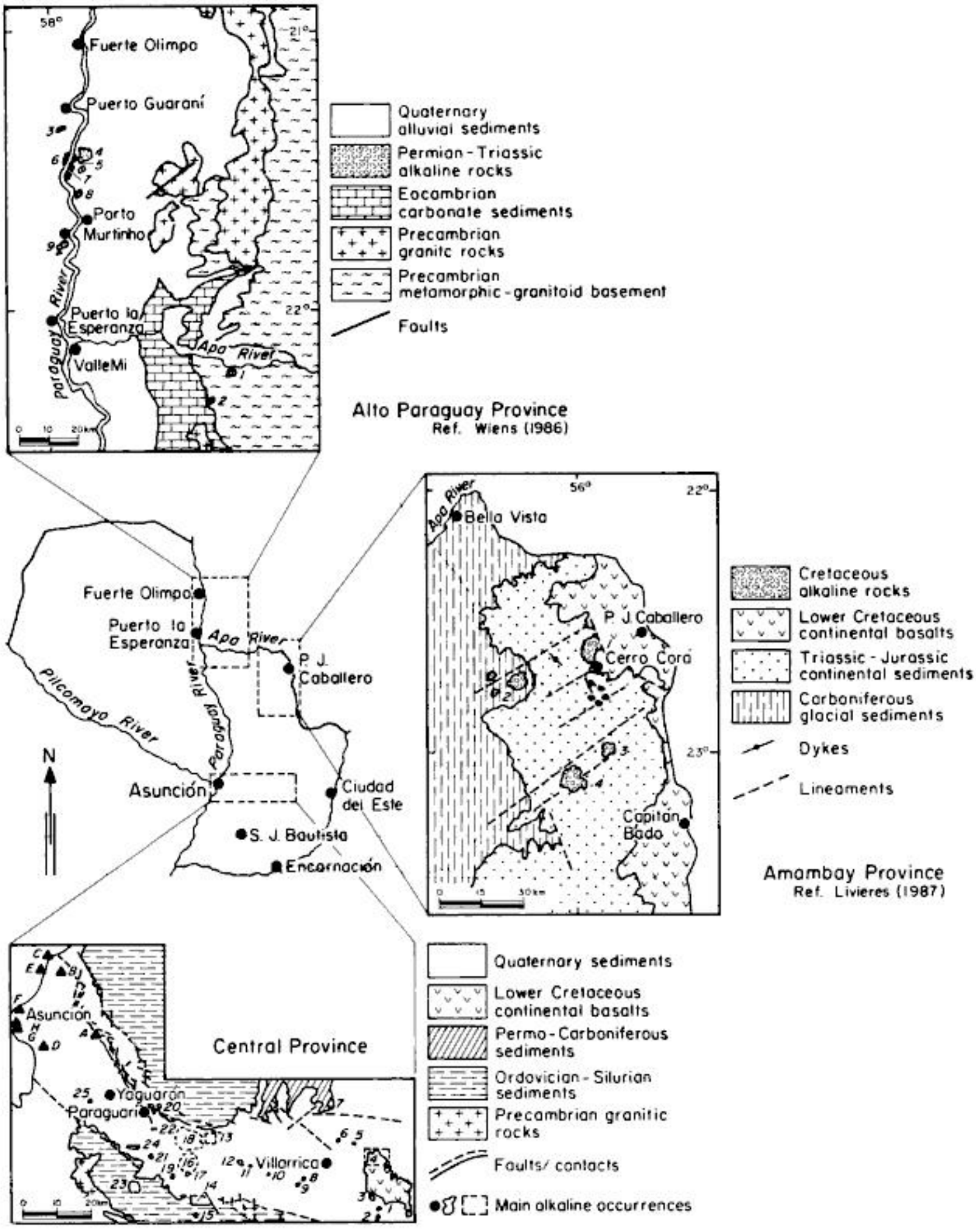

Figure 5 - Locality map of alkaline occurrences in Paraguay. *Alto Paraguay Province*: 1. San Carlos; 2. Buena Vista; 3. Cerro Boggiani; 4. Pão de Açúcar; 5. Ilha Fecho dos Morros; 6. Cerrito; 7. Porto Conceição; 8. Pedreira; 9. Cerro Siete Cabezas. *Amambay Province*: 1. Cerro Chiriguelo; 2. Cerro Sarambí; 3. Cerro Guazú; 4. Cerro Tayay. *Central Province*: 1. Cerro Km 23; 2. Cerro San Benito; 3. Cerro E Santa Helena; 4. Northwestern Ybytyruzú; 5. Cerro Capiitindy; 6. Mbocayaty; 7. Aguapety Portón; 8. Cerro Itapé; 9. Cerrito Itapé; 10. Colonia Vega; 11. Cañada; 12. Cerro Chobí; 13. Cerro Yaguarú; 14. Cerro Achón area; 15. Cerro San José; 16. Potrero Ybaté; 17. Cerro Medina; 18. Sapucai; 19. Cerro Gimenez; 20. Cerro Santo Tomás; 21. Cerro Yarigua-á; 22. Cerro Porteño; 23. Cerro Acahay; 24. Cerro Ybypyté; 25. Cerro Arrúa-í; A. Cerro Patiño; B. Limpio; C. Cerro Verde; D. Ñemby; E. Cerro Confuso; F. Nueva Tablada; G. Lambaré; H. Tacumbú.

of a "trachyte porphyry" dyke at Arroyo Gasory, about 15 km WSW of Cerro Chiriguelo.

The Cerro Sarambí complex is a near circular structure, about 7 km in diameter, emplaced into Precambrian metamorphic rocks which are domed and surrounded by Silurian and Permo-Carboniferous sedimentary rocks (Mariano, 1978; Haggerty & Mariano, 1983; Mariano & Druecker, 1985). It is composed mainly of an inner pyroxenite-syenite body that is transected by trachyte and phonolite dykes as well as very thin sövite veins. These probably emanate from a larger carbonatite core which is presumed to occur in the centre of the intrusion (Mariano, 1978). Fenites showing well developed flow structures occur as radial dykes cutting the up-domed country rock ridges in the southern rim of the complex. Some additional information on the complex can be found in Palmieri et al. (1974), Sanders (1981) and Almeida (1983). Mariano (1978) also noticed the existence of "trachyte porphyry" dykes at Cerro Peró and Cerro Apuá adjacent to Cerro Sarambí.

Cerro Guazú is described as a stock of shonkinite surrounded by strongly silicified sandstones, and with a radial swarm of lamprophyre dykes (OEA, 1975; Mariano, 1978; Druecker, 1981). Carbonatite has not been found yet, but it is suspected to occur at depth on the basis of geophysical evidence and geochemical anomalies for REE, Nb, Sr and Ba (Mariano, 1978).

Unfortunately, little information exists for Cerro Tayay and Ypané. Livieres & Quade (1987) have referred to the former as a morphological feature conical in shape, with a radial structure and made up of ultramafic (?) rocks; for Ypané the reference mentions only its semicircular structure and the presence of alkaline rocks.

Central Province

The highest concentration of alkaline rocks in the country is found in the Central Province. Livieres & Quade (1987) listed a total of 20 different bodies over central-eastern Paraguay. However, on the basis of recent work, that number has increased. Excluding dykes, it reachs now at least 30 distinct occurrences (Fig. 5).

The rocks mainly occur associated with the rift zone between Asunción and Villarrica, an extensional NW-SE tectonic structure about 200 km long and 25-40 km wide the basement of which subsided at least 2 km relative to the adjacent area (DeGraff, 1985). They form stocks, plugs, lava flows, ring complexes and dyke swarms in the central portion of the region, cutting Silurian sandstones of the Caacupé Group. In the eastern part of the outcrop area however, the country rocks are Triassic sandstones of the Misiones Formation, and occasionally Carboniferous sediments of the Coronel Oviedo Formation. Furthermore, the alkaline rocks are tectonically related to the NE-trending antiform structures of Igatimí and Caagazú, to the WNW-ESE faulting zone of Acahay and can be found at the intersection of these and other linear features.

Sapucai, Potrero Ybaté and Cerro Acahay seem to constitute the largest Mesozoic alkaline occurrences found in central-eastern Paraguay. Recently, they have been the object of numerous investigations which also provided information on other associated bodies. However, of great importance in the Sapucai region is the presence of a dyke swarm, mainly NW-SE-trending, of at least 200 intrusions, 0.5 to 20 m thick, and composed of several rock-types. A systematic study of these rocks was made by Gomes et al. (1989) and Comin-Chiaramonti et al. (1990a, 1991d, 1992b). Tertiary rocks from the Asunción area are represented by at least eight different bodies, forming plugs, lava flows and dykes (Bitschene, 1987; Comin-Chiaramonti et al., 1991c).

Mesozoic alkaline rocks of the Central Province are variable in texture and composition. Intrusive types show dominantly alkali gabbroic to syenodioritic or theralitic to essexitic affinities; volcanic material is represented by two different sequences, a) tephrite-phono-tephrites to phonolites and peralkaline phonolites and b) alkali basalts to trachyandesites and trachytes or trachyphonolites. The Tertiary bodies mainly consist of nephelinitic and ankaratritic rocks.

In contrast to the other two provinces, the literature on this province, particularly the most recent, is extensive and focusses on various aspects of these rocks. Therefore individual descriptions are more conveniently given in the Appendix.

As already mentioned, alkaline rocks have recently been found in the San Juan Bautista re-

gion at the southern extremity of Paraguay (Comin-Chiaramonti et al., 1992c). They form the small plugs of Cerro Caá Jhovy (26°43.2'S, 57°18.3'W) and Estancia Guavira-y (26°57.7'S, 57°06.7'W), but at Estancia Ramirez (26°56.5'S, 57°10.0'W) is a NW-trending dyke possibly associated with the latter. The rock-types include K-peralkaline phonolite in Cerro Caá Jhovy and Na-nephelinites in Estancia Guavira-y and Estancia Ramirez; in Estancia Guavira-y the host nephelinites also bear mantle xenoliths. The country rocks are Triassic sandstones of the Misiones Formation.

Rock associations

Petrographic descriptions of Paraguayan alkaline rocks are still generally inadequate. For the Alto Paraguay Province in particular, information on samples comes principally from older studies, with few new data being available. As a result, instead of trying to define classification scheme for those rocks, it seems more reasonable to tentatively group them according to the rock associations outlined by Ulbrich & Gomes (1981) for the comparable Brazilian material.

For the Alto Paraguay Province, a type I association is suggested on the basis of the occurrence of undersaturated to saturated syenites and their corresponding fine-grained varieties, tinguaites and phonolites.

Carbonatites are found in the Cerro Chiriguelo and Cerro Sarambí complexes, but, according to Mariano (1978), they also occur at Cerro Guazú. At Cerro Sarambí they are associated with ultramafic (pyroxenite) and syenitic (trachytic) rocks. Thus, a type III association is clearly indicated for the Amambay Province intrusions.

As previously mentioned, the Mesozoic complexes of the Central Province show great variation in mineralogy and petrography, but, in general, they may be placed into two suites. The first one includes intrusive rock-types having dominantly alkali gabbroic to syenodioritic or theralitic to essexitic compositions. It is slightly to strongly undersaturated, the intrusions of Aguapety Portón, Cerro Acahay, Cerro Arrúa-í and Cerro San José being typical examples. In a few cases (e.g. Cerro Acahay, small dykes and veins; Cerro Chobí) syenitic rocks can also be found.

The second suite is made up of volcanic material. Two lineages - tephrite-phonotephrite to phonolite and peralkaline phonolite; alkali basalt to trachyandesite and trachyte or trachyphonolite - are distinguished. In some complexes, e.g. Cerro Acahay and Sapucai, intrusive and extrusive suites are present. The intrusive rocks point to a type IV association, whereas the volcanic ones to a type V. The ultra-alkaline and strongly undersaturated rocks (nephelinites and, subordinately, ankaratrites) cropping out in the neighbourhood of Asunción could be tentatively considered as representative of the type VII association in Paraguay.

Radiometric ages

The first geochronological study of Paraguayan alkaline rocks is due to Comte & Hasui (1971), following extensive researches carried out by Amaral et al. (1967) and others (see Ulbrich & Gomes, 1981, for references) on Brazilian formations. Other important contributions are those by Palmieri & Arribas (1975) and Bitschene (1987), the former dealing specifically with the Sapucai rocks and the latter focussing on several occurrences of central-eastern Paraguay. In all cases only K/Ar ages were obtained. In addition to some K/Ar data, Eby & Mariano (1986) also provided fission-track ages for a few intrusions of the Amambay Province. However, a more systematic investigation of rocks belonging to the Central Province has been recently conducted by Velázquez et al. (1990b, 1992) and Velázquez (1992) using K/Ar and Rb/Sr methods. Fission-track ages were also made available by Green et al. (1991a,b) for Cerro Acahay and Cerro Santo Tomás rocks.

K/Ar results of Paraguayan rocks are plotted in Figure 6, which shows histograms for individual intrusions and the cumulative distribution of the data. Data range from Triassic up to Oligocene (Table 1).

The oldest age relates to the Pão de Açúcar complex, mostly occurring on the Brazilian side of the Paraguay river. New data available for this occurrence and farther rocks of the Alto Paraguay Province are given in other section of the volume.

The second age group clusters around 120-140 Ma, and correlates well with the chronogroup of 133 Ma defined by Ulbrich et al.

You have either reached a page that is unavailable for viewing or reached your viewing limit for this book.

Table 1 - K/Ar results for samples from the Alto Paraguay, Amambay and Central Provinces.

	Locality	Rock-type	Material	K %	^{40}Ar Rad. (10^{-6} cSTP/g)	Ar atm. %	Age (Ma)	Refer.
			Alto Paraguay Province					
1	Pão de Açúcar	NS	Bi	7.46	75.96	3.10	244.6	1
2	Pão de Açúcar	NS	Bi	7.54	75.60	3.80	241.7	1
3	Pão de Açúcar	NS	AF	5.71	49.75	11.20	211.3	1
4	Pão de Açúcar	NS	AF	5.68	40.07	12.00	209.6	1
5	Pão de Açúcar	P	WR	4.72	41.70	7.00	214.1±13.3	3
6	Cerro Chiriguelo	MDi	Bi	6.95	41.30	10.30	146.7±9.2	3
7	Cerro Chiriguelo	MDi	WR	7.11	39.90	13.70	138.9±9.2	3
			Amambay Province					
8	Cerro Chiriguelo	Sc	Bi				130±5	*
9	Arroyo Gasory	Tr	WR				137±7	*
10	Arroyo Gasory	Tr	Bi				145±8	*
11	Cerro Guazú	L	Bi				119±4	*
12	Arroyo Blanco	Sh	Bi				117±4	*
			Central Province					
13	Cerro Km 23	Th	Bi	7.68	40.84	16.90	131.9±5.0	7
14	Cerro Km 23	Th	WR	6.43	29.90	10.20	115.8±4.2	7
15	Ybytyruzú (C.Acatí)	Tp	Bi	7.71	39.07	11.90	125.9±4.6	7
16	Ybytyruzú (S. Boni)	La	Bi	8.16	40.91	6.90	124.6±4.2	7
17	Ybytyruzú (C.Itatí)	Pte	Bi	7.17	37.20	9.20	128.8±4.6	7
18	Mbocayaty	NSd	AF	9.17	47.97	8.86	130.0±3.4	8
19	Mbocayaty	NSd	Bi	6.63	34.45	25.94	129.2±6.8	8
20	Mbocayaty	E	Bi	7.87	40.65	6.80	128.2±4.5	7
21	Aguapety Portón	Ma	WR	2.50	13.94	15.90	138.1±4.8	7
22	Aguapety Portón	E	Bi	7.54	40.38	23.60	132.9±5.5	7
23	Potrero Ybaté	NSd	AF	5.97	30.68	9.76	127.8±5.6	8
24	Sapucai	E	WR	7.79	41.16	17.50	131.0±8.2	5
25	Sapucai	P	WR	5.42	29.86	3.70	136.4±5.1	5
26	Sapucai	Ba	WR	3.42	16.34	19.50	119.6±7.2	5
27	Sapucai	E	WR	3.82	15.35	28.30	100.0±10.0	4
28	Sapucai	Te	WR	5.57	24.17	26.10	108.3±10.2	5
29	Sapucai	AB	WR	4.03	16.12	29.80	98.0±5.0	4
30	Sapucai	AB	WR	3.97	21.00	14.50	131.2±5.1	5
31	Sapucai	Tb	WR	4.75	20.15	104.70	122.0±4.0	9
32	Sapucai	Pte	WR	4.65	19.93	70.56	119.0±4.0	9
33	Sapucai	P	WR	6.18	29.99	95.90	121.0±4.0	9
34	Sapucai	Sg	WR	3.77	18.02	82.20	119.0±4.0	9
35	Sapucai	Te	WR	3.87	18.36	92.80	118.0±4.0	9
36	Sapucai	Pte	WR	4.13	19.70	97.50	119.0±4.0	9
37	Sapucai	Te	WR	4.13	10.78	93.40	66.0±2.0	9
38	Sapucai	Te	WR	1.92	2.47	90.10	32.8±0.9	9

Table 1 (conclusion).

	Locality	Rock-type	Material	K %	^{40}Ar Rad. (10^{-6} cSTP/g)	Ar atm. %	Age (Ma)	Refer.
			Central Province					
39	Cerro Gimenez	P	WR	4.44	11.58	21.18	66.0±4.6	8
40	Cerro Santo Tomás	Sg	Bi	8.05	40.84	7.50	126.0±4.5	7
41	Cerro Santo Tomás	Sg	C	4.63	25.57	8.20	136.8±5.0	7
42	Cerro Santo Tomás	E	WR	2.80	15.44	47.00	136.5±10.2	5
43	Cerro Santo Tomás	Te	Bi	8.48	44.46	12.40	130.1±4.8	7
44	Cerro Santo Tomás	Te	Bi	8.31	42.79	10.70	127.9±4.8	7
45	Cerro Santo Tomás	Di	Bi	7.25	38.60	45.80	132.0±11.5	3
46	Cerro Acahay	Tb	WR	3.33	21.52	99.40	118.0±4.0	9
47	Estancia las Rosas	Ta	WR	2.71	13.62	11.05	124.8±3.4	10
48	Cerro Arruá-í	NSd	Bi	5.44	28.90	48.19	132.3±8.4	8
49	Cerro Patiño	A	WR	0.86	1.31	43.2	38.8±2.3	6
50	Limpio	Ne	WR	1.09	2.15	14.7	50.2±1.9	6
51	Cerro Verde	A	WR	0.83	1.86	22.0	57.0±2.3	6
52	Villa Hayes	A	WR	1.30	2.99	18.0	58.4±2.2	6
53	Ñemby	Ne	WR	1.58	2.84	23.2	45.7±1.8	6
54	Remanso Castillo	Ne	WR	1.16	1.85	26.3	40.6±1.6	6
55	Cerro Confuso	P	WR	4.97	1.08	20.7	55.3±2.1	6
56	Cerro Confuso	P	WR	1.42	3.42	41.1	60.9±4.4	6
57	Cerro Confuso	P	WR	1.97	4.61	29.1	59.3±2.4	6
58	Nueva Tablada	Ne	WR	1.26	2.29	32.7	46.3±2.0	6
59	Nueva Tablada	Ne	WR	1.28	2.86	26.2	56.7±2.3	6
60	Lambaré	Ne	WR	1.09	2.09	32.7	48.9±2.2	6
61	Lambaré	Ne	WR	1.09	1.88	25.9	48.9±2.0	6
62	Tacumbú	B	WR	1.04	1.95	82.0	46.0±7.0	2
63	Tacumbú	Ne	WR	1.50	2.43	30.9	41.3±1.8	6

Abbreviations: 1) Material: AF, alkali feldspar; Bi, biotite; C, felsic concentrate; WR, whole-rock. 2) Rock-types: A, ankaratrite; AB, alkali basalt; B, basalt; Ba, basanite; Di, diorite; E, essexite; L, lamprophyre; La, latite; Ma, malignite; MDi, microdiorite; Ne, nephelinite; NS, nepheline syenite; NSd, nepheline syenodiorite; P, phonolite; Pte, phonotephrite; Sc, silico-carbonatite; Sg, syenogabbro; Sh, shonkinite; Ta, trachyandesite; Tb, trachybasalt; Te, tephrite; Th, theralite; Tp, trachyphonolite; Tr, trachyte.

References: 1. Amaral et al. (1967), Sonoki & Garda (1988); 2. Conte & Hasui (1971); 3. Conte & Hasui (1971), Sonoki & Garda (1988); 4. Palmieri & Arribas (1975); 5. Palmieri & Arribas (1975), Sonoki & Garda (1988); 6. Bitschene (1987); 7. Bitschene (1987), Sonoki & Garda (1988); 8. Velázquez et al. (1990b), Velázquez (1992); 9. and 10. G.Capaldi and V.F.Velázquez, respectively (unpublished data); *, ages reported by Mariano (1978) and Eby & Mariano (1986).

Also according to Mariano (1978), the above analyses 6 and 7 were actually made on rocks (trachyte porphyry dyke) cropping out at the Arroyo Gasory, approximately 15 km WSW of Cerro Chiriguelo (Cerro Corá).

(1990) for some Brazilian rocks. Most of its representatives are found in the Central Province in association with the rift-graben structure of Asunción-Sapucai, but this set also includes rocks of the Amambay Province (Cerro Chiriguelo, Arroyo Gasory, Cerro Guazú, Arroyo Blanco) at northeastern Paraguay. The spread of ages registered for the Central Province intrusions could be a result of analytical errors or, as also suggested by Velázquez (1992), could be due to the rifting geodynamic which led to different stages of activation.

After an apparent hiatus, alkaline magmatism in Paraguay resumed during late Cretaceous to Tertiary times as evidenced by the existence of scarce Na-rich phonolitic plugs (e.g. Cerro

You have either reached a page that is unavailable for viewing or reached your viewing limit for this book.

You have either reached a page that is unavailable for viewing or reached your viewing limit for this book.

You have either reached a page that is unavailable for viewing or reached your viewing limit for this book.

straints to mantle metaso-matism. In: E.M. Piccirillo & A.J. Melfi (eds.) The Mesozoic flood volcanism on the Paraná Basin: petrogenetic and geophysical aspects. IAG-USP, São Paulo, p.207-227.

DERBY, O.A. (1887) On nepheline rocks in Brazil. Quart. J. Geol. Soc., *43*:457-473.

DERBY, O.A. (1898) A study on consanguinity on eruptive rocks. J. Geol., *1*:597-605.

DRUECKER, M.D. (1981) Chiriguelo carbonatite complex. T.A.C. (int. rep.), Asunción, 5p.

DRUECKER, M.D. & GAY, S.P. (1987) Mafic dyke swarms associated with Mesozoic rifting in Eastern Paraguay. In: H.C. Halls & W.F. Fahrig (eds.) Geol. Ass. Can., Spec. Paper, *34*:187-193.

DUGRATY, A.M. (1865) La Republique de Paraguay, 2d ed., Brussels, C. Muquardt, 407p.

EBY, N.G. & MARIANO, A.N. (1986) Geol-ogy and geochronology of carbonatites peripheral to the Paraná Basin, Brazil-Paraguay. Carbonatites Symposium, Ottawa, 13p.

ECKEL, E.B. (1959) Geology and mineral resources of Paraguay - A reconnaissance. U.S. Geol. Surv. Prof. Paper, *327*:110p.

ERNESTO, M.; RODAS, C.S.R.; COMIN-CHIARAMONTI, P.; GOMES, C.B.; PICCIRILLO, E.M.; BELLIENI, G.; CASTILLO, A.M.C.; VELÁZQUEZ, J.C.; CUNDARI, A. (1990) Paleomagnetismo de los diques asociados al complejo alcalino de Sapucai, Paraguay Oriental. 1er. Coloquio de Rocas Magmaticas de Paraguay, San Lorenzo, Paraguay. Rev. Geol., *1*:125-128.

EVANS, J.W. (1894) The geology of Mato Grosso (particularly the region drained by the upper Paraguay). Quart. J. Geol. Soc., *50*:85-104.

FACETTI, J.R. & PRATS, M. (1973) Correlaciones de escandio, tierras raras y otros elementos en el stock of Arrúa-í. Rev. Soc. Cient. Paraguay, *13*:7-17.

FÚLFARO, V.J.; SAAD, A.R.; SANTOS, M.V.; VIANNA, R.B. (1982) Compartimentação e evolução tectônica da Bacia do Paraná. Rev. Bras. Geoc., *12*:590-611.

GALLO, P. (1988) Studio petrografico del massiccio alcalino di Acahay (Paraguay Orientale). Bs.D. Dissertation, University of Palermo, 188p.

GOLDSCHLAG, M. (1913) Zur Petrographie Paraguay und Mato Grosso. Mitt. Geog. Gesell., *8*:293-301.

GOMES, C.B.; COMIN-CHIARAMONTI, P.; DE MIN, A.; MELFI, A.J.; BELLIENI, G.; ERNESTO, M.; CASTILLO, A.M.C.; VELÁZQUEZ, J.C.; VELÁZQUEZ, V.F.; PICCIRILLO, E.M. (1989) Atividade filoniana associada ao complexo alcalino de Sapukai, Paraguai Oriental. Geochim. Brasil., *3*:93-114.

GREEN, P.F.; DUDDY, I.R.; O'SULLIVAN, P.; HEGARTY, K.A.; COMIN- CHIARAMONTI, P.; GOMES, C.B. (1991a) Análise de traços de fissão em apatita de rochas alcalinas do Paraguai Oriental e sua implicação para a exploração de hidrocarbonetos. 3º Congr. Bras. Geoq./1º Congr. Geoq. PLOP, São Paulo, Brazil, Resumos, 2:627.

GREEN, P.F.; DUDDY, I.R.; HEGARTY, K.A.; O'SULLIVAN, P.; COMIN-CHIARAMONTI, P.; GOMES, C.B. (1991b) Mesozoic potassic magmatism from the Asunción-Sapucai graben (Paraguay): apatite fission track analysis of the Acahay suite and implications for hydrocarbon exploration. Geochim. Brasil., *5*:79-87.

GROSSI-SAD, J.H. (1972) Relatório preliminar sobre as possibilidades minerais do complexo ígneo de Chiriguelo em Pedro Juan Caballero. GEOSOL (int. rep.), Belo Horizonte, 42p.

HAGGERTY, S.E. & MARIANO, A.N. (1983) Strontian loparite and strontio-chevkinite: two new minerals in rheomorphic fenites from the Paraná Basin carbonatites, South America. Contr. Mineral. Petrol., *84*:365-381.

HALES, F.W. (1980) An interpretation of the data from the airbone magnetic surveys in northern areas of Eastern Paraguay. T.A.C. (int. rep.), Asunción, 19p.

HARRINGTON, H.J. (1950) Geologia del Paraguay Oriental. Fac. Ci. Ex., Fis. Mat., Contr. Cient., Ser. E, Geologia, *1*:1-88.

HARRINGTON, H.J. (1956) Paraguay. In: Jenks (ed.) Handbook of South America Geology. Geol. Soc. Amer. Mem., *65*:99-114.

HARRINGTON, H.J. (1972) Silurian of Paraguay. In: W.B.Berry & A.J. Boucot (eds.)

You have either reached a page that is unavailable for viewing or reached your viewing limit for this book.

You have either reached a page that is unavailable for viewing or reached your viewing limit for this book.

You have either reached a page that is unavailable for viewing or reached your viewing limit for this book.

Age: K/Ar, 128-130 Ma (Bitschene, 1987; Velázquez et al., 1990b, 1992; Velázquez, 1992). Comte & Hasui (1971) reported very old ages for microdioritic rocks. Rb/Sr, 127.8±7.2 Ma (Velázquez et al., 1990b, 1992; Velázquez, 1992), determined from an internal isochron based on mineral concentrates (biotite and plagioclase) and whole rock data.
References: Harrington (1950), Eckel (1959), Putzer (1962), Mariano (1978), Almeida (1983), Bitschene & Lippolt (1984), Bitschene (1987), Livieres & Quade (1987), Woolley (1987), Velázquez et al. (1990b, 1992), Comin-Chiaramonti et al. (1991a,b) and Velázquez (1992).

06. Aguapety Portón 25°35.2'S; 56°26.6'W

A theralite-essexite stock forming a conical hill, height 205 m, area 0.2 km^2, emplaced into Carboniferous sediments of the Coronel Oviedo Formation. Rocks have been quarried for rough building stone and road surfacing. Other rock types described in the literature include shonkinite, malignite and nepheline syenite. Mariano (1978) detected an apparent gradation between shonkinite and malignite of the Mbocayaty-Aguapety Portón area; this author also refers to the shonkinitic rocks as porphyritic-aphanitic varieties (shonkinite lamprophyres) mainly having phenocrysts of clinopyroxene and lesser amounts of olivine.
Age: K/Ar, 133-138 Ma (Bitschene, 1987). Rb/Sr, 126.5±7.6 Ma (Velázquez et al., 1990b, 1992; Velázquez, 1992), based on a reference isochron for six complexes of the Central Province including two Aguapety Portón samples.
References: Putzer (1962), Putzer & van den Boom (1962), Mariano (1978), Almeida (1983), Bitschene (1987), Livieres & Quade (1987), Woolley (1987), Velázquez et al. (1990b, 1992), Comin-Chiaramonti et al. (1991a,b) and Velázquez (1992).

07. Cerro Itapé 25°51.5'S; 56°33.3'W

A small plug, height 339 m, area 0.8 km^2, associated with sandstones of the Misiones Formation. Rock types include trachybasalts and trachyphonolites.

08. Cerrito Itapé 25°52.6'S; 56°35.4'W

Two Na-rich tephritic plugs, approximately 0.5 km^2 in area, lying SE of the village of Itapé and intruded into Triassic sandstones of the Misiones Formation.

09. Colonia Vega 25°49.6'S; 56°42.6'W

A peralkaline phonolitic volcanic dome, height 200 m, area 0.4 km^2, ESE of Colonia Hector L.Vega. Country rocks are Triassic sandstones of the Misiones Formation.

10. Cañada 25°47.6'S; 56°46.8'W

A stock of essexite and nepheline syenite, area 0.8 km^2, lying SSE of the village of Ybytymí and emplaced into Triassic sandstones of the Misiones Formation. In Comin-Chiaramonti et al. (1991a,b) it has been erroneously referred to as Garay.

11. Cerro Chobí 25°47.5'S; 56°48.7'W

A stock of gabbroic to essexitic rock types, height 475 m, area 1.0 km^2, cutting Triassic sandstones of the Misiones Formation and cropping out a few kilometers S of Ybytymí.

You have either reached a page that is unavailable for viewing or reached your viewing limit for this book.

You have either reached a page that is unavailable for viewing or reached your viewing limit for this book.

You have either reached a page that is unavailable for viewing or reached your viewing limit for this book.

26. Ñemby 25°24.2'S; 57°32.1'W

A nephelinite plug, height 208 m, area 0.3 km^2, emplaced into Triassic sandstones of the Misiones Formation. Mantle xenoliths of spinel peridotite (ca. 10-15% by volume and up to 40 cm across) are abundant, whereas crustal xenoliths (up to 100 cm across) occur rarely.
Age: K/Ar, 45.7±1.8 Ma (Bitschene, 1987).
References: Putzer (1962), Palmieri & Velázquez (1981), Comin- Chiaramonti et al. (1986, 1991c), Bitschene (1987), Livieres & Quade (1987) and Demarchi et al. (1988).

27. Cerro Confuso 25°07.9'S; 57°32.7'W

A Na-rich peralkaline phonolite plug, area 0.2 km^2, occurring on the western bank of the Paraguay river.
Age: K/Ar, 55-61 Ma (Bitschene, 1987).
References: Putzer (1962), Bitschene (1987), Livieres & Quade (1987) and Censi et al. (1991).

28. Nueva Tablada 25°15.2'S; 57°35.6'W

A lava flow of nephelinite, about 10 m thick and with abundant mantle xenoliths of spinel peridotite (up to 20 cm across), associated with Triassic sandstones of the Misiones Formation.
Age: K/Ar, 46.3±2.0 Ma (Bitschene, 1987).
References: Comin-Chiaramonti et al. (1986, 1991c) and Bitschene (1987).

29. Lambaré 25°20.4'S; 57°38.5'W

A small plug of nephelinite, height 156 m, area 0.2 km^2, emplaced into Triassic sandstones of the Misiones Formation. Mantle xenoliths of spinel peridotite (up to 10 cm across) are abundant, while crustal xenoliths (up to 30 cm in size) are scarce.
Age: K/Ar, 48.9±2.2 Ma (Bitschene, 1987).
References: Putzer (1962), Comin-Chiaramonti et al. (1986, 1991c), Bitschene (1987) and Livieres & Quade (1987).

30. Tacumbú 25°18.7'S; 57°39.9'W

A small plug of nephelinite, height 65 m, area 0.1 km^2, cutting Triassic sandstones of the Misiones Formation. Mantle xenoliths of spinel peridotite (up to 7 cm across) are very common and crustal xenoliths (up to 50 cm across) can occasionally be found.
Age: K/Ar, 41-46 Ma (Comte & Hasui, 1971; Bitschene, 1987).
References: Putzer (1962), Comte & Hasui (1971), Comin-Chiaramonti et al. (1986, 1991c), Bitschene (1987) and Livieres & Quade (1987).

Not included in the above list are the occurrences of *Apyraguá* (dyke: 25°54.7'W, 56°53.5'W; also referred to *Apitaguá*, an essexite stock, cf. Putzer, 1962; Putzer & van den Boom, 1962; Livieres & Quade, 1987; Woolley, 1987) and *Cerro Verá* (25°54.9'S, 56°55.7'W; also an essexite stock, cf. Putzer, 1962; Putzer & van den Boom, 1962; Livieres & Quade, 1987; Woolley, 1987), at 3.5 and 4.5 km SW of La Colmena, respectively, corresponding to outcrops of high-Ti andesi-basalts of the Alto Paraná Formation. Also of tholeiitic affinity is *Cerro Obí* (25°55.2'S, 56°57.6'W), lying 6 km SW of La Colmena.

You have either reached a page that is unavailable for viewing or reached your viewing limit for this book.

You have either reached a page that is unavailable for viewing or reached your viewing limit for this book.

You have either reached a page that is unavailable for viewing or reached your viewing limit for this book.

Table 1 - Catalogue of earthquakes in Paraguay and neighbouring regions compiled from NEIC, ISC and Brazilian Seismic catalogues.

Date Y/M/D	Lat.	Long.	Depth (km)	Mag. (m_b)	Date Y/M/D	Lat.	Long.	Depth (km)	Mag. (m_b)
1744/09/24	-15.30	-58.00		1.2	1961/07/20	-20.80	-64.70	128.0	
1860/10/01	-15.60	-56.10			1961/09/10	-22.80	-63.50	527.0	
1876/06/26	-16.57	-57.82		1.2	1961/09/19	-20.50	-62.90	580.0	
1879/03/01	-15.60	-56.10		1.2	1962/09/27	-17.90	-64.90	120.0	
1906/10/24	-19.00	-57.64		4.2	1962/09/29	-27.00	-63.60	575.0	
1916/07	-15.60	-56.10			1962/12/08	-25.80	-63.40	620.0	
1918/01	-15.60	-56.10			1962/12/25	-28.20	-63.20	589.0	
1919/06/01	-18.00	-56.00		4.9	1963/04/18	-23.00	-65.00	33.0	
1919/07/16	-15.60	-56.10			1963/09/02	-18.20	-62.60	33.0	4.5
1928	-21.82	-52.05			1963/10/17	-21.50	-63.40	33.0	4.5
1934	-29.45	-51.50			1963/11/01	-29.50	-64.20	33.0	4.0
1939/06/04	-15.60	-56.10			1964/02/13	-18.06	-56.69		5.4
1941/04/11	-16.10	-54.50		4.4	1964/02/13	-18.05	-56.75	16.0	5.2
1942/07/21	-20.50	-64.00			1964/06/25	-22.86	-63.80	532.0	4.2
1947/12/15	-21.70	-57.90		1.2	1964/07/09	-17.20	-64.61	33.0	4.4
1949/01/31	-21.00	-65.00	250.0		1964/12/09	-27.46	-63.23	578.0	5.7
1949/06/13	-28.00	-63.50	650.0		1964/12/23	-27.35	-63.00	579.0	4.2
1950/01/20	-28.00	-63.50	600.0		1965/02/18	-22.50	-63.50	542.0	4.4
1950/02/20	-19.50	-63.00	600.0		1965/02/18	-22.87	-63.73	536.0	3.9
1955/02/08	-20.00	-62.50	600.0		1965/03/05	-26.89	-63.25	555.0	5.6
1955/02/19	-20.50	-65.00	250.0		1965/03/30	-22.00	-63.20	260.0	4.0
1955/04/24	-17.00	-65.00			1965/04/20	-25.98	-63.00	601.0	3.9
1955/06/21	-27.50	-63.00			1965/05/13	-19.24	-63.84	602.0	5.0
1957/01/18	-15.60	-56.10			1965/06/07	-22.80	-65.00	78.0	4.3
1957/05/25	-25.50	-65.00			1965/07/30	-22.88	-63.67	533.0	4.3
1957/05/31	-27.50	-63.00	600.0		1965/09/03	-27.39	-63.20	586.0	4.5
1957/08/26	-19.00	-63.00			1966/01/24	-23.58	-64.27	28.0	4.9
1957/11/06	-24.50	-65.00			1966/01/31	-24.93	-64.48	20.0	5.5
1958/02/23	-27.50	-63.00	600.0		1966/04/14	-24.91	-64.40	30.0	5.1
1958/05/31	-21.50	-64.00			1966/08/04	-19.00	-57.80		
1958/06/01	-19.00	-64.50			1966/08/08	-28.86	-63.30	635.0	3.8
1958/08/06	-24.50	-63.00	550.0		1966/10/30	-22.42	-63.90	20.0	4.8
1958/08/21	-20.00	-65.00	300.0		1966/11/03	-17.80	-63.90	64.0	4.5
1958/08/21	-26.50	-62.00	550.0		1966/12/20	-26.06	-63.10	571.0	5.8
1958/09/01	-18.00	-65.00			1967/01/17	-27.32	-63.24	586.0	5.6
1958/10/11	-23.50	-65.00	200.0		1967/02/19	-24.79	-63.40	562.0	4.0
1958/11/19	-27.50	-63.50	600.0		1967/08/10	-23.22	-63.90	550.0	3.6
1959/05/13	-22.50	-63.50			1967/09/04	-28.26	-63.21	607.0	4.3
1959/05/30	-22.00	-63.00	500.0		1967/09/09	-27.62	-63.15	577.0	5.9
1959/07/06	-26.50	-61.50	600.0		1967/10/05	-27.12	-64.47		4.6
1959/07/06	-26.50	-61.00	600.0		1967/11/06	-22.10	-64.00	541.0	3.9
1959/08/01	-27.50	-65.00	200.0		1968/01/20	-25.62	-64.58	33.0	4.1
1959/12/27	-28.00	-63.00	650.0		1968/01/28	-23.64	-65.00	68.0	4.4
1960/06/11	-21.00	-64.50	300.0		1968/01/31	-27.69	-63.22	585.0	5.1
1960/08/10	-23.50	-64.70	183.0		1968/04/01	-23.63	-63.65	540.0	4.2
1960/08/23	-27.40	-63.10	568.0		1968/05/11	-28.72	-63.11	598.0	5.3
1960/11/15	-15.60	-56.10			1968/08/22	-17.24	-64.80	72.0	4.5
1961/04/16	-22.70	-61.80	176.0		1968/08/23	-21.95	-63.64	513.0	5.6
1961/04/28	-22.00	-62.90	82.0		1968/08/23	-21.86	-63.57	533.0	5.2

You have either reached a page that is unavailable for viewing or reached your viewing limit for this book.

You have either reached a page that is unavailable for viewing or reached your viewing limit for this book.

You have either reached a page that is unavailable for viewing or reached your viewing limit for this book.

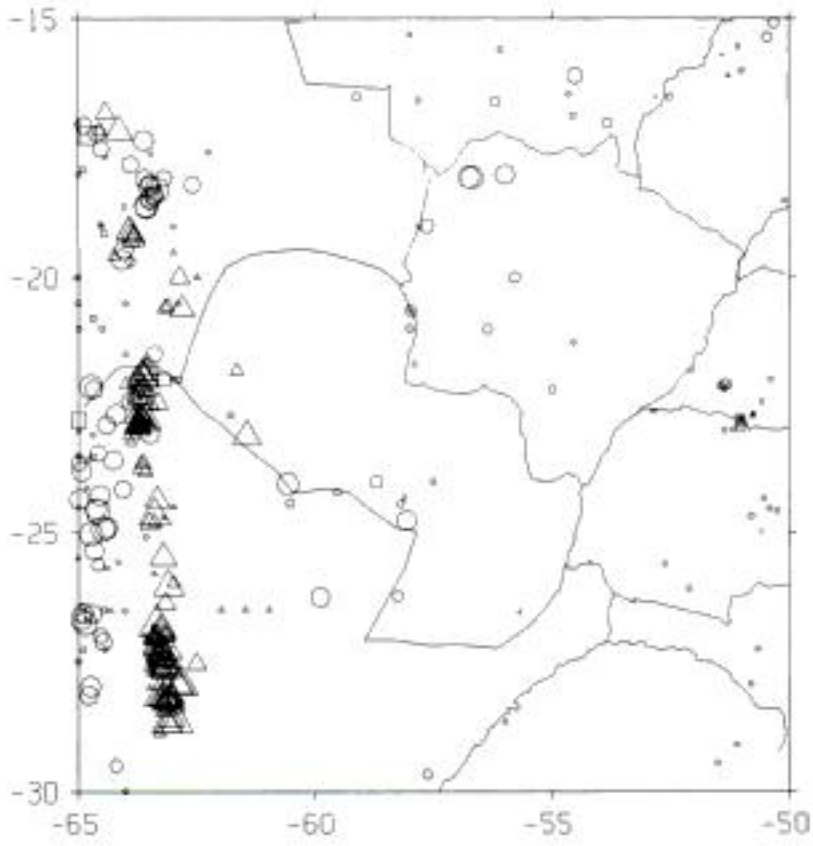

Figure 3 - Seismicity of Paraguay and neighbouring regions by using selected data from the NEIC and ISC files and all reliable data from the Brazilian Seismic Catalogue, showing earthquakes occurred in the interval July 1942 - June 1993. The shapes of the symbols are explained in Fig. 1 and their sizes represent events with m_b magnitude among 1.0 and 6.6.

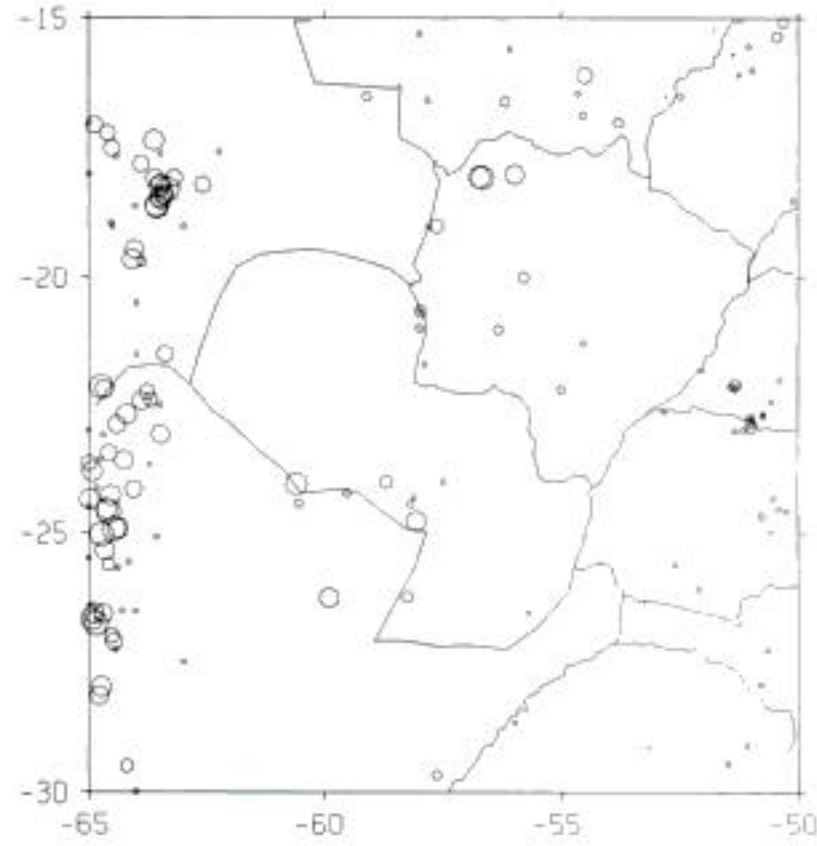

Figure 4 - Same as Fig. 3, showing only the earthquakes with surface foci (h<70 km).

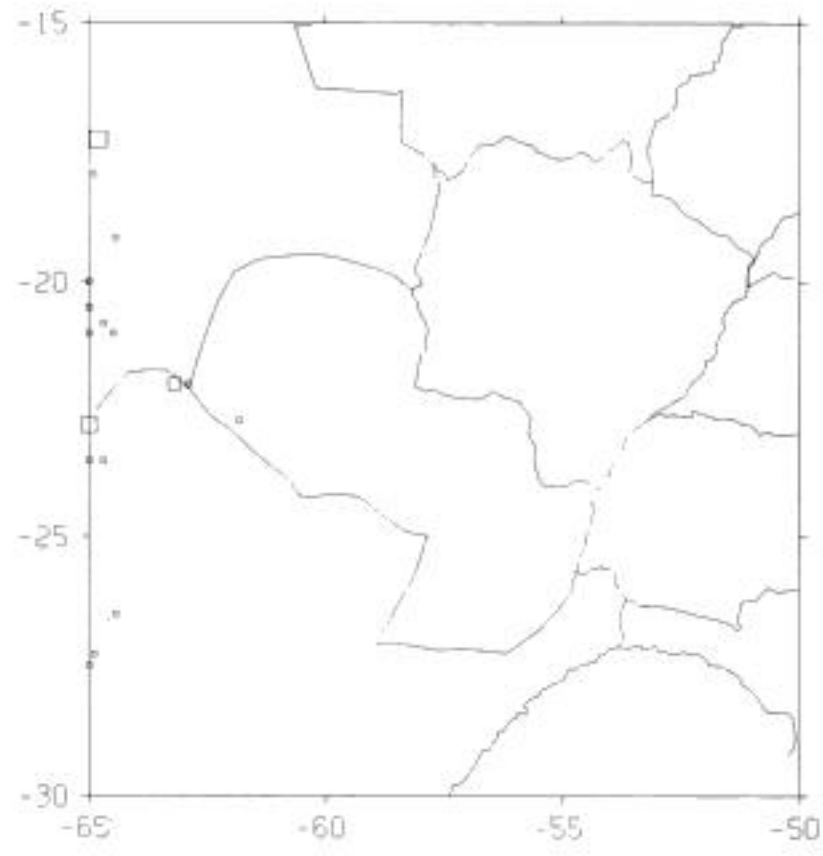

Figure 5 - Same as Fig. 3, showing only events of intermediate depth (70<h<300 km).

crust and are also called intraplate events.

The intermediate earthquakes, with depths among 70 and 300 km, are shown in Figure 5. They are present, as expected, only in the portion associated with the subduction zone. No intermediate events occur in the other portions of the region of study. Those earthquakes are directly associated with the subduction of the Nazca plate. The important features observed in Figure 5 are the relatively low level of intermediate activity as compared to the superficial one, the main NS trend of those epicenters and a probable SE-NW branch of the slab at these depths, present under the western portion of the Paraguayan territory.

The deep events, with depths larger than 300 km, are shown in Figure 6. Those earthquakes are also associated directly with the subducted Nazca plate. Most of those earthquakes have depths larger than 500 km. They form most of the southern zone of deep activity in South America that goes from northern Argentina to central Bolivia. The main features presented by the deep activity are: a) the NS trend also presented by the shallower events, dislocated around two degrees to the East from the trend presented by the intermediate earthquakes of Figure 5, showing the geometry of the Nazca slab under the region of study, as stated before and b) the presence of deep activity well to the East from the main NS trend, especially the epicenters shown in the western portion of Paraguay. These dislocated events also agree with the idea of a SE-NW branch of the slab suggested by the intermediate depth earthquakes (Berrocal et al., 1994). The three small deep events distributed in a WE orientation at around 26 South may be mislocations due to the small magnitude of those events. However, the larger

You have either reached a page that is unavailable for viewing or reached your viewing limit for this book.

You have either reached a page that is unavailable for viewing or reached your viewing limit for this book.

You have either reached a page that is unavailable for viewing or reached your viewing limit for this book.

basin hosting massive basaltic lava flows related to the openning of the nearby South Atlantic (Fig. 1). AFTA is a technique which provides direct information about the thermal history of individual samples and in particular constrains the time and magnitude of specific thermal events.

The Paraná Basin and its margins are ideally suited for a rigorous thermal history study as the presence of the largest basaltic flow on continental crust (i.e. Paraná flood basalts) and thousands of diabase intrusives are a testament to the complex history of this area. Furthermore, the presence of hydrocarbons in the region is not well understood and timing relationships sought in this study should help constrain aspects of the basins development and improve assessments of the hydrocarbon prospectivity in the area.

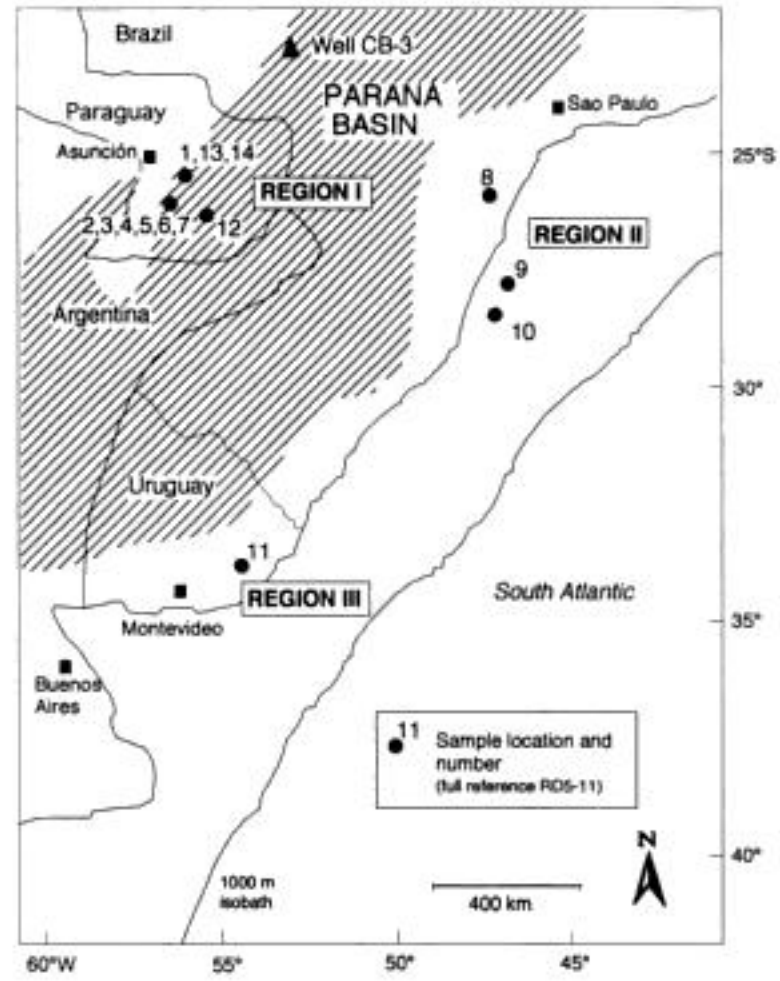

Figure 1 - Location of AFTA (Apatite Fission Track Analysis) samples from in and around the Paraná Basin (sample numbers shown as 1 to 14, full sample reference number is RD5-1 to RD5-14.). Samples consist of igneous, sedimentary and metamorphic rocks varying in age from Upper Ordovician to Cretaceous (see Table 1 for details). Both the Paraná Basin and its margins were sampled as part of this preliminary study to identify the thermal history of the basin and its flanks using AFTA. Location of Well CB-3 in Brazil is also shown above.

GEOLOGICAL SETTING AND SAMPLE DETAILS

The Paraná Basin is an Ordovician-to-Cretaceous composite basin comprising an area of more than 1.6 million km² extending through Brazil, Paraguay, Uruguay and Argentina. Review of the stratigraphy, structure and evolution of the Paraná Basin can be found in this volume as well as in Piccirillo & Melfi (1988) and Zalán et al. (1990). Zalán et al. (1990) suggest that the present basinal geometry is controlled by the superposition of at least three basins which formed at different times due to different tectonic forces related to plate interactions. The present configuration of the basin does not reflect patterns related to periods of basinal deposition, but rather the combined effect of several phases of deformation.

The basin is bounded by numerous basement arches which appear to have been re-activated several times throughout the basins history. Perhaps the most profound and well-studied feature of the Paraná Basin is the Paraná continental flood basalts (part of the Serra Geral Formation) representing a major magmatic event in which vast amounts of basaltic material (typically estimated at 1 to 2 million km³) erupted during the Early Cretaceous in less than 2 Ma. In places, the cumulative thickness of Paraná volcanics is more than a kilometre. In addition to the Paraná flood tholeiites and potassic magmas which are also Early Cretaceous in age (see Comin-Chiaramonti et al., Appendix I, and Cundari & Comin-Chiaramonti, this volume), the Paraná Basin is also host to Eocene-Oligocene magmatism characterised by ultra-alkaline shallow-level intrusives such as those found at the western limit of the Asunción-Sapucai graben of central-eastern Paraguay (Comin-Chiaramonti et al., 1991).

The location of the AFTA samples collected in and around the Paraná Basin can be grouped into three general regions (Fig. 1) and represent a broad range in rock-type and age (see Table 1). Samples RD5-1 to -7 and -12, -13 and -14 were collected from the Asunción-Sapucai graben or its flanks and include both igneous and sedimentary rocks ranging in age from Late Ordovician to Early Cretaceous (Table 1). Details of the structural setting and rock-types found in the Asunción-Sapucai graben are given in several papers in this volume (Comin-Chiaramonti et al.,

You have either reached a page that is unavailable for viewing or reached your viewing limit for this book.

You have either reached a page that is unavailable for viewing or reached your viewing limit for this book.

You have either reached a page that is unavailable for viewing or reached your viewing limit for this book.

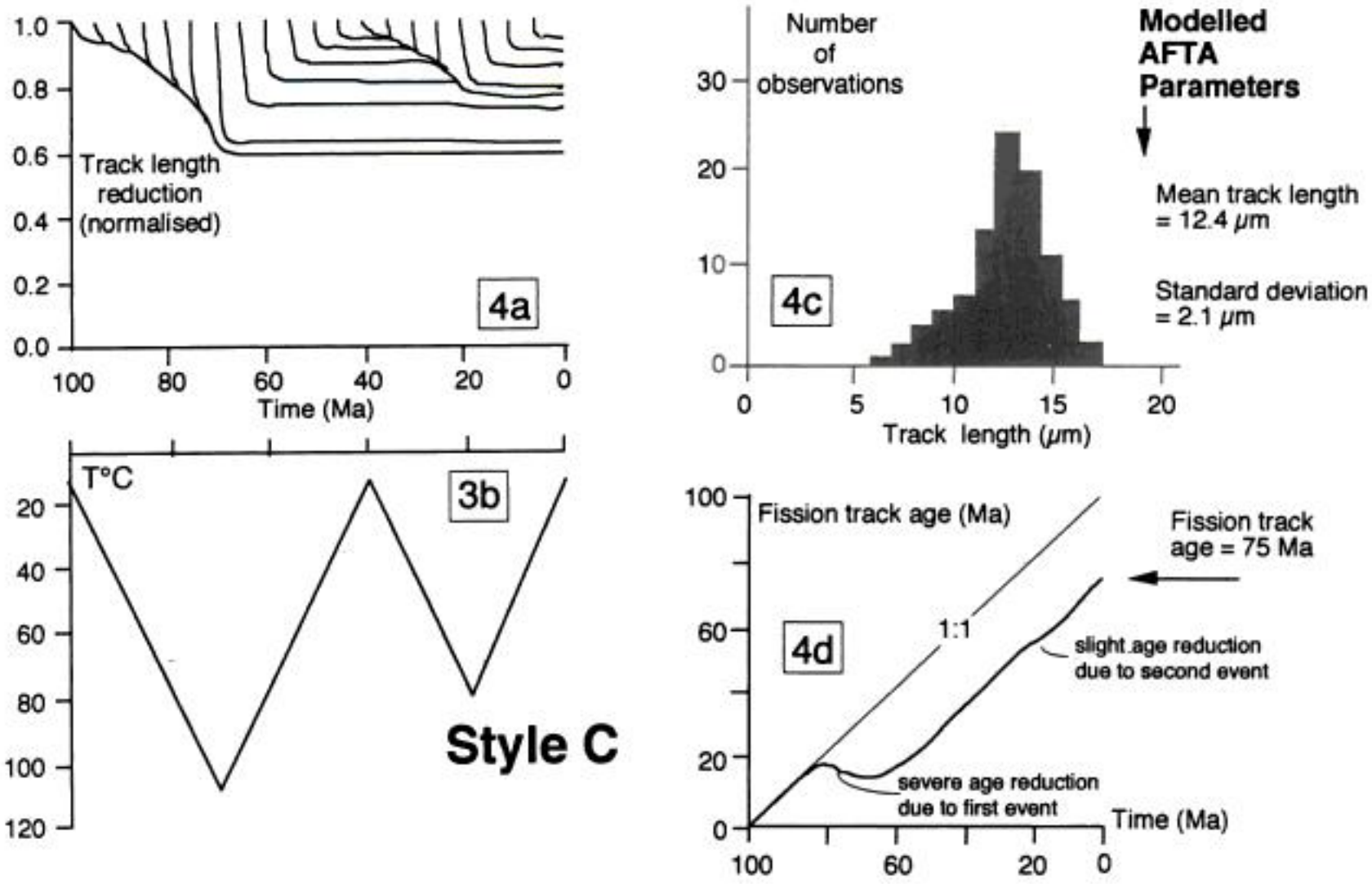

Figure 4 - Example of the fission track response to a specific thermal history, Style C, involving two thermal peaks (Fig. 4b). In this example the maximum paleotemperature is 105°C at ~ 70 Ma and as such none of the tracks is totally annealed (i.e. the oldest formed tracks retain ~60 % of their original length; Fig. 4a). Like the previous examples, tracks form constantly through time and the length of each individual track is a direct consequence of the maximum temperature experienced by that track. Like Style B, the length histogram (Fig. 4c) gives a relatively short mean track length of 12.4μm and a broad standard deviation (2.1μm), but the age is significantly greater (75.5 Ma) compared to Style B. Note the slight reduction in age (Fig. 4d) due to the second cooling event at ~ 20 Ma where a paleotemperature of 80°C was reached. The final fission track age for this sample is 75 Ma and as with Style B, the final age does not give direct information about the time of cooling, but rather, must be interpreted together with the length information to determine the two-event history.

(Fig. 2a; note that all tracks shown to experience greater than ~60 % track reduction are not represented in the lenght histogram as they are typically not observed). Following rapid cooling at ~60 Ma, paleotemperatures of 15°C were retained until the present-day. All those tracks that formed between 60 Ma and the present, retained their original length (note in Fig. 2a that there is an initial minor amount of length reduction associated with each track due to general track instabilities, known to be insignificant and not related to temperature). As a result, all tracks observed in the sample today are relatively long giving a mean length of ~15μm (Fig. 2c), with a narrow distribution (~1.2μm), and having formed after a rapidly cooling event, they give us a direct estimate of the time of cooling, in this case, 58 Ma (Fig. 2d).

Compare the effect of rapid cooling (Style A) with that of slow cooling referred to as Style B in Figure 3. In particular, note that the maximum paleotemperature experienced by each individual track after the 60 Ma event is different, i.e. systematically lower with time (Fig. 3b), and as a result the length of the *younger* tracks are systematically longer than the *older* tracks (Fig. 3a). This history results in a length distribution displaying a relatively shorter mean and broader distribution (Fig. 3c) when compared to the predicted track length distribution corresponding to Style A (Fig. 2c). Note also that in contrast to Style A, the prolonged higher paleotemperatures in Style B have the effect of greater age reduction (Fig. 3d) and give a fission track age of 49 Ma, significantly less than in the case of rapid cooling (Style A).

In Figure 4, an alternative thermal history (Style C) involving two periods of elevated paleotemperature is shown. Note that the first episode of heating is associated with a higher

You have either reached a page that is unavailable for viewing or reached your viewing limit for this book.

You have either reached a page that is unavailable for viewing or reached your viewing limit for this book.

You have either reached a page that is unavailable for viewing or reached your viewing limit for this book.

lengths (Table 2) similar to the Style A cooling history (Fig. 2) in which the corresponding fission track age is giving us direct information about the time of cooling from maximum paleotemperature. Furthermore, these long lengths require that since cooling, paleotemperatures probably never exceeded ~50°C, as indicated in Table 3.

Results from Precambrian sample RD5-8 show clear evidence of two episodes of cooling (Table 3). Furthermore, elevated paleotemperatures during the Early Tertiary (105-115°C) would have erased evidence of any earlier heating/cooling, and therefore there could have been *more than* two episodes as would seem likely for such an old sample. Evidence for more recent heating (with cooling beginning some time in the last 30 Ma) is taken from the track length distribution which is characterised by a relative low mean length (Table 2) indicating cooling from moderate paleotemperatures (50-60°C) is required relatively recently. The AFTA data from sample RD5-8 is typical of a sample which has experienced a thermal history similar to Style C.

Solutions for samples RD5-9 and -10 are consistent with the results from RD5-8. AFTA data from sample RD5-10 also provide clear evidence of two events, while the interpretation for RD5-9 is somewhat tenuous because of limited data from this sample. Age data from sample RD5-9 clearly requires a significant amount of heating to account for the substantial amount of age reduction in the sample, but the limited length data disallow more detailed constraints on the subsequent cooling history.

The solution for sample RD5-11 is poorly controlled because of limited AFTA data in the sample. However, despite this shortcoming, the data clearly show evidence of higher temperatures in the past with cooling commencing some time between 150 and 30 Ma.

AFTA data from the Misiones Formation (sample RD5-12) provides a strong constraint on the thermal history of this unit at this locality. Two cycles of cooling are clear in the data with most of the age reduction occurring during the first episode (Style C). Cooling commenced some time between 110 and 60 Ma, and in a subsequent episode moderate paleotemperatures (70-80°C) were reached followed by cooling beginning between 60 and 10 Ma.

Results from Upper Ordovician sandstones (samples RD5-13 and -14) are also consistent with two episodes (Table 3), however in the case of sample RD5-14, the AFTA data are limited and therefore, constraints on timing of cooling are broad with no control on subsequent heating/cooling in the Tertiary.

Overall, the AFTA parameters and thermal history solutions are similar across the study area which is notable given the wide range in rock type and stratigraphic (or emplacement) age of the fourteen samples. It is possible that there were more than two events affecting the region, but the data do not *see through* the Late Cretaceous episode because of the masking effect of the more recent elevated paleotemperatures (as an example of this masking effect, consider the thermal history illustrated by Style A, i.e. any "memory" of an earlier event are erased by the high temperatures associated with the event at 60 Ma).

Finally, the discussion above and in the following section points to "episodes" of cooling identified in the AFTA data. Note that for those samples in which two episodes have been identified, the solution does not necessarily require two distinct thermal pulses or events (e.g. burial followed by erosion or igneous activity). However, the data do require that the cooling path experienced by the sample passes through the paleotemperature ranges indicated within the time ranges shown (Table 3). In other words, for those samples in which two episodes are indicated, the data could either be explained by two distinct heating events or slow progressive cooling through the time-temperature control points provided by AFTA.

Summary of results in a regional context

The solutions presented in Table 3 are based on modelling the AFTA parameters of a single sample independent of any knowledge of the regional geology or results from neighboring samples. By inspecting the results from structurally related samples, the overlap in time ranges identified by AFTA can be used to improve the control on the time of cooling and to identify specific regional events.

Figure 5 summarises the results in a regional context. We refer to the area of the Asunción-Sapucai graben of central-eastern Paraguay as

You have either reached a page that is unavailable for viewing or reached your viewing limit for this book.

You have either reached a page that is unavailable for viewing or reached your viewing limit for this book.

You have either reached a page that is unavailable for viewing or reached your viewing limit for this book.

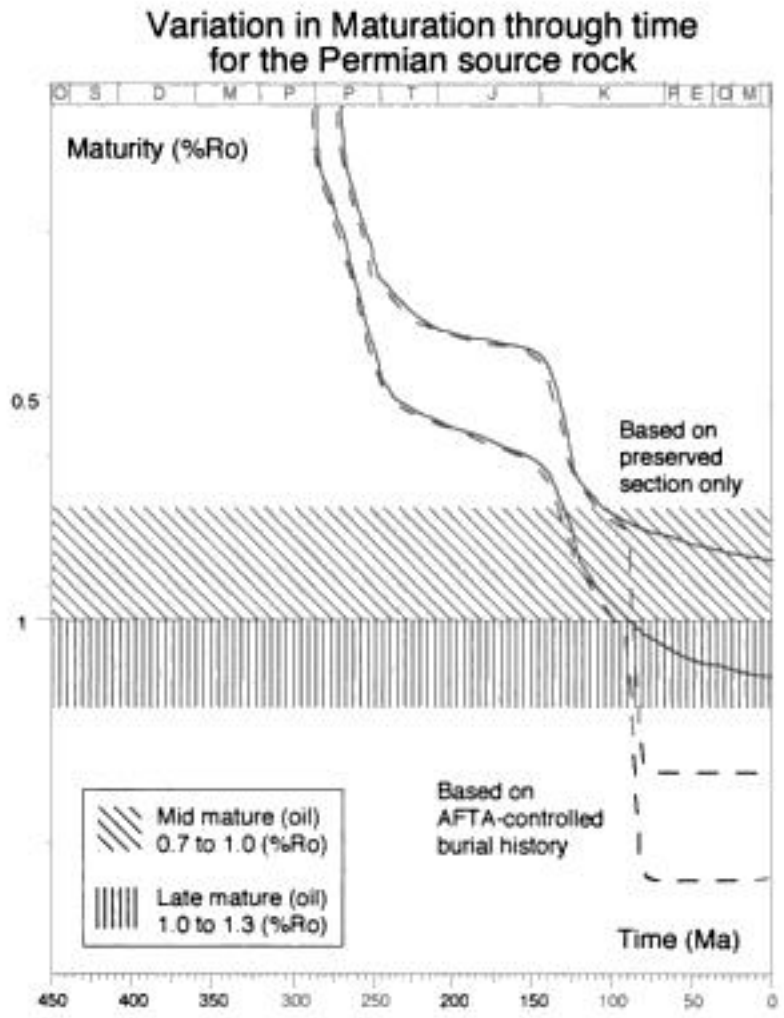

Figure 8 - Comparison of the evolution of maturity at the top and bottom of the Permian source rock for histories shown in Figure 6 (based on preserved section only) and Figure 7 (AFTA-controlled history) constructed for Well CB-3 in the Paraná Basin. Note that the Lower Permian section enters the maturity windows at the same time for both histories but diverge significantly following the event at ~80 Ma. Using the AFTA-controlled history, present-day maturities in the Lower Permian section are predicted to be 0.2-0.3% greater than maturities predicted from models based on the burial of the preserved section only.

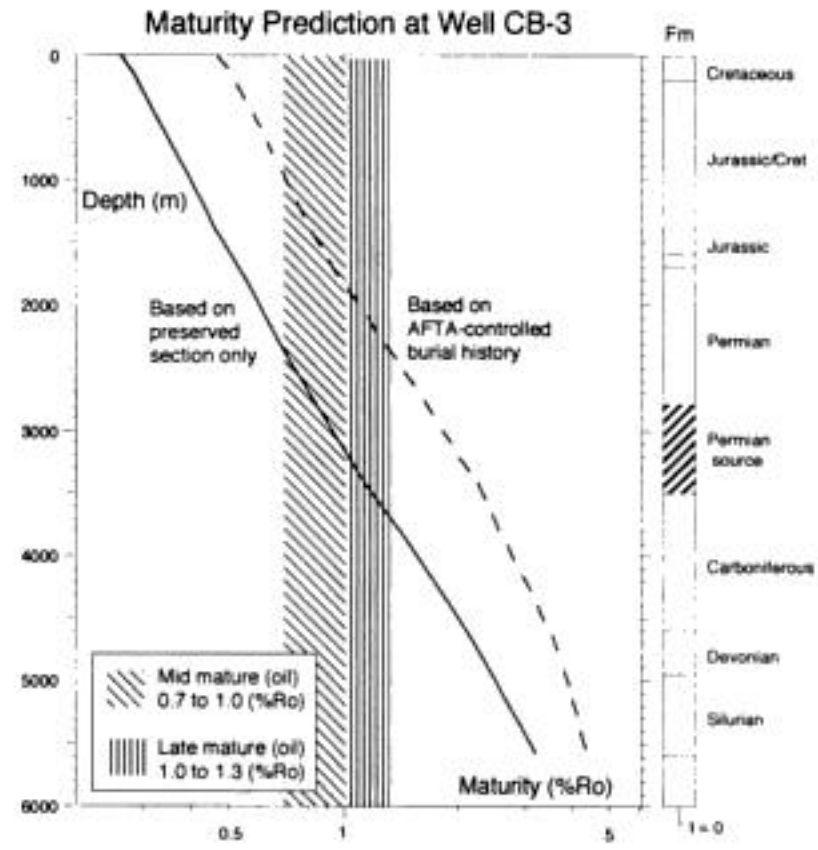

Figure 9 - Comparison of the present-day VR profile based on the burial model from the preserved section only (solid line) shown in Figure 6 and the AFTA-controlled history (dashed line) shown in Figure 7. In the AFTA-controlled history, the time of maximum paleotemperature post-dates the time of deposition preserved at Well CB-3. Therefore, the maturity profile corresponding to this history is everywhere greater than predictions based on the preserved section only. The difference between the two predictions is significant throughout most of the section, such that with reliable VR data from suitable portions of the section, the more appropriate model can be identified.

phases of heating (burial) and cooling (erosion) in the region (Fig. 7):

1) Note that the high levels of maturity predicted within the section are a result of Late Cretaceous burial followed by erosion (commencing between 90 and 80 Ma), and not controlled by localised contact heating caused by intrusions. While localised heating may account for some VR data in the section (Zalán et al., 1990), it is expected that the overall profile is principally a consequence of additional burial and erosion. Note in Figure 7, that Late Cretaceous cooling is rapid as required by the AFTA data.

2) The subsidence histories shown in our Figure 6 and Zalán et al. (1990, Fig. 33-13) do not portray the actual geohistory at the location of Well CB-3, and as such, should not be used to evaluate mechanisms of extension or heating. In contrast, the reconstructed history shown in Figure 7 which attempts to include episodes of heating/cooling is required in order to comment on basin models or the maturation and migration of hydrocarbons.

While the AFTA-based reconstruction for Well CB-3 provides an important revision to previous attempts, we note that there are still significant deficiencies that can be improved in future work. Firstly, we have assumed that the thermal events identified in the Asunción-Sapucai graben in Paraguay and on the Brazilian coast are related to exhumation and apply to the location of Well CB-3. While the evidence does suggest the events are regional, it would be more appropriate to evaluate paleotemperature directly from sediments in the well of interest. In particular, for future work we recommend collection of a complete suite of AFTA and VR samples from Well CB-3 or a well nearby. Good stratigraphic control and bottom-hole temperature coverage are also required from the well. The AFTA suite of samples should be complemented with a suite of

You have either reached a page that is unavailable for viewing or reached your viewing limit for this book.

You have either reached a page that is unavailable for viewing or reached your viewing limit for this book.

You have either reached a page that is unavailable for viewing or reached your viewing limit for this book.

PALAEOMAGNETIC DATA FROM THE CENTRAL ALKALINE PROVINCE, EASTERN PARAGUAY

M.Ernesto, P.Comin-Chiaramonti, C.B.Gomes, A.M.C.Castillo, J.C.Velázquez

Alkaline Magmatism in Central-Eastern Paraguay. Relationships with Coeval Magmatism in Brazil. Comin-Chiaramonti, P. & Gomes, C. B. (eds.), 1996, Edusp/Fapesp, São Paulo, pp. 85-102.

ABSTRACT

A palaeomagnetic study has been carried out on Mesozoic (125 sites) and Tertiary (10 sites) alkaline rocks of the Central Province. The Mesozoic sites correspond mainly to dykes cropping out near the Sapucai city; the Tertiary rocks were sampled near Asunción.

Most of the Mesozoic rocks belong to two chemical differentiation trends, apparently emplaced contemporaneously; the most evolved types seem to constitute the final episodes. After alternating field and thermal demagnetizations these rocks revealed mainly reversed polarity remanences corresponding to a palaeomagnetic pole at 62.3°E 85.4°S (N = 75; A_{95} = 3.1°; k = 29). By comparing this pole with those calculated for the Serra Geral Formation in the Paraná Basin it is concluded that the central-eastern Paraguay alkaline rocks were emplaced while the tholeiitic magmatic activity was taking place.

The Asunción Tertiary results revealed high between-site remanence scattering probably induced by high frequency-large amplitude variations in the geomagnetic field while the intrusions were gradually cooling.

INTRODUCTION

The Mesozoic tholeiitic volcanism in the Paraná Basin was followed by an intense alkaline magmatic activity which is presently observed around the borders of the basin, especially along the northeastern one. Most of the alkaline rocks are of Late Cretaceous age in the interval 80-53 Ma (Ulbrich & Gomes, 1981; Sonoki & Garda, 1988). Early Cretaceous alkaline occurrences are also present and are located at higher latitudes than the younger rocks. Piccirillo et al. (1988a) suggested that this pattern is due to the migration of the thermal anomaly associated with the Paraná volcanism, away from the most affected area.

New dating on the Paraná magmatism based on the Ar/Ar method (Renne et al., 1992a, b; Hawkesworth et al., 1992; G. Féraud, personnal communication) indicated a very short interval of a few million years for the emplacement of most of the Paraná tholeiitic rocks, roughly from 133 to 130 Ma. In contrast, the scattering observed in the K-Ar ages of the related alkaline rocks leaves unclear the temporal relationship between the two types of magmatism. Clarification of this rela-

You have either reached a page that is unavailable for viewing or reached your viewing limit for this book.

You have either reached a page that is unavailable for viewing or reached your viewing limit for this book.

You have either reached a page that is unavailable for viewing or reached your viewing limit for this book.

Table 1 (continuation).

74*	56°54'	25°43'	1.0	315	68.9	66.1	-	-	-	-	-	-	-	P	
75	56°54'	25°43'	3.0	315	4958.0	83.6	3	177.9	18.4	5.1	583	115.7	-73.6	Pte	
76	56°53'	25°42'	1.0	325	2825.0	819.5	3	132.5	47.5	15.2	66	18.0	-47.9	Pte	
76*	56°54'	25°42'	?	?	5240.3	5769.2	3	37.0	10.4	9.9	154	357.6	42.6		
77	56°54'	25°43'	2.0	30	786.6	2034.7	3	204.0	69.3	9.2	181	276.0	-57.4	Tp	
83	56°57'	25°51'	4.5	325	2141.0	9448.3	3	163.4	16.0	6.4	376	78.4	-66.3	Tb	D87
84	56°57'	25°51'	4.5	325	761.8	20.9	3	171.9	29.5	5.1	576	84.5	-77.4	Tb	D90
85	56°59'	25°50'	2.0	20	2795.0	101.2	5	169.4	38.1	8.0	92	55.3	-79.3	Lb	D100
86	56°59'	25°50'	(flow)		4128.9	208.0	7	171.8	46.7	6.1	98	15.0	-82.4	Ta	116
87*	56°58'	25°50'	3.0	315	4570.3	5243.9	-	-	-	-	-	-	-	Ta	D98
j) Sapucai															
1*	56°57'	25°42'	(intrusive)		8567.7	555.4	1	191.0	39.2	-	-	196.1	-79.4	EG	127
2	56°59'	25°45'	?	30	3357.2	90.6	3	172.7	59.0	12.6	96	324.8	-74.7	Te	D206
3*	56°59'	25°45'	?	29	3215.1	235.4	2	171.3	58.0	11.0	512	330.5	-75.2	Te	D204
4	56°59'	25°45'	4.0	45	1904.5	229.5	6	174.3	41.3	3.4	378	53.3	-84.2	AB	D203
5*	56°59'	25°45'	2.0	340	3951.0	18784.2	2	86.8	-62.4	25.3	99	73.0	19.7	Tb	D202
6*	56°57'	25°41'	2.0	10	163.9	55.1	-	-	-	-	-	-	-	PaP	D127
7*	56°57'	25°41'	6.0	325	116.9	98.7	4	247.6	52.7	11.7	62	237.8	-31.7	PaP	D147
8*	56°57'	25°41'	6.0	325	4301.9	2359.1	-	-	-	-	-	-	-	Pte	D148
9*	56°57'	25°41'	4.0	E-W	4727.0	3200.4	-	-	-	-	-	-	-	Te	D144
10	56°57'	25°41'	7.0	340	6798.2	6643.8	3	177.7	61.1	5.4	519	309.2	-73.4	Pte	D145
11*	56°57'	25°41'	10.0	355	601.0	50.5	-	-	-	-	-	-	-	PaP	D146
12*	56°57'	25°41'	2.0	N-S	5540.6	16183.2	-	-	-	-	-	-	-	Pte	D143
12	56°57'	25°41'	8.0	295	745.0	22.7	3	185.2	54.0	6.2	395	277.4	-80.1	Pte	D142
13	56°57'	25°41'	4.5	322	30.3	12.7	6	161.7	-0.7	7.6	78	86.1	-58.5	PaP	D141
14*	56°57'	25°42'	2.0	30	5754.0	5238.1	-	-	-	-	-	-	-	Pte	D151
15*	56°57'	25°41'	1.0	N-S	991.4	320.8	-	-	-	-	-	-	-	PaP	D117
15*	56°56'	25°41'	20.0	10	2389.8	442.9	-	-	-	-	-	-	-	P	D119
15*	56°56'	25°40'	1.0	N-S	4427.3	564.3	-	-	-	-	-	-	-	P	D116
16*	56°57'	25°41'	4.0	320	3708.3	291.4	2	177.1	31.0	11.9	438	106.1	-80.6	Te	D122
17	56°58'	25°40'	1.0	332	1376.5	34.3	6	25.3	-56.7	4.3	238	67.6	65.6	P	D171
18*	56°57'	25°40'	1.0	345	1881.1	57.5	2	345.4	-26.2	3.5	5056	251.5	71.9	Tp	D164
19*	56°58'	25°40'	1.0	315	5575.5	237.6	-	-	-	-	-	-	-	Pte	D169
20*	56°58'	25°41'	5.0	315	2573.2	21236.2	2	1.1	-29.8	19.4	166	309.3	80.2	Te	D176
21*	56°58'	25°41'	2.0	325	7755.5	1279.3	-	-	-	-	-	-	-	Pte	D180
22	56°58'	25°41'	1.0	318	1715.6	294.6	4	178.0	21.3	4.9	345	115.3	-75.2	Tp	D181
23	56°58'	25°41'	1.0	307	3091.6	1934.9	3	173.5	12.4	5.4	152	104.2	-69.6	Pte	D183

You have either reached a page that is unavailable for viewing or reached your viewing limit for this book.

You have either reached a page that is unavailable for viewing or reached your viewing limit for this book.

You have either reached a page that is unavailable for viewing or reached your viewing limit for this book.

*Table 2 - Palaeomagnetic results for the Paraná Basin tholeiitic flows (k, susceptibility; M_n, magnetization intensity; A_{95} and k, Fisher's, 1953, statistical parameters; * samples not referenced in this volume).*

	Coordinates					Characteristic Magnetization				VGP		Rock-type	
Site	Long. (°W)	Lat. (°S)	k(10^{-6}) (emu)	M_n(10^{-5}) (emu)	N	Dec. (°)	Inc. (°)	A_{95} (°)	K	Long. (°E)	Lat. (°N)	Code	Sample
98	56°17'	25°46'	3127.0	138.6	9	179.3	55.7	8.8	35	306.8	-79.5	Ab	17
106	55°54'	27°19'	3153.5	268.1	9	342.2	-60.9	10.2	26	164.3	69.4	Ab	PS286'
107	55°46'	27°10'	1800.3	65.2	6	358.7	-47.4	5.1	175	163.8	88.2	Ab	PS287'
108	55°35'	27°02'	2180.3	68.4	2	309.3	52.1	29.8	72	262.4	13.2	Ab	PS288'
109	55°22'	26°49'	1694.4	248.2	3	353.6	-39.5	3.6	1124	250.4	82.7	Ab	PS289'
110	55°13'	26°46'	2537.8	223.7	6	67.6	-71.0	3.7	323	85.4	34.3	Ab	PS290'
111	55°10'	26°32'	1634.5	195.3	3	73.5	-69.4	2.5	2328	83.1	30.6	Ab	PS291'
112	55°10'	26°28'	2104.5	356.8	3	79.5	-66.7	11.5	114	79.6	26.4	Ab	PS292'

Code: Ab, Andesi-basalt.

Table 3 - Palaeomagnetic results for the Tertiary alkaline rocks (k, susceptibility; M_n, magnetization intensity; A_{95} and k, Fisher's, 1953, statistical parameters).

	Coordinates						Characteristic Magnetization					VGP		Rock-type
Site	Long. (°W)	Lat. (°S)	Width (m)	Trend (°E)	k(10^{-6}) (emu)	M_n(10^{-5}) (emu)	N	Dec. (°)	Inc. (°)	A_{95} (°)	K	Long. (°E)	Lat. (°N)	Code
a) Cerro Verde														
103A	57°33'	25°07'	-	-	1073.6	141.9	2	144.1	77.0	7.2	1198	322.4	-43.9	A
103A	57°33'	25°07'	-	-	1657.1	367.7	3	168.4	70.8	5.0	610	315.3	-58.9	A
103B	57°33'	25°07'	-	-	1813.0	35.5	3	167.1	63.3	4.2	837	326.8	-67.5	A
103B	57°33'	25°07'	-	-	1085.9	67.3	3	190.8	57.9	14.1	78	270.8	-73.8	A
103C	57°33'	25°07'	-	-	2509.7	606.0	3	186.8	47.6	8.4	214	244.5	-83.0	A
103C	57°33'	25°07'	-	-	1441.0	362.9	3	195.9	41.5	7.2	288	210.8	-75.5	A
b) Ñemby														
100	57°29'	25°27'	-	-	1819.7	42.9	3	142.4	43.3	6.0	418	24.6	-56.1	Ne
100	57°29'	25°27'	-	-	3263.7	41.7	3	138.2	45.1	9.2	178	21.3	-52.6	Ne
100	57°29'	25°27'	-	-	2971.4	53.5	3	111.7	31.6	4.8	642	25.2	-26.5	Ne
c) Remanso Castillo														
105	57°35'	25°16'	?	330	1649.5	255.3	3	200.2	56.9	4.5	724	278.2	-48.1	Ne
105	57°35'	25°16'	?	330	1357.3	154.5	3	223.5	58.4	5.3	539	244.1	-51.1	Ne
105	57°35'	25°16'	?	330	922.3	132.1	3	210.0	60.4	5.1	569	252.9	-60.4	Ne
d) Cerro Confuso														
104A	57°34'	25°11'	-	-	80.2	17.2	3	133.6	76.9	12.2	103	326.1	-40.4	P
104A	57°34'	25°11'	-	-	60.4	38.9	3	174.3	43.7	6.7	332	26.7	-84.8	P
104B	57°34'	25°11'	-	-	6.8	3.8	3	227.8	83.0	9.3	176	290.2	-33.9	P
104B	57°34'	25°11'	-	-	32.1	1.7	-	-	-	-	-	-	-	P
e) Lambaré														
101A	57°38'	25°24'	-	-	1400.7	109.8	3	135.3	70.9	13.2	88	337.5	-45.9	Ne
101A	57°38'	25°24'	-	-	1923.3	1570.8	3	308.9	-24.0	9.8	159	217.4	40.3	Ne
101B	57°38'	25°24'	-	-	2290.7	300.4	3	105.3	58.7	7.5	268	359.4	-27.1	Ne
101B	57°38'	25°24'	-	-	1561.0	171.7	3	115.6	55.5	5.1	574	4.7	-34.6	Ne
f) Tacumbú														
102	57°40'	25°21'	-	-	1513.3	426.9	3	151.5	37.3	4.9	636	36.2	-63.5	Ne
102	57°40'	25°21'	-	-	1492.2	120.6	2	165.1	33.7	20.5	150	55.9	-74.6	Ne

Code: A, Ankaratrite; Ne, Nephelinite; P, Phonolite.

cussed later this behaviour was especially noticed in the more evolved alkaline types.

Some sites showed anomalous results possibly caused by an isothermal magnetization due to lightning strikes as suggested by the extremely high NRM intensities; others are probably rolled blocks.

MAGNETIC PROPERTIES

Mesozoic rocks

Large variations in magnetic properties were observed between sites as indicated by the mean values per site of the susceptibility (k) and the intensity of the natural remanent magnetization (M_n) listed in Table 1. These variations are partially due to the varying chemical composition of the investigated rocks since the majority of the samples belong to the trachybasalt to trachyte (*sequence I*) and tephrite to peralkaline phonolite (*sequence II*) differentiation trends of De La Roche et al. (1980), the latter being more abundant.

Sequence I tends to show higher values of susceptibility than *sequence II* (Fig. 4) as a consequence of the higher content of iron oxides normally exhibited by the less evolved alkaline types. The medium destructive a.c. fields (MDF)

You have either reached a page that is unavailable for viewing or reached your viewing limit for this book.

You have either reached a page that is unavailable for viewing or reached your viewing limit for this book.

You have either reached a page that is unavailable for viewing or reached your viewing limit for this book.

this can be considered a good indication that the characteristic magnetizations of these rocks are of primary origin. Few sites have normal magnetization indicating that the magmatic activity in the area was of short duration.

Data from the two main chemical groups (*sequence I* in Fig. 8a and *sequence II* in Fig. 8b) do not show significant difference regarding the mean magnetization directions giving palaeomagnetic poles (Table 4) which are not statistically distinguishable although the shape of the data distributions differ slightly. This is an indication that although these rocks are of very similar age they were not emplaced simultaneously and therefore might have recorded different stages of the secular variation cycles.

Most of the sites with normal or transitional directions correspond to the more evolved alkaline types and occasionally they have been seen crosscutting others of reversed polarity. This was observed for example at sites 38, 49 and 50 indicating that normal polarity rocks are younger than most of the reversed ones. However, at site 32, a reversed-polarity dyke cutting a normal-polarity dyke was observed. Although based on this single observation, it is possible to assume that the magmatism lasted for at least three magnetic polarity intervals. Nevertheless, the main activity seems to have been concentrated in the first reversed interval. Flows and other intrusions, the host rock for the dykes, probably belong to the first reversed polarity chron since they are all of reversed polarity (Fig. 8c; except for one essexitic gabbro with anomalous direction).

The temporal relationship between the NW- and NE-trending systems is difficult to ascertain. Most of the younger normal polarity dykes trend NE. However, in this group secondary fractures of varying azimuths and widths of less than 0.5 m are included. When only the most important fracture system (dykes more than 1.0 m wide) are considered the small number of NE dykes allows no statistical comparison based on the magnetization directions.

The andesi-basalt flows of the Paraná Basin sampled on the western bank of the Paraná river recorded normal polarities (Fig. 8c) at the base of the sequence near Encarnación town changing to transitional directions (sites 110 to 112 in Table 2) upwards and culminating with a reversed direction (the andesi-basalt flow near Ybytyruzú, site 98) where the Paraná flows are closer to the alkaline rocks of the Central Province. It is worth noting that the trachyandesite dyke emplaced in that flow is of normal polarity. The reversed-polarity flow near Ybytyruzú is very well in accordance with the directions recorded by the alkaline flows. However, considering that the Lower Cretaceous geomagnetic field was a high frequency reversing field it may be not reasonable to expect that this Paraná flow and the alkaline rocks were emplaced during the same polarity chron.

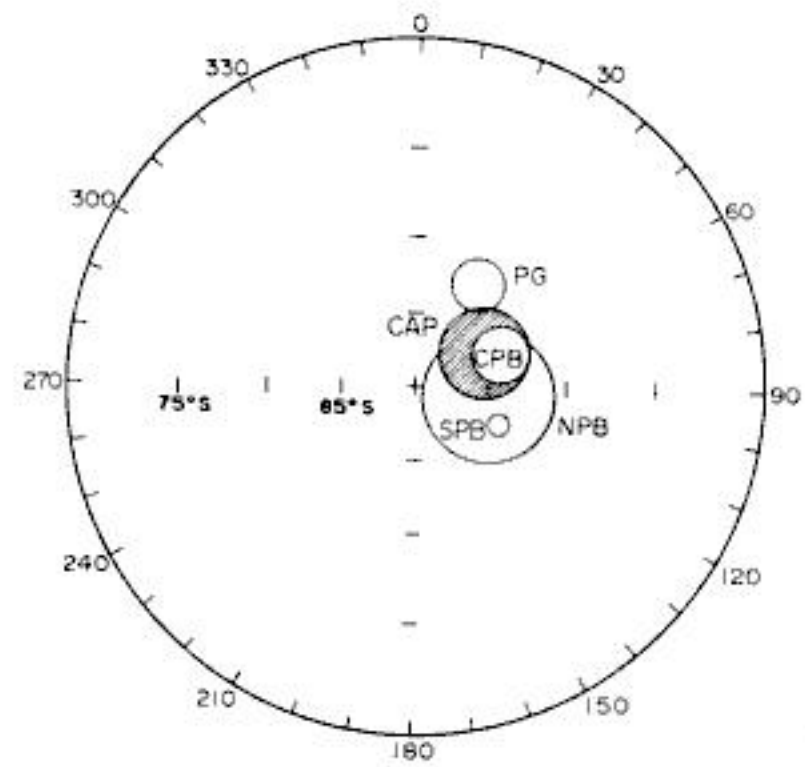

Figure 9 - Mean palaeomagnetic pole for the Mesozoic alkaline rocks of the Central Province (shaded area coded CAP) along with the Southern (SPB), Central (CPB) and Northern (NPB) Paraná Basin poles (Ernesto et al., 1988) and the Ponta Grossa (PG) dykes pole (Raposo & Ernesto, 1995) represented by their A_{95} confidence circles.

A well determined palaeomagnetic pole (Table 4) has been computed for all reliable Mesozoic data from the Central Province, coded CAP in Table 4 and Figure 9. The CAP pole is in good agreement with the Serra Geral Formation poles (Fig. 9) computed by Ernesto & Pacca (1988). These poles correspond to the southern (SPB), central (CPB) and northern (NPB) Paraná Basin following the subdivision imposed by the variation in titanium content of those rocks (Piccirillo et al., 1988b). The NPB pole used here was modified to incorporate new data from the northeastern part of the basin (Diogo, 1989; unpublished data). The Ponta Grossa dykes (pole PG in Fig. 9) although also corresponding to the NPB was considered independently because palaeomagnetic and field evidence point to a

You have either reached a page that is unavailable for viewing or reached your viewing limit for this book.

You have either reached a page that is unavailable for viewing or reached your viewing limit for this book.

You have either reached a page that is unavailable for viewing or reached your viewing limit for this book.

de los complejos alcalinos del Paraguay. Zbl. Geol. Paläont. Teil. *I*:791-805.

MONTES-LAUAR, C.R. (1988) Estudo paleomagnético dos maciços alcalinos de Poços de Caldas, Passa Quatro e Itatiaia. M.Sc. Thesis, University of São Paulo, 101p.

MONTES-LAUAR, C.R. (1993) Paleomagnetismo de rochas magmáticas Mesozóico-Cenozóicas da Plataforma Sul-Americana. Ph.D. Thesis, University of São Paulo, 250p.

PALMIERI, J.H. (1973) El complejo alcalino de Sapucai (Paraguay Oriental). Ph.D. Thesis, University of Salamanca, 298p.

PALMIERI J.H. & ARRIBAS A. (1975) El complejo alcalino-potássico de Sapukai (Paraguay Oriental). Congr. Ibero-Americano de Geol. Econ., Buenos Aires, 2:267-300.

PICCIRILLO, E.M., BELLIENI, G.; COMIN-CHIARAMONTI, P.; ERNESTO, M.; MELFI, A.J.; PACCA, I.G.; USSAMI, N. (1988a) Significance of the Paraná flood volcanism in the disruption of western Gondwanaland. In: E. M. Piccirillo & A.J. Melfi (eds.) The Mesozoic flood volcanism of the Paraná Basin: petrogenetic and geophysical aspects. IAG-USP, São Paulo, p. 285-295.

PICCIRILLO, E.M.; MELFI, A.J.; COMIN-CHIARAMONTI, P.; BELLIENI, G.; ERNESTO, M.; MARQUES, L.S.; NARDY, A.J.R.; PACCA, I.G.; ROISEMBERG, A.; STOLFA, D. (1988b) Continental flood volcanism from the Paraná Basin (Brazil). In: J.D. MacDougall (ed.) Continental flood basalts. Kluwer Academic Publ., Dordrecht, The Netherlands, p.195-238.

POZZI, J.P.; WESTPHAL, M.; ZHOU, Y.X.; XING, L.S.; CHEN, X.Y. (1982) The position of the Lhasa block (South Tibet) during late Cretaceous time: new paleomagnetic results. Nature, *297*:319-321.

PROYECTO PAR 83/005 (1986) Mapa geologico del Paraguay 1:500000. Comissión Nacional de desarrollo Regional, Ministério de Defensa Nacional, Asunción.

RAPOSO, M.I.B. & ERNESTO, M. (1995) An Early Cretaceous paleomagnetic pole from Ponta Grossa dykes (Brazil): implications for the South America Mesozoic APWP. J. Gephys. Res., *100(310)*:20.095-20.109.

RENNE, P.R.; ERNESTO, M.; PACCA, I.G.; COE, R.S.; GLEN, J.M.; PRÉVOT, M.; PERRIN, M. (1992a) The age of Paraná flood volcanism, rifting of Gondwanaland, and the Jurassic-Cretaceous boundary. Science, *258*:975-979.

RENNE, P.R.; ERNESTO, M.; PACCA, I.G.; NARDY, A.J.R.; COE, R.S.; GLEN, J.M.; PRÉVOT, M.; PERRIN, M. (1992b) Age and duration of Paraná flood volcanism in Brazil. American Geophysical Union, 1992 Fall Meeting, EOS (suppl.), p.531-532.

SCHULT, A. & GUERREIRO, S.D.C. (1980) Palaeomagnetism of Upper Cretaceous volcanic rocks from Cabo de Santo Agostinho, Brazil. Earth Planet. Sci. Lett., *50*:311-315.

SOFFEL, H. (1972) Anticlockwise rotation of Italy between the Eocene and the Miocene: paleomagnetic evidence from the Colli Euganei, Italy. Earth Planet. Sci. Lett., *17*:207-210.

SOFFEL, H. (1975) The paleomagnetism of age dated Tertiary volcanites of the Monti Lessini (Northern Italy) and its implication for the rotation of Northern Italy. J. Geophys., *41*:385-400.

SONOKI, I.K. & GARDA, G.M. (1988) Idades K-Ar de rochas alcalinas do Brasil Meridional e Paraguai Oriental: compilação e adaptação às novas constantes de decaimento. Bol. IG-USP, Sér. Cient., *19*:63-85.

STORMER, J.R.F.; GOMES, C.B.; TORQUATO, J.R.F. (1975) Spinel-lherzolite nodules in basanite lavas from Asunción, Paraguay. Rev. Bras. Geoc., *5*:176-185.

ULBRICH, H.H.G.J. & GOMES, C.B. (1981) Alkaline rocks from continental Brazil. Earth Sci. Rev., *17*:135-145.

VALENCIO, D.A.; VILAS, J.F.; SOLA, P.; LOPEZ, M.G. (1983) Palaeomagnetism of Upper Cretaceous-Lower Tertiary igneous rocks from Central Argentina. Geophys. J.R. Astr. Soc., *73*:129-134.

VELÁZQUEZ, V.F.; GOMES, C.B.; CAPALDI, G.; COMIN-CHIARAMONTI, P.; ERNESTO, M.; KAWASHITA, K.; PETRINI, R.; PICCIRILLO, E.M. (1992) Magmatismo alcalino Mesozóico na porção centro-oriental do Paraguai: aspectos geocronológicos. Geochim. Brasil., *6*:23-35.

You have either reached a page that is unavailable for viewing or reached your viewing limit for this book.

You have either reached a page that is unavailable for viewing or reached your viewing limit for this book.

You have either reached a page that is unavailable for viewing or reached your viewing limit for this book.

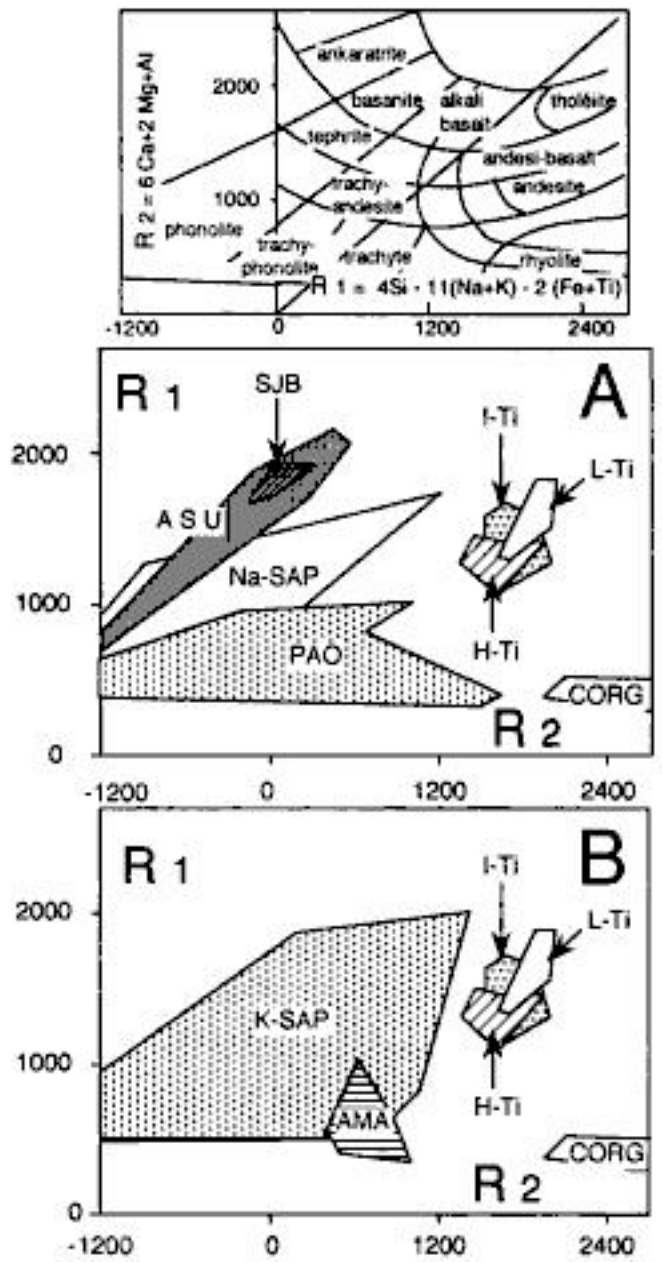

Figure 2 - Magmatic rocks from Eastern Paraguay projected in the R1-R2 diagram (R1 = 4Si - 11(Na + K) - 2(Fe + Ti), R2 = 6Ca + 2Mg + Al; De La Roche, 1986). A, and B: sodic and potassic alkaline associations compared with subalkaline ones, respectively. Data sources: Eckel, 1959; Bellieni et al., 1986; Comin-Chiaramonti et al., this volume, Appendix II and unpublished data; N = number of analyzed samples. CORG: Cambro-Ordovician rhyolites and granites of the Ciclo Brasiliano (N=34); PAO: Permo-Triassic alkaline (sodic) phonolites to trachytes and intrusive equivalents of Alto Paraguay (N=101) and Rio Apa (N=1) Provinces; L-Ti, I-Ti, H-Ti: Early Cretaceous stratoid volcanics and dykes (tholciitic basalts and andesi-basalts of Alto Paraná, = Serra Geral, Formation: low-titanium, L-Ti (TiO_2 < 2 wt %; N=12); intermediate titanium, I-Ti (2 ≤TiO_2≤ 3 wt %; N = 47); high titanium, H-Ti (TiO_2 > 3 wt %; N=43), respectively; AMA: Early Cretaceous alkaline (potassic) trachytes of the Amambay Province (N=12); K-SAP: Early Cretaceous alkaline (potassic) dykes, volcanics and intrusive equivalents of the Asunción-Sapucai graben (N=389); SJB: Early Cretaceous alkaline (sodic) rocks from the San Juan Bautista region (N=12); Na-SAP and ASU: Late Cretaceous to Oligocene alkaline (sodic) rocks of the Asunción-Sapucai Province (N=106).

Potassic and sodic rocks (see classification) forming dykes, plugs, lava domes, lava flows and shallow-level intrusive complexes (Fig. 3; cf. Comin-Chiaramonti et al., this volume, Appendix I) are unconformable on Palaeozoic to Mesozoic sandstones and tholeiitic stratoid volcanics of the Alto Paraná Formation (Serra Geral Formation of the Brazilian stratigraphy). The latter are widespread in the Ybytyruzú block (Fig. 3) at the eastern side of the graben, consisting of basaltic flow sequences up to 800 m thick.

Apatite fission track data (Hegarty et al., this volume) show two main peaks of tectonic activity at 120-70 Ma and 60-10 Ma, roughly corresponding to the waning of the potassic and sodic magmatisms, respectively.

As a whole, it is estimated that the volume of potassic rocks is less than 1,000 km^3, whereas that of the sodic rocks is lower by one order of magnitude. Therefore, this province is very small, compared with the flood basalts of the Paraná Basin (more than 750,000 km^3; Piccirillo & Melfi, 1988). However, this alkaline province is important in significantly extending the petrological spectrum of basaltic rocks related with the splitting of Western Gondwana, and in providing a more accurate insight of the subcontinental mantle sources of these basaltic rocks.

It is proposed to first introduce classification criteria and nomenclature of a representative specimen collection in order to designate the various occurrences in terms of certain chemical groups. These will be based on chemical data as the investigated specimens are mostly aphyric to microcrystalline and are best classified chemically rather than modally.

CLASSIFICATION AND NOMENCLATURE

Alkaline rocks may be distinguished in sodic or potassic. Conventionally, potassic rocks are those in which K_2O (wt %) exceeds Na_2O (wt %). Le Maitre (1989) suggested to apply the terms sodic and potassic to rocks with (Na_2O - 2) ≥ K_2O and (Na_2O - 2)≤ K_2O, respectively. Middlemost (1975) proposed 0.5<K_2O/Na_2O<2 and >2 for potassic and high-potassic groups, respectively, at SiO_2 ≤ 53.5 wt %.

The chemical screens adopted here are:

1) Na_2O - 2 ≥ K_2O: *sodic* (N);
2) Na_2O - 2 < K_2O to K_2O/Na_2O ≤ 1: *transitional* (tK);
3) 1 < K_2O/Na_2O ≤ 2: *potassic* (K);
4) K_2O/Na_2O > 2: *highly potassic* (HK).

You have either reached a page that is unavailable for viewing or reached your viewing limit for this book.

You have either reached a page that is unavailable for viewing or reached your viewing limit for this book.

You have either reached a page that is unavailable for viewing or reached your viewing limit for this book.

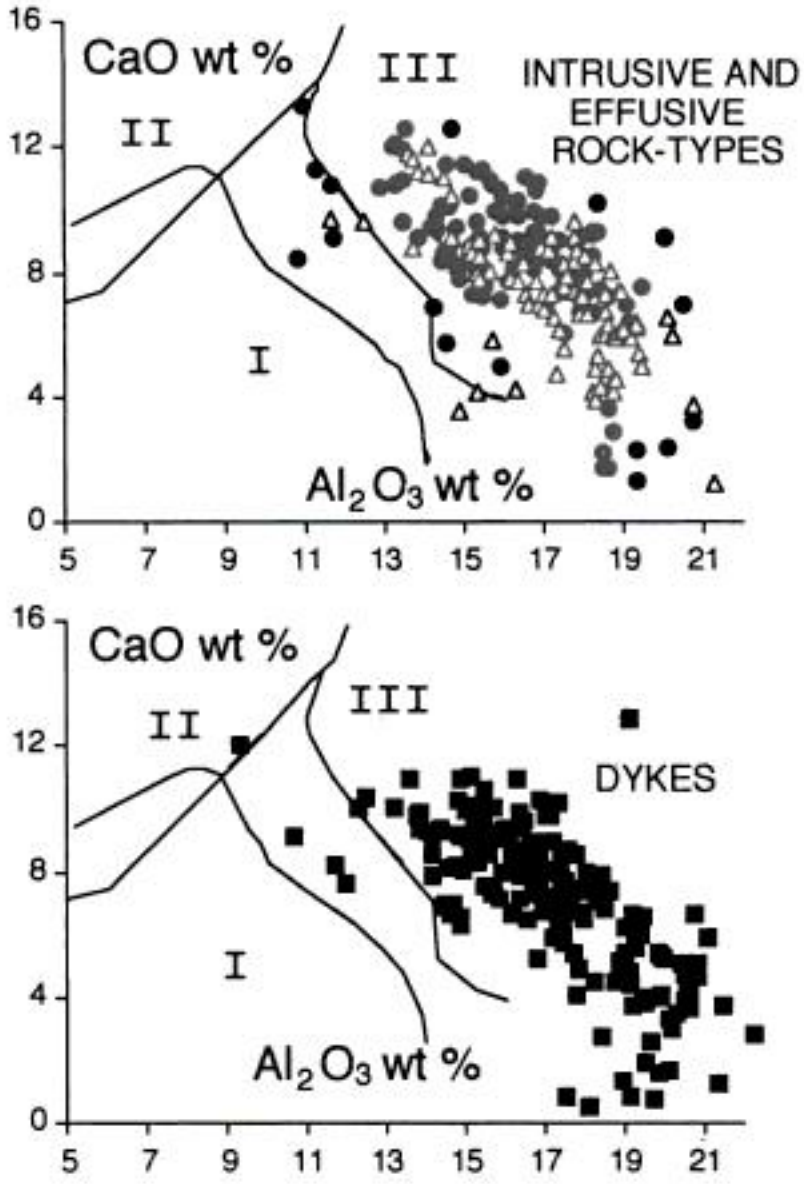

Figure 8 - CaO vs. Al_2O_3 (wt %, on a water-free basis) of the ASU potassic rocks. The lines are the boundaries of the groups as defined by Foley et al. (1987). Symbols: full circles=intrusives; open triangles=effusives; full squares=dykes.

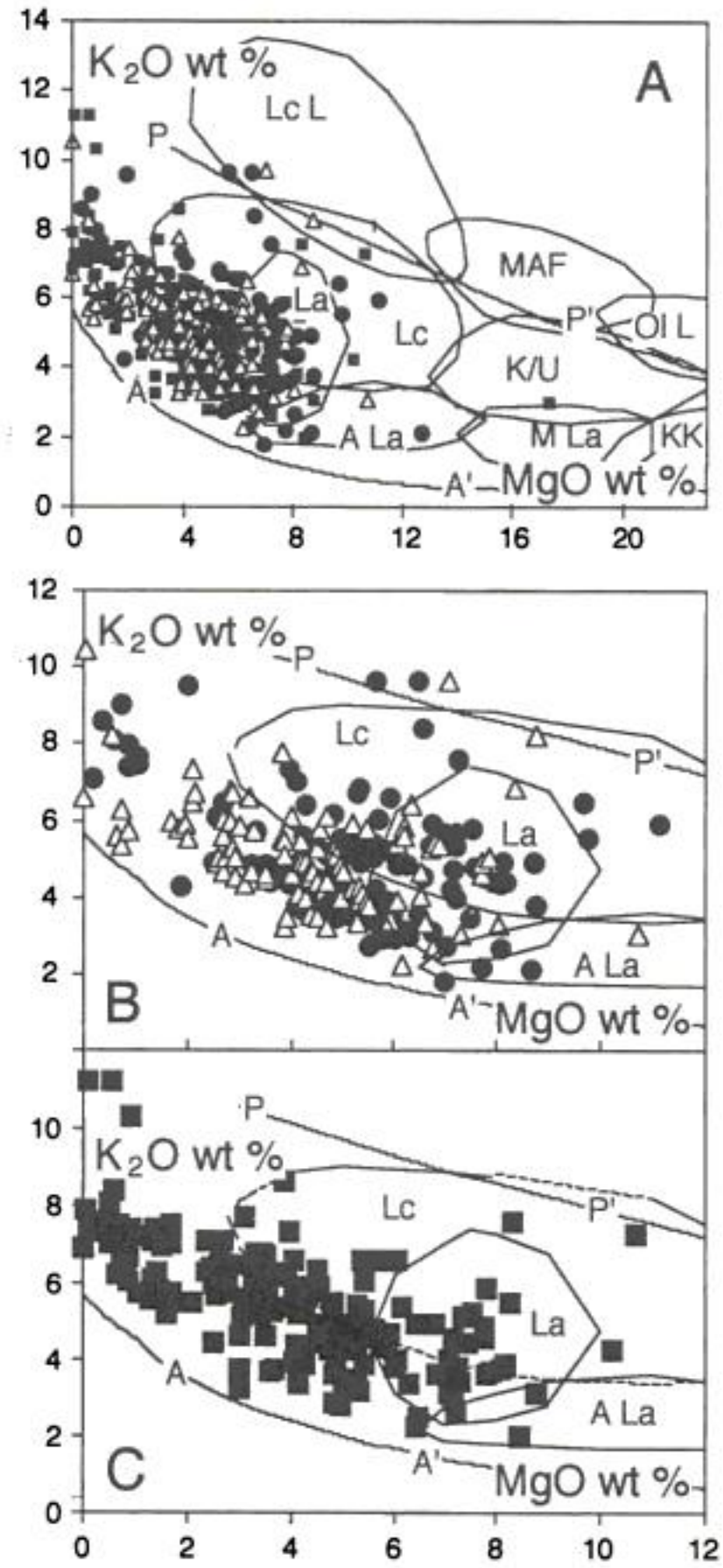

Figure 9 - ASU potassic rocks in terms of MgO vs. K_2O (wt %, on a water-free basis). Boundaries (A-A', alkalic; P-P', perpotassic) and fields (Lc L, leucite lamproites; MAF, mafurites; Ol L, olivine lamproites; Lc, leucitites; La, ordinary lamprophyres; K/U, katungites/ugandites; A La, alkaline lamprophyres; M La, melilitic lamprophyres; KK, kimberlite kindred) are from Middlemost (1986).
A, general diagram showing all the potassic rocks from ASU; B,intrusive + effusive rock-types; C, dykes (symbols as in Fig. 8).

occur as lava domes and dykes from various localities, mainly in the central ASU area (i.e. lava domes: areas 10, 21, 24, 26, 29, and E of Fig. 3; dykes: area 25 (twenty-four dykes), area 16 (three dykes) and area 12 (one dyke). Tephrites occur as plugs (area 9 of Fig. 3) and dykes (area 9: three dykes; area 25: two dykes; Fig. 3). Alkali basalts, hawaiites and mugearites occur as dykes (one dyke in each of areas 3, 23 and 33 in Fig. 3, respectively).

Notably, 18% of the whole population of the sampled dykes show both NW and NE strikes and crosscut the other occurrences of potassic rocks (Fig. 10).

Nephelinite and ankaratrite

Ankaratrites and nephelinites contain olivine, clinopyroxene and magnetite phenocrysts and microphenocrysts set in a hypocrystalline groundmass. The latter is composed of 40-49% vol salitic clinopyroxene (mg# 0.80-0.75), 7-16% vol olivine (Fo_{89-74}) and 4-8% vol titanomagnetite, interstitial glass, nepheline, accessory apatite and very rare alkali feldspar, plagioclase, carbonate and biotite microlites.

Mantle xenoliths and associated olivine, clinopyroxene, orthopyroxene and/or spinel xenocrysts are abundant in the ASU ankaratrites/ nephelinites.

You have either reached a page that is unavailable for viewing or reached your viewing limit for this book.

You have either reached a page that is unavailable for viewing or reached your viewing limit for this book.

You have either reached a page that is unavailable for viewing or reached your viewing limit for this book.

HK variants are characterized by clinopyroxene ($Wo_{44-51}En_{47-36}Fs_{9-16}$), olivine ($Fo_{67-60}$), Ti-biotite, Ti-magnetite with ilmenite exsolutions, leucite/pseudoleucite, alkali feldspar, nepheline, occasional K-magnesio katophorite, and accessory apatite and zircon.

K variants from the eastern ASU show clinopyroxene ($Wo_{43-49}En_{44-37}Fs_{13-15}$), occasionally with uralite rims (kaersutite), olivine (Fo_{76-53}), Ti-biotite, Ti-magnetite, alkali feldspar, pseudoleucite and/or nepheline and accessory plagioclase (An_{30-23}), sphene, apatite and zircon.

K variants from the western ASU systematically yielded strongly zoned plagioclase (An_{76-10}) as the most important phase and subordinate clinopyroxene ($Wo_{45-50}En_{41-31}Fs_{13-22}$), alkali feldspar ($Or_{81-33}$), nepheline/analcime ($Ne_{80-64}Ks_{13-23}$), olivine ($Fo_{76-50}$), Ti-biotite, Ti-magnetite and ilmenite, amphibole (ferroan pargasite to Mg-hastingsite) and accessory apatite and zircon.

tK variants are rare and they are characterized by clinopyroxene ($Wo_{49-50}En_{42-37}Fs_{9-13}$) alkali feldspar ($Or_{94-56}$), plagioclase ($An_{50-10}$), Ti-biotite, Ti-magnetite, olivine (Fo_{60-35}), nepheline and accessory apatite and zircon.

Nepheline syenite

K variants are pegmatoid facies with dominant alkali feldspar and nepheline, subordinate

Table 1 - Modal analyses of ASU intrusive, potassic rocks. Numbers as in Comin-Chiaramonti et al. (this volume, Appendix I). Modal constituents (vol %): Af, alkali feldspar; Pl, plagioclase; Fd, feldspathoids; Ol, olivine; Cpx, clinopyroxene; M, mica (biotite/phlogopite); Am, amphibole; Op, opaques; Ac, accessory minerals (mainly apatite and zircon); M', Colour index.

	Cerro Km 23							*Cerro San Benito*					*C.E.S. Helena*	
	18	19	20	21	22	23	24	25	27	28	29	30	38	39
	PS544A	PS544	PS540	PS539	PS543	PS542	PS541	PS536	PS535	PS538	PS537	PS534	PS529	PS530
Af	13.8	31.9	31.4	36.8	24.0	27.1	31.6	32.8	35.1	29.6	27.1	30.6	32.0	5.2
Pl	3.3	5.2	8.0	7.2	4.8	6.4	7.1	0.0	0.0	0.0	2.5	0.2	0.5	0.0
Fd	30.8	19.6	21.6	18.8	19.2	17.8	12.2	24.9	24.8	28.4	28.9	23.5	25.5	40.4
Ol	4.7	2.3	1.1	1.0	0.4	0.0	0.0	0.0	0.0	5.5	7.6	1.3	6.8	1.3
Cpx	37.9	28.2	27.8	25.1	33.6	31.7	33.3	27.0	25.7	30.5	27.4	31.2	25.3	38.2
M	3.5	3.7	3.5	4.2	12.3	11.1	8.4	6.8	7.3	1.0	1.0	6.6	4.0	9.2
Am	0.0	0.7	0.4	0.0	0.0	0.0	0.0	0.0	0.0	0.0	0.0	0.0	0.0	0.0
Op	5.4	6.4	5.3	6.0	4.7	4.8	6.5	7.3	5.4	4.6	5.0	5.4	5.1	5.4
Ac	0.6	1.0	0.9	0.9	1.0	1.1	0.9	1.3	1.7	0.4	0.5	1.2	0.8	0.3
M'	51.5	41.3	38.1	36.3	51.0	47.6	48.2	41.1	38.4	41.6	41.0	44.5	41.2	54.1
F	64	34	35	30	40	35	21	43	41	49	50	43	44	89
A	29	57	52	59	50	53	53	57	59	51	46	56	55	11
P	7	9	13	11	10	12	26	0	0	0	4	1	1	0

	Mbocayaty		*Aguapety Portón*				*Cañada*		*Cerro Chobí*					
	47	51	52	56	63	66	77	78	80	81	82	83	84	85
	PS263	3152	PS264	PS268	PS273	3147	PS245	PS243	PS583	PS584	PS585	PS586	PS587	PS588
Af	45.7	23.7	21.4	6.5	41.0	34.7	0.0	28.6	39.5	25.2	20.3	31.5	32.2	35.1
Pl	0.0	0.0	0.0	0.0	0.0	1.0	0.0	0.0	0.0	0.0	0.0	0.0	2.6	0.6
Fd	15.5	11.7	27.6	14.4	15.7	17.6	29.5	19.2	20.8	20.1	24.0	20.7	17.7	21.2
Ol	4.1	10.9	7.1	11.8	4.6	6.5	2.8	2.9	1.0	0.0	4.1	0.0	0.0	1.2
Cpx	20.8	39.1	36.4	54.1	25.4	30.2	45.6	31.6	28.0	37.7	34.6	25.2	27.0	22.7
M	6.0	6.7	1.7	3.1	4.0	3.4	18.8	12.5	4.8	7.4	8.6	14.7	12.1	9.0
Am	0.9	2.1	0.0	0.0	3.7	0.0	0.0	0.0	0.0	0.0	0.0	0.0	0.0	0.0
Op	6.2	5.1	4.6	8.2	5.0	5.7	3.0	4.5	4.9	6.6	8.0	6.7	7.6	8.5
Ac	0.8	0.7	1.1	1.9	0.6	0.9	0.3	0.7	1.0	3.0	0.8	1.2	0.8	1.7
M'	38.0	63.9	49.8	77.2	42.7	45.8	70.2	51.5	38.7	51.7	55.3	46.6	46.7	41.4
F	25	33	56	69	28	33	100	40	34	44	54	40	34	37
A	75	67	44	31	72	65	0	60	66	56	46	60	61	62
P	0	0	0	0	0	2	0	0	0	0	0		5	1

You have either reached a page that is unavailable for viewing or reached your viewing limit for this book.

You have either reached a page that is unavailable for viewing or reached your viewing limit for this book.

You have either reached a page that is unavailable for viewing or reached your viewing limit for this book.

You have either reached a page that is unavailable for viewing or reached your viewing limit for this book.

You have either reached a page that is unavailable for viewing or reached your viewing limit for this book.

You have either reached a page that is unavailable for viewing or reached your viewing limit for this book.

You have either reached a page that is unavailable for viewing or reached your viewing limit for this book.

MIN, A.; VELÁZQUEZ, V.F.; COMIN-CHIARAMONTI, P. (this volume) Alkaline magmatism from northern Paraguay (Alto Paraguay): a Permo-Triassic province.

HARLAND, W.B.; COX, A.V.; LLEWELLIN P.G.; PICKTON, C.A.; SMITH, A.G.; WALTERS, R. (1982) A geological time scale. Cambridge University Press, 131p.

HEGARTY K.A.; DUDDY, I.R.; GREEN, P.F. (this volume) The thermal history in around the Paraná Basin using apatite fission track analysis - Implications for hydrocarbon occurrences and basin formation.

LE BAS, M.J.; LE MAITRE, R.W.; WOOLLEY, A.R. (1992) The construction of the Total Alkali-Silica chemical classification of volcanic rocks. Mineralogy and Petrology, *46*:1-22.

LE MAITRE, R.W. (1989) A classification of igneous rocks and glossary of terms. Blackwell Sci. Publ., Oxford, 193p.

LIVIERES, R.A. & QUADE, H. (1987) Distribución regional y asentamiento tectónico de los complejos alcalinos del Paraguay. Zbl. Geol. Paläont., Teil I, *7/8*:791-805.

MAALØE, S. & PRINZLAU, I. (1979) Natural partial melting of spinel lherzolite. J. Petrol., *20*:727-741.

MARIANO, A.N. & DRUECKER, M.D. (1985) Alkaline igneous rocks and carbonatites of Paraguay. Geol. Soc. Amer., Abstracts with Programs, *17*, p.166.

MIDDLEMOST, E.A.K. (1986) The nomenclature and origin of the noncumulate ultramafic rocks and the systematic position of the kimberlites. Geol. Soc. Australia, Abstracts, *16*:72-74.

MITCHELL, R.H. & BERGMAN, S.C. (1991) Petrology of lamproites. Plenum Press, New York, 447p.

NORTHFLEET, A.; MEDEIROS, R.; MÜHLMANN, H. (1969) Reavaliação dos dados geológicos da Bacia do Paraná. Bol. Técn. Petrobrás, *12*:291-346.

ODIN, G.S.; CURRY, D.; GALE, N.H.; KENNEDY, W.J. (1982) The Phanerozoic time scale in 1981. In: G.S. Odin (ed.) Numerical Dating in Stratigraphy, vol. 2. John Wiley, New York, p.957-960.

PALMER, A.R. (1983) The decade of North America geology. 1983 geologic time scale. Geology, *11*:503-504.

PICCIRILLO, E.M. & MELFI, A.J. (eds.) (1988).The Mesozoic flood volcanism of the Paraná Basin: petrogenetic and geophysical aspects. IAG-USP, São Paulo, 600p.

RENNE, P.R.; ERNESTO, M.; PACCA, I.G.; COE, R.S.; GLEN, J.M.; PRÉVOT, M.; PERRIN, M. (1992) The age of Paraná flood volcanism, rifting of Gondwanaland, and the Jurassic-Cretaceous boundary. Science, *258*:975-979.

STRECKEISEN, A. (1976) To each plutonic rock its proper name. Earth Sci. Rev., *12*:1-33.

TURNER, S.; REGELOUS, M.; KELLEY, S.; HAWKESWORTH, C.; MANTOVANI, M. (1994) Magmatism and continental break-up in the South Atlantic: high precision ^{40}Ar-^{39}Ar geochronology. Earth Planet. Sci. Lett., *121*:333-348.

VELÁZQUEZ V.F.; GOMES, C.B.; COMIN-CHIARAMONTI, P.; ERNESTO, M.; KAWASHITA, K.; PETRINI, R.; PICCIRILLO, E.M. (1992) Magmatismo alcalino mesozóico na porção centro-oriental do Paraguai: aspectos geocronológicos. Geochim. Brasil., *6*:23-35.

WILSHIRE, H.G. & SHERVAIS, J.W. (1975) Al-augite and Cr-diopside ultramafic xenoliths in basaltic rocks from the Western United States. Phys. Chem. Earth, *9*:257-272.

You have either reached a page that is unavailable for viewing or reached your viewing limit for this book.

You have either reached a page that is unavailable for viewing or reached your viewing limit for this book.

You have either reached a page that is unavailable for viewing or reached your viewing limit for this book.

You have either reached a page that is unavailable for viewing or reached your viewing limit for this book.

You have either reached a page that is unavailable for viewing or reached your viewing limit for this book.

You have either reached a page that is unavailable for viewing or reached your viewing limit for this book.

You have either reached a page that is unavailable for viewing or reached your viewing limit for this book.

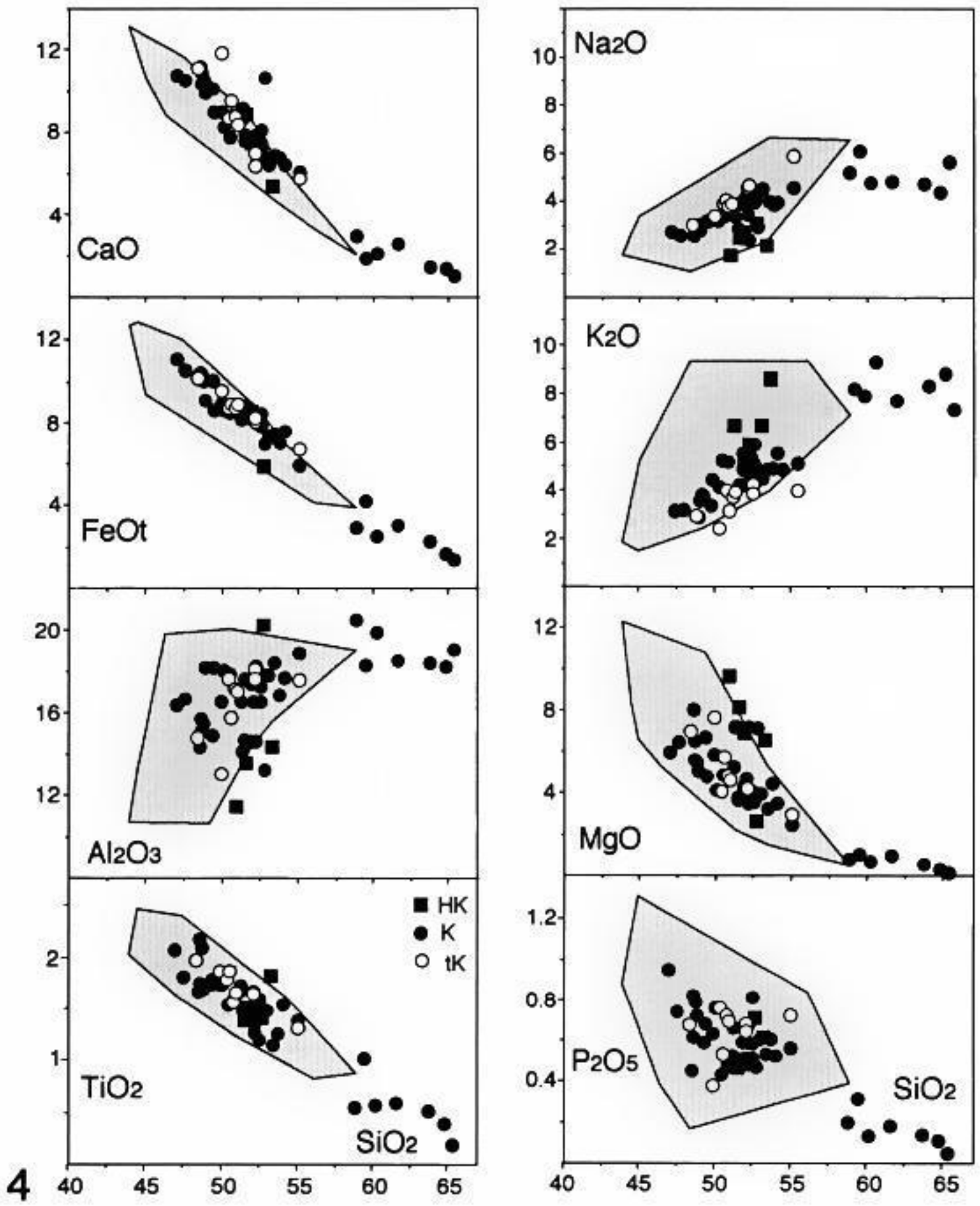

Figure 5A - SiO_2 vs. major elements (wt %) for intrusives of the AB-T suite. Dotted area: variation of the B-P suite. Other symbols as in Fig. 4A.

You have either reached a page that is unavailable for viewing or reached your viewing limit for this book.

You have either reached a page that is unavailable for viewing or reached your viewing limit for this book.

You have either reached a page that is unavailable for viewing or reached your viewing limit for this book.

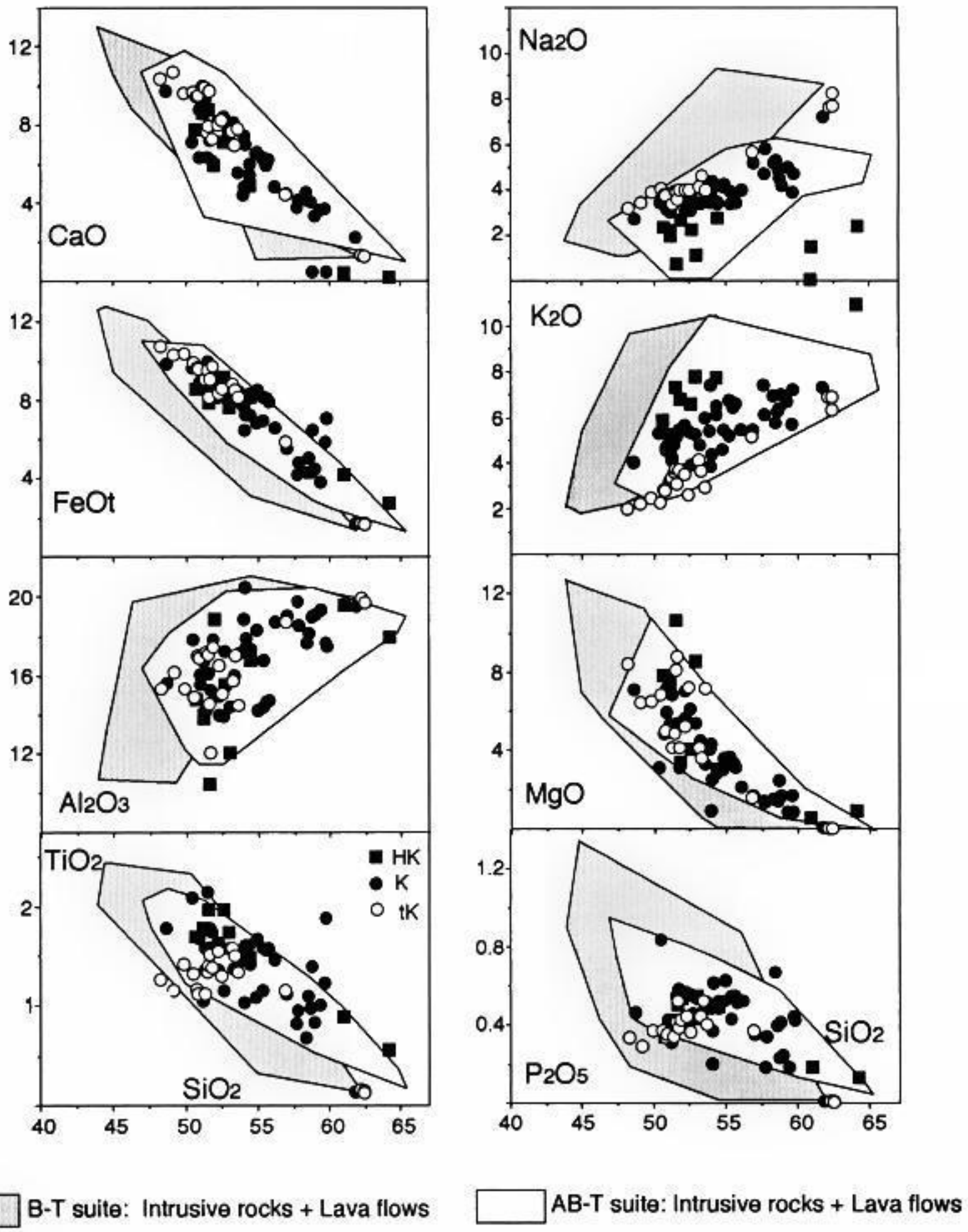

Figure 9A - SiO_2 vs. major elements (wt %) for dykes of the AB-T suite. Symbols as in Fig. 4A.

You have either reached a page that is unavailable for viewing or reached your viewing limit for this book.

You have either reached a page that is unavailable for viewing or reached your viewing limit for this book.

You have either reached a page that is unavailable for viewing or reached your viewing limit for this book.

Table 1-A. Average major (wt %) and trace (ppm) element contents for rocks with $SiO_2 \leq 54$ wt %, B-P suite (standard deviations in parentheses); HK, K, tK: highly potassic, potassic and transitional potassic groups, respectively; N, number of samples.

	B-P SUITE												
	INTRUSIVE ROCKS				LAVA FLOWS				DYKES				WHOLE
	HK (N=9)	K (N=54)	tK (N=13)	TOTAL (N=77)	HK (N=2)	K (N=31)	tK (N=7)	TOTAL (N=40)	HK (N=2)	K (N=59)	tK (N=19)	TOTAL (N=80)	LINEAGE (N=197)
wt %													
SiO_2	50.29 (2.14)	49.96 (1.91)	49.75 (2.92)	50.08 (2.33)	48.66 (1.61)	50.28 (1.39)	50.01 (1.88)	50.15 (1.49)	51.00 (2.97)	50.33 (2.67)	50.25 (1.41)	50.33 (1.59)	50.20 (1.86)
TiO_2	1.67 (0.19)	1.70 (0.22)	1.77 (0.46)	1.70 (0.28)	1.90 (0.02)	1.63 (0.20)	1.48 (0.44)	1.62 (0.26)	1.70 (0.38)	1.68 (0.32)	1.80 (0.34)	1.71 (0.33)	1.69 (0.30)
Al_2O_3	14.04 (1.60)	15.54 (1.92)	16.19 (1.44)	15.52 (1.91)	14.46 (0.02)	17.17 (1.81)	16.28 (2.76)	16.88 (2.03)	16.08 (0.59)	16.64 (1.89)	15.30 (1.66)	16.31 (1.89)	16.12 (1.93)
FeOt	8.46 (1.25)	9.04 (1.05)	9.29 (1.95)	8.95 (1.38)	9.99 (0.78)	8.89 (1.08)	9.09 (2.15)	9.01 (1.32)	7.88 (0.87)	8.90 (1.32)	9.32 (1.15)	8.97 (1.29)	8.97 (1.33)
MnO	0.15 (0.03)	0.17 (0.02)	0.17 (0.03)	0.17 (0.03)	0.17 (0.02)	0.16 (0.01)	0.17 (0.01)	0.17 (0.01)	0.14 (0.01)	0.17 (0.02)	0.17 (0.02)	0.17 (0.02)	0.17 (0.02)
MgO	6.96 (1.91)	5.70 (1.77)	5.15 (1.74)	5.69 (1.90)	6.27 (0.11)	4.59 (1.46)	5.06 (2.49)	4.76 (1.66)	3.92 (0.06)	4.77 (1.71)	5.61 (1.58)	4.95 (1.69)	5.20 (1.76)
CaO	8.25 (1.98)	8.78 (1.32)	9.12 (1.96)	8.69 (1.70)	9.45 (0.93)	7.69 (1.47)	8.54 (3.11)	7.93 (1.84)	6.90 (0.12)	7.79 (1.52)	8.53 (0.85)	7.95 (1.41)	8.23 (1.61)
Na_2O	2.51 (0.66)	3.55 (0.64)	4.27 (1.05)	3.59 (0.92)	1.76 (0.98)	3.77 (0.61)	4.73 (1.67)	3.84 (1.05)	3.72 (0.11)	3.79 (0.71)	4.62 (0.72)	3.98 (0.79)	3.80 (0.89)
K_2O	7.09 (1.63)	4.90 (0.90)	3.54 (0.97)	4.96 (1.40)	6.14 (0.38)	5.23 (0.75)	4.20 (1.93)	5.10 (1.11)	7.99 (0.93)	5.39 (0.97)	3.80 (0.54)	5.07 (1.20)	5.03 (2.12)
P_2O_5	0.57 (0.23)	0.66 (0.19)	0.74 (0.24)	0.66 (0.21)	0.62 (0.34)	0.54 (0.11)	0.44 (0.19)	0.53 (0.14)	0.68 (0.02)	0.56 (0.16)	0.61 (0.17)	0.57 (0.16)	0.60 (0.18)
ppm													
Rb	175 (71)	98 (20)	64 (21)	108 (62)	145 (19)	104 (19)	71 (30)	101 (27)	203 (81)	109 (31)	68 (21)	101 (38)	103 (49)
Sr	1341 (356)	1639 (352)	1680 (318)	1609 (358)	2199 (161)	1713 (319)	1803 (455)	1753 (350)	1671 (64)	1797 (476)	1832 (104)	1803 (463)	1722 (440)
Zr	256 (36)	273 (69)	286 (55)	273 (72)	224 (52)	259 (55)	252 (144)	286 (75)	310 (78)	308 (74)	332 (125)	314 (88)	291 (88)
Y	16.5 (7.8)	21.1 (5.6)	22.3 (4.0)	21.5 (5.1)	19.5 (4.9)	19.3 (4.22)	16.1 (5.9)	18.8 (4.6)	17.5 (6.4)	20.7 (5.7)	22.1 (7.3)	21.0 (6.1)	21 (6)
Nb	38 (13)	41 (17)	36 (12)	40 (16)	44 (7)	44 (9)	43 (23)	44 (12)	54 (11)	51 (14)	54 (18)	52 (15)	45 (17)
Ba	1563 (129)	1470 (425)	1357 (334)	1463 (406)	1695 (226)	1578 (245)	1481 (456)	1566 (286)	1855 (112)	1527 (333)	1550 (458)	1540 (363)	1523 (392)
La	83 (36)	89 (27)	82 (9)	87(26)	83 (0)	92 (14)	85 (32)	90 (18)	103 (6)	96 (22)	103 (27)	98 (23)	92 (25)
Ce	158 (67)	161 (42)	153 (20)	159 (42)	140 (13)	161 (24)	143 (40)	157 (27)	187 (1)	168 (36)	181 (46)	171 (38)	162 (40)
Nd	60 (20)	72 (14)	75 (19)	68 (16)	64 (4)	67 (12)	57 (10)	65 (12)	68 (7)	68 (15)	75 (19)	70 (16)	68 (16)

You have either reached a page that is unavailable for viewing or reached your viewing limit for this book.

You have either reached a page that is unavailable for viewing or reached your viewing limit for this book.

You have either reached a page that is unavailable for viewing or reached your viewing limit for this book.

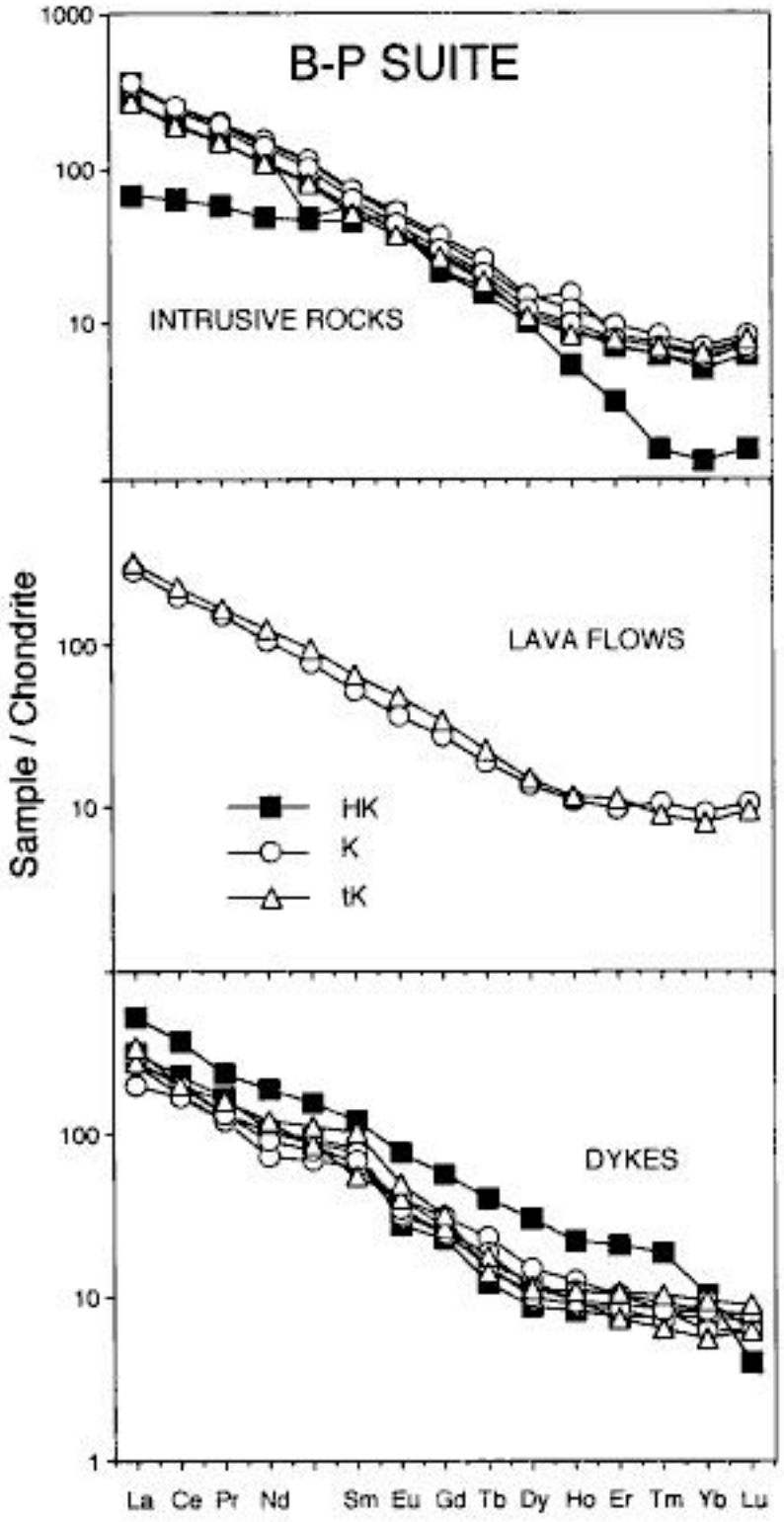

Figure 12 - Chondrite-normalized REE diagram for compositions from the B-P suite. HK, K and tK: highly potassic, potassic and transitional potassic groups, respectively. Normalizing values are from Boynton (1984).

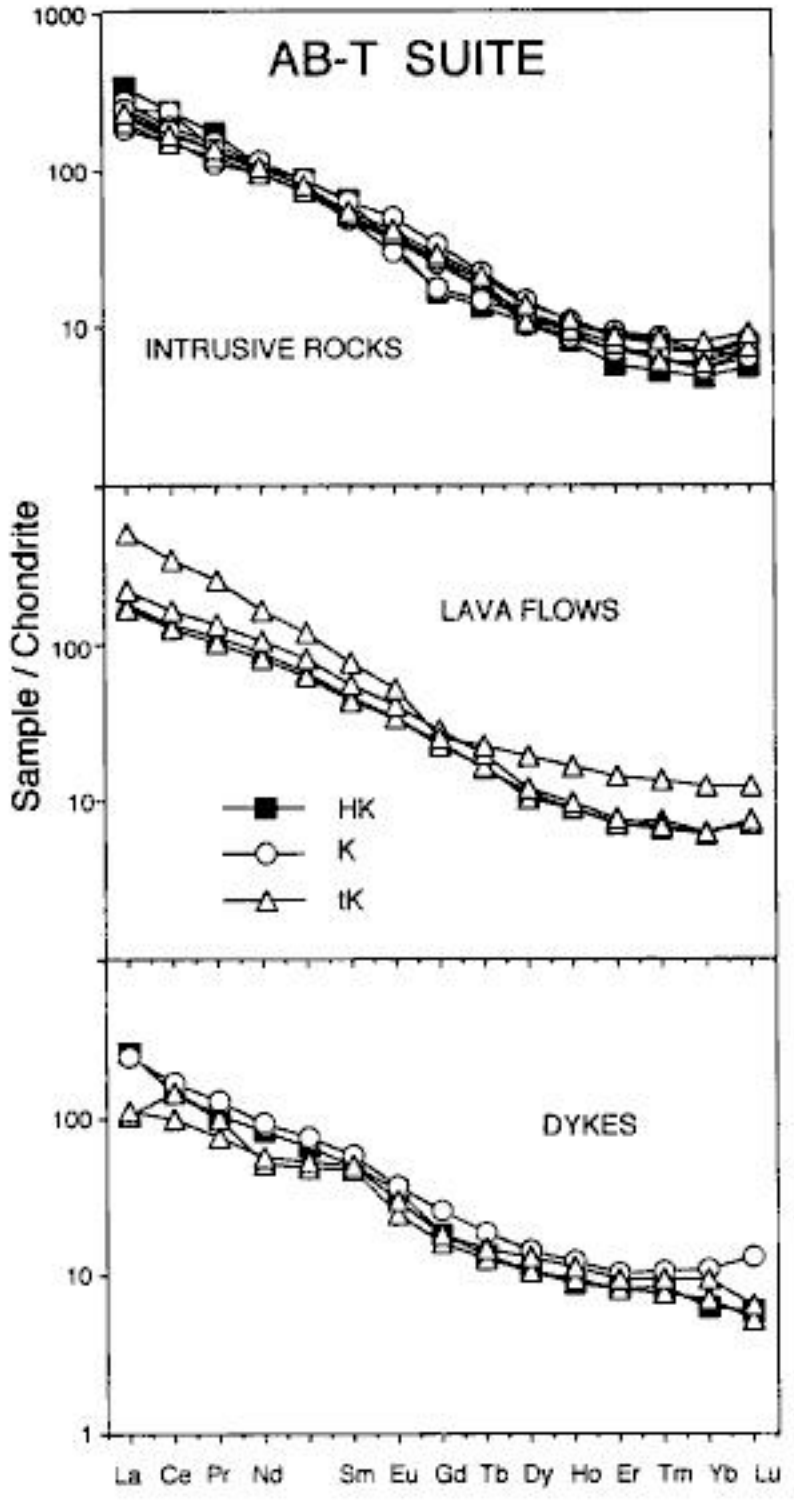

Figure 13 - Chondrite-normalized REE diagram for rocks from the AB-T suite. Symbols as in Fig. 12.

The origin of Eu anomalies has not been satisfactorily explained. Feldspar fractionation, cumulus processes, or mixtures of phenocryst (xenocryst)-loaded liquids from different stages of magmatic evolution (Comin-Chiaramonti et al., 1993) are plausible means for producing slightly deficiency or excess in Eu. However, it should be noted that both anomalies are present in the less evolved potassic compositions (mg#$\geq$0.6, for both groups), suggesting that these anomalies may have also been inherited from the magma source.

The incompatible element-enriched nature of the alkaline magma(s) of the Asunción-Sapucai graben is also apparent from the normalized trace element plots which include some of the REE data (Figs. 14 and 15).

In general, B-P and AB-T compositions have similar element enrichment patterns for large ion lithophile elements (LILE), i.e. Rb, Ba, and other incompatible elements like La, Ce, Sm and Tb. Th and U show relative enrichments in the lavas and dykes, but generally tend to be depleted.

The high-field-strenght elements (HFSE), particularly Ta, Nb and Ti, display marked depletion and yielded negative Ta/Nb-Ti anomalies. These anomalies were generally interpreted (e.g. Pearce, 1983; Thompson et al., 1984; Nelson, 1992) as characteristic of magmas generated in subduction-related environments.

In general, the B-P suite displays higher Ti, K, Zr, Nb, Y and REE contents than those shown by the AB-T one.

You have either reached a page that is unavailable for viewing or reached your viewing limit for this book.

You have either reached a page that is unavailable for viewing or reached your viewing limit for this book.

You have either reached a page that is unavailable for viewing or reached your viewing limit for this book.

INFLUENCE OF COOLING HISTORY ON Mg-Fe^{2+} INTRACRYSTALLINE DISTRIBUTION IN OLIVINES FROM PARAGUAY (ASUNCIÓN-SAPUCAI GRABEN)

F.Princivalle, D.Sabelli, M.Tirone

Alkaline Magmatism in Central-Eastern Paraguay. Relationships with Coeval Magmatism in Brazil. Comin-Chiaramonti, P. & Gomes, C. B. (eds.), 1996, Edusp/Fapesp, São Paulo, pp. 151-156.

ABSTRACT

The distribution of Mg-Fe^{2+} (K_D) between M1 and M2 sites in olivines is principally influenced by temperature and composition. These two factors produce the same effect because their increase cause an increase of Fe^{2+} in M1 (i.e. a K_D increase). Three olivines from Paraguay (Asunción-Sapucai graben) are considered: two from medium to coarse-grained essexitic rocks, and one from a fine-grained essexitic rock. The olivine intracrystalline configuration confirms that the Mg-Fe^{2+} exchange is primarily controlled by temperature variation coincident with conditions deduced from textural evidence.

INTRODUCTION

The cooling history of the rocks can be studied using the intracrystalline Mg-Fe^{2+} exchange reaction between M1 and M2 sites of olivines. In fact, olivines are not only important and common rock-forming minerals, but as a consequence of two very similar cationic sites (M1 and M2) the Mg-Fe^{2+} exchange reaction may continue even at temperatures lower than 500°C as indicated by Ottonello et al. (1990) and Princivalle (1990).

Several factors such as temperature, composition, oxygen fugacity and pressure may influence the intracrystalline Mg-Fe^{2+} distribution in olivine. This exchange reaction is evaluated as follows:

$$Fe^{2+}_{M1}+Mg_{M2} \leftrightarrow Fe^{2+}_{M2}+Mg_{M1}$$

The effect of temperature over the quoted exchange reaction was studied by using heating experiments.

Brown & Prewitt (1973) and Smith & Hazen (1973) performed experiments at 375 and 710°C, and 300 and 600°C, respectively. Only at temperatures of 600°C (Smith & Hazen, 1973) and 710°C (Brown & Prewitt, 1973) it was found a significant Fe^{2+} ordering in M1 , i.e. increase of $(Fe^{2+}/Mg)_{M1}/(Fe^{2+}/Mg)_{M2}$ ratio (K_D).

Aikawa et al. (1985) carried out heating experiments on olivine Fa_{33} in the 700-1000°C range, followed by a "millisecond quenching technique". They have demonstrated that the quenching of Mg-Fe^{2+} distribution can be achieved only for temperatures lower than 800°C. In fact, at higher temperatures the rate of Mg-Fe^{2+} exchange is too high to obtain the quench, even with their quenching technique.

You have either reached a page that is unavailable for viewing or reached your viewing limit for this book.

You have either reached a page that is unavailable for viewing or reached your viewing limit for this book.

You have either reached a page that is unavailable for viewing or reached your viewing limit for this book.

BROWN, G.E. & PREWITT, C.T. (1973) High temperature crystal chemistry of hortonolite. Amer. Mineral., *58*:577-587.

GANGULY, D. (1977) Crystal chemical aspects of olivine structure. Neues Jb. Mineral Abh., *130*:303-318.

GHOSE, S.; WAN, C.; McCALLUM, I.S. (1976) Mg-Fe^{2+}order in an olivine from the lunar anorthosite 67075 and the significance of cation order in lunar and terrestrial olivines. Indian J. Earth Sci., *3*:1-8.

KISINA, N.R.; BELOKONEVA, L.; UKHANANOV, A.V.; URUSOV, S.V. (1985) Petrological consequences of the intracrystalline distributions of Fe and Mg in olivines. Translated from Geokhimiya, *2*: 153-162.

NOVER, G. & WILL, G. (1981) Structure refinement of seven natural olivine crystals and the influence of the oxygen partial pressure on cation distribution. Zeitschrift für Kristallographie, *155*:27-45.

OTTONELLO, G.; DELLA GIUSTA, A.; MOLIN, G.M. (1989) Cation ordering in Ni-Mg olivines. Amer. Mineral., *74*:411-421.

OTTONELLO, G.; PRINCIVALLE, F.; DELLA GIUSTA, A. (1990) Temperature, composition and fO_2 effects on intersite distribution of Mg and Fe^{2+} in olivines: experimental evidence and theoretical interpretation. Phys. Chem. Minerals, *17*:301-312.

PRINCIVALLE, F. (1990) Influence of temperature and composition on Mg-Fe^{2+} intracrystalline distribution in olivines. Mineral. Petrol., *43*:121-129.

PRINCIVALLE, F. & SECCO, L. (1985) Crystal structure refinement of 13 olivines in the forsterite-fayalite series from volcanic rocks and ultramafic nodules. Tschermaks Min. Petr. Mitt., *34*:105-115.

ROBINSON, K.; GIBBS, G.V.; RIBBE, P.H. (1971) Quadratic elongation: a quantitative measure of distortion in coordination polyhedra. Science, *172*:567-570.

SAXENA, S.K.; DOMENEGHETTI, M.C.; MOLIN, G.M.; TAZZOLI, V. (1989) X- ray diffraction study of Mg-Fe^{2+} order-disorder in orthopyroxene. Some kinetic result. Phys. Chem. Minerals, *16*:421-427.

SMITH, J.R. & HAZEN, R.M. (1973) The crystal structure of forsterite and hortonolite at several temperatures up to 900°C. Amer. Mineral., *58*:588-593.

WENK, H.R. & RAYMOND, K.N. (1973) Four new structure refinements of olivine. Zeitschrift für Kristallographie, *137*:86-105.

You have either reached a page that is unavailable for viewing or reached your viewing limit for this book.

You have either reached a page that is unavailable for viewing or reached your viewing limit for this book.

You have either reached a page that is unavailable for viewing or reached your viewing limit for this book.

Table 2 - Cell parameters and site geometry of the clinopyroxene samples.

Sample	G99		G5		G4		G3		G2		G1		G8		G6	
a	9.7477	(10)	9.7693	(8)	9.7678	(7)	9.7692	(10)	9.7576	(8)	9.7650	(10)	9.7732	(6)	9.7720	(11)
b	8.9192	(10)	8.9205	(11)	8.9183	(9)	8.9211	(13)	8.9225	(10)	8.9132	(14)	8.9075	(8)	8.9064	(14)
c	5.2589	(4)	5.2776	(4)	5.2791	(3)	5.2782	(4)	5.2696	(3)	5.2786	(5)	5.2919	(3)	5.2958	(5)
ß(°)	106.010	(10)	105.940	(7)	105.949	(6)	105.930	(10)	105.960	(7)	105.980	(10)	105.847	(5)	105.840	(10)
Vc	439.48		442.24		442.17		442.34		441.10		441.68		443.18		443.41	
Obs. Refl.	604		604		604		589		627		599		564		531	
R(%) (a)	1.86		1.54		1.49		1.63		1.80		1.99		1.75		2.20	
M1-O2	2.050	(1)	2.044	(1)	2.040	(1)	2.044	(1)	2.048	(1)	2.038	(1)	2.031	(2)	2.025	(2)
M1-O1A2	2.061	(1)	2.067	(1)	2.065	(1)	2.067	(1)	2.063	(1)	2.064	(1)	2.068	(1)	2.073	(2)
M1-O1A1	2.126	(1)	2.131	(1)	2.131	(1)	2.130	(1)	2.129	(1)	2.130	(1)	2.132	(1)	2.129	(2)
M1-O mean	2.079	(2)	2.081	(2)	2.079	(2)	2.080	(2)	2.080	(2)	2.077	(3)	2.077	(4)	2.076	(4)
VM1	11.892	(3)	11.915	(3)	11.873	(3)	11.905	(3)	11.906	(3)	11.853	(4)	11.844	(5)	11.815	(6)
λoct. (b)	1.0053		1.0057		1.0059		1.0058		1.0056		1.0059		1.0064		1.0065	
σ²oct. (c)	16.9916		18.2093		18.6510		18.5587		17.8890		18.6277		20.1984		20.7330	
M2-O2	2.325	(1)	2.342	(1)	2.342	(1)	2.344	(1)	2.337	(1)	2.342	(2)	2.365	(2)	2.367	(2)
M2-O1	2.354	(1)	2.363	(1)	2.364	(1)	2.362	(1)	2.360	(1)	2.364	(1)	2.378	(2)	2.377	(2)
M2-O3C1	2.571	(1)	2.572	(1)	2.569	(1)	2.570	(1)	2.572	(1)	2.569	(1)	2.555	(2)	2.557	(2)
M2-O3C2	2.729	(1)	2.721	(1)	2.723	(1)	2.723	(1)	2.725	(1)	2.718	(1)	2.711	(1)	2.711	(2)
M2-O mean	2.495	(3)	2.500	(3)	2.500	(3)	2.500	(3)	2.499	(3)	2.498	(3)	2.502	(5)	2.503	(5)
VM2	25.637	(6)	25.817	(5)	25.817	(5)	25.830	(5)	25.763	(5)	25.788	(6)	25.948	(8)	25.961	(6)
T-O2	1.591	(1)	1.598	(1)	1.600	(1)	1.597	(1)	1.594	(1)	1.601	(1)	1.605	(2)	1.607	(2)
T-O1	1.605	(1)	1.614	(1)	1.615	(1)	1.615	(1)	1.611	(1)	1.615	(1)	1.622	(1)	1.625	(1)
T-Onobr	1.598		1.606		1.608		1.606		1.603		1.608		1.614		1.616	
T-O3A1	1.666	(1)	1.671	(1)	1.670	(1)	1.670	(1)	1.669	(1)	1.670	(1)	1.673	(1)	1.672	(2)
T-O3A2	1.688	(1)	1.692	(1)	1.692	(1)	1.691	(1)	1.683	(1)	1.692	(2)	1.690	(2)	1.690	(3)
T-Obr	1.677		1.682		1.681		1.681		1.676		1.681		1.682		1.681	
T-O mean	1.638	(2)	1.644	(2)	1.644	(2)	1.643	(2)	1.639	(2)	1.645	(3)	1.648	(3)	1.649	(4)
VT	2.234	(1)	2.259	(1)	2.262	(1)	2.260	(1)	2.247	(1)	2.263	(2)	2.276	(2)	2.281	(3)
λtet. (d)	1.0063		1.0061		1.0062		1.0061		1.0061		1.0061		1.0057		1.0056	
σ²tet. (e)	26.9145		25.7170		26.2140		25.6481		25.7280		25.7652		24.0998		23.6643	
ΔSi(f)	0.079		0.075		0.074		0.075		0.074		0.073		0.068		0.065	

Sample	53CC		530C		530S		245C		245D		201A	
a	9.7547	(7)	9.7552	(7)	9.7605	(8)	9.7562	(10)	9.7657	(8)	9.7605	(6)
b	8.9233	(9)	8.9182	(9)	8.9015	(11)	8.9214	(13)	8.9231	(11)	8.9239	(8)
c	5.2640	(3)	5.2683	(3)	5.2867	(4)	5.2696	(4)	5.2747	(4)	5.2714	(3)
ß(°)	105.997	(6)	105.987	(6)	105.951	(7)	105.938	(8)	105.882	(7)	105.947	(5)
Vc	440.46		440.61		441.64		441.03		442.09		441.48	
Obs. Refl.	560		566		552			563	574		568	
R(%) (a)	2.16		2.60		1.99		1.86		1.82		1.74	
M1-O2	2.048	(2)	2.045	(2)	2.028	(2)	2.049	(1)	2.044	(1)	2.044	(1)
M1-O1A2	2.061	(2)	2.059	(1)	2.061	(1)	2.062	(1)	2.066	(1)	2.066	(1)
M1-O1A1	2.129	(2)	2.128	(2)	2.130	(1)	2.126	(1)	2.129	(1)	2.130	(1)
M1-O mean	2.079	(4)	2.077	(4)	2.073	(4)	2.079	(2)	2.080	(2)	2.080	(2)
VM1	11.894	(6)	11.856	(6)	11.771	(5)	11.882	(3)	11.891	(3)	11.908	(3)
λoct. (b)	1.0056		1.0058		1.0064		1.0057		1.0058		1.0057	
σ²oct. (c)	17.6437		18.3676		20.1476		18.2215		18.6116		18.4078	
M2-O2	2.333	(2)	2.335	(2)	2.350	(1)	2.342	(1)	2.351	(1)	2.325	(1)
M2-O1	2.358	(2)	2.359	(2)	2.367	(1)	2.364	(1)	2.370	(1)	2.354	(1)
M2-O3C1	2.574	(2)	2.572	(2)	2.561	(2)	2.567	(1)	2.564	(1)	2.571	(1)
M2-O3C2	2.727	(2)	2.725	(2)	2.710	(2)	2.725	(1)	2.724	(1)	2.729	(1)
M2-O mean	2.498	(5)	2.498	(5)	2.497	(5)	2.500	(3)	2.502	(3)	2.495	(3)
VM2	25.743	(10)	25.743	(10)	25.745	(9)	25.807	(6)	25.913	(6)	25.637	(5)
T-O2	1.593	(2)	1.594	(2)	1.604	(2)	1.591	(1)	1.595	(1)	1.594	(1)
T-O1	1.608	(2)	1.612	(1)	1.621	(1)	1.610	(1)	1.611	(1)	1.612	(1)
T-Onobr	1.601		1.603		1.613		1.601		1.603		1.603	
T-O3A1	1.666	(2)	1.667	(2)	1.676	(2)	1.669	(1)	1.668	(1)	1.669	(1)
T-O3A2	1.691	(3)	1.689	(3)	1.689	(3)	1.690	(1)	1.692	(1)	1.686	(1)
T-Obr	1.679		1.678		1.683		1.680		1.680		1.678	
T-O mean	1.640	(4)	1.641	(4)	1.648	(3)	1.640	(2)	1.642	(2)	1.640	(2)
VT	2.242	(2)	2.247	(2)	2.276	(2)	2.244	(2)	2.251	(1)	2.246	(1)
λtet.(d)	1.0062		1.0062		1.0060		1.0063		1.0063		1.0060	
σ²tet.(e)	26.1443		26.1051		25.5300		26.8261		26.8365		25.3271	
ΔSi(f)	0.078		0.075		0.070		0.079		0.077		0.074	

(a) R%=| |ΣFo|-|ΣFc| | / |ΣFo|

(b) λoct. (Robinson et al., 1971) defined by: $\sum_{i=1}^{6} (\lambda i / \lambda o)\ 2 / 6 = 112$

(c) σ^2oct. (Robinson et al., 1971) defined by: $\sum_{i=1}^{12} (\theta_i / 90)\ 2 / 11 = 14$

(d) λtet. (Robinson et al., 1971) defined by: $\sum_{i=1}^{4} (\lambda i / \lambda o)\ 2 / 4 = 112$

(e) σ^2oct. (Robinson et al., 1971) defined by: $\sum_{i=1}^{5} (\theta_i / 109.47)\ 2 / 5 = 1$

(f) ΔSi (Mozimoto et al., 1975) defined by: T-Obr-T-Onbr

You have either reached a page that is unavailable for viewing or reached your viewing limit for this book.

You have either reached a page that is unavailable for viewing or reached your viewing limit for this book.

You have either reached a page that is unavailable for viewing or reached your viewing limit for this book.

Table 3 (continuation).

Sample	53CC-49	53CC-50	53CC-51	53CC-52	53CC-53	Avg. of 9 53CC	201A-54	201A-55	201A-56	201A-57	Represent. 201A-58	201A-59	201A-60	201A-61
SiO_2	53.41	53.66	53.88	53.56	53.19	53.32	50.82	51.47	52.38	51.66	50.79	50.81	49.76	50.34
Al_2O_3	1.48	1.42	1.52	1.30	1.41	1.53	2.66	2.49	2.30	2.49	2.56	3.21	3.91	3.16
FeO	4.12	3.65	3.82	3.82	3.71	3.92	9.34	9.17	9.37	8.99	8.09	8.26	8.54	8.48
MgO	16.76	16.80	16.63	16.89	16.84	16.61	12.28	12.28	12.32	12.38	12.80	12.93	12.20	12.22
MnO	0.11	0.04	0.10	0.06	0.05	0.08	0.34	0.44	0.33	0.25	0.33	0.30	0.27	0.29
TiO_2	0.39	0.45	0.43	0.37	0.38	0.42	0.79	0.69	0.66	0.69	0.89	1.31	1.61	1.17
Cr_2O_3	0.30	0.25	0.32	0.29	0.33	0.27	0.03	0.06	0.00	0.05	0.02	0.03	0.00	0.00
CaO	23.92	24.16	24.21	24.38	23.76	24.11	22.64	22.61	22.80	22.92	22.71	22.48	22.70	22.74
Na_2O	0.21	0.24	0.24	0.26	0.23	0.23	0.81	0.80	0.80	0.79	0.70	0.76	0.82	0.79
Sum	100.70	100.67	101.15	100.93	99.90	100.49	99.71	100.01	100.96	100.22	98.89	100.09	99.81	99.19
According to Papike et al. (1974)														
Si	1.938	1.945	1.947	1.939	1.942	1.938	1.903	1.922	1.939	1.924	1.911	1.889	1.859	1.893
Al^{IV}	0.062	0.055	0.053	0.055	0.058	0.062	0.097	0.078	0.061	0.076	0.089	0.111	0.141	0.107
T	2.000	2.000	1.994	2.000	2.000	2.000	2.000	2.000	2.000	2.000	2.000	2.000	2.000	2.000
Al^{VI}	0.001	0.006	0.012	0.000	0.003	0.004	0.020	0.032	0.039	0.033	0.025	0.030	0.031	0.033
Fe^{2+}	0.079	0.076	0.089	0.070	0.072	0.076	0.203	0.224	0.248	0.219	0.190	0.195	0.189	0.201
Fe^{3+}	0.046	0.034	0.026	0.045	0.041	0.043	0.089	0.063	0.042	0.060	0.064	0.062	0.078	0.066
Mg	0.906	0.908	0.895	0.911	0.916	0.900	0.685	0.684	0.680	0.687	0.718	0.716	0.679	0.685
Mn	0.003	0.001	0.003	0.002	0.002	0.002	0.011	0.014	0.010	0.008	0.011	0.009	0.009	0.009
Ti	0.011	0.012	0.012	0.010	0.010	0.011	0.022	0.019	0.018	0.019	0.025	0.037	0.045	0.033
Cr	0.009	0.007	0.009	0.008	0.010	0.008	0.001	0.002	0.000	0.001	0.001	0.001	0.000	0.000
Ca	0.930	0.938	0.937	0.946	0.930	0.939	0.909	0.905	0.904	0.914	0.916	0.895	0.909	0.916
Na	0.015	0.017	0.017	0.018	0.016	0.016	0.059	0.058	0.057	0.057	0.051	0.055	0.059	0.058
M1+M2	2.000	1.999	2.000	2.010	2.000	1.999	1.999	2.001	1.998	1.998	2.001	2.000	1.999	2.001
T+M1+M2	4.000	3.999	4.000	4.004	4.000	3.999	3.999	4.001	3.998	3.998	4.001	4.000	3.999	4.001

According to stoichiometric criteria (T + M1 + M2) = 4

Si	1.937
Altot	0.055
Fe^{2+}	0.053
Fe^{3+}	0.062
Mg	0.910
Mn	0.002
Ti	0.010
Cr	0.008
Ca	0.944
Na	0.018
T+M1+M2	3.999

You have either reached a page that is unavailable for viewing or reached your viewing limit for this book.

You have either reached a page that is unavailable for viewing or reached your viewing limit for this book.

You have either reached a page that is unavailable for viewing or reached your viewing limit for this book.

Table 3 (continuation).

Sample	G3-38	G3-39	G3-40	G3-41	G3-42	G3-43	G3-44	Avg. of 14 G3	G4-1	G4-2	G4-3	G4-4	G4-5	G4-6
SiO_2	49.34	50.13	49.59	49.12	48.92	49.51	49.52	49.42	50.59	49.12	50.53	49.28	50.33	50.35
Al_2O_3	3.31	3.09	3.10	3.14	3.53	3.14	3.10	3.24	3.08	4.02	3.24	4.41	3.60	2.99
FeO	6.95	6.83	6.91	6.78	6.98	7.07	6.51	6.88	6.77	7.23	7.10	7.74	7.24	6.66
MgO	13.66	14.05	13.80	13.91	13.65	13.90	13.89	13.86	14.07	13.63	14.00	13.31	13.80	14.22
MnO	0.05	0.14	0.05	0.14	0.16	0.18	0.12	0.14	0.11	0.15	0.18	0.14	0.12	0.12
TiO_2	1.61	1.52	1.61	1.57	1.72	1.59	1.59	1.61	1.58	1.77	1.46	1.82	1.48	1.43
Cr_2O_3	0.00	0.05	0.01	0.04	0.00	0.02	0.01	0.02	0.05	0.03	0.00	0.06	0.01	0.09
CaO	23.52	23.41	23.56	23.51	23.54	23.45	23.54	23.54	23.88	23.49	23.33	23.21	23.35	23.91
Na_2O	0.38	0.31	0.35	0.35	0.32	0.35	0.42	0.37	0.35	0.38	0.44	0.44	0.39	0.32
Sum	98.82	99.53	98.98	98.56	98.82	99.21	98.70	99.08	100.48	99.82	100.28	100.41	100.32	100.09
According to Papike et al. (1974)														
Si	1.852	1.867	1.859	1.851	1.839	1.854	1.859	1.851	1.866	1.826	1.867	1.824	1.861	1.865
Al^{IV}	0.146	0.133	0.137	0.139	0.156	0.139	0.137	0.143	0.134	0.174	0.133	0.176	0.139	0.131
T	1.998	2.000	1.996	1.990	1.995	1.993	1.996	1.994	2.000	2.000	2.000	2.000	2.000	1.996
Al^{VI}	0.000	0.003	0.000	0.000	0.000	0.000	0.000	0.000	0.000	0.002	0.008	0.017	0.018	0.000
Fe^{2+}	0.135	0.146	0.145	0.139	0.137	0.148	0.127	0.137	0.139	0.125	0.144	0.152	0.157	0.135
Fe^{3+}	0.083	0.066	0.071	0.075	0.083	0.074	0.078	0.079	0.070	0.100	0.075	0.087	0.067	0.071
Mg	0.764	0.780	0.771	0.781	0.765	0.776	0.777	0.774	0.773	0.755	0.771	0.734	0.760	0.785
Mn	0.002	0.004	0.002	0.004	0.005	0.006	0.004	0.004	0.003	0.005	0.006	0.004	0.004	0.004
Ti	0.045	0.043	0.045	0.044	0.049	0.045	0.045	0.045	0.044	0.049	0.041	0.051	0.041	0.040
Cr	0.000	0.001	0.000	0.001	0.000	0.001	0.000	0.001	0.001	0.001	0.000	0.002	0.000	0.003
Ca	0.946	0.934	0.947	0.949	0.948	0.941	0.947	0.945	0.944	0.936	0.924	0.921	0.925	0.949
Na	0.028	0.022	0.025	0.026	0.023	0.025	0.031	0.027	0.025	0.027	0.032	0.032	0.028	0.023
M1+M2	2.003	1.999	2.006	2.019	2.010	2.016	2.009	2.012	1.999	2.000	2.001	2.000	2.000	2.010
T+M1+M2	4.001	3.999	4.002	4.009	4.005	4.009	4.005	4.006	3.999	4.000	4.001	4.000	4.000	4.006
According to stoichiometric criteria (T + M1 + M2) = 4														
Si	1.851		1.858	1.845	1.837	1.851	1.857	1.849						1.862
Altot	0.146		0.137	0.139	0.156	0.138	0.137	0.143						0.130
Fe^{2+}	0.130		0.134	0.109	0.122	0.125	0.114	0.119						0.121
Fe^{3+}	0.088		0.082	0.107	0.097	0.096	0.090	0.096						0.085
Mg	0.764		0.771	0.779	0.764	0.774	0.777	0.773						0.784
Mn	0.002		0.002	0.002	0.005	0.005	0.006	0.004						0.004
Ti	0.045		0.045	0.044	0.049	0.045	0.045	0.045						0.040
Cr	0.000		0.000	0.001	0.000	0.001	0.000	0.001						0.003
Ca	0.946		0.946	0.946	0.947	0.939	0.946	0.943						0.948
Na	0.028		0.025	0.025	0.023	0.025	0.030	0.027						0.023
T+M1+M2	4.000		4.000	4.000	4.000	4.000	4.000	4.000						4.000

You have either reached a page that is unavailable for viewing or reached your viewing limit for this book.

You have either reached a page that is unavailable for viewing or reached your viewing limit for this book.

You have either reached a page that is unavailable for viewing or reached your viewing limit for this book.

Table 3 (continuation).

Sample	G99-25	G99-26	G99-27	G99-28	Avg. of 23 G99	G6-15	G6-17	G6-18	G6-19	G6-20	G6-21	G6-22	G6-23	Represent. G6-24
SiO_2	51.50	51.10	51.21	54.09	54.32	45.69	45.51	45.71	45.12	45.41	47.98	46.54	44.82	45.48
Al_2O_3	2.16	2.49	2.54	0.89	0.92	6.35	6.76	7.14	6.94	7.02	4.86	6.60	7.61	6.81
FeO	5.79	6.02	5.91	2.45	2.66	15.92	10.97	11.91	13.65	11.83	10.25	9.89	10.41	14.03
MgO	14.79	14.67	14.41	17.69	17.46	6.55	9.34	8.91	7.37	8.82	10.34	10.10	9.43	7.36
MnO	0.09	0.06	0.11	0.18	0.06	0.82	0.31	0.49	0.70	0.48	0.32	0.28	0.32	0.76
TiO_2	0.98	1.29	1.34	0.31	0.30	1.45	2.72	2.69	2.31	2.63	1.97	2.30	3.02	1.97
Cr_2O_3	0.22	0.05	0.11	0.77	0.80	0.00	0.02	0.03	0.04	0.00	0.00	0.00	0.01	0.00
CaO	23.61	23.86	24.11	23.48	23.54	21.33	23.18	22.97	22.02	22.91	23.27	23.56	23.26	21.97
Na_2O	0.35	0.24	0.28	0.23	0.26	1.70	1.07	1.20	1.36	1.13	0.95	0.87	0.89	1.32
Sum	99.49	99.78	100.02	100.09	100.32	99.81	99.88	101.05	99.51	100.23	99.94	100.14	99.77	99.70
According to Papike et al. (1974)														
Si	1.891	1.892	1.893	1.964	1.970	1.754	1.725	1.712	1.731	1.716	1.807	1.747	1.695	1.742
Al^{IV}	0.093	0.108	0.107	0.036	0.030	0.246	0.275	0.288	0.269	0.284	0.193	0.253	0.305	0.258
T	1.984	2.000	2.000	2.000	2.000	2.000	2.000	2.000	2.000	2.000	2.000	2.000	2.000	2.000
Al^{VI}	0.000	0.001	0.004	0.002	0.009	0.042	0.025	0.028	0.044	0.029	0.023	0.040	0.035	0.049
Fe^{2+}	0.120	0.135	0.138	0.064	0.081	0.264	0.173	0.179	0.246	0.185	0.194	0.164	0.166	0.256
Fe^{3+}	0.058	0.051	0.045	0.011	0.000	0.247	0.174	0.194	0.192	0.188	0.128	0.146	0.163	0.193
Mg	0.864	0.810	0.794	0.957	0.944	0.375	0.525	0.497	0.421	0.497	0.580	0.565	0.532	0.420
Mn	0.003	0.002	0.003	0.006	0.002	0.027	0.010	0.016	0.023	0.015	0.010	0.009	0.010	0.025
Ti	0.027	0.036	0.037	0.008	0.008	0.042	0.077	0.076	0.067	0.075	0.056	0.065	0.086	0.057
Cr	0.006	0.001	0.003	0.022	0.023	0.000	0.001	0.001	0.001	0.000	0.000	0.000	0.000	0.000
Ca	0.929	0.947	0.955	0.914	0.915	0.877	0.937	0.922	0.905	0.928	0.939	0.947	0.943	0.902
Na	0.025	0.017	0.020	0.016	0.018	0.127	0.078	0.087	0.101	0.083	0.069	0.063	0.065	0.098
M1+M2	2.032	2.000	1.999	2.000	2.000	2.001	2.000	2.000	2.000	2.000	1.999	1.999	2.000	2.000
T+M1+M2	4.016	4.000	3.999	4.000	4.000	4.001	4.000	4.000	4.000	4.000	3.999	3.999	4.000	4.000

According to stoichiometric criteria (T + M1 + M2) = 4

Si	1.909
Altot	0.094
Fe^{2+}	0.128
Fe^{3+}	0.052
Mg	0.817
Mn	0.003
Ti	0.027
Cr	0.006
Ca	0.938
Na	0.025
T+M1+M2	3.999

You have either reached a page that is unavailable for viewing or reached your viewing limit for this book.

You have either reached a page that is unavailable for viewing or reached your viewing limit for this book.

You have either reached a page that is unavailable for viewing or reached your viewing limit for this book.

Table 4 (conclusion).

Sample	G99	G5	G4	G3	G2	G1	G8	G6
SiO_2	54.32	49.24	50.20	49.42	51.06	49.67	47.25	45.48
Al_2O_3	0.92	3.29	3.19	3.24	2.89	3.28	5.22	6.81
TiO_2	0.30	1.71	1.49	1.61	0.96	1.25	1.34	1.97
FeO	2.66	7.01	6.86	6.88	5.30	6.15	13.24	14.03
MgO	17.46	13.95	14.21	13.86	15.16	14.14	8.71	7.36
MnO	0.06	0.16	0.17	0.14	0.10	0.10	0.62	0.76
CaO	23.54	23.63	23.79	23.54	23.86	23.75	22.65	21.97
Na_2O	0.26	0.40	0.35	0.37	0.34	0.33	0.99	1.32
Cr_2O_3	0.80	0.02	0.04	0.02	0.22	0.20	0.00	0.00
Sum	100.32	99.41	100.30	99.08	99.89	98.87	100.02	99.70
T								
Si	1.970	1.835	1.853	1.849	1.879	1.856	1.797	1.742
Al^{IV}	0.030	0.145	0.139	0.143	0.121	0.144	0.203	0.258
Ti	0.000	0.020	0.008	0.008	0.000	0.000	0.000	0.000
Sum	2.000	2.000	2.000	2.000	2.000	2.000	2.000	2.000
M1								
Al	0.009	0.000	0.000	0.000	0.004	0.001	0.031	0.049
Fe^{2+}	0.067	0.089	0.102	0.103	0.073	0.095	0.253	0.256
Fe^{3+}	0.000	0.117	0.096	0.096	0.081	0.090	0.168	0.193
Cr	0.023	0.001	0.001	0.001	0.006	0.006	0.000	0.000
Mg	0.893	0.765	0.768	0.763	0.809	0.773	0.494	0.420
Ti	0.008	0.028	0.033	0.037	0.027	0.035	0.038	0.057
Mn	0.000	0.000	0.000	0.000	0.000	0.000	0.016	0.025
Sum	1.000	1.000	1.000	1.000	1.000	1.000	1.000	1.000
M2								
Ca	0.915	0.944	0.941	0.943	0.941	0.951	0.923	0.902
Na	0.018	0.029	0.025	0.027	0.024	0.024	0.073	0.098
Mn	0.002	0.005	0.005	0.004	0.003	0.003	0.004	0.000
Mg	0.051	0.010	0.015	0.010	0.023	0.015	0.000	0.000
Fe^{2+}	0.014	0.012	0.014	0.016	0.009	0.007	0.000	0.000
Sum	1.000	1.000	1.000	1.000	1.000	1.000	1.000	1.000

4) similar distortions observed in T(2) tetrahedron of some richterites are correlated with Ti^{4+} entry (Oberti et al., 1992);
5) examination of PS201 crystals by XANES spectroscopy confirms the presence of Ti^{4+} in T site;
then it can be reasonably inferred that, if (Si + Al_{tot}) < 2, Ti^{4+} is the cation which ensures full occupancy.

The eight-coordinated M2 site

The M2 polyhedron is characterized by high Ca content (> 0.90 a.f.u.), which constrains the other cations to very small amounts (maximum content of Na = 0.098 a.f.u. in aegirine-augite; on average Na = 0.035 a.f.u.; Mn = 0.003 a.f.u.; Mg and Fe^{2+} ~ 0.012 a.f.u.). Aegirine-augites and 245D have no residual electron density (M2' site), lacking completely small cations like Fe^{2+} and Mg (Table 4), virtually only Ca is present. It is apparent from Figure 3 that, excluding aegirine-augites and 530S, the investigated clinopyroxenes do not conform to the general trend defined by Ethiopian augites and Sabatini clinopyroxenes. This trend shows that, if Ca content increases, the longest M2-O3C2 bond lengths become progressively shorter. Instead, Paraguayan clinopyroxenes have significantly longer M2-O3C2 bond distances, quite similar to those in diopside. It should be stressed that 245D reaches one of the highest Ca content. The general characteristics of the M2 polyhedron are, therefore:
1) high Ca content does not correspond to shorter values in the longest bond distances;
2) scattering of the M2-O3C2 bond lengths is very low (2.718 - 2.729 Å) and corresponds to very lim-

You have either reached a page that is unavailable for viewing or reached your viewing limit for this book.

You have either reached a page that is unavailable for viewing or reached your viewing limit for this book.

You have either reached a page that is unavailable for viewing or reached your viewing limit for this book.

COMIN-CHIARAMONTI, P.; DE MIN, A.; GOMES, C.B. (this volume) Magmatic rock-types from the Asunción-Sapucai graben: description of the occurrences and petrographical notes. Appendix I.

COMIN-CHIARAMONTI, P.; DE MIN, A.; MARZOLI, A. (this volume) Magmatic rock-types from the Asunción-Sapucai graben: chemical analyses. Appendix II.

CUNDARI, A. & SALVIULO, G. (1989) Ti solubility in diopsidic pyroxenes from a suite of New South Wales leucitites (Australia). Lithos, *22*:191-198.

CUNDARI, A. & COMIN-CHIARAMONTI, P. (this volume) Mineral chemistry of the alkaline rocks from the Asunción-Sapucai graben (central-eastern Paraguay).

DAL NEGRO, A.; CARBONIN, S.; MOLIN, G.M.; CUNDARI, A.; PICCIRILLO, E.M. (1982) Intracrystalline cation distribution in natural clinopyroxenes of tholeiitic, transitional and alkaline basaltic rocks. In: S.K. Saxena (ed.) Advances in physical geochemistry, 2, Springer-Verlag, New-York, p.117-150.

DAL NEGRO, A.; CARBONIN, S.; SALVIULO, G.; PICCIRILLO, E.M.; CUNDARI, A. (1985) Crystal chemistry and site configuration of the clinopyroxene from leucite-bearing rocks and related genetic significance: The Sabatini lavas, Roman Region, Italy. J. Petrol., *26*:1027-1040.

DAVOLI, P. (1987) A crystal-chemical study of aegirine-augites and some evaluations on the oxidation state of Mn. Neues Jb. Miner. Abh., *158*:67-87.

DE LA ROCHE, H. (1986) Classification et nomenclature des roches ignées: un essai de restauration de la convergence entre systématique quantitative, typologie de l'usage et modélisation génétique. Bull. Soc. Géol. France, *8*:337-353.

MORIMOTO, N.; NAKAJIMA, Y.; SYONO, Y.; AKIMOTO, S.; MATSUI, Y. (1975) Crystal structures of pyroxene type $ZnSiO_3$ and $ZnMgSi_2O_6$. Acta Cryst., *B31*:1041-1049.

NORTH, A.C.T.; PHILLIPS, D.C.; SCOTT MATHEWS, F. (1968) A semi-empirical method of absorption correction. Acta Cryst., *A24*:351-359.

OBERTI, R.; UNGARETTI, L.; CANNILLO, E.; HAWTHORNE, F.C. (1992) The behaviour of Ti in amphiboles: I. Four- and six-coordinate Ti in richterite. Eur. J. Mineral., *4*:425-439.

PAPIKE, J.J.; CAMERON, K.L.; BALDWIN, K. (1974) Amphiboles and pyroxenes: characterization of other than quadrilateral components and estimates of ferric iron from microprobe data. Geol. Soc. Amer. Abstracts with Programs, *6*:1053-1054.

QUARTIERI, S.; ANTONIOLI, G.; ARTIOLI, G.; LOTTICI, P.P. (1993) XANES study of Titanium coordination in natural diopsidic pyroxenes. Eur. J. Mineral., *5*:1101-1109.

ROBINSON, K.; GIBBS, G.V.; RIBBE, P.H. (1971) Quadratic elongation: a quantitative measure of distortion in coordination polyhedra. Science, *172*:567-570.

ROSSI, G.; TAZZOLI, V.; UNGARETTI, L. (1981) Crystal-chemical studies on sodic pyroxenes. XI Gen. Meet. I.M.A. (abstract), *1*:29.

ROSSI, G.; OBERTI, R.; DAL NEGRO, A.; MOLIN, G.M.; MELLINI, M. (1987) Residual electron density at the M2 site in C2/c clinopyroxenes: relationship with bulk chemistry and sub-solidus evolution. Phys. Chem. Minerals, *14*:514-520.

You have either reached a page that is unavailable for viewing or reached your viewing limit for this book.

You have either reached a page that is unavailable for viewing or reached your viewing limit for this book.

You have either reached a page that is unavailable for viewing or reached your viewing limit for this book.

Feldspathoids

These are represented by leucite (pseudoleucite), analcime and nepheline, characteristic of the B-P assemblages. Notably, the former two minerals tend to cluster along the analcime-leucite tie line of Petrogeny's Residual System and fall in the primary leucite field, coexisting with analcime-rich compositions (Comin-Chiaramonti et al., 1992b). The feldspathoids are generally altered and by far the majority of electron microprobe analyses failed to yield compositions approaching stoichiometry. It is well known that nepheline may alter to analcime during subsolidus interaction with deuteric and/or hydrothermal fluids (Deer et al., 1992) and that leucite readily changes to compositions approaching analcime through similar processes (Comin-Chiaramonti et al., 1979), notably in the rocks from the Roman Region (e.g. Cundari, 1975).

Structural formulae were calculated on the basis of 32, 6 and 7 oxygens for nepheline, leucite and analcime, respectively.

Most *nepheline* compositions yielded $(Si+Al+Fe^{3+})=16.00\pm0.10$ a.f.u., which is well within 1% of the expected theoretical value. However, about half the nepheline compositions from B-P rocks are cation deficient (Fig. 2), probably reflecting vacancies in the potassium sites by omission solid solution.

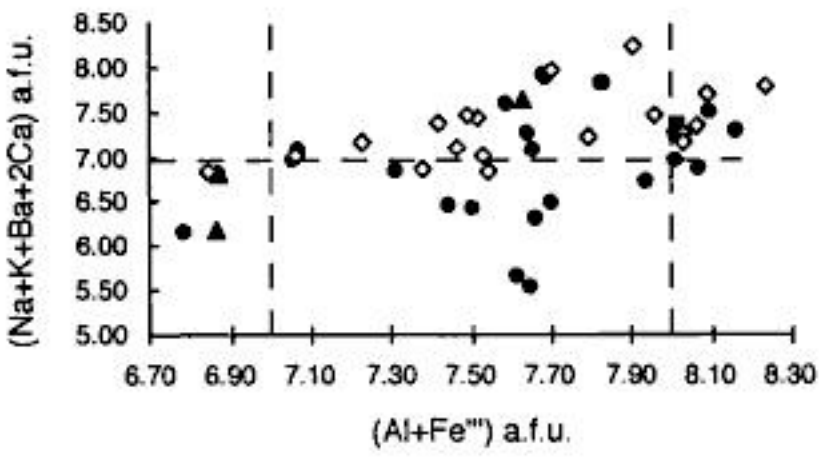

Figure 2 - ASU nepheline plotted in terms of $(Al+Fe^{3+})$ vs. (Na+K+Ba+2Ca), a.f.u. KG nepheline: full circles, intrusives; triangles, lava flows; squares, dykes. NaG nepheline: open diamonds.

Similar to the associated feldspar, significant Sr (up to 0.02 a.f.u.) is present in the nepheline from Mbocayaty.

Only one analysis was obtained from Cerro E Santa Helena (essexite 39/PS530), which closely corresponds to *leucite* in composition. The latter is strongly anisotropic and coarsely twinned.

The nepheline compositions from NaG rocks, characterized by a higher Na/K ratio relative to the B-P analogues, show virtually no cation deficiency.

Presumed *analcime* in some NaG phonolites are notable in their high $(Si+Al+Fe^{3+})$, mainly due to excess Si (0.23-0.34 a.f.u.) above the expected theoretical value of 2.00 a.f.u. Variable potassium (0.01-1.14 a.f.u.), often above the expected range, i.e. 0.03-0.07 a.f.u., suggests that residual potassium may be present from leucite transformation to analcime.

Olivine

Olivine compositions from a wide spectrum of KG and NaG rocks consistently yielded a sum of cation better than 1% of the theoretical 3.00 a.f.u., based on 4 oxygens. The $Mgx100/(Mg+Fe^{2+})$ ratio, mg#, averages 67 for KG intrusives and lavas, respectively, and 73 for dyke rocks, the most forsteritic olivine compositions occurring at Mbocayaty {mean (N=10) mg# 79} and Cañada {mean (N=4) mg# 77}. mg# for NaG ankaratrites and nephelinites averages 81.

Olivine from the B-P suite gave mg# ranging from 0.86 (basanite/theralite) to 0.53 (phonolite/nephelinic syenite). Olivine megacrysts, phenocrysts and microphenocrysts occur in the rocks of the AB-T suite with mg# ranging from 0.83 to 0.46 (alkali basalt/alkali gabbro to trachybasalt/syenodiorite).

mg# relationships between olivine and host rock compositions indicate that olivine is rarely in equilibrium with his host rock and that olivine-host rock pairs from the B-P suite are closer to equilibrium compositions than the analogues from the AB-T suite (Fig. 3A).

Calculated temperatures of olivine equilibration with their host bulk rock composition (Roeder & Emslie, 1970; Leeman, 1977) range from 1250 to 950°C (± 50°C), for both B-P and AB-T olivine-bulk rock pairs, respectively (Fig. 3B).

Olivine from NaG ankaratrites and nephelinites yielded equilibration temperatures between 1300 and 1249°C.

Intracrystalline $Mg-Fe^{2+}$ exchange reaction indicates variable cooling rate for intrusive as-

You have either reached a page that is unavailable for viewing or reached your viewing limit for this book.

You have either reached a page that is unavailable for viewing or reached your viewing limit for this book.

You have either reached a page that is unavailable for viewing or reached your viewing limit for this book.

The B site is filled to 2.00 a.f.u. with Na_B<0.50 a.f.u. for all compositions, except those from Mbocayaty and Aguapety Portón (Na_B=1.10-1.21 a.f.u.), while the A site is in all cases close to 1.00 a.f.u. (0.88-1.09 a.f.u.).

Significant SrO (up to 0.2 wt %) occurs in the amphibole from Cerro Arrúa-í (257/ PS204) and Mbocayaty (47/PS263), associated with high F (1.1-1.3% wt) in the latter. Carmichael (1967) and Mason (1977) reported similar SrO concentrations in amphiboles from lamproite (see Mitchell & Bergman, 1991, p.230).

Following Leake's (1978) recommended nomenclature, most amphibole compositions in rocks from the AB-T suite fall in the *pargasite* field, but transitional compositions close to or straddling the pargasite-kaersutite fields are also present (Fig. 9).

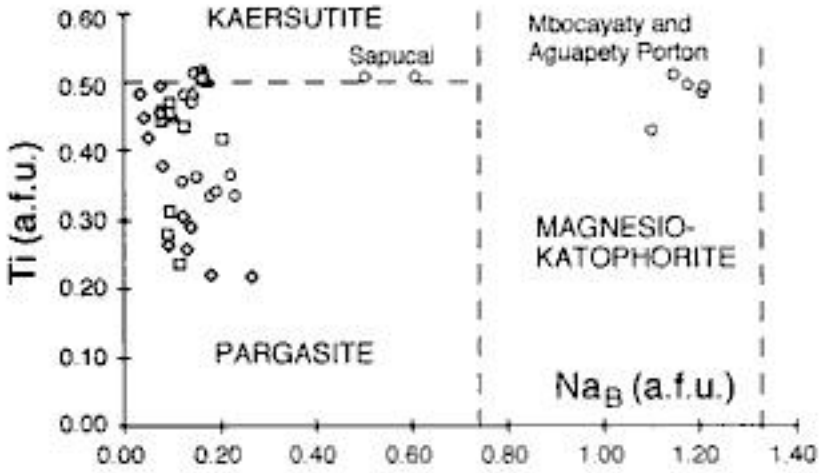

Figure 9 - Amphibole compositions from ASU rocks projected onto Leake's (1978) Ti vs. Na_B (a.f.u.) diagram. Amphibole from KG rocks: circles, intrusives; triangles, lava flows; squares, dykes. Amphibole from NaG rocks: open diamonds, phonolitic rocks.

Quite distinct are the compositions from Mbocayaty and Aguapety Portón (B-P suite), which fall in the *magnesio-katophorite* field. This amphibole is higher in its Na/K ratio and lower in Ti, K, mg#, relative to the magnesio-katophorite from the Western Australian lamproites (Mitchell & Bergman, 1991, Table 6.17).

Compared with amphibole compositions from the Sabatini (Cundari, 1979) and Vulsini (Holm, 1982) HKS lavas, all Paraguayan amphibole compositions are distinctly higher in Ti, relative to Al (Ti/Al>0.1; Fig. 10A) and mg# (Ti/mg#>0.5; Fig. 10B). On the other hand, Ti appears to be generally consistent, relative to Na/K, with the amphibole variation trend from the New South Wales leucitites (Fig. 10C).

The amphibole from NaG rocks was found only in phonolite/peralkaline phonolite and is distinct from the KG analogue in its high Ca on the B site (Ca_B=1.7-3.6 a.f.u.) and low mg# (31-50), which places it in the *ferroedenite-ferropargasite* range. Notably, some late-crystallized (gm) compositions from Cerro Medina (118/PS221, 119/PS218) and a phenocryst from Cerro Gimenez (178/PS214) required Ti^{IV} to complete the T site to 8.00 a.f.u. The amphibole compositions from these occurrences are distinct from those from Sapucai and closely match the amphibole variation trend from the NSW leucitites (Fig. 10D).

While most compositions fall above the line Ti/Al=0.1 (cf. Fig. 10), phenocrystal (P) and microphenocrystal (mP) core (c) to rim (r) variation trends from Sapucai (D101/PS106) straddle this line and fall within the amphibole compositional envelope of the Sabatini HKS lavas.

Mica

Ti-rich mica is characteristic of KG rocks, where it is represented by a wide compositional spectrum, particularly in the intrusive assemblages. Mica from lavas and dyke rocks appears to be generally similar in its chemical variation.

Cations were calculated on the basis of 24(O, OH, F) and H_2O estimated assuming (OH, F)=4.00 a.f.u. All compositions belong to the *phlogopite-annite* series, phlogopitic mica typically occurring in intrusive rocks from Mbocayaty (47/PS263, 51/3152), Aguapety Portón (52/PS 264), Cañada (77/PS245), Cerro San José (58/PS236, 103/PS237), Sapucai (142/PS30, 152/PS56, 154/PS58), Cerro Acahay (197/3346, 200/3327, 208/3341, 214/3162, 230/3354), and Cerro Arrúa-í (259/PS201).

Only three micas from dyke rocks, out of 15, yielded (Si+Al)>8.00 a.f.u. (Fig. 11A). Intrusive rocks from Mbocayaty consistently contain micas with (Si+Al)=7.40-7.69 a.f.u. Likewise, most mica compositions from Cañada, Cerro San José, and Cerro Arrúa-í are Al-deficient to complete the Z site to 8.00 a.f.u. and it is expected that Ti^{IV} compensates for this deficiency. Compositions from Cerro San José and Sapucai (143/PS31) lavas are also notable in their Al-deficiency in the Z site.

You have either reached a page that is unavailable for viewing or reached your viewing limit for this book.

You have either reached a page that is unavailable for viewing or reached your viewing limit for this book.

You have either reached a page that is unavailable for viewing or reached your viewing limit for this book.

Accessory minerals like high-Ti garnet and primary carbonate, virtually identical in both the Paraguayan and Roman Region assemblages, reflect crystallization from closely related liquids and point to a genetic link with carbonatites, reported from both provinces (Comin-Chiaramonti et al., 1992a; Stoppa & Lavecchia, 1992).

Generally, the mineral chemistry indicates mild interprovincial variation of parental liquid compositions, from metaluminous to peralkaline, higher in Ti relative to their analogues from the Roman Region and sharing in the signature of the southwest Ugandan and New South Wales provinces. This suggests bridging or transitional conditions of magmas genesis and evolution, particularly with respect to alkali- and Ti-bearing mantle phases and their melting behaviour under different lithospheric configurations.

In spite of considerable time and space differences, the ASU-KG mineralogy is remarkably similar to that of HKS lavas from intraplate continental setting, e.g. Bufumbira and NSW, and also shows characteristic parageneses and chemical signatures typical of the Roman Region HKS assemblages. These are important indicators of common genetic links in potassic magmas from different continental rifts.

ACKNOWLEDGEMENTS

Thanks are due to Brazilian (FAPESP) and Italian (CNR and MURST) agencies and to University of Trieste for financial support.

AC gratefully acknowledges the assistance of Pat Kelly (Geotrack International) in the microanalytical work carried out at the School of Earth Sciences, Melbourne University.

REFERENCES

CARBONIN, S. & PRINCIVALLE, F. (this volume) A crystal-chemical study of pyroxenes with diopsidic structures in alkaline rocks from central-eastern Paraguay: some considerations on tetrahedrally coordinated Ti^{4+}.

CARBONIN, S.; SALVIULO, G.; MUNNO, R.; DESIDERIO, M.; DAL NEGRO, A. (1989) Crystal-chemical examination of natural diopside: some geometrical indications of Si-Ti tetrahedral substitution. Mineral. Petrol., *41*:1-10.

CARMICHAEL, I.S.E. (1967) The mineralogy and petrology of the volcanic rocks from the Leucite Hills, Wyoming. Contrib. Mineral. Petrol., *15*:24-66.

CASTORINA, F.; CENSI, P.; BARBIERI, M..; COMIN-CHIARAMONTI, P.; CUNDARI, A.; GOMES, C.B.; PARDINI, G. (this volume) Carbonatites from Eastern Paraguay: a comparison with coeval carbonatites form Brazil and Angola.

COMIN-CHIARAMONTI, P.; MERIANI, S., MOSCA, R.; SINIGOI, S. (1979) On the occurrence of analcime in northeastern Azerbaijan volcanics (northwestern Iran). Lithos, *12*:187-198.

COMIN-CHIARAMONTI, P.; GOMES, C.B.; PICCIRILLO, E.M.; BELLIENI, G.; CASTILLO, A.M.C.; DEMARCHI, G.; GALLO, P.; VELÁZQUEZ, J.C. (1990a) Petrologia do maciço alcalino de Acahay, Paraguai Oriental. Rev. Bras. Geoc., *20*:133-152.

COMIN-CHIARAMONTI, P.; CUNDARI, A.; GOMES, C.B.; PICCIRILLO, E.M.; BELLIENI, G.; DE MIN, A.; CENSI, P.; ORUÉ, D.; VELÁZQUEZ, V.F. (1990b) Mineral chemistry and its genetic significance of major and accessory minerals from a potassic dyke swarm in the Sapucai graben, Central-Eastern Paraguay. Geochim. Brasil., *4*:175-206.

COMIN-CHIARAMONTI P.; CENSI, P.; CUNDARI, A.; GOMES, C.B. (1992a) A silico-beforsite from the Sapucai complex (central-eastern Paraguay). Geochim. Brasil., *6*:87-92.

COMIN-CHIARAMONTI, P.; CUNDARI, A.; GOMES, C.B.; PICCIRILLO, E.M.; CENSI, P.; DE MIN, A.; BELLIENI, G.; VELÁZQUEZ, V.F; ORUÉ, D. (1992b) Potassic dyke swarm in the Sapucai graben, Eastern Paraguay: petrographical, mineralogical and geochemical outlines. Lithos, *28*:283-301.

COMIN-CHIARAMONTI, P.; CUNDARI, A.; BELLIENI, G. (this volume) Mineral analyses of alkaline rock-types from the Asunción-Sapucai graben. Appendix III.

You have either reached a page that is unavailable for viewing or reached your viewing limit for this book.

You have either reached a page that is unavailable for viewing or reached your viewing limit for this book.

You have either reached a page that is unavailable for viewing or reached your viewing limit for this book.

(61-39 Ma; Comin-Chiaramonti et al., 1991) sodic magmatism, with nephelinitic lava flows, dykes and plugs yielding averaged initial $^{87}Sr/^{86}Sr$ and $^{143}Nd/^{144}Nd$ ratio of 0.70372(9) and 0.51274(6), respectively. Most nephelinitic plugs (e.g. Ñemby Hill) contain mantle xenoliths ranging in composition from spinel lherzolites to dunites (Demarchi et al., 1988). These xenoliths contain glassy patches (blebs) probably derived from the breakdown of K-rich phases (Comin-Chiaramonti et al., 1986; Demarchi et al., 1988), which may be interpreted as evidence of metasomatic enrichments in incompatible elements and LREE.

Whole-rock xenoliths and clinopyroxene (Cr-diopside) Nd isotopic ratios are in the range 0.51246-0.51325 and 0.51267-0.51317, respectively (Petrini et al., 1990), indicating both isotopically depleted and enriched components.

SAMPLE LOCATION AND DESCRIPTION

Detailed geological and petrographic descriptions of the investigated rocks are given by Comin-Chiaramonti et al. (this volume, Appendix I). Location, formation, caption and rock-type of the selected samples analyzed for Sr-Nd isotopes are given herein.

B-P and AB-T are the identified ASU suites.

Cordillera del Ybytyruzú

Cerro Km 23. Stock: 21-PS539, B-P, essexite. 131.9±5.0 Ma.

Cerro San Benito. Stock: 27-PS535, B-P, essexite. 126.5±7.6 Ma.

Cerro E Santa Helena. Complex: 39-PS530, B-P, essexite. 126.5±7.6 Ma.

Northwestern Ybytyruzú. Dyke: D14-PS260, AB-T, trachyandesite. 124.6±4.2 to 128.4±4.6 Ma.

Villarrica

Cerro Capiitindy. Volcanic dome: 43-PS500, AB-T, trachyphonolite. 126.5± Ma.

Mbocayaty. Stock: 47-PS263, AB-T, nepheline syenodiorite. 128.2±4.5 to 130.0±3.4.

Aguapety Portón. Stock: 52-PS264, 55-PS267, 56-PS268, 60-PS270C, B-P, theralite, essexitic gabbro and essexite. 132±5.5 to 138.1±4.8 Ma.

Serranía de Ybytymí

Cañada. Stock: 75-PS246 and 77-PS245, AB-T nephelinic syenite and B-P ijolite, respectively. 126.5±7.6 Ma.

Cerro Chobí. Dyke: D46-PS256, AB-T, peralkaline trachyphonolite. 126.5±7.6 (?) Ma.

Cerro Yaguarú

Catalán. Dyke: D59-PS119, B-P, phonotephrite.

Cerro San José

Cerro San José. Stock: 94-PS231A and 100-PS233, B-P, essexite and phonotephrite, respectively; 99-PS235, 103-PS237, AB-T, syenogabbro and alkali gabbro, respectively. 126.5±7.6 Ma.

Potrero Ybaté

Potrero Ybaté. Complex: 110-PS167 and 113-PS228, AB-T, nepheline syenodiorite; 111-PS227, AB-T, trachybasalt. Dykes: D88-PS129 and D99-PS131, AB-T, trachybasalt. 127.8 ±5.6 Ma.

Sapucai

Sapucai. Complex: 142-PS30, AB-T, syenogabbro; 143-PS31 and 167-PS72, B-P, phonotephrite and silico-beforsite, respectively. Dykes: D144-PS21, D185-PS50 and D207-PS111, B-P, tephrite; D145-PS22, D151-PS28 and D208-PS114, B-P, phonotephrite; D105-PS105, D108-PS125 and D162-PS29, B-P, phonolite; D159-PS9 and D164-PS40, AB-T, trachybasalt and trachyphonolite, respectively. 119±4 to 136±5 Ma.

Paraguarí

Cerro Santo Tomás. Stock: 181-3090, AB-T, nepheline syenodiorite; 186-PS136A, B-P, essexite. Dyke: basanite D211-3088, B-P, basanite. 126.5±7.6 Ma.

Carapeguá-Acahay

Cerro Acahay. Complex: 243-3360 and 193-3164, B-P, essexitic gabbro and nepheline syenite, respectively; 208-3341, AB-T, alkali gabbro; 199-3344, 203-3329 and 207-3334, AB-T, trachybasalt, trachyandesite and trachyte, respectively. 118±4 Ma.

You have either reached a page that is unavailable for viewing or reached your viewing limit for this book.

You have either reached a page that is unavailable for viewing or reached your viewing limit for this book.

You have either reached a page that is unavailable for viewing or reached your viewing limit for this book.

You have either reached a page that is unavailable for viewing or reached your viewing limit for this book.

You have either reached a page that is unavailable for viewing or reached your viewing limit for this book.

You have either reached a page that is unavailable for viewing or reached your viewing limit for this book.

You have either reached a page that is unavailable for viewing or reached your viewing limit for this book.

DeGRAFF, I.M. (1985) Late Mesozoic crustal extension and rifting on the western edge of the Paraná basin, Paraguay. Geol. Soc. Amer., Abstract with programs, *17*:560.

DeGRAFF, I.M.; FRANCO, R.; ORUÉ, D. (1981) Interpretación geofisica y geologica del valle de Ypacaray (Paraguay) y su formación. Ass. Geol. Argent., *36*:240-246.

DEMARCHI, G.; COMIN-CHIARAMONTI, P.; DE VITO, P.; SINIGOI, S.; CASTILLO, C.A.M. (1986) Lherzolite-dunite xenoliths from Eastern Paraguay: petrological contraints to mantle metasomatism. In: E.M. Piccirillo & A.J. Melfi (eds.) The Mesozoic flood volcanism from the Paraná Basin (Brazil): petrogenetic and geophysical aspects. IAG-USP, São Paulo, p.207-227.

DRUECKER, M.D. & GAY, S.P. Jr. (1987) Mafic dyke swarms associated with Mesozoic rifting in Eastern Paraguay, South America. In H.C. Halls & W.F. Fahrig (eds.) Mafic dyke swarms. Geol. Assoc. Canada, Spec. Publ., *34*:187-193.

EDGAR, A.D. & VUKADINOVIC, D. (1992) Implications of experimental petrology to the evolution of ultrapotasic rocks. Lithos, *28*:205-220.

EDGAR, A.D.; CHARBONNEAU, H.E.; MITCHELL, R.H. (1992) Phase relations of an armalcolite-phlogopite lamproite from Soky Butte, Montana: applications to lamproite genesis. J. Petrol., *33*:505-520.

ERLANK, A.J.; WATERS, F.G.; HAWKESWORTH, C. J.; HAGGERTY, S.E.; ALLSOPP, H.L.; RICHARD, R.S.; MENZIES, M.A. (1987) Evidence for the mantle metasomatism in peridotite nodules from the Kimberley pipes, South Africa. In: M.A. Menzies & C.J. Hawkesworth (eds.) Mantle metasomatism. London Academic Press, p.221-329.

ERNESTO, M.; PACCA, I.G.; HIODO, S.Y.; NARDY, A. Jr. (1990) Paleomagnetism of the Mesozoic Serra Geral Formation, Southern Brazil. Phys. Earth Planet. Int., *64*:153-175.

ERNESTO, M; COMIN-CHIARAMONTI, P.; GOMES, C.B., CASTILLO, A.M.C.; VELÁZQUEZ, J.C. (this volume) Palaeomagnetic data from the Central Alkaline Province, Eastern Paraguay.

FAURE, G. (1986) Principles of isotope geology. J. Wiley & Sons, New York, 589p.

FODOR, R.V.; CRICKET, C.; SIAL, A.N. (1985) Crustal signature in the Serra Geral flood-basalt province, southern Brazil: O and Sr-isotopic evidence. Geology, *13*:763-765.

FOLEY, S. (1992) Petrological characterization of the source components of potassic magmas: geochemical and experimental constraints. Lithos, *28*:187-204.

FOLEY, S. & PECCERILLO, A. (1992) Potassic and ultrapotassic magmas and their origin. Lithos, *28*:181-185.

FREY, F.A.; GREEN, D.H.; ROY, S.D. (1978) Integrated models of basalt petrogenesis: a study of quartz tholeiites to olivine melilitites from South Eastern Australia utilizing geochemical and experimental petrological data. J. Petrol., *19*:453-513.

GAST, P.W. (1968) Trace element fractionation and the origin of tholeiitic and alkaline magma types. Geochim. Cosmochim. Acta, *32*:1057-1086.

HART, S.R.; GERLACH, D.C.; WHITE, W.M. (1986) A possible new Sr-Nd-Pb mantle array and consequences for mantle mixing. Geochim. Cosmochim. Acta, *50*:1551-1557.

HAWKESWORTH, C. J.; MANTOVANI, M.; PEATE, D. (1988) Lithosphere remobilization during Paraná CFB magmatism. J. Petrol., Special Lithosphere Issue, p.205-223.

HAWKESWORTH, C. J.; HERGT, J.M., ELLAM, R.M.; MAC DERMOTT, J. (1991) Element fluxes associated with subduction related magmatism. Phil. Trans. R. Soc. London, *335A*:395-405.

HEGARTY, K.A.; DUDDY, I.R.; GREEN, P.F. (this volume) The thermal history in around the Paraná Basin using apatite track analysis - Implications for hydrocarbon occurrences and basin formation.

LUDWIG, K.R. (1987) User's for "analyst", a computer program for control of an isomass 54E thermal-ionization, single collector mass-spectrometer. U.S. Geol. Open File Report, p.485-513.

McKENZIE, D.P. (1989) Some remarks on the movement of small melt fractions in the mantle. Earth Planet. Sci. Lett., *95*:53-72.

You have either reached a page that is unavailable for viewing or reached your viewing limit for this book.

You have either reached a page that is unavailable for viewing or reached your viewing limit for this book.

You have either reached a page that is unavailable for viewing or reached your viewing limit for this book.

Table 1 - Major (wt %) and trace (ppm) element average contents, relative standard deviations (s.d.) of ASU magmas. B-P suite: B, basanite; T, tephrite; PT, phonotephrite; P, phonolite. AB-T suite: AB, alkali basalt; TB, trachybasalt; TA, trachyandesite; TP, trachyphonolite; TR, trachyte. N = number of samples, mg# = atomic Mg/(Mg+Fe²⁺), assuming Fe³⁺/Fe²⁺ ratio = 0.18.

B-P suite

	B (N=3)	s.d.	T (N=74)	s.d.	PT (N=101)	s.d.	P (N=23)	s.d.
SiO_2	48.86	(0.34)	49.36	(1.21)	50.85	(1.47)	54.28	(2.49)
TiO_2	1.55	(0.12)	1.79	(0.25)	1.65	(0.25)	1.04	(0.40)
Al_2O_3	13.30	(0.25)	15.17	(1.69)	16.68	(1.49)	19.48	(1.07)
FeO_t	9.33	(0.95)	9.60	(0.82)	8.67	(1.03)	5.41	(1.65)
MnO	0.17	(0.01)	0.17	(0.02)	0.17	(0.02)	0.15	(0.03)
MgO	8.54	(1.50)	6.25	(1.19)	4.44	(0.98)	1.56	(1.07)
CaO	10.86	(0.93)	9.26	(0.89)	7.54	(0.97)	4.63	(1.51)
Na_2O	3.40	(0.21)	3.33	(0.61)	4.02	(0.60)	6.05	(1.39)
K_2O	3.53	(0.60)	4.48	(0.88)	5.37	(1.12)	7.00	(1.14)
P_2O_5	0.46	(0.08)	0.59	(0.17)	0.61	(0.16)	0.40	(0.26)
mg#	0.65		0.57		0.51		0.37	
Cr	388	(15)	161	(111)	70	(65)	16	(16)
Ni	140	(40)	51	(27)	34	(20)	6	(5)
Ba	1214	(4)	1470	(336)	1563	(357)	2022	(1104)
Rb	61	(20)	90	(28)	107	(37)	129	(39)
Sr	1383	(150)	1703	(323)	1731	(441)	2443	(719)
La	73	(13)	85	(22)	97	(23)	126	(36)
Ce	136	(27)	153	(36)	171	(39)	205	(47)
Nd	58	(3)	67	(14)	76	(28)	84	(18)
Zr	162	(36)	258	(74)	299	(72)	531	(150)
Y	18	(4)	20	(5)	21	(5)	25	(9)
Nb	38	(7)	40	(12)	48	(15)	77	(21)

AB-T suite

	AB (N=8)	s.d.	TB (N=52)	s.d.	TA (N=65)	s.d.	TP (N=20)	s.d.	TR (N=15)	s.d.
SiO_2	50.72	(1.74)	51.43	(1.17)	53.53	(1.97)	58.58	(2.39)	60.91	(2.45)
TiO_2	1.53	(0.27)	1.51	(0.22)	1.50	(0.23)	0.83	(0.43)	0.94	(0.44)
Al_2O_3	12.99	(1.73)	15.62	(1.62)	17.20	(1.36)	19.04	(0.90)	18.24	(0.84)
FeO_t	9.11	(1.38)	8.75	(0.61)	7.88	(1.24)	4..22	(1.74)	4.26	(1.70)
MnO	0.17	(0.03)	0.16	(0.02)	0.15	(0.02)	0.14	(0.04)	0.12	(0.10)
MgO	8.63	(1.44)	6.04	(1.45)	3.84	(1.27)	1.14	(0.81)	1.34	(0.73)
CaO	9.86	(0.79)	8.46	(0.74)	6.34	(1.22)	3.47	(1.31)	2.28	(1.54)
Na_2O	2.60	(1.19)	3.31	(0.67)	3.76	(0.90)	5.60	(1.21)	4.21	(1.02)
K_2O	3.93	(1.05)	4.24	(1.07)	5.27	(1.44)	6.71	(0.93)	7.43	(1.86)
P_2O_5	0.46	(0.09)	0.49	(0.11)	0.55	(0.11)	0.27	(0.19)	0.31	(0.18)
mg#	0.66		0.59		0.50		0.36		0.39	
Cr	316	(86)	165	(143)	64	(48)	8	(10)	10	(13)
Ni	91	(33)	59	(36)	24	(21)	6	(5)	8	(5)
Ba	1444	(344)	1310	(265)	1417	(376)	1334	(811)	1140	(482)
Rb	77	(35)	89	(28)	104	(32)	131	(34)	136	(32)
Sr	1251	(185)	1496	(288)	1440	(353)	1358	(692)	815	(325)
La	65	(38)	72	(18)	87	(22)	114	(36)	93	(39)
Ce	124	(58)	126	(32)	153	(34)	185	(59)	159	(62)
Nd	52	(19)	53	(12)	66	(15)	64	(25)	64	(28)
Zr	210	(90)	224	(52)	295	(54)	541	(167)	440	(130)
Y	18	(5)	19	(4)	21	(4)	22	(10)	22	(10)
Nb	29	(14)	31	(8)	40	(9)	66	(26)	50	(23)

You have either reached a page that is unavailable for viewing or reached your viewing limit for this book.

You have either reached a page that is unavailable for viewing or reached your viewing limit for this book.

You have either reached a page that is unavailable for viewing or reached your viewing limit for this book.

Crystal accumulation and crystal/liquid mixing

Petrographical evidences show that the ASU magmas were subjected to varying degrees of crystal accumulation and to variable degrees of mixing between magmas containing higher- and lower-temperature assemblages (cf. Cundari & Comin-Chiaramonti, this volume). This complex situation is summarized in Figure 2, in terms of olivine-bulk rock relationships. The liquid products of crystal fractionation lie along a trend parallel to, but below, the Roeder-Emslie equilibrium curve. The xenocryst vector represents the situation where high-temperature olivine is preserved in lower-temperature magma by non-equilibration with the host liquid.

Olivine accumulation produces MgO-rich magmas in which olivine is less magnesian than the equilibrium olivine for that bulk composition. Magma mixing results in a range of phenocryst/

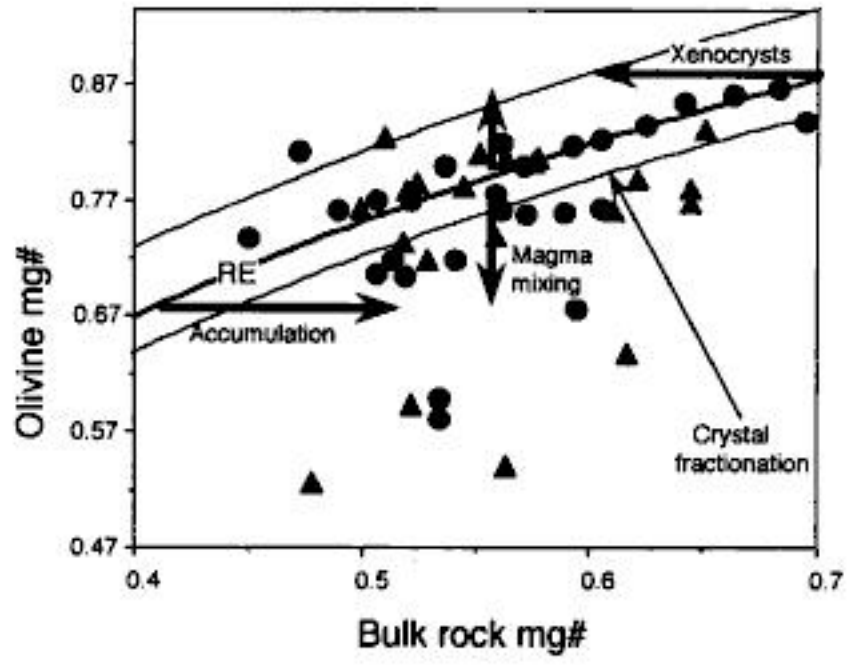

Figure 2 - Compositions of olivine phenocryst and microphenocryst cores plotted against bulk-rock compositions to show the effects of crystal fractionation, xenocrystal retention, magma mixing and olivine accumulation on the range of phenocrysts in individual specimens (cf. Cundari & Comin-Chiaramonti, this volume, Fig. 3). Arrows indicate direction of spread of olivine compositions resulting from the various processes. Circles and triangles: B-P and AB-T suites, respectively. RE, Roeder & Emslie (1970) equilibrium curve.

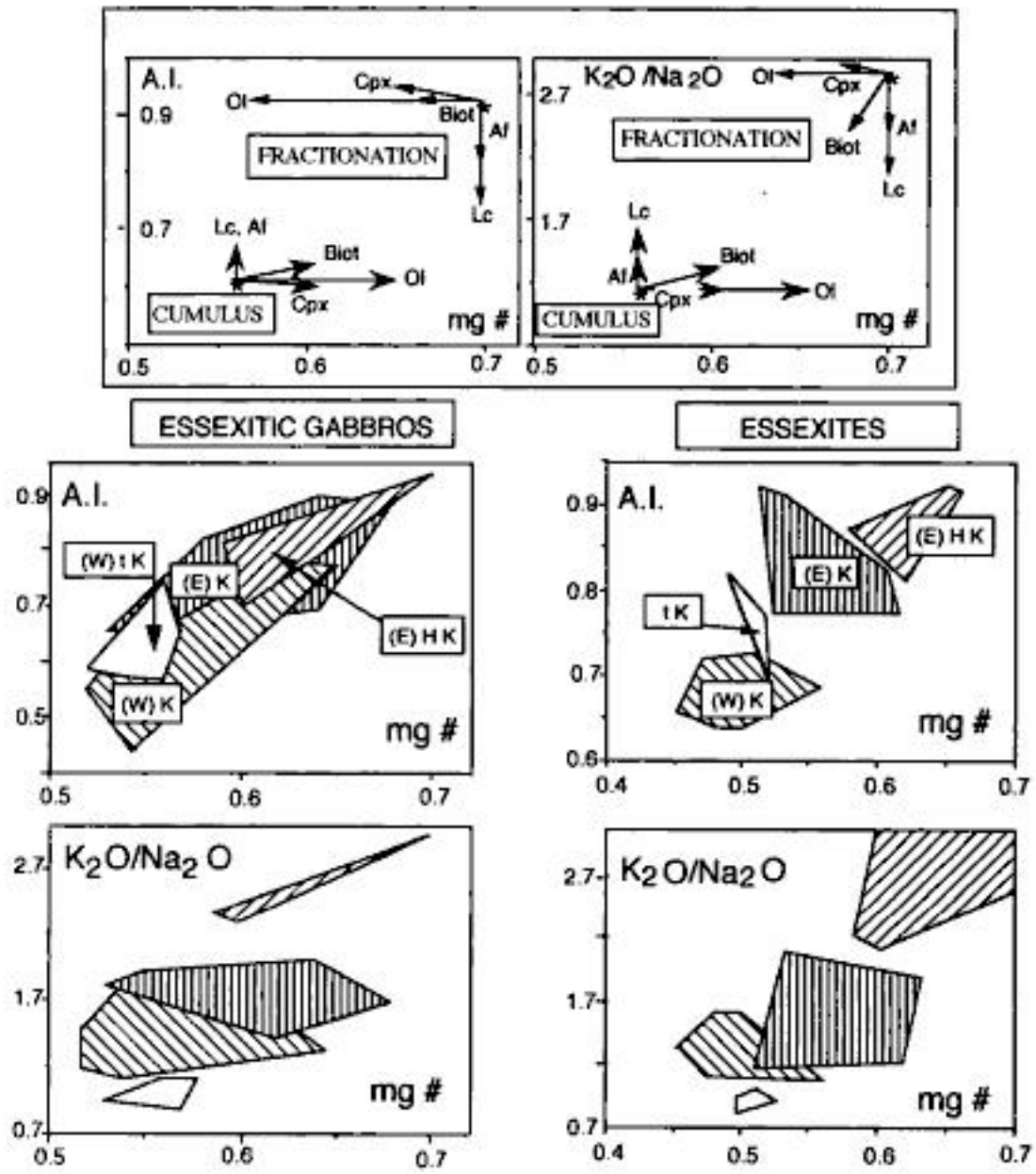

Figure 3 - Relationships between mg# and alkali index (A.I.) and K_2O/Na_2O ratio (wt %) for ASU essexitic gabbros and essexites. HK, K, tK: high potassic, potassic and transitional potassic rock-types, respectively. (E) and (W): eastern and western region, respectively. Insect: vectors (proportional intensities) representative of fractionation and cumulus processes (whole-rocks and minerals from Comin-Chiaramonti et al., Appendices II and III). Ol, Olivine; Cpx, clinopyroxene; Biot, biotite; Af, alkali feldspar; Lc, leucite.

You have either reached a page that is unavailable for viewing or reached your viewing limit for this book.

You have either reached a page that is unavailable for viewing or reached your viewing limit for this book.

You have either reached a page that is unavailable for viewing or reached your viewing limit for this book.

Table 6 - A. Calculated primary magmas and compositions of added minerals. Basanite, B-P suite, from basanite of Table 1, adding 23.0 % Ol + Cpx (38.6% Ol, 61.4% Cpx); alkali basalt, AB-T suite, from alkali basalt of Table 1, adding 21.5 % of Ol + Cpx (31.4% Ol, 68.6% cpx). Trace elements calculated according to Raileygh's fractionation and crystal/liquid partition coefficients as in Table 4. B. Equilibrium partial melting models (Shaw equation, according to Hanson, 1978: $C_L/C_O = 1/\{D(1-F)+F\}$, where C_L is the concentration of a given trace element in a derived melt, C_O is the composition of that element in the parent solid prior to melting, D is the bulk distribution coefficient for the mineral assemblage left in the residue, and F is the fraction of melting); data source: C, Chen, 1971; M, MacGregor, 1974; W, Wilkinson & Le Maitre, 1987. C. crystal/liquid partition coefficients (McKenzie & O'Nions, 1991 and therein references). ΣR^2: sum of the square residuals.

A

	Basanite	Alkali basalt	Olivine	Clinopyroxene
SiO_2	47.76	50.40	40.98	53.78
TiO_2	1.40	1.20		0.32
Al_2O_3	10.45	11.01		3.09
FeO_t	8.25	8.04	9.38	3.27
MnO	0.16	0.15	0.16	0.09
MgO	13.31	12.67	49.46	16.60
CaO	11.98	11.08	0.02	21.97
Na_2O	2.82	2.14		0.87
$0.K_2O$	3.42	2.95		0.01
P_2O_5	0.47	0.36		
mg#	0.74	0.76	0.90	0.90
Cr	801	674		
Ni	710	323		
Rb	45	61		
Ba	899	1147		
Th	7.5	7.9		
U	1.9	2.5		
Ta	2.4	2.6		
Nb	29	23		
La	56	53		
Ce	106	103		
Nd	48	46		
Sr	1124	1038		
Zr	121	168		
Sm	12.3	11.3		
Tb	0.64	0.58		
Y	15	16		
Yb	1.4	0.9		
Lu	0.21	0.16		

B

	Gt Per (C)	Ol (M)	Opx (M)	Cpx (M)	Gt (M)	Amph (W)
SiO_2	45.70	41.54	57.43	53.42	42.17	41.49
TiO_2	0.10	0.02	0.28	0.49	0.30	4.79
Al_2O_3	1.60	0.01	0.99	2.49	20.61	14.40
FeO_t	8.62	9.28	6.43	4.89	12.45	11.32
MnO	0.01	0.10	0.02	0.02	0.30	0.10
MgO	40.97	49.00	33.62	16.79	18.50	12.49
CaO	2.53	0.03	0.94	20.86	4.46	10.67
Na_2O	0.36		0.26	1.01	0.79	2.76
K_2O	0.09			0.01	0.40	1.96
P_2O_5	0.02					0.01

	B-P 1	B-P 2	AB-T 1	AB-T 2
F %	3.11	3.19	3.18	3.19
Ol	67.71	67.77	68.20	68.79
Opx	19.00	18.99	18.46	18.29
Cpx	8.70	8.69	8.71	8.69
Gt	4.52	4.54	4.15	4.22
Amph	0.07		0.47	
ΣR^2	0.039	0.040	0.042	0.043

You have either reached a page that is unavailable for viewing or reached your viewing limit for this book.

You have either reached a page that is unavailable for viewing or reached your viewing limit for this book.

You have either reached a page that is unavailable for viewing or reached your viewing limit for this book.

COMIN-CHIARAMONTI, P.; CENSI, P.; CUNDARI, A.; GOMES, C.B.; MARZOLI, A.; PICCIRILLO, E.M. (this volume) Petrochemistry of the Early-Cretaceous potassic rocks from the Asunción-Sapucai graben, central-eastern Paraguay.

COMIN-CHIARAMONTI, P.; CUNDARI, A.; BELLIENI, G. (this volume) Mineral analyses of alkaline rock-types from the Asunción-Sapucai graben. Appendix III.

COMIN-CHIARAMONTI, P.; CUNDARI, A.; DE MIN., A; GOMES, C.B.; VELÁZQUEZ, V.F. (this volume) Magmatism in Eastern Paraguay: occurrence and petrography.

COMIN-CHIARAMONTI, P.; DE MIN, A.; GOMES, C.B. (this volume) Magmatic rock-types from the Asunción-Sapucai graben: description of the occurrences and petrographical notes. Appendix I.

COMIN-CHIARAMONTI, P.; DE MIN, A.; MARZOLI, A. (this volume) Magmatic rock-types from the Asunción-Sapucai graben: chemical analyses. Appendix II.

CUNDARI, A. & COMIN-CHIARAMONTI, P. (this volume) Mineral chemistry of alkaline rocks from the Asunción-Sapucai graben (central-eastern Paraguay).

DE MIN, A. (1993) Il magmatismo Mesozoico K-alcalino del Paraguay Orientale: aspetti petrogenetici ed implicazioni geodinamiche. Ph.D. Thesis, Trieste University, 242p.

DEMARCHI, G.; COMIN-CHIARAMONTI, P.; DE VITO, P.; SINIGOI, S.; CASTILLO, C.A.M. (1986) Lherzolite-dunite xenoliths from Eastern Paraguay: petrological contraints to mantle metasomatism. In: E.M. Piccirillo & A.J. Melfi (eds.) The Mesozoic flood volcanism from the Paraná Basin (Brazil): petrogenetic and geophysical aspects. IAG-USP, São Paulo, p.207-227.

EDGAR, A.D. (1980) Role of subduction on the genesis of leucite-bearing rocks: discussion. Contrib. Mineral. Petrol., *73*:429-431.

ERNESTO, M.; COMIN-CHIARAMONTI, P.; GOMES, C.B.; CASTILLO, A.M.C.; VELÁZQUEZ, J.C. (this volume) Paleomagnetic data from the Central Alkaline Province, Eastern Paraguay.

FOLEY, S. (1992) Petrological characterization of the source components of potassic magmas: geochemical and experimental constraints. Lithos, *28*:187-204.

FOLEY, S. & WHELLER, G.E. (1990) Parallels in the origin of the geochemical signatures of island arc volcanics and continental potassic igneous rocks: the role of residual titanates. Chem. Geol., *85*:1-18.

FREY, F.A.; GREEN, D.H.; ROY, S.D. (1978) Integrated models of basalt petrogenesis: a study of quartz tholeiites to olivine melilites from South Eastern Australia utilizing geochemical and experimental petrological data. J. Petrol., *19*:463-513.

GOMES, C.B.; COMIN-CHIARAMONTI, P.; VELÁZQUEZ, D.; ORUÉ, D. (this volume) Alkaline magmatism in Paraguay: a review.

HAMILTON, D.L. & MacKENZIE, W.S. (1965) Phase equilibrium studies in the system $NaAlSiO_4$ (nepheline) - $KAlSiO_4$ (kalsilite) - SiO_2-H_2O. Mineral. Mag., *34*:214-231.

HANSON, G.N. (1978) The application of trace elements to the petrogenesis of igneous rocks of granitic composition. Earth Planet. Sci. Lett., *38*:26-43.

HAWKESWORTH, C.J.; MANTOVANI, M.S.M.; TAYLOR, P.N.; PALACZ, Z. (1986) Evidence from the Paraná of South Brazil for a continental contribution to Dupal basalts. Nature, *322*:356-359.

LUTH, W.C. (1967) Studies in the system $KAlSiO_4$ - Mg_2SiO_4 - SiO_2 - H_2O: Part 1, Inferred phase relations and petrological applications. J. Petrol., *8*:372-416.

MacGREGOR, I.D. (1974) The system MgO-Al_2O_3-SiO_2: solubility of Al_2O_3 in enstatite for spinel and garnet peridotite compositions Amer. Mineral., *59*:110-119.

MARQUES, L.S.; PICCIRILLO, E.M.; MELFI, A.J.; COMIN-CHIARAMONTI, P.; BELLIENI, G. (1989) Distribuição de terras raras e outros elementos traços em basaltos da Bacia do Paraná (Brasil Meridional). Geochim. Brasil., *3*:33-50.

MARZOLI, A. (1991) Studio petrologico e geochimico di complessi alcalini del rift di Sapucai (Paraguay). Bs.D. Thesis, Trieste University, 201p.

McKENZIE, D.P. & O'NIONS, R.K. (1991) Partial melt distributions from inversion of Rare Earth element concentrations. J. Petrol., *32*:1021-1091.

You have either reached a page that is unavailable for viewing or reached your viewing limit for this book.

You have either reached a page that is unavailable for viewing or reached your viewing limit for this book.

You have either reached a page that is unavailable for viewing or reached your viewing limit for this book.

Table 1 - Representative and average chemical compositions and CIPW norm for alkaline rocks from the Alto Paraguay Province. Analyses recalculated to 100% on anhydrous basis; mg# = MgO/(MgO+FeO), assuming Fe_2O_3/FeO ratio = 0.3. CB, Cerro Boggiani; FDM, Fecho dos Morros; P, Pedreira; CSC, Cerro Siete Cabezas (sample RP-61).

	1 CB	2 CB	3 CB	4 FDM	5 FDM	6 FDM	7 FDM	8 FDM	9 FDM	10 P	11 P	12 CSC	13 CSC	14 CSC	15 CSC	16 CSC
SiO_2	58.63	58.59	57.20	53.94	56.22	58.49	59.45	65.15	61.90	61.07	70.00	62.31	61.25	63.10	65.28	65.84
TiO_2	0.25	0.29	0.55	2.01	1.07	0,50	1.03	0.75	0.70	1.28	0.51	0.58	0.84	0.86	0.49	0.47
Al_2O_3	20.06	19.59	17.56	17.76	18.67	17.83	19.65	16.91	18.22	16.70	14.94	17.68	17.85	17.07	17.01	17.43
FeO_t	2.07	3.14	5.26	6.13	5.38	5.24	3.03	3.00	3.47	4.47	3.38	3.75	4.07	4.12	3.53	2.71
MnO	0.12	0.20	0.53	0.18	0.30	0.36	0.08	0.12	0.22	0.16	0.20	0.22	0.19	0.18	0.16	0.10
MgO	0.05	0.12	0.07	2.64	1.26	0.74	1.03	0.96	0.58	2.12	0.14	0.57	0.77	1.03	0.30	0.28
CaO	0.55	0.95	1.19	4.44	1.76	1.28	3.68	1.46	1.42	2.88	0.96	1.04	1.86	1.23	0.53	0.43
Na_2O	12.58	11.43	13.15	7.25	9.21	10.10	7.47	6.37	7.80	6.45	5.04	8.31	7.93	6.65	6.87	6.91
K_2O	5.67	5.66	4.48	4.35	5.18	5.27	3.99	4.99	5.47	4.20	4.78	5.29	4.88	5.42	5.70	5.68
P_2O_5	0.02	0.05	0.01	1.29	0.92	0.18	0.57	0.29	0.22	0.68	0.04	0.25	0.35	0.33	0.12	0.14
Cr	<2	<2	<2	2	4	<2	<2	4	<2	4	<2	<2	2	<2	<2	<2
Ni	6	8	10	11	8	13	7	8	4	8	5	7	9	6	6	6
Cs		4.4	3.8					8.8	1.7	1.8	0.8	6.5	6.0	6.8	7.1	7.2
Rb	263	293	340	89	156	232	67	168	110	107	189	137	110	187	144	154
Ba	58	102	135	1389	901	164	2329	777	764	1029	85	679	877	1229	266	402
Th		11.5	28.7	3.4	5.3	36.7	6.2	15.1	9.6	10.7	19.7	9.0	16.33	7.9	5.7	6.0
U		10.3	78.8	6.0	9.4	110.6	2.3	3.2	3.5	2.9	16.0	4.3	7.3	4.9	7.5	4.0
Ta	12.1	17.1	52.1	13.2	29.6	245.8	13.1	12.7	15.9	16.4	49.3	14.2	14.9	18.5	22.3	15.1
Nb	150	200	687	124	277	2230	142	132	159	112	480	162	174	177	187	142
Sr	94	131	180	1481	741	213	2514	396	337	614	30	266	370	258	49	75
Zr	735	1673	7847	320	1436	5939	409	439	655	309	1337	905	621	487	889	587
Hf	16.8	38.4	149.4	8.4	39.1	162.9	10.6	10.9	17.4	7.3	33.7	22.1	16.5	14.4	27.8	11.6
Y	21	33.7	71.5	36	54	199	20.7	28.7	48.0	30.4	87.3	49	46	53	46.3	39.5
La	73	83.0	234	86	119.2	336.5	56.8	74.5	125.3	72.5	178.0	82.3	96.4	72.6	113.8	48.8
Ce	108	133.8	340	181	228.5	591.3	106.6	161.6	237.9	158.5	347.0	154.8	192.7	165.8	223.2	114.0
Pr		9.4	23.7		19.4	54.6	8.6	14.6	23.8	24.6	31.8	17.7	23.3	10.1	17.5	11.5
Nd	25	29.2	67.2	78	74.2	162.8	43.1	52.8	86.0	64.2	105.0	50.9	72.8	65.3	74.0	45.3
Sm		3.69	9.05		10.1	28.0	7.1	8.2	14.1	11.15	10.39	9.4	16.0	14.11	16.1	8.6
Eu		0.89	2.19		1.2	5.1	3.51	1.95	2.49	3.08	3.46	2.21	2.63	1.38	1.80	1.39
Gd		4.29	12.55		11.8	29.6	8.4	8.1	13.36	10.90	11.66	9.7	13.4	11.4	13.6	7.9
Tb		0.59	1.63		1.18	4.54	0.74	0.84	1.54	1.14	1.28	1.39	1.68	1.39	1.59	0.95
Dy		3.67	9.97		4.48	30.5	3.8	5.0	7.0	6.33	8.07	7.35	10.21	8.07	10.64	6.41
Ho		0.81	2.32		0.73	6.85	0.62	0.88	1.29	1.03	1.37		1.49	1.29	1.58	1.19
Er		2.99	8.57		2.70	24.91	1.89	2.56	4.49	2.93	4.26	4.76	5.22	4.10	5.97	3.39
Tm		0.59	1.56		0.39	4.69	0.26	0.34	0.70	0.42	0.57	0.75	0.82	0.63	0.88	0.46
Yb		4.52	12.49		2.35	34.81	1.65	2.17	3.66	2.03	3.40	3.72	4.57	2.69	4.56	2.10
Lu		0.65	1.78		0.30	5.12	0.22	0.322	0.53	0.29	0.52	0.57	0.51	0.43	0.57	0.51
Q								5.04		0.20	19.17				1.73	2.47
or	33.37	33.42	26.18	25.70	30.55	31.15	23.52	29.43	47.98	24.78	28.18	31.20	28.78	31.7	33.64	33.54
ab	30.99	31.09	30.77	34.42	31.61	34.99	50.01	53.81	32.30	54.49	42.56	49.89	49.92	56.17	55.68	57.42
an				3.04			8.25	2.80		4.22	3.99			0.74		0.29
ne	21.89	20.70	18.39	14.58	19.16	14.79	7.05		8.26			6.23	7.95			
ac	2.18	3.31	5.35		5.43	3.59			2.37			4.07	2.12		2.06	0.79
ns	7.48	5.16	9.16		1.06	4.43			0.01			0.97				
di	2.30	3.83	5.12	8.54	2.28	4.47	5.04	2.07	4.81	4.51	0.43	3.00	6.25	2.65	1.59	0.83
hy								2.02		5.43	2.46			3.44	3.09	2.29
ol	0.97	1.57	3.12	4.11	5.61	5.27	1.05		2.45			2.90	1.55	0.50		
mt				2.92			1.55	1.65		2.34	1.95		1.10	2.08	0.93	1.12
il	0.46	0.54	1.02	3.81	2.03	0.95	1.95	1.42	1.33	2.42	0.96	1.10	1.59	1.63	0.93	0.89
ap	0.03	0.11	0.02	3.05	2.17	0.42	1.35	0.68	0.51	1.61	0.09	0.59	0.82	0.78	0.28	0.32
A.I.	1.337	1.273	1.508	0.937	1.113	1.252	0.846	0.939	1.029	0.907	0.902	1.098	1.027	0.984	1.027	1.005
mg#	0.052	0.080	0.186	0.493	0.346	0.356	0.435	0.420	0.275	0.517	0.086	0.261	0.300	0.361	0.161	0.189

You have either reached a page that is unavailable for viewing or reached your viewing limit for this book.

You have either reached a page that is unavailable for viewing or reached your viewing limit for this book.

You have either reached a page that is unavailable for viewing or reached your viewing limit for this book.

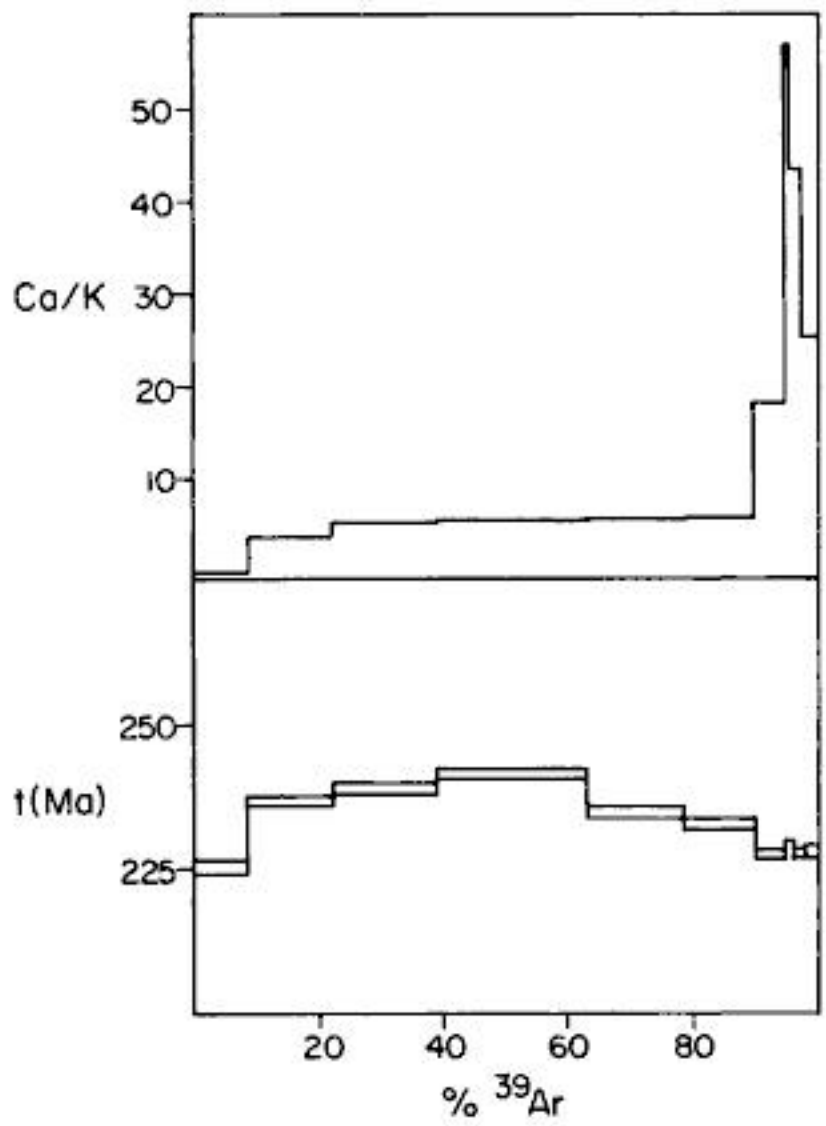

Figure 8 - $^{40}Ar/^{39}Ar$ analysis on amphibole from rock of Cerro Siete Cabezas (sample RP-61).

ACKNOWLEDGEMENTS

The authors are grateful to Brazilian (FAPESP) and Italian (CNR and MURST) agencies for financial support and to I. McReath for improving the manuscript.

REFERENCES

AMARAL, G. (1984) Províncias Tapajós e Rio Branco. In: F.F.A. Almeida & Y. Hasui (eds.) O Pré-Cambriano do Brasil. Editora Edgard Blücher Ltda., São Paulo, p.6-35.

AMARAL, G.; BUSHEE, J.; CORDANI, U.G.; REYNOLDS, J.H. (1967) Potassium-argon ages of alkaline rocks from southern Brazil. Geochim. Cosmochim. Acta, *31*:117-142.

ARAÚJO, H.J.T.; SANTOS NETO, A; TRINDADE, C.A.H.; PINTO, J.C.A.; MONTALVÃO, R.M.G.; DOURADO, T.D.C.; PALMEIRA, R.C.B.; TASSINARI, C.C.G. (1982) Geologia. In: Projeto Radambrasil, Folha SF 21. Campo Grande. MME/SG, Rio de Janeiro, p.82.

COMIN-CHIARAMONTI, P.; CUNDARI, A.; DE MIN, A.; GOMES, C.B.; VELÁZQUEZ, V.F. (this volume) Magmatism in Eastern Paraguay: occurrence and petrography.

COMTE, D. & HASUI, Y. (1971) Geochronology of Eastern Paraguay by the potassium-argon method. Rev. Bras. Geoc., *1*:33-43.

DE LA ROCHE, H.; LETERRIER, J.; GRANDCLAUDE, P.; MARCHAL, M. (1980) A classification of volcanic and plutonic rocks using R1-R2 diagram and major element analyses. Its relationships with current nomenclature. Chem. Geol., *29*:183-210.

FLETCHER, C.J.N. & BEDDOE-STEPHENS, B. (1987) The petrology, chemistry and crystallization history of the Velasco alkaline province, Eastern Bolivia. In: J.G.Fitton & B.G.J. Upton (eds.) Alkaline igneous rocks. Geol. Soc. Sp. Publ., 30. Blackwell Scientific Publications, p.403-413.

GOMES, C.B.; COMIN-CHIARAMONTI, P.; DE MIN, A.; ROTOLO, S.G.; VELÁZQUEZ, V.F. (1993) A Província Alcalina do Alto Paraguai (Mato Grosso do Sul e Paraguai): características geoquímicas. 4° Congr. Bras. Geoq., Brasília, Resumos Expandidos, p.55-58.

GOMES, C.B.; COMIN-CHIARAMONTI, P.; VELÁZQUEZ, V.F.; ORUÉ, D. (this volume) Alkaline magmatism in Paraguay: a review.

LAURENZI, M.A. & VILLA, I.M. (1987) $^{40}Ar/^{39}Ar$ chronostratigraphy of Vico ignimbrites. Per. Mineral., *56*:285-295.

LIVIERES, R.A. & QUADE, H. (1987). Distribución regional y assentamiento tectónico de los complejos alcalinos del Paraguay. Zbl. Geol. Pälont., Teil I, Heft 7/*8*:791-805.

MORAES, L.J. (1958) Rochas alcalinas da região dos Fechos dos Morros, no sul de Mato Grosso e República do Paraguai. I -Distribuição geográfica das montanhas sieníticas do Fecho dos Morros. An. Acad. brasil. Ciênc., *30*:165-169.

SAMSON, S.D. & ALEXANDER, E.C. Jr. (1987) Calibration of the interlaboratory $^{40}Ar/^{39}Ar$ dating standard, MMhb-1. Chem. Geol., *66*:27-34.

You have either reached a page that is unavailable for viewing or reached your viewing limit for this book.

You have either reached a page that is unavailable for viewing or reached your viewing limit for this book.

You have either reached a page that is unavailable for viewing or reached your viewing limit for this book.

formed by subhedral carbonate grains. The alvikite is aplitic in texture. Accessory minerals are apatite (1-2% by volume) and subordinate barite, quartz, phlogopite, sanidine, uranpyrochlore, magnetite, aegirine, zircon, strontianite, synchysite, goethite and pyrite.

2. Cerro Sarambí (22°45'S; 56°14'W)

This also forms an approximately circular structure of about 7 km in diameter, with strong doming of the peripheral country rocks (Mesozoic to Silurian sediments and Precambrian metasediments). The main rock-types are pyroxenites and trachytes crosscut by glimmeritic, søvitic and silico-carbonatitic dykes and veins (Lechner-Wiens & Quade, 1990).

A similar age to that of Cerro Chiriguelo can be inferred on the basis of geological and isotopic evidence.

The selected Cerro Sarambí specimens consist of a søvite vein and two medium-grained silico-søvite stringers. Euhedral quartz and accessory fluorite, vermiculite and opaques are present.

3. Sapucai (25°42'S; 56°58'W)

This complex, representing the major occurrence of alkaline rocks in Paraguay, is composed of hypabyssal and extrusive rocks extending over an area of more than 90 km^2. Hypabyssal rocks include dykes and small stocks, while the extrusive rocks are represented by thick sequences of lavas and pyroclastics with occasionally interbedded beforsitic flows (Comin-Chiaramonti et al., 1992a, b).

K/Ar ages show a main frequency class at 120-125 Ma (Gomes et al., this volume). A Rb/Sr isochron gave 126.5±7.6 Ma (Velázquez et al., 1992).

The selected Sapucai samples are a silico-beforsitic flow composed of alkali feldspar (61.3 wt %), dolomite (21.5 wt %), magnetite (8.6 wt %), biotite (5.2 wt %), calcite (2.8 wt%) and apatite (0.6 wt %) (Comin-Chiaramonti et al., 1992b) and a strongly carbonatated dyke (peralkaline phonolite on a $CaCO_3$-free basis) with very fine-grained groundmass calcite .

4. Ybytyruzú (25°46'S; 56°17'W)

This is a Cordillera formed by tholeiitic basalts of the Serra Geral Formation (cf. Bellieni et al., 1986) crosscut by dykes and igneous complexes formed by potassic rocks (see Comin-Chiaramonti et al., this volume). Some dykes containing sparry calcite may be conceivably related with contamination processes by calcareous sandstones of the Independencia Group (Upper Permian; Bitschene, 1987). A sparry calcite from a trachyphonolitic dyke (K/Ar age on biotite = 128±4.6 Ma, Bitschene, 1987) was selected.

5. Valle-mí (22°12'S; 57°57'W)

Very low grade metamorphic limestones, dolomitic limestones and dolostones of Early Ordovician age (480-500 Ma; Palmieri & Velázquez, 1982) extending on the left side of the Paraguay river, near Valle-mí township, represent the largest carbonate platform in Paraguay.

A calcareous dolostone (microsparitic dolomite+calcite) and a limestone (sparitic, well recrystallized calcite with ghosts of fossiliferous remnants) were selected.

Brazil

6. Jacupiranga (24°42'S; 48°08'W)

Oval-shaped alkaline complex c. 65 km^2 in surface area, intruded into Precambrian basement. Rock-types range from dunites and jacupirangites to syenites and alkali granites (Morbidelli et al., 1986).

The carbonatites occur near the center of the complex and consist of magnetite-apatite-phlogopite søvite with minor beforsitic dykes (Morikiyo et al., 1987). The age of intrusion is well constrained by both K/Ar determinations (Amaral et al., 1967; Amaral, 1978) and Rb/Sr isochron (Roden et al., 1985) at 131±3 Ma.

The investigated samples are medium-grained søvites having subhedral, granular texture with apatite less than 3 vol %. Data relative to apatite and/or magnetite-phlogopite-bearing søvites from Roden et al. (1985) and from Nelson et al. (1988) are also given for comparison, along with the C-O isotopic values from Morikiyo et al. (1987).

7. Juquiá (24°23'S; 47°49'W)

This is an asymmetric alkaline complex of about 14 km^2 intruded into Precambrian base-

You have either reached a page that is unavailable for viewing or reached your viewing limit for this book.

You have either reached a page that is unavailable for viewing or reached your viewing limit for this book.

You have either reached a page that is unavailable for viewing or reached your viewing limit for this book.

Table 2 - C-O isotopic composition of the carbonates. Source of data: 1. Nelson et al., 1988; 2., Morikiyo et al., 1987.

Locality	Sample	Rock-type	Carbonate Fraction (wt %)	Mineral	wt%	$\delta^{13}C$‰ vs PDB-1	$\delta^{18}O$‰ vs V-SMOW	Partial mineral analyses (wt %) MgO	CaO
				Paraguay					
C.Chiriguelo	3422	søvite	97	calcite	100	-7.26	+13.48	0.47	54.08
	3434	søvite	97	calcite	100	-6.52	+11.22	0.58	54.22
	3435A	alvikite	98	calcite	100	-7.77	+11.53	0.97	53.88
	3435B	søvite	98	calcite	100	-6.25	+14.94	0.70	53.76
	3442	søvite	97	calcite	100	-8.08	+11.76	0.10	54.24
C.Sarambí	SA90	søvite	96	calcite	100	-5.68	+21.68	0.31	54.55
	SA91	silico-søvite	53	calcite	100	-10.37	+17.11	0.61	55.20
	SA95	silico-søvite	38	calcite	100	-5.68	+14.96	0.72	54.46
Sapucai	PS72	silico-beforsite	24	dolomite	88	-5.63	+14.47	20.17	30.04
				calcite	12	-6.54	+14.00	0.10	55.93
	PS94	"carbonatic" phonolite	19	calcite	100	-7.37	+16.70	0.30	55.50
Ybytyruzú	PS260	trachy-phonolite		sparry calcite	100	-5.96	+11.55	0.16	55.85
Valle-mí	PS279	meta-dolostone	95	dolosparite	89	-0.27	+23.88		
				microsparite	11	-1.68	+20.55		
	PS280	meta-limestone	96	microsparite	100	+0.57	+22.85	0.20	55.80
				Brazil					
Jacupiranga	JCC99	søvite	92	calcite	100	-6.39	+10.05	3.37	51.81
	JM2	søvite	94	calcite	84	-6.07	+7.48		
				dolomite	16	-5.71	+7.60		
	JM6	søvite	95	calcite	79	-5.03	+8.12		
				dolomite	21	-4.59	+8.41		
	JM12	søvite	90	calcite	81	-4.12	+9.38		
				dolomite	19	-3.80	+9.51		
	JM15	søvite	91	calcite	84	-5.15	+8.62		
				dolomite	16	-4.80	+9.20		
	5961[1]	søvite		calcite		-6.1	+7.1		
	5963[1]	søvite		calcite		-5.6	+7.3		
	JC-11[2]	søvite		calcite		-6.4	+7.5		
	JC-18[2]	søvite		calcite		-6.4	+8.1		
	JC-26[2]	søvite		calcite		-6.2	+7.3		
				dolomite		-5.8	+7.1		
	JC-27[2]	beforsite		dolomite		-5.9	+7.7		
	JC-44[2]	beforsite		dolomite		-6.1	+7.3		
				calcite		-5.8	+9.6		
	JC-46[2]	søvite		calcite		-6.4	+7.7		
				dolomite		-5.6	+8.1		
Juquiá	S16C	beforsite	70	dolomite	78	-7.20	+15.83		
				calcite	22	-7.57	+16.58		
	S25	beforsite	84	dolomite	89	-7.27	+16.13		
				calcite	11	-7.60	+15.68		
	S26A	beforsite	84	dolomite	90	-7.45	+16.64		
				cafcite	10	-7.84	+16.42		
	S26B	beforsite	84	dolomite	90	-7.45	+16.64		
				calcite	10	-8.02	+15.68		
				Angola					
Bonga	316/14	silico-beforsite	75	ankeritic dolomite	93	-3.65	+15.53		
				calcite	7	-4.36	+21.49		
	316/32	beforsite	90	ankeritic dolomite	100	-3.09	+9.42		
	316/34	søvite	82	calcite	71	-4.00	+11.89		
				ankerite	29	-3.37	+12.59		
	316/42	søvite	88	calcite	76	-5.31	+9.69		
				ankerite	24	-4.85	+10.32		
	3616/66	beforsite	85	ankeritic dolomite	100	-1.88	+16.55		

You have either reached a page that is unavailable for viewing or reached your viewing limit for this book.

You have either reached a page that is unavailable for viewing or reached your viewing limit for this book.

You have either reached a page that is unavailable for viewing or reached your viewing limit for this book.

To be noted that the compositions of metasomites formed from a single metasomatizing melt will vary with the evolution of the melt. Consequentely, the veins will define a trend of shallow-slope, and mixing curves between veins and matrix will define an array towards the matrix (cf. a and b regression lines).
Model D.M.: Rb = 0; Sr = 0.133; Sm = 0.314; Nd = 0.628
Present day B.E.: $^{87}Sr/^{86}Sr = 0.70475$; $^{87}Rb/^{86}Sr = 0.0816$
$^{143}Nd/^{144}Nd = 0.512638$; $^{147}Sm/^{144}Nd = 0.1967$
$(Rb/Sr)_{Diopside}$: $(Rb/Sr)_{melt} \sim 0.125$
$(Sm/Nd)_{Diopside}$: $(Sm/Nd)_{melt} \sim 1.5$
K: Rb/Sr = 0.0957 Sm/Nd = 0.1344
Na: Rb/Sr = 0.0732 Sm/Nd = 0.2295
Th: Rb/Sr = 0.0733 Sm/Nd = 0.2082

agencies is gratefully acknowledged. We would like to express our thank to R. Alaimo for the use of a Perkin-Elmer mass spectrometer.

REFERENCES

ALAIMO, R. & CENSI, P. (1992) Quantitative determination of major, minor and trace elements on U.S.G.S. rock standards by inductively coupled plasma mass spectrometry. Atom. Spectr., *13*:113-121.

ALLSOPP, H.L. & HARGRAVES, R.B. (1985) Rb-Sr ages and palaeomagnetic data for some Angolan alkaline intrusives. Trans. Geol. Soc. South Africa, *88*:295-299.

AMARAL, G. (1978) Potassium-Argon age studies on the Jacupiranga alkaline district, State of São Paulo, Brazil. Proc. 1st Intern. Symp. Carbonatites. DNPM, Brasília, p. 297-302.

AMARAL, G.; BUSHEE, J.; CORDANI, U.G.; KAWASHITA, K.; REYNOLDS, J.H. (1967) Potassium-Argon ages of the alkaline rocks from the Southern Brazil. Geochim. Cosmochim. Acta, *31*:117-142.

ANDERSEN, T. (1987) Mantle and crustal components in a carbonatite complex, and the evolution of carbonatite magma: REE and isotopic evidence from the Fen complex, southeast Norway. Isotope Geoscience, *65*:147-166.

BECCALUVA, L.; BARBIERI, M.; BORN, H.; BROTZU, P.; COLTORTI, M.; CONTE, A.; GARBARINO, C.; GOMES, C.B.; MACCIOTTA, G.; MORBIDELLI, L.; RUBERTI, E.; SIENA, F.; TRAVERSA, G. (1992) Fractional crystallization and liquid immiscibility processes in the alkaline-carbonatite complex of Juquiá (São Paulo, Brazil). J. Petrol., *33*:1371-1404.

BELL, K. & BLENKINSOP, J. (1987) Nd and Sr isotopic compositions of East African carbonatites: implications for mantle heterogeneity. Geology, *15*:99-102.

BELL, K. & BLENKINSOP, J. (1989) Neodymium and Strontium isotope geochemistry of carbonatites. In: K. Bell (ed.) Carbonatites, genesis and evolution. London, p.278-300.

BELLIENI, G.; COMIN-CHIARAMONTI, P.; MARQUES, L.S.; MARTINEZ, L.A.; MELFI, A.J.; NARDI, A.J.R.; PICCIRILLO, E.M.; STOLFA, D. (1986) Continental flood basalts from the central-western regions of the Paraná plateau (Paraguay and Argentina): petrology and petrogenetic aspects. Neues Jb. Miner. Abh., *154*:111-139.

BITSCHENE, P. (1987) Mesozoischer und Känozoischer anorogener magmatismus in Ostparaguay: arbeiten zur geologie und petrologie zweier Alkaliprovinzen. Ph.D. Thesis, Heidelberg University, 317p.

BOYNTON, W.V. (1984) Cosmochemistry of the rare Earth elements: meteorite studies. In: P. Henderson (ed.) Rare element geochemistry. Elsevier, Amsterdam, p.90-103.

BUSHEE, J. (1974) Potassium-argon ages of some alkaline rocks from southern Brazil. Ph.D. Thesis, University of California, Berkeley, 145p.

CAHEN, L.; SNELLING, N.J.; DELHAL, J.; VAIL, J.R. (1984) The geochronology and evolution of Africa. Clarendon Press, Oxford, 512p.

CENSI, P.; COMIN-CHIARAMONTI, P.; ORUÉ, D.; DEMARCHI, G.; LONGINELLI, A. (1989) Geochemistry and C-O isotopes of the Chiriguelo carbonatite, northeastern Paraguay. J. South Amer. Earth Sci., *2*:295-303.

You have either reached a page that is unavailable for viewing or reached your viewing limit for this book.

You have either reached a page that is unavailable for viewing or reached your viewing limit for this book.

You have either reached a page that is unavailable for viewing or reached your viewing limit for this book.

COMPARATIVE ASPECTS BETWEEN POST-PALAEOZOIC ALKALINE ROCKS FROM THE WESTERN AND EASTERN MARGINS OF THE PARANÁ BASIN

C.B.Gomes, L.Morbidelli, E.Ruberti, P.Comin-Chiaramonti

Alkaline Magmatism in Central-Eastern Paraguay. Relationships with Coeval Magmatism in Brazil. Comin-Chiaramonti, P. & Gomes, C. B. (eds.), 1996, Edusp/Fapesp, São Paulo, pp. 249-274.

ABSTRACT

The comparison of alkaline rocks from western and eastern regions of the Paraná Basin (Paraguay and Brazil, respectively) show that:

1. The alkaline occurrences are widespread in areas tectonically well defined, i.e. Eastern Paraguay, *Asunción-Sapucai graben* and *Amambay tectonic depression*; Southeastern Brazil, *Alto Paranaíba Arch*, *Ponta Grossa Arch*, *Ribeira Belt* and *Taiúva-Cabo Frio lineament*. 2. The Paraguay alkaline occurrences are mainly represented by subvolcanic-volcanic mafic-intermediate rock-types of "plagioleucititic" affinity, Early Cretaceous in age and by Eocene-Oligocene ankaratrites/nephelinites and their derivatives. 3. The Alto Paranaíba Arch is characterized by prevailing Late Cretaceous kamafugitic associations. 4. The Ponta Grossa Arch, Ribeira Belt and Taiúva-Cabo Frio lineament display a potassic magmatism of "plagioleucititic" affinity mainly represented by evolved intrusive rock-types with ages spanning from Early Cretaceous (Ponta Grossa Arch) to Late Cretaceous-Palaeocene (Taiúva-Cabo Frio lineament); cumulitic assemblages (clinopyroxenites, members of the ijolite series and dunites) are common mainly in association with carbonatite-bearing districts (e.g. Jacupiranga, Tapira). 5. Sr and Nd isotopic data point to distinct lithospheric mantle sources for the primitive magmas of all the investigated districts. 6. Model ages span from Transamazonico to Brasiliano thermo-tectonic events and point to distinct lithospheric keels.

INTRODUCTION

The alkaline rock-types from the Paraná Basin "sensu lato" occur in four South American countries, i.e. Brazil, Paraguay, Bolivia and Uruguay, but they are mostly concentrated in Brazilian and Paraguayan territories (Fig. 1).

The distribution of alkaline rocks in South America is due to Almeida (1971, 1972). This author drew attention to the important role played by regional tectonics in controlling the emplacement of alkaline rocks in Southern Brazil and Eastern Paraguay.

More recently, reviewing the tectonic setting of alkaline rocks south of the 15°S parallel, Almeida (1983) grouped several occurrences into three major areas: 1) borders of the Paraná Basin, which includes the largest number of bodies

You have either reached a page that is unavailable for viewing or reached your viewing limit for this book.

You have either reached a page that is unavailable for viewing or reached your viewing limit for this book.

You have either reached a page that is unavailable for viewing or reached your viewing limit for this book.

glimmeritic rocks (N=18; data source: Meyer et al., 1994; Bizzi et al., 1994 and references therein) gave ranges of 0.70500 to 0.70592 (av. 0.70545±0.00034) and -4.8 to -7.9 (av. -5.56±0.87), respectively. T^{DM} Nd isotope model ages gave 908±56 Ma. The nepheline syenites and phonolites from Poços de Caldas have very restricted ranges of R_0 (78 Ma) and Nd (0.70486 to 0.70561, av. 0.70514±0.00013 and -2.69 to -3.46, av. -3.46±0.37, respectively), with T^{DM} model ages fitting 740±76 Ma (cf. Shea, 1992).

Notably, the potassic rocks from Alto Paranaíba and Poços de Caldas display isotopic R_0 variations close to those of the flood basalts of the Paraná Basin (130 Ma, Fig. 3; data source: Piccirillo & Melfi, 1988).

INTERCRATONIC PARANÁ BASIN

The Paraná Basin is mainly characterized by extensive flood tholeiitic magmatism at 137-128 Ma over an area of more than 1,200,000 km² (Bellieni et al., 1984; Piccirillo & Melfi, 1988; Turner et al., 1994).

The alkaline magmatism was widespread mainly at the western and eastern sides (Eastern Paraguay and southeastern Brazil, respectively; cf. Figs. 1 and 2).

Eastern Paraguay

Eastern Paraguay was the site of alkaline magmatic activity mainly in Early Cretaceous (118-132 Ma; Gomes et al., this volume, Review) and in Tertiary times (39-61 Ma; Comin-Chiaramonti et al., 1991c; G. Capaldi, unpublished data).

The oldest rock-types are potassic and the younger ones are sodic. They are clearly controlled by major tectonic structures (Livieres & Quade, 1987).

In northeastern Paraguay (Amambay tectonic depression) carbonatitic complexes and associated potassic rocks occur at Cerro Chiriguelo, Cerro Sarambí and Cerro Guazú. The major controlling structure is a NE-trending (~N50E) fault zone that stretches from north of Pedro Juan Caballero to soutwest, along a straight trajectory south of Conceptión (Livieres & Quade, 1987).

In central-eastern Paraguay the major structure is the Asunción-Sapucai graben (ASU; cf. Comin-Chiaramonti et al., this volume, Magmatism), where potassic magmatism is widespread in the central-eastern side of the graben and sodic magmatism occurs at the western fringe. Two main suites are represented, i.e. basanite to phonolite (B-P) and alkali basalt to trachyphonolite/trachyte (AB-T) and intrusive equivalents. On the whole, the two suites belong to the plagioleucitite group of Foley (1992) and are distinct with respect to the APR kamafugitic-kimberlitic rock-types.

The sodic magmatism is essentially bimodal and represented by ankaratrites/nephelinites and phonolites/peralkaline phonolites. Notably, the ankaratrites/nephelinites contain mantle spinel-bearing xenoliths (Comin-Chiaramonti et al., 1986). These yielded an apparent $^{87}Rb/^{86}Sr$ vs. $^{87}Sr/^{86}Sr$ correlation from which a crude isochron can be inferred at 130.9±6.4 Ma and R_0 = 0.70361 (P. Comin-Chiaramonti, unpublished data).

Some poorly documented sodic occurrences were found in southeastern Paraguay (San Juan Bautista region), apparently controlled by NW-trending faults (Comin-Chiaramonti et al., 1992b).

The two poles of alkaline activity show distinct initial R_0 ratios, i.e. potassic 0.70714±0.00024 (N=49), and sodic 0.70375±0.00012 (N=8), respectively (Fig. 4).

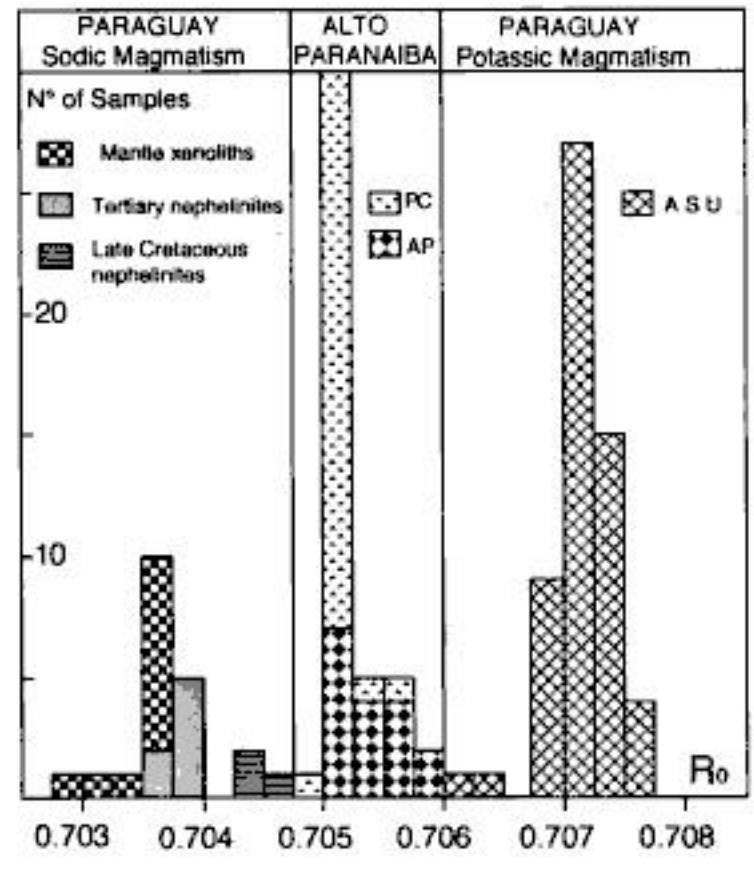

Figure 4 - Histogram of initial Sr-isotopic ratios of alkaline rock-types from Eastern Paraguay (both sodic and potassic), compared with the rock-types from Alto Paranaíba (AP) and Poços de Caldas (PC).

You have either reached a page that is unavailable for viewing or reached your viewing limit for this book.

You have either reached a page that is unavailable for viewing or reached your viewing limit for this book.

You have either reached a page that is unavailable for viewing or reached your viewing limit for this book.

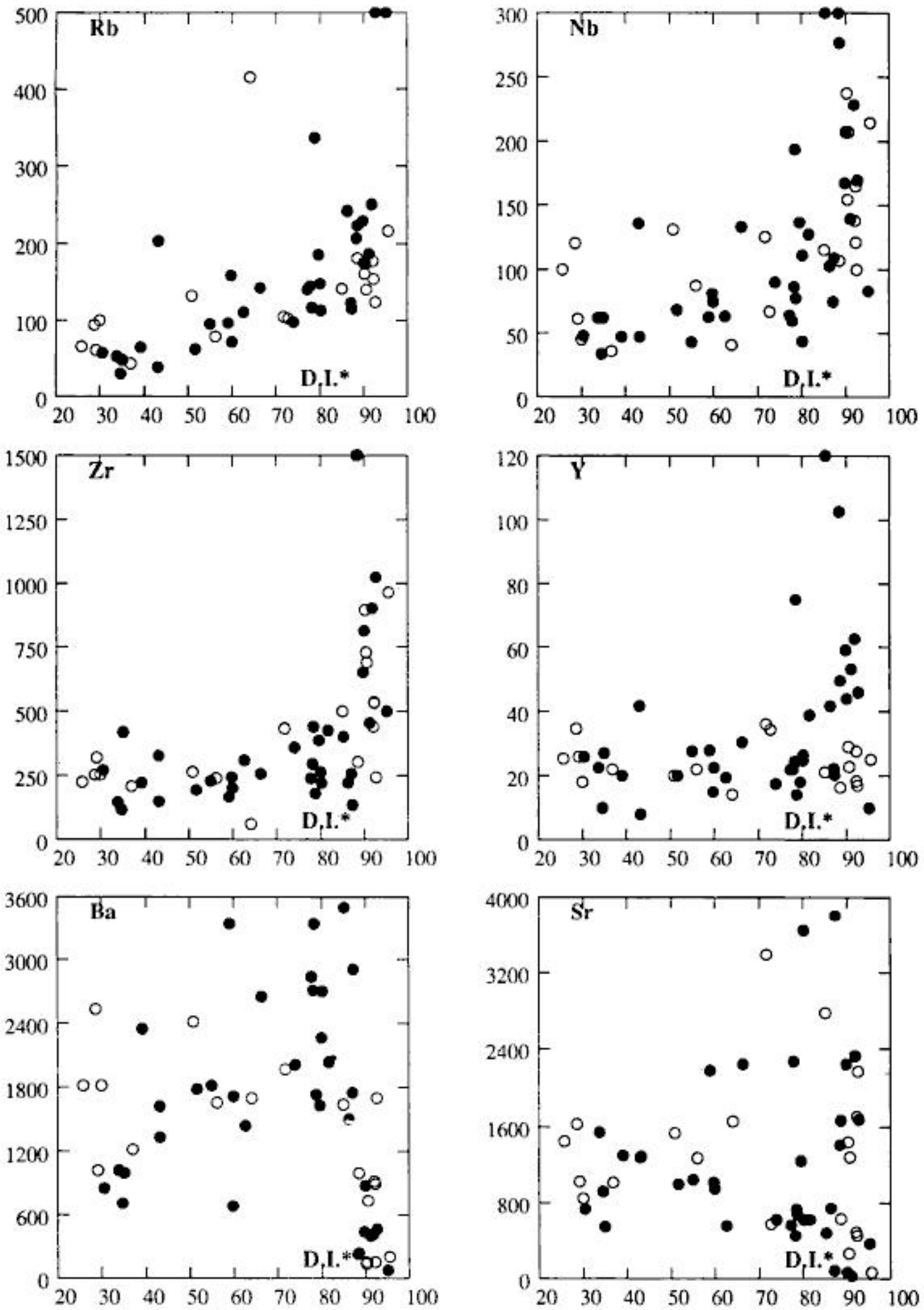

Figure 15 - Trace element variations against differentiation index (D.I.* = Q + Or + Ab + Ne + Kp + Lc + Ac) values for average Brazilian alkaline rocks. Symbols as in Fig. 10.

You have either reached a page that is unavailable for viewing or reached your viewing limit for this book.

You have either reached a page that is unavailable for viewing or reached your viewing limit for this book.

You have either reached a page that is unavailable for viewing or reached your viewing limit for this book.

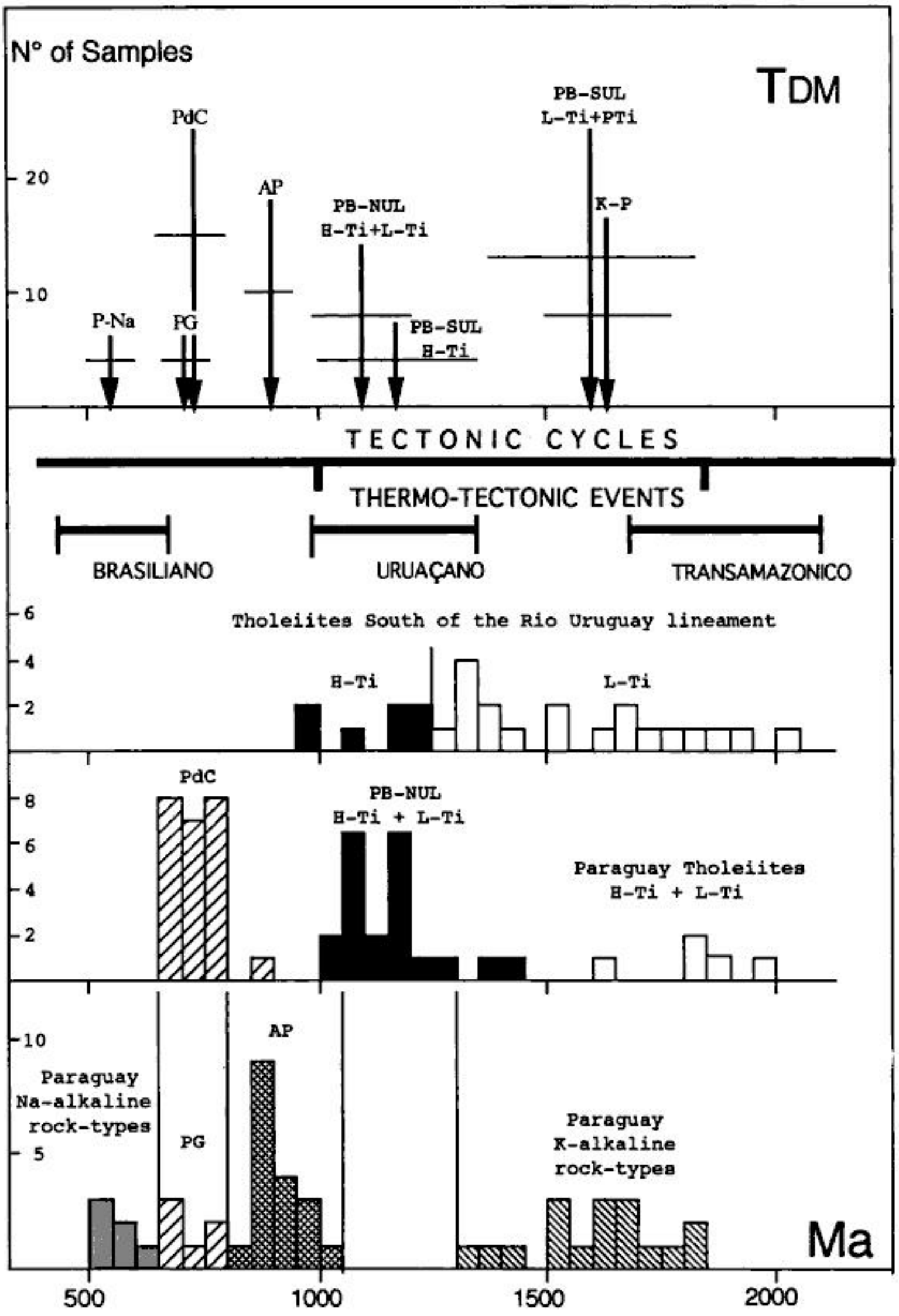

Figure 23 - Time integrated model ages (depleted mantle; cf. Faure, 1986) for alkaline rock-types and tholeiites from the Paraná Basin. Data source: Piccirillo & Melfi (1988); Comin-Chiaramonti et al. (1991c); Bizzi et al. (1994); Meyer et al. (1994); Castorina et al., this volume, Carbonatites and Sr-Nd. Tectonic, thermo-tectonic framework after Trompette (1994). Abbreviations: P-Na, Eastern Paraguay sodic magmatism; PG, Ponta Grossa Arch alkaline rocks; PdC, Poços de Caldas alkaline complex; AP, Alto Paranaíba kamafugitic magmatism; PB-NUL, SUL, Paraná Basin tholeiites North and South of the Rio Uruguay lineament, respectively; K-P, Eastern Paraguay potassic magmatism; H-Ti and L-Ti, high- and low-titanium tholeiites believed not affected by crustal contamination, respectively.

You have either reached a page that is unavailable for viewing or reached your viewing limit for this book.

You have either reached a page that is unavailable for viewing or reached your viewing limit for this book.

You have either reached a page that is unavailable for viewing or reached your viewing limit for this book.

APPENDIX I

MAGMATIC ROCK-TYPES FROM THE ASUNCIÓN-SAPUCAI GRABEN: DESCRIPTION OF THE OCCURRENCES AND PETROGRAPHICAL NOTES

P.Comin-Chiaramonti, A.De Min, C.B.Gomes

Alkaline Magmatism in Central-Eastern Paraguay. Relationships with Coeval Magmatism in Brazil. Comin-Chiaramonti, P. & Gomes, C. B. (eds.), 1996, Edusp/Fapesp, São Paulo, pp. 275-330.

ABSTRACT

The outcrops of magmatic rock-types from the Asunción-Sapucai graben are described on the basis of data collected during field seasons between 1981 to 1991. The region was subdivided into 13 main groups of occurrences and into 41 main areas. A synthetic picture with basic information relative to each area is drawn and petrographic description of the rocks are given for 530 samples.

INTRODUCTION

The Appendix I deals with the description of alkaline rocks cropping out in central-eastern Paraguay (Asunción-Sapucai graben). However, all the occurrences of magmatic rocks as indicated from field work are described, since some tholeiitic outcrops were reported as alkaline rocks in the past. Moreover some occurrences of the crystalline basement (Cambro-Ordovician rhyolites) are also considered, because they represent an important stratigraphic marker in the investigated area.

The description of the occurrences, as well as those relative to individual samples, are ordered into a east to west and south to north sequence. The order numbers (flows and intrusive rock-types: 1, 2..., 307; dykes: D1, D2..., D220) correspond to those of Appendix II, Tables A and B, respectively, and are reported along with the field numbers. The rock-types of Na-alkaline and K-alkaline affinities are either specified or not for each sample, respectively. The Group Name points to the main fields of outcropping magmatic rock-types, being ulteriorly subdivided in areas (Fig. 1). The petrographic nomenclature uses a petrochemical basis (De La Roche, 1986) and the textural nomenclature conforms to Comin-Chiaramonti et al. (1988), following the geological glossary after Bates & Jackson (1980).

The phases (subdivided into: phenocrysts, maximum diameter > 1 mm; microphenocrysts, maximum diameter in the range of 0.2-1 mm; groundmass, crystals with maximum diameter < 0.2 mm, including glass and/or interstitial phases and accessory minerals) are ordered into decreasing volume abundances.

You have either reached a page that is unavailable for viewing or reached your viewing limit for this book.

You have either reached a page that is unavailable for viewing or reached your viewing limit for this book.

You have either reached a page that is unavailable for viewing or reached your viewing limit for this book.

fringe lies about 6 km N of La Col-mena town. The highland is mainly composed of red sandstones of the Misiones Formation displaying a NW-SE orientation. Two main bodies of K-alkaline rocks, along with some dykes (Fig. 5), rest unconformably on the sediments.

11. Cañada

Location: 25°47.6'S, 56°46.8'W. The body crops out at 2 km E of Cerro Chobí.
Age: Not available; probably around 127 Ma, because Rb/Sr isotopic data fit the 126.5±7.6 Ma reference isochron of Velázquez et al. (1992).
Country rocks: Red sandstones of the Misiones Formation.
Intrusive/Extrusive Forms: Oval shaped stock, up to 165 m high.
Area/Volume: About 0.8 km^2; < 0.1 km^3.
Main rock-types: K-alkali gabbros to nephelinic syenites. Cumulates of ijolitic rocks are also present.

12. Cerro Chobí

Location: 25°47.5'S, 56°48.7'W. The main body lies about 3.5 km S of the Ybytymí town.
Age: Not available; probably the same age as the Cañada stock.
Country rocks: Red sandstones of the Misiones Formation.
Intrusive/Extrusive Forms: NW-SE elongated stock, up to 475 m high, with an associated dyke swarm.
Area/Volume: About 1 km^2; 0.5 km^3.
Main rock-types: K-essexites and essexitic gabbros; subordinate syenogabbros.

13. Potrero Garay

Location: 25°50.3'S, 56°49.2'W. Outcrops are found about 4 km N of La Colmena town.
Age: Post-Jurassic. Radiometric ages are not available.
Country rocks: Red sandstones of the Misiones Formation.
Intrusive/Extrusive Forms: Unknown, probable stock. Few blocks at the top of the hill.
Area/Volume: Unknown.
Main rock-types: K-alkaline essexites.

Cerro Yaguarú Group

The area extends between 56°50.8'-56°54.6'W and 25°45.0'-25°42.3'S. Two small lava domes of K-alkaline trachyandesites (samples 87-PS150 and 88-PS149A) and dykes of both K- and Na-alkaline affinity crop out in the field. Notably, a giant dyke consisting of Na-alkaline rocks (samples D49-PS116, D50-PS117 and D52-PS118) cuts all the other dykes (Fig. 6). The dykes belong to both basanite-phonolite and alkali basalt-trachyphonolite suites (Comin-Chiaramonti et al., this volume).

14. Valle-í

Location: 25°44.4'S, 56°51.2'W.
Age: Post-Jurassic.
Country rocks: Red sandstones of the Misiones Formation.
Intrusive/Extrusive Forms: Dyke.
Area/Volume: Unknown.
Main rock-types: K-peralkaline trachy-phonolites.

15. Cerro Yaguarú

Location: 25°43.5'S, 56°52.9'W.
Age: K-alkaline rock-types are post-Jurassic and pre-Tertiary. The giant Na-tephritic dyke (samples D49-PS116 to D52-PS118) has a K/Ar, whole-rock, age of 32.8±0.9 Ma (Gomes et al., this volume).
Country rocks: Red sandstones of the Misiones Formation.
Intrusive/Extrusive Forms: A small lava dome (87-PS150) and dykes of K- and Na-alkaline affinities.

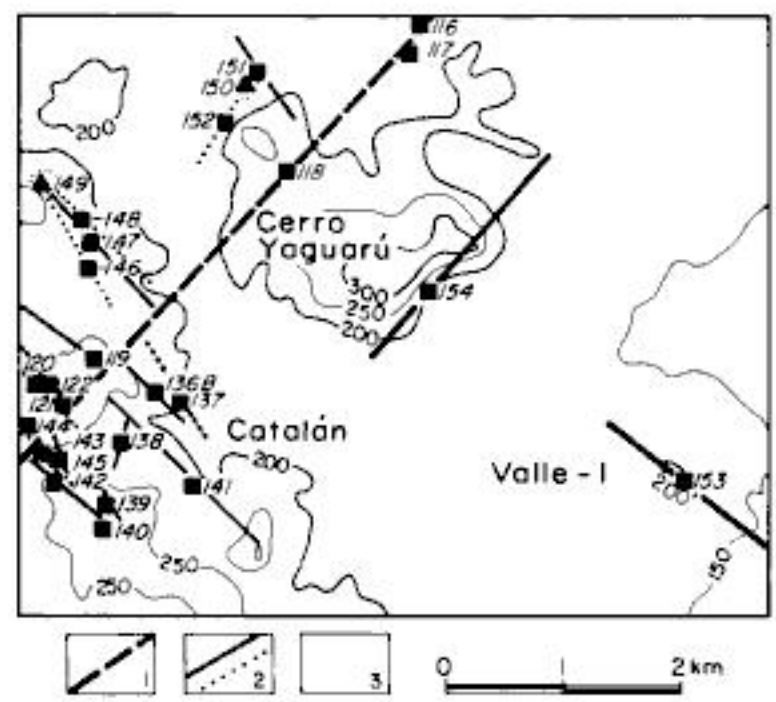

Figure 6 - Sketch map of the alkaline outcrops in the area of Cerro Yaguarú. 1. Na-alkaline mafic dyke; 2. K-alkaline mafic and phonolitic dykes (full and dotted lines, respectively); 3. red sandstones of the Misiones Formation (Triassic-Jurassic). Other symbols as in Fig. 2.

You have either reached a page that is unavailable for viewing or reached your viewing limit for this book.

You have either reached a page that is unavailable for viewing or reached your viewing limit for this book.

You have either reached a page that is unavailable for viewing or reached your viewing limit for this book.

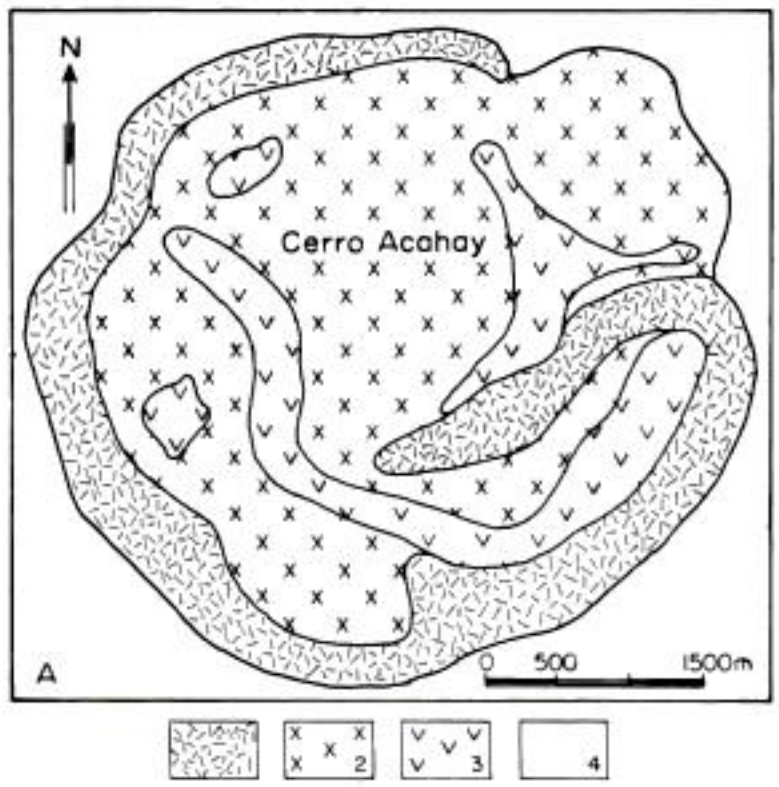

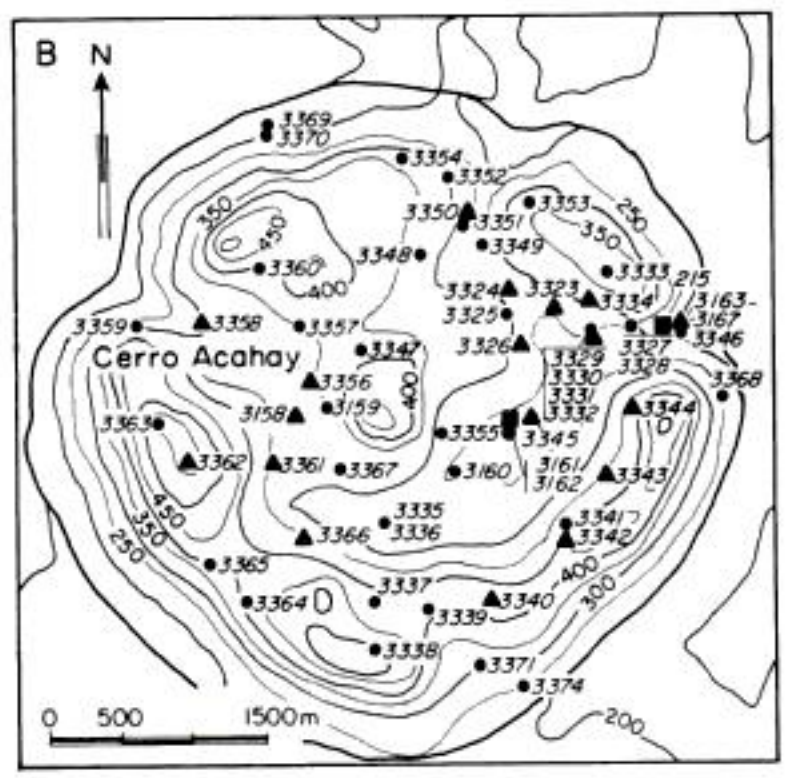

Figure 16 - Sketch map of Cerro Acahay complex (Comin-Chiaramonti et al., 1990). A. geological sketch (computer interpolation): 1. essexite + syenodiorite; 2. theralite + essexitic gabbro + syenogabbro; 3. trachybasalt + trachyandesite + trachyte; 4. sandstones of the Caacupé Group (Silurian). B. topographic map showing the collected samples (circles, intrusive facies; triangles, effusive facies; squares, dykes).

Intrusive/Extrusive Forms: Lava flow.
Area/Volume: A few hundred square meters; <0.1 km^3.
Main rock-types: K-alkaline trachyandesites

32. Cerro Ybypyté

Location: 25°44.9'S, 57°11.1'W.
Age: Post-Jurassic. A lava-flow sample (254-PS206, Estancia las Rosas) gives a K/Ar, whole-rock, age of 124±2.4 Ma.
Country rocks: Red sandstones of the Caacupé and Itacurubí Groups and red sandstones of the Misiones Formation.

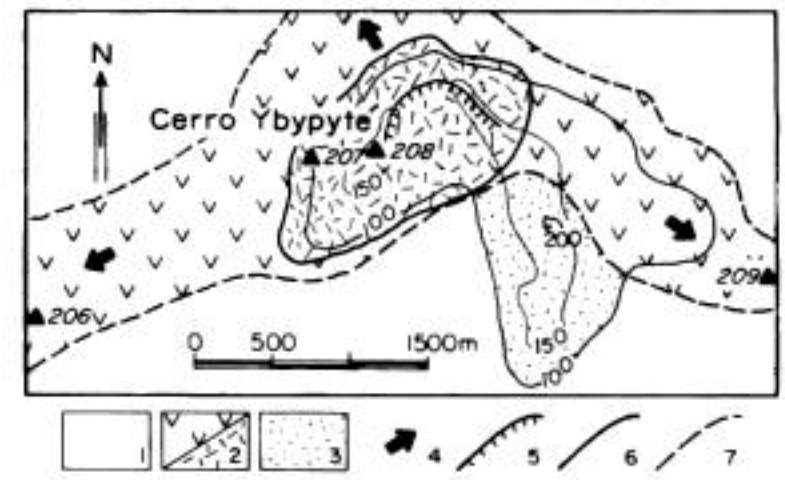

Figure 17 - Sketch map of Cerro Ybypyté dome. 1. alluvial sediments; 2. lava flows (a) and lava dome (b); 3. sandstones of the Caacupé and Itacurubí Groups; 4. orientation of the lava flows; 5. remnant of the caldera; 6. limit of the lava dome; 7. actual limit of the lava flows. Other symbols as in Fig. 2.

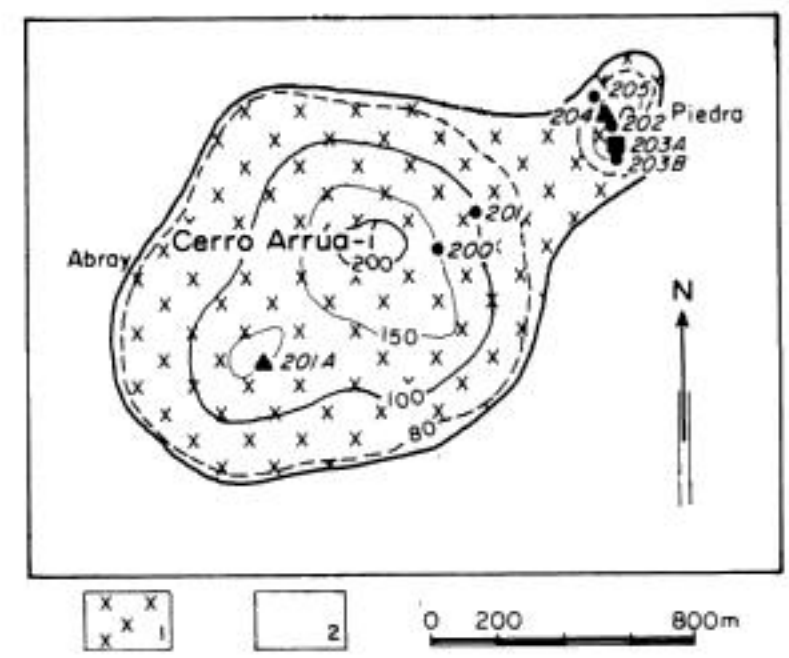

Figure 18 - Sketch map of Cerro Arrúa-í stock. 1. magmatic rocks; 2. red sandstones of the Misiones Formation.

Intrusive/Extrusive Forms: Emission center with a partially preserved caldera. Lava dome, 156 m high, and lava flows.
Area/Volume: About 3 km^2; < 0.5 km^3.
Main rock-types: K-alkaline trachybasalts, latibasalts and trachyandesites.

Yaguarón Group

The Yaguarón area is characterized by several circular hills and blocks (e.g. Cerro Arrúa-í, Cerro Ñanduá, Cerro Yaguarón, Cerro Curupayty) similar in morphology to the occurrences of alkaline domes and/or stocks of the region (e.g. Cerro Gimenez, Cerro Medina, Cerro Yarigua-á). Only Cerro Arrúa-í clearly represents a stock of alkaline rocks (Fig. 18), the other being knolls of red sandstones of the Misiones Formation.

You have either reached a page that is unavailable for viewing or reached your viewing limit for this book.

You have either reached a page that is unavailable for viewing or reached your viewing limit for this book.

You have either reached a page that is unavailable for viewing or reached your viewing limit for this book.

You have either reached a page that is unavailable for viewing or reached your viewing limit for this book.

You have either reached a page that is unavailable for viewing or reached your viewing limit for this book.

You have either reached a page that is unavailable for viewing or reached your viewing limit for this book.

You have either reached a page that is unavailable for viewing or reached your viewing limit for this book.

Rock-type	Sample	Texture	Phenocrysts	Microphenо.	Groundmass	Miscellaneous
Essexitic gabbro	**83** PS586	Holocrystalline			Seriate Af, Cpx, Ne, Biot, Op, Pl, Ap	
Essexitic gabbro	**84** PS587	Holocrystalline			Seriate Af, Cpx, Ne, Biot, Op, Pl, Ap	
Essexite	**85** PS588	Porphyritic	Cpx, Lc*		Holocrystalline, seriate Af, Ne, Cpx, Op, Biot, Ap	Ol with fayalitic rims and Biot overgrowth; Zeol patches
ASSOCIATED DYKES						
Trachy-andesite	**D23** PS591	Strongly porphyritic	Cpx	Cpx, Ol, Lc*, Op	Hypohyaline Cpx, Op, Ol, Ap	
Peralkaline trachy-phonolite	**D24** PS596	Porphyritic	Af	Af, Lc*, Biot	Hyalotrachytic Af, Gar, Cpx	
Trachy-basalt	**D25** PS589	Strongly porphyritic	Cpx	Cpx, Lc*, Ol, Op	Hypohyaline Cpx, Op, Ol, Biot	Ol → felty mass of Op
Trachy-basalt	**D26** PS590	Strongly porphyritic	Cpx, Ol, Lc*	Cpx, Ol, Lc*, Op	Hyaline Cpx, Op, Biot	"Exsolved" Ol with fayalitic rims
Peralkaline phonolite	**D27** PS592	Porphyritic	Af	Af, Lc*, Biot	Hyalotrachytic Af, Gar, Cpx	
Syeno-gabbro	**D28** PS593	Holocrystalline			Seriate Cpx, Af, Ne, Op, Biot, Op, Sp, Ap	Xenolith in PS592 dyke
Phono-tephrite	**D29** PS594	Strongly porphyritic	Cpx, Lc*	Cpx, Op, Ol, Lc*	Hypohyaline Op, Cpx, Af	Zeol patches
Tephrite	**D30** PS595	Strongly porphyritic	Cpx	Cpx, Ol, Op, Lc*	Hypohyaline Cpx, Op, Ol	Strongly zoned Cpx with pink rims
Tephrite	**D31** PS597	Strongly porphyritic	Cpx, Lc*	Cpx, Ol, Lc*, Op	Hypohyaline Cpx, Op, Biot, Ap	Strongly zoned Cpx with pink rims
Phono-tephrite	**D32** PS599	Strongly porphyritic	Cpx, Lc*	Cpx, Ol, Op, Pl	Hyaline Cpx, Af, Op, Ap	
Peralkaline phonolite	**D33** PS598 (sodic)	Aphyric			Hyalotrachytic Af, Cpx	
Tephrite	**D34** PS602	Strongly porphyritic	Cpx, Lc*, Ol, Af	Cpx, Lc*, Ol, Op	Hyaline Cpx, Op, Ol, Ap	Strongly zoned Cpx with pink rims
Phono-tephrite	**D35** PS601	Strongly porphyritic	Cpx, Lc*	Cpx, Op, Ol	Hypohyaline Cpx, Af, Biot, Ap	

You have either reached a page that is unavailable for viewing or reached your viewing limit for this book.

You have either reached a page that is unavailable for viewing or reached your viewing limit for this book.

You have either reached a page that is unavailable for viewing or reached your viewing limit for this book.

You have either reached a page that is unavailable for viewing or reached your viewing limit for this book.

You have either reached a page that is unavailable for viewing or reached your viewing limit for this book.

You have either reached a page that is unavailable for viewing or reached your viewing limit for this book.

You have either reached a page that is unavailable for viewing or reached your viewing limit for this book.

Rock-type	Sample	Texture	Phenocrysts	Microphenо.	Groundmass	Miscellaneous
Trachy-basalt	**D96** PS162	Strongly porphyritic	Cpx, Ol	Ol, Cpx, Op	Hypocrystalline Af, Cpx, Op, Ne*, Pl, Ol, Ap	
Alkali basalt	**D97** PS159	Strongly porphyritic	Cpx, Ol	Cpx, Ol, Op	Hypohyaline Cpx, Op, Pl, Af, Ap	Rare Zeol patches
Trachy-andesite	**D98** PS225	Weakly porphyritic	Cpx	Cpx, Ol, Op	Hypocrystalline Pl, Af, Cpx, Op, Ne*, Ap, Zr	
Trachy-basalt	**D99** PS131	Porphyritic	Cpx, Ol	Cpx, Ol, Pl, Op	Hypocrystalline Cpx, Pl, Af, Op, Ol, Ap	
Latibasalt	**D100** PS223	Strongly porphyritic	Ol, Cpx	Cpx, Ol, Op	Hypocrystalline Pl, Cpx, Af, Op, Cc, Ap	
24. CERRO MEDINA						
Peralkaline phonolite	**117** PS220 (sodic)	Porphyritic	Af, Cpx, Ne	Af, Ne, Cpx, Am	Hypocrystalline Af, Ne, Cpx, Am	
Phonolite	**118** PS221 (sodic)	Porphyritic	Cpx, Am, Af, Ne	Cpx, Am, Af, Ne	Hyaline	Pl xenocrysts
Peralkaline phonolite	**119** PS218 (sodic)	Holocrystalline			Microgranular Af, Ne, Cpx, Am	
Peralkaline phonolite	**120** PS219 (sodic)	Porphyritic	Af, Cpx, Ne	Af, Ne, Cpx, Am	Hypocrystalline Af, Ne, Cpx, Am	

Sapucai Group

25. SAPUCAI						
Essexitic gabbro	**121** PS109	Porphyritic	Cpx		Holocrystalline, seriate Cpx, Af, Ne, Am, Biot, Pl, Op, Ap, Zr	
Tephrite	**122** 3389	Strongly porphyritic	Cpx, Lc*	Cpx, Lc*, Ol, Op	Hypohyaline Cpx, Af, Lc*, Ol, Op, Biot, Pl, Ap	
Essexitic gabbro	**123** 3395	Porphyritic	Cpx		Holocrystalline, seriate Cpx, Af, Ne, Am, Biot, Pl, Op, Ap, Zr	
Phono-tephrite	**124** PS15	Weakly porphyritic	Cpx, Lc*	Cpx, Lc*, Op	Hypohyaline Cpx, Pl, Lc*, Op, Ol	

You have either reached a page that is unavailable for viewing or reached your viewing limit for this book.

You have either reached a page that is unavailable for viewing or reached your viewing limit for this book.

You have either reached a page that is unavailable for viewing or reached your viewing limit for this book.

Rock-type	Sample	Texture	Phenocrysts	Microphenо.	Groundmass	Miscellaneous
Phono-tephrite	**D104** PS123	Strongly porphyritic	Cpx, Pl, Ol	Cpx, Pl, Lc*, Ol, Op	Hypohyaline Cpx, Pl, Af, Lc*, Op, Ap	
Phonolite	**D105** PS105	Strongly porphyritic	Cpx, Pl	Pl, Cpx, Op, Biot, Am, Sp	Hypohyaline Cpx, Op, Af, Pl, Ap	
Tephrite	**D106** PS104	Porphyritic	Cpx, Lc*	Cpx, Lc*, Op, Ol	Hypohyaline Cpx, Op, Ol, Lc*, Af, Pl, Ap	
Tephrite	**D107** PS124	Strongly porphyritic	Cpx, Lc*	Cpx, Op	Hypohyaline Cpx, Op, Af, Lc*, Biot, Ap	
Phonolite	**D108** PS125	Porphyritic	Cpx, Op	Cpx, Op, Pl, Ol, Lc*	Hypocrystalline Cpx, Ol, Op, Pl, Af, Biot, Ap	
Phonolite	**D109** PS101	Porphyritic	Cpx, Lc*, Biot	Cpx, Lc*, Biot, Op	Hyaline Cpx, Lc*, Biot, Op, Ap, Zr	
Phonolite	**D110** PS102	Strongly porphyritic	Cpx, Lc*	Cpx, Lc*, Op, Ol	Hypohyaline Cpx, Lc*, Op, Ol, Ap	
Phono-tephrite	**D111** PS103	Strongly porphyritic	Cpx, Lc*	Cpx, Op, Ol	Hypohyaline Cpx, Op, Ol, Ap	
Trachy-basalt	**D112** PS100	Porphyritic	Cpx, Ol, Lc*	Cpx, Ol, Op	Hyaline Ap	
Phono-tephrite	**D113** PS97	Strongly porphyritic	Cpx	Cpx, Op, Ol	Hypohyaline Cpx, Af, Pl, Ne, Op, Biot, Ap	
Phono-tephrite	**D114** PS98	Strongly porphyritic	Cpx, Pl, Ol	Cpx, Ol, Pl, Op	Hypocrystalline Cpx, Pl, Af, Lc*, Op, Ol, Ap	Exsolved Ol
Phonolite	**D115** PS99	Porphyritic	Cpx, Op, Pl, Af, Lc*	Pl, Cpx, Op, Af, Lc*, Biot, Am, Ol	Holocrystalline Pl, Cpx, Op, Af, Lc*, Biot, Am, Ap	
Phonolite	**D116** PS37	Porphyritic	Cpx, Am, Sp, Lc*	Cpx, Am, Op, Sp, Biot, Ol, Op	Hyaline Zr	
Peralkaline phonolite	**D117** PS38 (sodic)	Strongly porphyritic	Cpx, Af, Lc*, Sp, Am	Cpx, Op, Sp, Am	Hyaline	Pl xenocrysts
Phonolite	**D118** PS35	Porphyritic	Pl, Cpx, Am, Lc*	Cpx, Am, Op, Sp	Hyaline Zr	
Phonolite	**D119** PS36	Porphyritic	Am, Cpx, Af	Cpx, Am, Op, Gar, Af, Lc*	Hyaline Cpx, Af, Ne, Ap, Zr	

You have either reached a page that is unavailable for viewing or reached your viewing limit for this book.

You have either reached a page that is unavailable for viewing or reached your viewing limit for this book.

You have either reached a page that is unavailable for viewing or reached your viewing limit for this book.

Rock-type	Sample	Texture	Phenocrysts	Micropheno.	Groundmass	Miscellaneous
Trachy-basalt	**D199** PS197	Porphyritic	Cpx, Ol	Cpx, Ol, Op	Hypocrystalline Pl, Af, Cpx, Op, Ol, Ne*, Ap	Ol → Biot
Phonolite	**D200** 3377 (sodic)	Porphyritic	Pl, Cpx, Ne, Am, Gar, Sp,	Cpx, Am, Gar, Sp, Zr, Op, Zr, Op	Hyalotrachytic Af	
Phonolite	**D201** PS79	Strongly porphyritic	Cpx, Lc*, Ol, Pl	Cpx, Lc*, Ol, Pl, Op, Af	Hypohyaline Cpx, Af, Pl, Lc*, Op, Ap	Pl xenocrysts
Trachy-basalt	**D202** PS171	Porphyritic	Cpx	Cpx, Ol, Op	Hypohyaline Pl, Cpx, Af, Op, Ne*, Ap	
Alkali basalt	**D203** PS170	Strongly porphyritic	Cpx, Ol	Cpx, Ol, Op	Hypohyaline Pl, Cpx, Op, Af, Ap	Rare Zeol patches
Tephrite	**D204** PS169 (sodic)	Porphyritic	Cpx, Ol	Cpx, Ol, Op	Hypohyaline Af, Ne, Cpx, Op, Pl	
Phono-tephrite	**D205** PS110	Porphyritic	Cpx, Ol	Cpx, Ol, Op	Hyaline Cpx, Pl, Af, Op	
Tephrite	**D206** PS168 (sodic)	Porphyritic	Cpx, Ol	Cpx, Ol, Op	Hypohyaline Af, Ne, Cpx, Op, Pl	
Tephrite	**D207** PS111	Strongly porphyritic	Ol, Cpx, Lc*	Cpx, Ol, Lc*, Op	Hypohyaline Cpx, Ol, Lc*, Op, Ap	
Phono-tephrite	**D208** PS114	Porphyritic	Cpx, Ol	Cpx, Ol, Pl, Op	Hypohyaline Cpx, Op, Pl, Af, Ap	
Phonolite	**D209** PS112	Porphyritic	Pl, Cpx, Ol	Pl, Cpx, Ol, Op	Hyaline Cpx, Pl, Af, Op, Biot, Ap	
Peralkaline phonolite	**D210** PS115 (sodic)	Strongly porphyritic	Af, Cpx, Gar, Anl	Af, Cpx, Biot, Gar, Sp, Ap	Hyaline Cpx	

Cerro Gimenez Group

26. CERRO GIMENEZ

Peralkaline phonolite	**178** PS214 (sodic)	Porphyritic	Cpx, Am, Af, Ne	Cpx, Am, Af, Ne	Hypocrystalline Af, Ne, Am , Zr	
Peralkaline phonolite	**179** PS231B (sodic)	Aphyric			Microgranular Af, Ne, Cpx, Zr	

You have either reached a page that is unavailable for viewing or reached your viewing limit for this book.

You have either reached a page that is unavailable for viewing or reached your viewing limit for this book.

You have either reached a page that is unavailable for viewing or reached your viewing limit for this book.

You have either reached a page that is unavailable for viewing or reached your viewing limit for this book.

You have either reached a page that is unavailable for viewing or reached your viewing limit for this book.

You have either reached a page that is unavailable for viewing or reached your viewing limit for this book.

You have either reached a page that is unavailable for viewing or reached your viewing limit for this book.

Rock-type	Sample	Texture	Phenocrysts	Microphenо.	Groundmass	Miscellaneous
Nephelinite	**284** 3270	Weakly porphyritic	Ol	Ol, Cpx, Op	Hypocrystalline Cpx, Ol, Op, Ne, Ap	Cpx xenocrysts and mantle microxenoliths
Nephelinite	**285** 3275	Weakly porphyritic	Ol	Ol, Cpx, Op	Hypocrystalline Cpx, Ol, Op, Ne, Ap, Biot, Cc, Af	Cpx xenocrysts and mantle microxenoliths
Nephelinite	**286** 3277	Weakly porphyritic	Ol	Ol, Cpx, Op	Hypocrystalline Cpx, Ol, Op, Ne, Ap	Cpx xenocrysts and mantle microxenoliths
Nephelinite	**287** 3281	Weakly porphyritic	Ol	Ol, Cpx, Op	Hypocrystalline Cpx, Ol, Op, Ne, Ap	Cpx xenocrysts and mantle microxenoliths
Nephelinite	**288** 3283	Weakly porphyritic	Ol	Ol, Cpx, Op	Hypocrystalline Cpx, Ol, Op, Ne, Ap	Cpx xenocrysts and mantle microxenoliths
Nephelinite	**289** 3284	Weakly porphyritic	Ol	Ol, Cpx, Op	Hypocrystalline Cpx, Ol, Op, Ne, Ap, Biot, Cc	Cpx xenocrysts and mantle microxenoliths
Nephelinite	**290** 3290	Weakly porphyritic	Ol	Ol, Cpx, Op	Hypocrystalline Cpx, Ol, Op, Ne, Ap, Biot, Cc	Cpx xenocrysts and mantle microxenoliths
Nephelinite	**291** 3292	Weakly porphyritic	Ol	Ol, Cpx, Op	Hypocrystalline Cpx, Ol, Op, Ne, Ap	Cpx xenocrysts and mantle microxenoliths
Nephelinite	**292** 3295	Weakly porphyritic	Ol	Ol, Cpx, Op	Hypocrystalline Cpx, Ol, Op, Ne, Ap	Cpx xenocrysts and mantle microxenoliths
Nephelinite	**293** 3300	Weakly porphyritic	Ol	Ol, Cpx, Op	Hypocrystalline Cpx, Ol, Op, Ne, Ap, Biot, Cc, Af	Cpx xenocrysts and mantle microxenoliths
Nephelinite	**294** 3301	Weakly porphyritic	Ol	Ol, Cpx, Op	Hypocrystalline Cpx, Ol, Op, Ne, Ap	Cpx xenocrysts and mantle microxenoliths
Nephelinite	**295** 3303	Weakly porphyritic	Ol	Ol, Cpx, Op	Hypocrystalline Cpx, Ol, Op, Ne, Ap	Cpx xenocrysts and mantle microxenoliths
Nephelinite	**296** 3305	Weakly porphyritic	Ol	Ol, Cpx, Op	Hypocrystalline Cpx, Ol, Op, Ne, Ap	Cpx xenocrysts and mantle microxenoliths
Nephelinite	**297** 3309	Weakly porphyritic	Ol	Ol, Cpx, Op	Hypocrystalline Cpx, Ol, Op, Ne, Ap, Biot, Cc, Af	Cpx xenocrysts and mantle microxenoliths

You have either reached a page that is unavailable for viewing or reached your viewing limit for this book.

You have either reached a page that is unavailable for viewing or reached your viewing limit for this book.

You have either reached a page that is unavailable for viewing or reached your viewing limit for this book.

Table A - Chemical analyses of lava flows and intrusive rock-types of the Asunción-Sapucai graben (order numbers: 1...307; THF, tholeiitic lava flow; F, alkaline lava flow; S, sill; I, intrusive facies; LA, layering; X, xenolith; LD, lava dome).

Group Name	Area		Samples (order numbers)
Cordillera del Ybytyruzú	*Ybytyruzú*		1-17
	1)	*Cerro Km 23*	18-24
	2)	*Cerro San Benito*	25-30
	3)	*Cerro E Santa Helena*	31-41
Villarrica	5)	*Cerro Capiitindy*	42-45
	6)	*Mbocayaty*	46-51
	7)	*Aguapety Portón*	52-69
Colonia Vega	8)	*Cerro Itapé*	70-71
	9)	*Cerrito Itapé*	72-73
	10)	*Colonia Vega*	74
Serranía de Ybytymí	11)	*Cañada*	75-79
	12)	*Cerro Chobí*	80-85
	13)	*Potrero Garay*	86
Cerro Yaguarú	15)	*Cerro Yaguarú*	87
	16)	*Catalán*	88
Cerro Achón	18)	*Cerro Verá*	89-91
	19)	*Cerro Obí*	92-93
Cerro San José	20)	*Cerro San José*	94-103
Potrero Ybaté	21)	*Paso Villán-Franco I*	104-107
	23)	*Potrero Ybaté*	108-116
	24)	*Cerro Medina*	117-120
Sapucai	25)	*Sapucai*	121-177
Cerro Gimenez	26)	*Cerro Gimenez*	178-179
Paraguarí	27)	*Cerro Santo Tomás*	180-187
Carapeguá-Acahay	29)	*Cerro Yarigua-á*	188-190
	30)	*Cerro Acahay*	191-249
	31)	*Cerro Pinto*	250
	32)	*Cerro Ybypyté*	251-254
Yaguarón	33)	*Cerro Arrúa-í*	255-261
Asunción	A)	*Cerro Patiño*	262
	B)	*Limpio*	263-264
	C)	*Cerro Verde*	265-266
	D)	*Ñemby*	267-301
	E)	*Cerro Confuso*	302
	F)	*Nueva Tablada*	303-304
	G)	*Lambaré*	305-306
	H)	*Tacumbú*	307

You have either reached a page that is unavailable for viewing or reached your viewing limit for this book.

You have either reached a page that is unavailable for viewing or reached your viewing limit for this book.

You have either reached a page that is unavailable for viewing or reached your viewing limit for this book.

Table A (continuation).

	41 PS532 F	42 PS315 LD	43 PS500 LD	44 PS314 LD	45 PS313 LD	46 PS263A I	47 PS263 I	48 PS262 F	49 3152A I	50 3153 I
SiO_2	46.43	56.92	56.50	56.02	57.28	52.10	51.66	50.31	49.68	50.50
TiO_2	1.71	0.90	0.88	0.84	0.78	1.50	1.76	1.61	1.53	1.68
Al_2O_3	13.59	17.54	17.84	17.82	18.08	15.26	13.89	12.96	11.22	13.69
Fe_2O_3	2.13	1.70	2.28	2.13	2.17	1.83	3.30	2.11	2.49	4.40
FeO	7.61	3.21	2.67	2.44	2.60	4.57	4.11	5.86	6.22	3.49
MnO	0.18	0.15	0.16	0.15	0.16	0.09	0.11	0.13	0.14	0.14
MgO	6.76	0.71	0.86	0.72	0.60	5.50	6.37	7.44	9.46	7.08
CaO	10.53	4.47	4.45	4.05	4.09	4.56	5.25	8.13	8.58	6.42
Na_2O	3.20	6.10	5.71	5.76	6.01	2.31	2.04	3.03	1.65	2.67
K_2O	5.26	5.21	5.59	6.03	5.44	9.41	8.13	4.44	6.30	7.41
P_2O_5	0.71	0.32	0.28	0.27	0.22	0.52	0.59	0.47	0.46	0.55
L.O.I.	1.08	2.73	2.36	3.42	2.40	1.88	2.17	2.85	1.88	1.49
Σ	99.19	99.96	99.58	99.67	99.83	99.53	99.38	99.34	99.61	99.52
mg#	0.595	0.279	0.320	0.299	0.254	0.647	0.651	0.665	0.698	0.663
Al	0.806	0.894	0.866	0.897	0.873	0.916	0.875	0.755	0.850	0.907
Cr	255	3	5	2	2	241	429	445	471	415
Ni	59	11	7	7	3	91	131	119	112	141
Rb	80	70	77	79	74	236	162	80	123	135
Sr	1517	1864	1956	2170	2262	1590	1618	1550	1354	1440
Zr	139	318	474	549	542	397	382	298	225	373
Y	18	28	29	31	28	12	19	17	18	14
Nb	32	37	59	65	62	50	48	39	40	n.d.
Ba	1653	2101	2684	2308	2446	2090	1995	1606	1436	1872
La	67	159	154	147	153	115	91	82	86	121
Ce	131	258	251	230	242	226	178	147	161	220
Nd	60	89	84	74	78	75	73	50	53	n.d.
Rock-type	Tephrite	Trachy-phonolite	Trachy-phonolite	Trachy-phonolite	Trachy-phonolite	Essexite	Nepheline syenodiorite	Trachy-basalt	Syeno-gabbro	Essexite
Lat. S	25°53.8'	25°43.4'	25°43.1'	25°43.3'	25°43.4'	25°42.5'	25°42.5'	25°42.5'	25°42.2'	25°42.2'
Long. W	56°17.3'	56°20.7'	56°20.8'	56°20.9'	56°21.0'	56°24.8'	56°24.8'	56°25.0'	56°25.2'	56°26.0'
Q										
or	14.20	31.66	33.94	37.05	32.99	53.85	49.46	27.15	36.74	44.71
ab		38.34	34.54	32.24	37.86		5.42	15.58		0.56
an	7.33	5.23	6.73	5.15	6.48	3.55	4.86	8.94	4.69	3.58
lc	13.62					2.40			1.00	
ne	14.89	7.96	8.24	9.96	7.75	10.83	6.68	5.93	7.74	12.17
ac										
ns										
wo		1.23	0.20	0.73	0.45					
di	33.84	10.63	11.54	10.29	10.08	13.20	14.68	24.11	29.10	20.69
hy										
ol	8.93					10.56	12.39	12.16	14.75	12.01
cs										
mt	2.19	2.43	2.43	2.27	2.34	1.44	1.64	1.81	1.93	1.71
il	3.30	1.76	1.73	1.65	1.52	2.93	3.43	3.16	2.96	3.25
ap	1.70	0.77	0.67	0.67	0.54	1.24	1.45	1.18	1.11	1.31

You have either reached a page that is unavailable for viewing or reached your viewing limit for this book.

You have either reached a page that is unavailable for viewing or reached your viewing limit for this book.

You have either reached a page that is unavailable for viewing or reached your viewing limit for this book.

Table A (continuation).

	111 PS227 F	112 PS229 F	113 PS228 I	114 PS160 F	115 PS222 F	116 PS224 F	117 PS220 LD	118 PS221 LD	119 PS218 LD	120 PS219 LD
SiO_2	50.05	51.45	52.56	47.99	49.76	51.05	57.71	57.02	58.05	56.53
TiO_2	1.16	1.14	1.22	1.04	1.31	1.42	0.35	0.39	0.32	0.39
Al_2O_3	17.22	17.16	16.46	16.26	14.51	16.00	19.58	19.38	19.71	19.36
Fe_2O_3	6.52	4.27	2.23	6.63	3.56	6.82	1.14	1.35	1.23	1.54
FeO	2.51	4.40	4.84	1.68	5.01	1.97	2.21	2.17	2.06	1.97
MnO	0.18	0.17	0.12	0.16	0.13	0.15	0.19	0.18	0.20	0.18
MgO	4.21	3.82	4.40	4.80	6.44	3.72	0.30	0.37	0.27	0.33
CaO	7.95	7.89	6.60	8.60	7.83	6.62	1.86	2.18	1.70	2.00
Na_2O	3.66	3.88	3.76	1.68	4.17	4.57	9.03	8.10	9.39	8.81
K_2O	3.39	3.43	5.16	3.92	2.54	3.08	5.08	5.21	5.06	4.76
P_2O_5	0.43	0.40	0.59	0.33	0.54	0.51	0.13	0.14	0.11	0.14
L.O.I.	2.42	1.41	1.38	6.57	3.62	3.74	2.07	3.23	1.54	3.74
Σ	99.70	99.42	99.32	99.66	99.42	99.65	99.65	99.72	99.64	99.75
mg#	0.510	0.490	0.571	0.565	0.619	0.487	0.195	0.221	0.183	0.204
AI	0.563	0.588	0.715	0.431	0.662	0.678	1.040	0.979	1.062	1.015
Cr	51	55	106	57	330	62	2	2	2	2
Ni	24	30	39	28	104	24	2	2	2	2
Rb	105	30	97	102	53	43	230	218	227	204
Sr	1496	1338	1834	1255	1785	1749	322	361	270	299
Zr	208	208	262	173	246	262	829	744	837	675
Y	20	20	17	18	16	20	38	36	39	31
Nb	22	22	36	20	32	33	197	184	197	158
Ba	1031	1057	1426	1041	1191	2427	485	498	436	515
La	49	52	91	57	72	81	112	119	111	117
Ce	89	95	143	85	117	132	180	183	176	186
Nd	41	47	54	41	50	55	53	52	49	51
Rock-type	Trachy-basalt	Trachy-basalt	Nepheline syenodiorite	Olivine basalt	Trachy-basalt	Trachy-andesite	Peralkaline phonolite	Phonolite	Peralkaline phonolite	Peralkaline phonolite
Lat. S	25°47.9'	25°48.3'	25°48.1'	25°47.7'	25°50.2'	25°50.0'	25°50.3'	25°50.2'	25°50.5'	25°50.4'
Long. W	56°57.5'	56°57.6'	56°57.7'	56°57.8'	56°58.1'	56°59.4'	56°58.4'	56°58.4'	56°58.5'	56°58.5'
Q										
or	20.68	20.73	31.08	25.02	15.67	19.06	30.42	31.89	30.07	29.33
ab	23.26	26.04	21.50	15.40	27.35	32.70	36.14	38.71	36.95	38.57
an	21.23	19.67	13.11	27.21	14.00	14.73		1.17		
lc										
ne	4.71	4.07	5.94		5.12	4.21	20.14	17.52	19.80	20.31
ac							3.33		3.32	1.39
ns							0.05		0.59	
wo							0.12			
di	13.86	14.72	13.59	13.69	18.79	13.58	7.17	7.77	6.67	8.06
hy				6.17						
ol	11.00	9.65	9.43	7.73	13.22	9.74		0.03	0.05	0.13
cs										
mt	1.94	1.90	1.57	1.85	1.92	1.92	1.67	1.78	1.67	1.07
il	2.28	2.22	2.37	2.12	2.59	2.82	0.67	0.76	0.61	0.77
ap	1.04	0.98	1.41	0.84	1.34	1.24	0.30	0.37	0.27	0.37

You have either reached a page that is unavailable for viewing or reached your viewing limit for this book.

You have either reached a page that is unavailable for viewing or reached your viewing limit for this book.

You have either reached a page that is unavailable for viewing or reached your viewing limit for this book.

Table A (continuation).

	161 PS86 I	162 PS83 F	163 PS53 F	164 PS71 F	165 PS90 F	166 PS91 F	167 PS72 F	168 PS81 F	169 PS78 F	170 PS77 F
SiO_2	50.19	48.98	47.73	47.24	50.61	47.32	42.17	49.22	45.01	47.02
TiO_2	1.33	1.49	1.81	1.60	1.34	1.64	1.67	1.38	1.86	1.68
Al_2O_3	14.04	17.16	13.86	14.87	18.50	16.22	13.17	17.62	14.08	16.21
Fe_2O_3	3.35	4.61	5.16	4.30	3.80	5.54	8.42	3.31	7.71	4.27
FeO	4.86	4.00	4.93	5.31	3.74	4.09	0.67	4.75	3.04	5.90
MnO	0.13	0.17	0.15	0.15	0.16	0.18	0.15	0.14	0.16	0.16
MgO	6.92	3.71	5.94	6.27	2.60	4.78	4.54	4.05	7.39	4.68
CaO	7.48	7.11	8.43	8.54	5.68	8.41	7.57	6.76	8.10	8.08
Na_2O	2.27	3.49	2.35	2.99	4.33	2.90	3.01	3.48	2.42	2.96
K_2O	5.42	5.26	5.63	4.49	5.87	4.45	5.15	5.28	4.76	4.90
P_2O_5	0.48	0.53	0.36	0.34	0.62	0.43	0.29	0.45	0.46	0.45
L.O.I.	2.50	2.36	2.59	2.79	2.03	3.09	12.00	2.56	4.11	2.45
Σ	98.97	98.87	98.94	98.89	99.28	99.05	98.81	99.00	99.10	98.76
mg#	0.645	0.485	0.562	0.586	0.429	0.522	0.533	0.520	0.605	0.499
Al	0.684	0.666	0.719	0.658	0.728	0.591	0.799	0.649	0.649	0.628
Cr	338	30	168	107	18	40	51	35	183	38
Ni	79	15	51	43	2	18	18	16	65	22
Rb	118	114	126	96	121	107	148	119	130	102
Sr	1823	1995	2086	2364	1721	2469	1126	1639	2068	1841
Zr	218	260	260	202	307	213	280	232	292	248
Y	20	26	16	15	24	27	18	22	15	17
Nb	34	51	39	37	59	50	35	48	45	36
Ba	1299	1460	1535	1437	1563	1361	1350	1480	1734	1430
La	76	98	83	80	106	90	80	93	99	84
Ce	123	184	130	143	176	152	145	139	165	146
Nd	53	66	61	55	68	64	62	56	70	65
Rock-type	Syeno-gabbro	Phono-tephrite	Tephrite	Tephrite	Phono-tephrite	Trachy-basalt	Silico-beforsite	Phono-tephrite	Tephrite	Tephrite
Lat. S	25°42.7'	25°42.3'	25°41.5'	25°40.8'	25°42.4'	25°42.4'	25°41.0'	25°41.9'	25°41.7'	25°41.6'
Long. W	56°58.4'	56°58.4'	56°58.5'	56°58.5'	56°58.6'	56°58.6'	56°58.6'	56°58.7'	56°58.7'	56°58.7'
Q										
or	33.21	32.29	34.59	27.66	35.71	27.51	28.59	32.41	29.72	30.07
ab	12.19	11.57	1.65	5.81	14.83	9.30		12.21	1.06	5.88
an	12.55	16.20	11.04	14.47	14.15	18.89	8.35	17.48	14.30	17.16
lc							5.23			
ne	4.19	10.35	10.30	11.12	12.41	8.85	16.01	9.96	11.14	10.91
ac										
ns										
wo										
di	18.59	14.02	24.73	22.57	9.03	18.04	27.29	11.85	20.52	17.88
hy										
ol	13.63	9.41	10.95	12.23	8.11	10.93	7.90	10.46	15.98	11.39
cs										
mt	1.85	1.90	2.24	2.15	1.64	2.13	2.14	1.81	2.38	2.27
il	2.62	2.94	3.59	3.16	2.63	3.25	3.68	2.72	3.74	3.32
ap	1.18	1.31	0.91	0.84	1.51	1.08	0.81	1.11	1.18	1.11

You have either reached a page that is unavailable for viewing or reached your viewing limit for this book.

You have either reached a page that is unavailable for viewing or reached your viewing limit for this book.

You have either reached a page that is unavailable for viewing or reached your viewing limit for this book.

Table A (continuation).

	201 3328 I	202 3333 I	203 3329 F	204 3330 F	205 3331 I	206 3332 I	207 3334 F	208 3341 I	209 3342 X	210 3345 F
SiO_2	49.77	47.73	53.35	53.58	63.25	64.36	57.94	46.01	46.57	58.90
TiO_2	1.53	1.72	1.47	1.44	0.51	0.39	1.27	2.02	1.71	0.96
Al_2O_3	16.80	15.40	17.41	16.52	18.27	18.11	17.77	16.01	17.14	17.84
Fe_2O_3	1.96	2.76	3.79	3.62	1.74	1.34	2.39	3.64	3.61	3.08
FeO	6.77	7.40	4.12	3.78	0.70	0.48	2.87	7.55	6.37	1.55
MnO	0.15	0.16	0.13	0.12	0.05	0.05	0.12	0.19	0.16	0.10
MgO	4.79	6.42	3.48	4.35	0.58	0.35	1.69	5.88	3.74	2.07
CaO	8.53	10.11	6.18	6.35	1.42	1.37	3.73	10.51	8.54	3.51
Na_2O	3.69	2.77	3.93	3.86	4.68	4.32	4.74	2.61	1.58	4.50
K_2O	3.44	3.28	4.56	4.57	8.03	8.54	5.91	2.88	7.56	6.37
P_2O_5	0.71	0.60	0.44	0.48	0.14	0.11	0.52	0.93	0.81	0.31
L.O.I.	1.11	0.82	0.68	0.89	0.54	0.53	0.73	0.94	1.51	0.65
Σ	99.25	99.17	99.54	99.56	99.91	99.95	99.68	99.17	99.30	99.84
mg#	0.537	0.574	0.489	0.561	0.346	0.301	0.467	0.529	0.446	0.498
AI	0.583	0.526	0.655	0.684	0.897	0.903	0.799	0.463	0.629	0.801
Cr	94	115	11	107	2	2	2	57	21	32
Ni	32	48	19	33	9	6	8	33	29	16
Rb	78	99	102	101	112	120	116	53	152	151
Sr	1725	1716	1289	1255	273	422	1235	2057	1136	1007
Zr	238	216	281	268	93	118	410	224	242	533
Y	18	14	19	12	4	9	22	23	25	24
Nb	23	18	31	33	12	22	54	16	15	105
Ba	1131	943	1180	1191	276	336	1450	1003	598	1015
La	71	53	73	79	39	48	87	81	76	102
Ce	141	117	127	120	63	88	177	166	176	179
Nd	65	63	65	61	25	40	76	87	91	70
Rock-type	Syeno-gabbro	Alkali gabbro	Trachy-andesite	Trachy-andesite	Syenite	Syenite	Trachyte	Alkali gabbro	Phono-tephrite	Trachyte
Lat. S	25°52.7'	25°52.5'	25°52.7'	25°52.7'	25°52.7'	25°52.7'	25°52.6'	25°53.5'	25°53.5'	25°52.9'
Long. W	57°09.4'	57°09.4'	57°09.5'	57°09.5'	57°09.5'	57°09.5'	57°09.5'	57°09.6'	57°09.6'	57°09.7'
Q					0.81	2.82				
or	20.72	19.71	27.25	27.41	47.81	50.83	35.33	17.33	23.34	38.05
ab	20.62	11.47	28.66	28.40	39.96	36.82	40.19	11.52		37.65
an	19.45	20.20	16.62	14.50	5.15	4.84	9.84	23.90	17.75	9.73
lc									17.56	
ne	6.04	6.68	2.76	2.55			0.18	5.93	7.41	0.44
ac										
ns										
wo										
di	15.68	22.10	9.57	11.73	0.88	1.07	4.48	19.08	16.96	4.86
hy					3.58	2.24				
ol	10.85	12.80	9.54	9.84			3.75	13.62	9.48	5.70
cs										
mt	1.97	2.26	1.71	1.62	0.51	0.37	2.57	2.47	2.22	1.00
il	2.95	3.31	2.82	2.78	0.97	0.74	2.43	3.91	3.32	1.84
ap	1.71	1.45	1.08	1.18	0.34	0.27	1.24	2.25	1.95	0.74

You have either reached a page that is unavailable for viewing or reached your viewing limit for this book.

You have either reached a page that is unavailable for viewing or reached your viewing limit for this book.

You have either reached a page that is unavailable for viewing or reached your viewing limit for this book.

Table A (continuation).

	261	262	263	264	265	266	267	268	269	270
	PS201A	3399	3082	3082A	3080	3080A	3092	3188	3197	3204
	F	LD	LD	LD	LD	LD	LD	LD	LD	LD
SiO_2	51.14	42.52	41.88	42.32	40.03	40.47	41.03	44.60	42.76	42.04
TiO_2	1.43	2.32	2.46	2.49	2.58	2.54	2.14	2.02	2.06	1.96
Al_2O_3	16.18	14.40	13.52	13.57	11.98	12.19	12.93	12.99	13.56	13.21
Fe_2O_3	3.49	3.99	4.60	4.62	6.27	6.07	4.83	3.28	3.52	4.06
FeO	4.99	6.13	6.64	6.64	5.46	5.63	6.87	6.83	6.91	6.77
MnO	0.18	0.17	0.21	0.21	0.23	0.22	0.23	0.19	0.20	0.20
MgO	4.06	9.77	9.51	9.63	11.77	11.68	10.48	9.57	9.07	10.46
CaO	6.44	11.71	10.52	10.51	12.15	12.38	10.90	9.77	10.16	10.24
Na_2O	4.86	5.00	5.60	5.97	4.55	4.77	5.07	5.46	6.19	6.11
K_2O	4.01	0.67	1.22	1.41	0.91	0.92	1.79	1.56	1.59	1.06
P_2O_5	0.74	0.87	0.94	0.91	1.19	1.16	1.10	1.00	1.17	1.09
L.O.I.	1.79	1.87	2.29	2.37	2.44	2.11	2.64	1.98	2.05	2.03
Σ	99.31	99.42	99.39	100.65	99.56	100.14	100.01	99.25	99.24	99.23
mg#	0.508	0.679	0.650	0.652	0.690	0.689	0.663	0.673	0.654	0.678
Al	0.762	0.622	0.779	0.836	0.707	0.725	0.795	0.821	0.878	0.848
Cr	36	542	385	358	480	483	438	504	583	745
Ni	25	207	223	200	277	271	273	275	261	294
Rb	88	22	39	44	55	53	69	68	46	49
Sr	1566	1016	1111	1141	1278	1309	1071	1062	1046	982
Zr	337	152	288	313	300	304	287	216	234	217
Y	24	26	29	29	27	26	22	32	33	31
Nb	41	86	96	91	122	135	n.d.	98	105	92
Ba	1028	1090	1050	1094	1258	1305	1051	942	1017	974
La	90	81	105	115	130	135	115	101	111	104
Ce	158	145	157	172	188	195	172	165	185	162
Nd	66	49	n.d.	n.d.	n.d.	n.d.	n.d.	n.d.	n.d.	n.d.
Rock-type	Phono-tephrite	Ankaratrite	Nephelinite	Nephelinite	Ankaratrite	Ankaratrite	Nephelinite	Nephelinite	Nephelinite	Nephelinite
Lat. S	25°35.7'	25°21.8'	25°11.6'	25°11.6'	25°05.1'	25°05.1'	25°24.2'	25°24.2'	25°24.2'	25°24.2'
Long. W	56°21.4'	57°19.9'	57°28.7'	57°28.7'	57°30.8'	57°30.8'	57°32.1'	57°32.1'	57°32.1'	57°32.1'
Q										
or	24.28	4.05	7.43	8.10				9.48	9.66	6.43
ab	25.11	4.60	1.77					9.30	2.27	1.96
an	10.75	15.25	8.37	6.16	9.84	9.31	7.45	6.48	4.65	5.66
lc				0.31	4.35	4.35	8.48			
ne	9.28	20.98	25.45	27.82	21.50	22.32	23.83	20.63	27.90	27.69
ac										
ns										
wo										
di	14.17	31.26	31.93	33.27	33.49	33.35	33.04	29.77	32.08	32.01
hy										
ol	9.92	14.80	15.22	14.63	19.10	18.73	17.45	15.48	14.04	17.14
cs					0.95	1.42	0.07			
mt	1.88	2.44	2.72	2.70	2.81	2.79	2.84	2.47	2.54	2.63
il	2.78	4.50	4.81	4.81	5.05	4.91	4.16	3.93	4.01	3.82
ap	1.82	2.11	2.28	2.21	2.92	2.81	2.68	2.44	2.85	2.65

You have either reached a page that is unavailable for viewing or reached your viewing limit for this book.

You have either reached a page that is unavailable for viewing or reached your viewing limit for this book.

You have either reached a page that is unavailable for viewing or reached your viewing limit for this book.

Table B (continuation).

	D1 PS545	D2 PS523	D3 PS528	D4 PS550	D5 PS553	D6 PS553B	D7 PS508	D8 PS535	D9 PS509	D10 PS510
SiO_2	48.26	46.35	57.05	51.16	46.91	51.66	53.11	51.99	51.24	52.46
TiO_2	1.47	1.41	0.65	1.60	1.78	1.69	1.21	1.40	1.52	1.53
Al_2O_3	14.70	12.65	17.23	13.63	9.49	11.70	15.89	15.33	13.87	14.02
Fe_2O_3	3.67	5.82	1.37	2.52	4.66	n.d.	2.40	3.45	3.66	2.66
FeO	5.80	4.62	3.00	6.38	2.96	7.46	4.50	4.00	4.83	5.18
MnO	0.18	0.23	0.12	0.17	0.20	0.11	0.14	0.13	0.15	0.14
MgO	5.52	7.09	1.49	5.55	9.69	8.30	2.61	3.88	5.26	5.29
CaO	10.54	9.65	4.44	8.00	7.99	7.30	6.00	6.68	7.57	6.51
Na_2O	3.71	3.98	5.06	3.02	0.64	1.11	4.21	3.57	3.34	3.65
K_2O	4.71	1.11	6.80	5.55	6.64	7.59	6.87	7.18	5.10	6.50
P_2O_5	0.42	0.37	0.65	0.56	0.46	0.54	0.57	0.65	0.52	0.54
L.O.I.	0.82	6.61	1.89	1.64	8.32	n.d.	2.27	1.50	2.75	1.33
Σ	99.80	99.89	99.75	99.78	99.74	97.46	99.78	99.76	99.81	99.81
mg#	0.557	0.598	0.476	0.571	0.737	0.697	0.448	0.531	0.573	0.591
AI	0.762	0.613	0.910	0.805	0.868	0.858	0.904	0.890	0.794	0.930
Cr	61	207	14	204	273	237	36	70	223	170
Ni	33	76	11	49	113	123	20	34	52	44
Rb	96	83	171	150	137	158	138	146	88	127
Sr	1478	432	2027	1523	1416	1304	1736	1716	1385	1253
Zr	176	164	135	256	400	406	287	254	211	207
Y	22	21	20	25	24	22	24	22	22	21
Nb	35	34	30	43	59	56	52	46	37	38
Ba	1277	948	2520	1764	1859	1709	1816	1776	1629	1610
La	75	72	88	106	144	147	128	107	100	99
Ce	135	143	141	187	253	270	222	187	185	173
Nd	62	73	53	74	91	91	87	73	75	71
Rock-type	Tephrite	Alkali basalt	Trachy-phonolite	Trachy-basalt	Alkali basalt	Trachy-basalt	Phono-tephrite	Phono-tephrite	Trachy-andesite	Phono-tephrite
Direction		N80W			N45E		N30W		N45W	
Thickness		0.2			8.0		3.0		4.0	
Lat. S	25°56.5'	25°52.8'	25°54.0'	25°38.4'	25°46.8'	25°46.8'	25°46.8'	25°58.5'	25°47.2'	25°47.3'
Long. W	56°14.6'	56°16.3'	56°17.2'	56°06.1'	56°14.2'	56°14.2'	56°15.2'	56°15.3'	56°15.7'	56°15.8'
Q										
or	24.92	7.05	41.04	33.39	38.00	45.86	41.63	43.19	31.06	38.99
ab	23.65	29.13	11.40			2.87	13.51	6.60	16.31	10.98
an	9.62	14.34	4.31	7.38	3.75	4.61	4.30	4.72	8.02	2.72
lc	2.48				3.88					
ne	17.20	6.80	7.89	7.91	3.20	3.66	12.45	13.08	6.97	11.02
ac										
ns										
wo										
di	33.45	28.45	11.59	24.21	29.39	23.42	18.71	20.52	22.42	21.75
hy										
ol	6.44	13.52	1.08	9.28	15.14	13.29	4.12	6.01	9.11	8.53
cs										
mt	2.07	2.37	2.15	1.99	1.75	1.71	1.53	1.62	1.88	1.74
il	2.81	2.87	1.26	3.09	3.69	3.28	2.35	2.72	2.96	2.95
ap	1.01	0.94	1.55	1.34	1.21	1.31	1.41	1.55	1.28	1.31

You have either reached a page that is unavailable for viewing or reached your viewing limit for this book.

You have either reached a page that is unavailable for viewing or reached your viewing limit for this book.

You have either reached a page that is unavailable for viewing or reached your viewing limit for this book.

Table B (continuation).

	D41 PS156	D42 PS157	D43 PS158	D44 PS257	D45 3322	D46 PS256	D47 PS153	D48 PS154	D49 PS116	D50 PS117
SiO_2	59.75	56.51	47.30	46.87	55.84	59.92	60.47	47.43	46.74	46.85
TiO_2	0.14	0.95	1.39	1.91	0.79	0.13	0.12	1.44	1.66	1.65
Al_2O_3	19.12	18.35	15.44	13.97	18.03	18.88	19.05	16.14	13.31	13.59
Fe_2O_3	0.90	3.04	5.33	4.79	3.48	1.00	1.06	3.38	5.40	4.38
FeO	0.87	0.95	3.35	5.55	1.16	0.79	0.68	5.25	4.53	5.46
MnO	0.18	0.16	0.15	0.20	0.11	0.18	0.20	0.15	0.15	0.16
MgO	0.02	0.83	4.93	5.03	1.60	0.02	0.01	4.82	6.95	6.23
CaO	1.26	3.49	7.77	9.49	3.19	1.21	1.20	8.25	8.70	8.79
Na_2O	7.34	4.73	3.87	4.00	3.99	7.36	8.00	3.32	4.40	5.02
K_2O	6.62	6.35	4.09	3.13	6.64	6.61	6.15	4.30	2.60	2.26
P_2O_5	0.02	0.18	0.52	0.84	0.24	0.02	0.01	0.45	0.60	0.62
L.O.I.	3.51	4.21	5.32	3.60	4.79	3.65	2.84	4.04	3.93	3.86
Σ	99.73	99.75	99.46	99.38	99.86	99.77	99.79	98.97	98.97	98.87
mg#	0.031	0.368	0.556	0.514	0.489	0.030	0.016	0.546	0.605	0.578
Al	1.006	0.799	0.699	0.714	0.763	1.020	1.040	0.627	0.755	0.788
Cr	2	3	38	59	2	2	2	63	237	207
Ni	2	6	27	33	1	2	2	32	61	41
Rb	157	119	82	38	133	167	198	67	67	81
Sr	448	975	1140	2717	600	625	275	1264	1950	1918
Zr	1026	402	315	465	392	952	1078	258	270	275
Y	8	29	22	26	23	9	5	20	12	15
Nb	88	58	45	66	61	84	94	38	44	38
Ba	28	2164	1584	1991	1726	167	16	1184	1476	1506
La	104	134	88	133	136	109	116	72	96	96
Ce	171	207	162	220	206	170	166	125	171	175
Nd	39	74	63	92	78	37	33	49	70	74
Rock-type	Peralkaline trachyphon.	Trachy-phonolite	Phono-tephrite	Tephrite	Trachyte	Peralkaline trachyphon.	Peralkaline trachyphon.	Tephrite	Tephrite	Tephrite
Direction	N60W	N63W	N60W		N40W	NS	N55W	N47E	N45E	N45E
Thickness	3.0	1.5	2.0		25.0	10.0	3.0	4.0	10.0	10.0
Lat. S	25°46.2'	25°46.2'	25°46.2'	25°46.4'	52°46.2'	25°46.2'	25°44.4'	25°43.5'	25°42.3'	25°42.5'
Long. W	56°51.9'	56°51.9'	56°51.9'	56°52.1'	56°52.3'	56°52.4'	56°51.2'	56°52.5'	56°52.6'	56°52.7'
Q										
or	40.64	39.34	25.73	19.32	41.34	40.64	37.20	26.78	16.22	14.10
ab	40.57	35.55	12.73	13.92	34.25	39.98	43.19	10.57	15.71	17.38
an		10.56	13.49	11.43	12.30			17.30	9.35	8.27
lc										
ne	12.69	3.46	11.99	11.62	0.73	12.35	11.93	10.32	12.75	14.81
ac	0.51					1.80	1.78			
ns							0.49			
wo	0.95					0.52	0.95			
di	3.68	5.35	19.81	26.63	2.24	4.38	3.31	18.80	26.38	27.57
hy										
ol		1.48	10.17	8.91	4.74			10.23	12.60	10.80
cs										
mt	0.65	1.92	1.97	2.31	2.22	0.02	0.89	1.97	2.21	2.21
il	0.29	1.90	2.80	3.78	1.58	0.27	0.23	2.88	3.31	3.30
ap	0.03	0.44	1.31	2.07	0.61	0.03	0.03	1.14	1.48	1.55

You have either reached a page that is unavailable for viewing or reached your viewing limit for this book.

You have either reached a page that is unavailable for viewing or reached your viewing limit for this book.

You have either reached a page that is unavailable for viewing or reached your viewing limit for this book.

Table B (continuation).

	D121 PS173	D122 PS34	D123 PS175	D124 PS174	D125 PS181	D126 PS182	D127 PS16	D128 3391	D129 PS184	D130 PS186
SiO_2	58.48	44.17	54.35	52.52	53.53	54.25	53.55	52.15	52.14	52.66
TiO_2	1.84	2.29	0.22	1.52	1.26	0.20	0.24	0.30	0.95	0.60
Al_2O_3	17.06	12.78	19.89	18.30	18.23	20.19	20.80	20.74	18.54	19.70
Fe_2O_3	6.85	7.05	1.67	5.81	3.97	1.41	1.67	1.97	5.09	4.35
FeO	0.80	4.96	0.96	2.24	3.06	1.06	0.95	0.85	1.05	0.75
MnO	0.09	0.18	0.17	0.13	0.15	0.16	0.17	0.15	0.20	0.19
MgO	0.80	6.96	0.09	4.00	2.46	0.05	0.04	0.16	0.66	0.46
CaO	0.47	10.19	1.23	4.33	4.92	1.13	1.12	1.52	3.34	3.23
Na_2O	4.65	3.30	9.30	3.35	3.45	8.83	10.55	10.75	6.78	6.93
K_2O	7.07	3.26	6.61	5.26	5.47	6.55	7.15	4.24	7.19	7.80
P_2O_5	0.42	0.56	0.02	0.48	0.58	0.02	0.02	0.02	0.17	0.06
L.O.I.	1.27	3.14	5.10	1.64	2.39	5.88	3.52	7.07	3.25	2.82
Σ	99.80	98.84	99.61	99.58	99.47	99.73	99.78	99.92	99.36	99.55
mg#	0.231	0.560	0.086	0.526	0.434	0.053	0.040	0.134	0.230	0.200
Al	0.897	0.701	1.129	0.612	0.636	1.071	1.206	1.074	1.021	1.007
Cr	23	190	2	12	6	2	6	2	4	5
Ni	11	85	4	16	10	2	2	2	3	4
Rb	117	69	147	108	106	125	166	97	110	144
Sr	647	1913	1134	1157	1672	1143	1029	1448	4121	3096
Zr	400	358	579	297	355	447	718	634	1074	545
Y	37	29	11	25	27	5	4	17	44	12
Nb	60	52	64	42	45	52	97	95	131	84
Ba	1653	1626	93	2924	2874	192	122	216	2302	2318
La	140	106	135	107	99	131	133	115	218	159
Ce	245	161	168	137	177	158	166	179	323	227
Nd	104	73	32	66	71	30	34	46	98	43
Rock-type	Trachyte	Tephrite	Peralkaline phonolite	Trachy-andesite	Trachy-andesite	Peralkaline phonolite	Peralkaline phonolite	Peralkaline phonolite	Peralkaline phonolite	Peralkaline phonolite
Direction	N5E	N40W	N20W	N25E	N37W	N45W	N10E	N42E	N25E	N43E
Thickness	0.5	4.0	3.0	1.0	3.5	2.0	2.0	2.0	0.3	2.5
Lat. S	25°41.6'	25°41.3'	25°41.9'	25°41.7'	25°42.4'	25°42.4'	25°40.8'	25°43.2'	25°43.2'	25°43.2'
Long. W	56°56.8'	56°56.8'	56°56.9'	56°56.9'	56°57.1'	56°57.1'	56°57.1'	56°57.2'	56°57.2'	56°57.2'
Q	1.47									
or	42.59	20.20	40.49	30.69	33.39	40.68	42.58	26.60	44.34	47.80
ab	40.12	1.89	23.18	15.33	30.10	23.49	15.92	29.28	10.01	7.09
an		10.90		18.07	18.74					
lc										
ne		14.84	24.24	6.86		25.69	28.07	31.94	25.83	28.68
ac			2.54			2.46	2.38	2.64	1.89	0.69
ns			2.51			1.12	4.56	1.25		
wo			0.15			0.20	0.05	0.51	0.14	1.48
di		31.56	5.18	14.99	2.15	4.71	4.78	5.83	13.58	11.00
hy	5.92				1.24					
ol		11.98		8.04	8.97					
cs										
mt	3.66	2.65	1.27	1.67	1.53	1.23	1.19	1.32	1.90	1.97
il	3.57	4.57	0.43	2.85	2.47	0.38	0.46	0.60	1.88	1.18
ap	0.87	1.41	0.03	1.14	1.41	0.03	0.03	0.03	0.44	0.13

You have either reached a page that is unavailable for viewing or reached your viewing limit for this book.

You have either reached a page that is unavailable for viewing or reached your viewing limit for this book.

You have either reached a page that is unavailable for viewing or reached your viewing limit for this book.

Table B (continuation).

	D181 PS46	D182 PS47	D183 PS48	D184 PS49	D185 PS50	D186 PS55	D187 PS52	D188 PS64	D189 PS65	D190 PS66
SiO_2	55.59	49.27	49.59	48.91	47.26	52.45	52.51	49.20	47.33	47.41
TiO_2	0.79	1.53	1.25	1.52	1.61	0.64	0.71	1.76	1.56	1.65
Al_2O_3	18.98	15.80	19.74	17.38	14.42	18.73	18.85	15.86	15.98	16.49
Fe_2O_3	1.40	3.66	4.16	4.64	4.44	2.52	2.01	6.94	3.74	4.63
FeO	2.80	4.61	3.09	4.16	5.18	1.63	2.12	2.52	5.56	5.20
MnO	0.14	0.14	0.14	0.16	0.15	0.15	0.14	0.14	0.15	0.18
MgO	1.31	5.10	2.40	3.39	6.50	0.43	0.46	4.01	5.15	4.64
CaO	3.62	7.49	6.08	6.46	8.66	2.78	3.48	6.55	8.29	7.60
Na_2O	4.56	3.35	3.73	3.34	2.79	10.16	8.56	3.46	3.22	2.76
K_2O	7.13	5.22	5.73	5.62	4.71	6.29	6.73	5.64	4.79	5.26
P_2O_5	0.18	0.43	0.42	0.52	0.35	0.13	0.21	0.38	0.41	0.40
L.O.I.	3.12	2.42	2.96	2.96	2.83	3.69	3.76	2.84	2.68	2.71
Σ	99.62	99.02	99.29	99.06	98.90	99.60	99.54	99.30	98.86	98.93
mg#	0.453	0.572	0.421	0.457	0.595	0.220	0.230	0.486	0.544	0.506
Al	0.802	0.706	0.625	0.666	0.672	1.256	1.133	0.744	0.656	0.621
Cr	12	77	19	25	107	5	13	40	54	61
Ni	2	27	11	11	43	2	2	24	26	32
Rb	117	108	106	115	107	114	140	156	103	107
Sr	1218	1933	3321	2451	1856	2753	2226	1600	1764	2293
Zr	515	300	278	273	240	1129	652	312	268	234
Y	25	19	22	23	16	31	21	23	18	17
Nb	74	43	42	42	39	100	64	41	41	38
Ba	1863	1297	1507	1662	1492	1014	938	1774	1430	1500
La	132	84	93	84	77	133	101	92	83	75
Ce	243	144	158	152	133	186	139	160	144	134
Nd	94	63	63	71	58	56	40	72	61	56
Rock-type	Trachy-phonolite	Phono-tephrite	Phono-tephrite	Phono-tephrite	Tephrite	Peralkaline phonolite	Peralkaline phonolite	Phono-tephrite	Tephrite	Phono-tephrite
Direction	N42W	N42W	N53W	N40W	N48W	N25W	N35W	N29W	N29W	N55W
Thickness	1.0	1.0	1.0	2.0	2.0	5.0	4.0	3.0	5.0	2.0
Lat. S	25°41.0'	25°41.0'	25°41.0'	25°41.0'	25°41.0'	25°41.6'	25°41.4'	25°41.3'	25°41.3'	25°41.3'
Long. W	56°58.2'	56°58.2'	56°58.2'	56°58.2'	56°58.2'	56°58.3'	56°58.3'	56°58.3'	56°58.3'	56°58.3'
Q										
or	43.67	31.94	35.27	34.64	29.00	37.36	40.55	34.69	29.44	32.35
ab	25.36	10.00	12.98	11.69	4.37	16.48	12.56	10.69	5.42	6.22
an	10.59	13.10	21.02	16.51	13.46			11.55	15.60	17.75
lc										
ne	7.92	10.49	10.74	9.65	10.96	24.45	26.07	10.71	12.43	9.82
ac						3.78	3.88			
ns						4.79	2.04			
wo						1.38	2.71			
di	5.67	18.50	6.33	11.25	23.78	8.32	8.38	16.42	20.23	15.56
hy										
ol	2.72	10.03	8.57	10.00	12.23			9.44	10.71	11.84
cs										
mt	2.08	1.85	1.60	1.97	2.15	1.90	1.94	2.06	2.08	2.20
il	1.56	3.01	2.47	3.02	3.18	1.22	1.38	3.48	3.09	3.25
ap	0.44	1.08	1.04	1.28	0.87	0.33	0.49	0.94	1.01	1.01

You have either reached a page that is unavailable for viewing or reached your viewing limit for this book.

You have either reached a page that is unavailable for viewing or reached your viewing limit for this book.

You have either reached a page that is unavailable for viewing or reached your viewing limit for this book.

Padova laboratory an energy dispersive spectrometer EDS EG 1G connected to a SEM AUTOSCAN electron microprobe operating at 15 kV was employed. A MAGIC program (Colby, 1972) in the ORTEC MAGIC IV M version was used to convert count rates into oxide weight %.

The standards were oxides or simple silicate compositions and several samples were systematically analyzed in the different microprobe equipements; the reported analyses are averaged by at least three point-analyses and the results are considered accurate to within 2-3% for major elements and to about 10% for the minor ones.

SYNOPSIS OF THE MINERAL ANALYSES

Table 1 represents a synopsis where the order- and field-numbers are the same as those in the Appendix I and Appendix II. The microprobe analyses are subdivided here into Appendix III.1 {Table 2 (potassic intrusives); Table 3 (potassic effusives) and Table 4 (potassic dykes)} and Appendix III.2 (Table 5, sodic rock-types).

The following symbols are adopted:

Intrusive rock-types: (E) and (L): minerals of early and late crystallization, respectively; (C) core, (I) intermediate portions and (R) rim of the crystals; Mxl, megacryst; mxl, microlites.

Effusive rock-types and dykes: (X) xenocrysts, (P) phenocrysts, (mP) microphenocrysts and (gm) groundmass microlites. (C) core, (I) intermediate portions and (R) rim of the crystals.

The chemical analyses are presented under the following characteristics:

Clinopyroxene: total Fe, as FeO, was partitioned to Fe_2O_3 and FeO, assuming charge balance and a theoretical formula containing 4 cations and 6 oxygens.

Olivine: structural formula calculated on the basis of 4 oxygens.

Fe-Ti oxides: Fe_2O_3, FeO, ulvöspinel (ulv. mole %: magnetite) and R_2O_3 (mole %: ilmenite) calculated according to Carmichael (1967).

Mica: structural formulae calculated on the basis of 24 (O, OH, F) and H_2O estimated assuming (OH, F)=4.000 a.f.u.

Amphibole: structural formulae calculated on the basis of 24 (O, OH, F) and H_2O estimated assuming (OH,F)=2.000 a.f.u.

Plagioclase and alkali feldspars: expressed in terms of Or-Ab-An (wt %), and structural formulae from theoretical $X_4Z_6O_{32}$.

Feldspathoids: expressed in terms of Ne-Ks-An-Qz and Ne-Ks-Qz (wt %). Anc: analcime; Lc: leucite; Lc*: pseudoleucite; Ne*: altered nepheline (e.g. hydronepheline). Structural formulae, calculated on the basis of 32, 6 and 7 oxygens for nepheline, leucite and analcime, respectively, are presented only for compositions close to stoichiometry.

Garnet: structural formulae on 24 oxygen basis and Fe_2O_3 as from charge balance.

Sphene: structural formulae on the basis of 4 Si and assuming all Fe as FeO.

ACKNOWLEDGEMENTS

The authors gratefully acknowledge the support of the Australian Research Grant Committee and of Italian (CNR and MURST) agencies. Special thanks are due to C.Garbarino (Cagliari University), to M. Molin, A. Fioretti, P. Da Roit (Padova University), for their generous and continuous assistance during the microanalytical work.

A.C. gratefully acknowledges the assistance of Pat Kelly (Geotrack International) in the microanalytical work carried out at the School of Earth Sciences, Melbourne University.

REFERENCES

CARMICHAEL, I.S.E. (1967) The iron-titanium oxides of salic volcanic rocks and their associated ferro-magnesian silicates. Contr. Miner. Petrol., *5*:310-357.

COLBY, J.W. (1972) Magic IV, a computer program for quantitative electron microprobe analysis. Bell Telephone Laboratories Inc., Alletown, Pennsylvania.

COMIN-CHIARAMONTI, P.; GOMES, C.B.; PICCIRILLO, E.M.; BELLIENI, G.; CASTILLO, A.M.C.; DEMARCHI, G.; GALLO, P; VELÁZQUEZ, J.C. (1990a) Petrologia do maciço alcalino de Acahay, Paraguai Oriental. Rev. Bras. Geoc., *20*:133-152.

You have either reached a page that is unavailable for viewing or reached your viewing limit for this book.

You have either reached a page that is unavailable for viewing or reached your viewing limit for this book.

You have either reached a page that is unavailable for viewing or reached your viewing limit for this book.

Table 2.1 (continuation).

	77				78			79			86	
	PS245	PS245	PS245 mxl	PS245	PS243 E	PS243	PS244 E	PS244 L	PS244	PS242 E	PS242 L	PS242
SiO_2	48.87	51.24	52.48	49.26	50.29	49.14	50.28	49.85	49.97	50.41	48.47	49.29
TiO_2	1.63	0.93	0.66	1.39	1.39	1.42	0.47	1.68	1.07	1.53	1.44	1.42
Al_2O_3	3.64	2.00	0.73	3.92	3.99	3.92	3.27	3.70	3.91	4.03	5.80	3.90
Cr_2O_3	0.05	0.05	0.04	0.05	0.02	0.03	0.03	0.00	0.11	0.01	0.02	0.00
Fe_2O_3*	6.05	3.37	2.86	1.95	1.59	3.00	6.21	2.12	2.76	1.80	2.77	2.53
FeO*	0.62	2.04	3.02	5.84	5.54	5.04	2.01	6.26	5.02	4.40	5.09	5.46
MnO	0.12	0.11	0.19	0.21	0.22	0.22	0.28	0.23	0.19	0.20	0.18	0.17
MgO	13.68	14.89	14.59	13.41	13.70	13.38	15.33	12.43	14.11	14.20	12.40	13.33
NiO												0.00
CaO	24.47	23.98	24.09	22.03	22.73	22.51	21.26	23.03	21.65	23.26	22.82	22.52
Na_2O	0.51	0.50	0.54	0.43	0.45	0.45	0.80	0.64	0.56	0.38	0.57	0.42
Sum	99.64	99.11	99.20	98.48	99.92	99.12	99.94	99.94	99.36	100.02	99.58	99.05
Si	1.818	1.904	1.952	1.860	1.868	1.846	1.857	1.865	1.864	1.864	1.813	1.853
Al^{IV}	0.182	0.096	0.048	0.140	0.132	0.154	0.142	0.135	0.136	0.136	0.187	0.147
Sum	2.000	2.000	2.000	2.000	2.000	2.000	2.000	2.000	2.000	2.000	2.000	2.000
Al^{VI}	0.000	0.000	0.000	0.035	0.042	0.020	0.000	0.028	0.036	0.039	0.069	0.026
Fe**	0.019	0.063	0.094	0.184	0.172	0.158	0.062	0.196	0.156	0.136	0.159	0.172
Mn	0.004	0.004	0.006	0.007	0.007	0.007	0.009	0.007	0.006	0.006	0.006	0.005
Mg	0.759	0.825	0.809	0.755	0.758	0.750	0.844	0.693	0.784	0.782	0.691	0.747
Ni												0.000
Fe***	0.170	0.094	0.080	0.055	0.044	0.085	0.173	0.060	0.078	0.050	0.078	0.072
Cr	0.001	0.001	0.001	0.002	0.000	0.001	0.000	0.000	0.003	0.000	0.000	0.000
Ti	0.024	0.018	0.003	0.039	0.039	0.040	0.013	0.047	0.030	0.037	0.041	0.040
Ca	0.976	0.955	0.960	0.891	0.904	0.906	0.842	0.923	0.865	0.921	0.915	0.907
Na	0.037	0.036	0.039	0.031	0.032	0.033	0.057	0.046	0.041	0.027	0.041	0.031
Sum	1.990	1.996	1.992	1.999	2.000	1.981	2.000	2.000	1.999	2.000	2.000	2..000
Ca	50.62	49.20	49.26	47.09	47.96	47.53	43.63	49.12	45.79	48.60	49.49	47.79
Mg	39.37	42.50	41.51	39.91	40.21	39.35	43.73	36.88	41.50	41.27	37.37	39.36
Fe**	10.01	8.30	9.23	13.00	11.83	13.12	12.64	14.00	12.71	10.13	13.14	12.85
mg#	0.98	0.93	0.90	0.80	0.82	0.83	0.93	0.78	0.83	0.85	0.81	0.81

	96								98			103
	PS230 E	PS230 L	PS230 mxl	PS230 mxl	PS230 Mxl	PS230 Mxl	PS236 E	PS236 L	PS236 R	PS236 R	PS236 mxl	PS237 E
SiO_2	51.51	49.81	50.86	50.09	49.92	52.22	50.49	49.11	49.15	49.23	49.21	49.08
TiO_2	1.23	1.46	0.76	0.96	1.34	0.61	1.27	1.48	1.25	1.25	1.63	1.68
Al_2O_3	3.73	3.41	2.79	2.68	3.37	2.27	3.25	4.52	3.13	3.44	4.04	4.94
Cr_2O_3	0.07	0.03	0.00	0.00	0.02	0.23	0.17	0.03	0.08	0.00	0.00	0.13
Fe_2O_3*	1.19	3.31	2.90	5.50	3.49	1.51	2.15	3.49	5.84	4.35	4.13	3.72
FeO*	6.07	5.83	7.37	3.23	5.22	3.96	3.38	4.20	2.78	3.89	4.56	2.16
MnO	0.22	0.25	0.37	0.31	0.25	0.13	0.17	0.23	0.32	0.32	0.25	0.28
MgO	14.44	13.30	11.62	13.28	13.29	15.80	15.17	13.95	13.52	13.53	13.11	16.52
NiO			0.00	0.00	0.00	0.00			0.00	0.02	0.03	
CaO	22.00	21.99	22.89	22.77	22.29	22.97	22.66	21.98	22.29	22.35	22.08	20.58
Na_2O	0.53	0.63	0.80	0.84	0.69	0.28	0.40	0.55	0.73	0.65	0.82	0.42
Sum	101.00	100.02	100.38	99.66	99.87	99.97	99.13	99.55	99.09	99.02	99.85	99.51
Si	1.887	1.860	1.905	1.872	1.864	1.920	1.876	1.830	1.846	1.851	1.837	1.808
Al^{IV}	0.113	0.140	0.095	0.128	0.136	0.080	0.124	0.170	0.154	0.149	0.163	0.192
Sum	2.000	2.000	2.000	2.000	2.000	2.000	2.000	2.000	2.000	2.000	2.000	2.000
Al^{VI}	0.048	0.010	0.028	0.000	0.012	0.018	0.018	0.029	0.000	0.003	0.015	0.022
Fe**	0.186	0.182	0.231	0.101	0.163	0.122	0.105	0.131	0.087	0.122	0.142	0.067
Mn	0.007	0.008	0.012	0.010	0.008	0.004	0.005	0.007	0.010	0.010	0.008	0.009
Mg	0.788	0.740	0.649	0.740	0.740	0.866	0.840	0.775	0.757	0.758	0.730	0.907
Ni			0.000	0.000	0.000	0.000			0.000	0.001	0.001	
Fe***	0.033	0.093	0.082	0.155	0.098	0.042	0.902	0.878	0.165	0.123	0.116	0.103
Cr	0.002	0.001	0.000	0.000	0.000	0.007	0.005	0.001	0.002	0.000	0.000	0.004
Ti	0.034	0.041	0.021	0.017	0.038	0.017	0.036	0.041	0.020	0.035	0.046	0.047
Ca	0.864	0.880	0.919	0.912	0.891	0.905	0.902	0.878	0.897	0.900	0.883	0.812
Na	0.038	0.046	0.058	0.061	0.050	0.020	0.029	0.040	0.053	0.047	0.059	0,030
Sum	2.000	2.001	2.000	1.996	2.000	2.001	2.000	2.000	1.991	1.999	2.000	2.000
Ca	46.01	46.24	48.55	47.55	46.89	46.67	47.18	46.48	46.82	47.05	46.99	42.78
Mg	41.96	38.89	34.28	38.58	38.95	44.66	43.93	41.03	39.51	39.62	38.85	47.79
Fe**	12.03	14.87	17.17	13.87	14.16	8.67	8.89	12.49	13.67	13.33	14.16	9.43
mg#	0.81	0.80	0.74	0.88	0.82	0.88	0.89	0.87	0.90	0.86	0.84	0.97

You have either reached a page that is unavailable for viewing or reached your viewing limit for this book.

You have either reached a page that is unavailable for viewing or reached your viewing limit for this book.

You have either reached a page that is unavailable for viewing or reached your viewing limit for this book.

Table 2.3 - Microprobe analyses of magnetite (MT) and ilmenite (IL). Stability relations in terms of TC-fO_2 for magnetite-ilmenite pairs were calculated according to Spencer & Lindsley (1981).

	39			47				50			51	
	PS530	PS530	PS263	PS263	PS263	PS263	3153	3153	3153	3152	3152	3152
	E	E	E	E	E	L	E	E	L	E	E	L
SiO_2	0.03	0.06	0.77	0.75	0.87	1.44	0.77	0.87	1.48	0.81	0.72	0.95
TiO_2	7.17	47.78	16.08	10.32	52.71	14.28	10.63	53.87	14.65	13.13	53.10	9.99
Al_2O_3	3.93	4.32	0.42	0.45	0.07	0.48	0.46	0.07	0.49	0.13	0.00	0.00
Cr_2O_3	0.20	0.07	0.80	1.19	0.14	0.24	1.23	0.14	0.25	1.25	0.05	0.70
Fe_2O_3*	50.98	13.76	38.10	48.21	1.91	42.59	40.35	0.00	43.49	44.30	1.38	52.46
FeO*	34.68	25.34	56.44	40.35	35.51	38.36	38.89	36.23	39.55	39.49	39.35	37.94
MnO	0.74	1.82	1.12	1.06	1.29	0.86	1.09	1.29	0.86	0.71	1.88	0.67
MgO	1.54	5.90	1.65	1.09	6.52	2.55	1.12	6.52	2.55	1.66	4.13	1.46
NiO	0.00	0.07	0.07	0.15	0.00	0.00	nd	nd	nd	nd	nd	nd
CaO	0.00	0.02	0.07	0.00	0.00	0.00	nd	nd	nd	nd	nd	nd
Sum	99.28	99.14	99.95	100.98	99.02	100.80	103.83	98.99	103.32	101.48	100.61	104.17
	MT	IL	MT	MT	IL	MT	MT	IL	MT	MT	IL	MT
	Host	Exsolved		Host	Exsolved		Host	Exsolved		Host	Exsolved	
Ulv. (mole%)	27.45		56.44	40.35		52.69	40.35			48.18		38.81
R_2O_3 (mole%)		9.78			0.99			0.12			1.29	
T(°C)		716			413			230			433	
-lof fO_2		14.9			32.1			51.3			30.2	

	52			57	66		67	68		77	78	79
	PS264	PS264	PS264	PS269	3147	3147	3149	3150	3150	PS245	PS243	PS244
	E	E	E		E	L	L	E	E	L	L	L
SiO_2	0.97	0.00	0.05	0.19	0.85	1.03	0.90	0.96	0.87	0.73	0.13	0.21
TiO_2	8.42	50.23	19.01	18.91	28.89	19.68	20.29	8.35	53.31	12.54	8.05	5.34
Al_2O_3	0.89	0.08	1.55	1.59	0.77	2.27	2.14	0.89	0.08	0.23	2.61	1.02
Cr_2O_3	0.63	0.12	0.54	0.35	0.22	0.22	0.26	0.65	0.12	0.28	0.16	0.70
Fe_2O_3*	50.12	5.95	31.48	31.73	13.41	29.19	27.13	49.71	0.00	47.73	50.28	57.83
FeO*	38.62	39.25	45.71	43.52	53.68	47.20	49.23	38.25	40.28	36.32	36.16	33.34
MnO	0.82	0.91	1.24	0.82	1.04	1.06	0.90	0.92	2.21	1.48	0.87	0.88
MgO	1.71	0.39	0.82	1.71	1.40	1.30	0.80	0.40	2.07	0.40	0.88	0.80
NiO	0.00	0.00	0.04	0.00	nd	nd	nd	nd	nd	0.05	0.03	0.08
CaO	0.00	0.00	0.01	0.01	0.21	0.16	0.09	0.00	0.00	0.61	0.07	0.09
Sum	100.95	99.91	100.45	98.83	100.50	102.11	101.74	100.13	98.94	100.37	99.24	100.29
	MT	IL	MT	MT	MT	MT	MT	MT	IL	MT	MT	MT
	Host	Exsolved						Host	Exsolved			
Ulv. (mole%)	35.81		62.39	62.42	85.84	65.68	67.66	35.79		47.16	31.13	21.88
R_2O_3 (mole%)		3.00							0.06			
T(°C)		560							206			
-lof fO_2		22.6							56.1			

	86	96	98	103	104	113	123		137	142	152	
	PS242	PS230	PS236	PS237	PS249	PS228	3395	3395	PS96	PS30	PS56	PS56
	L	L	L	E	L	L	L	L	E	L	L	L
SiO_2	0.47	0.03	0.09	0.15	0.09	0.19	0.00	0.00	0.06	0.15	0.05	0.00
TiO_2	11.62	15.47	16.42	16.63	15.18	13.51	21.36	48.11	15.73	21.93	24.70	44.34
Al_2O_3	1.87	2.19	2.89	3.27	5.83	6.26	2.44	0.23	11.03	2.64	2.34	0.15
Cr_2O_3	0.26	0.08	0.14	0.17	0.49	0.09	0.06	0.02	0.07	0.05	0.10	0.10
Fe_2O_3*	44.35	37.52	35.13	35.53	35.14	38.14	27.50	9.30	27.25	26.81	21.29	16.08
FeO*	40.30	42.49	42.07	40.50	38.29	37.53	46.71	38.81	41.34	46.57	49.90	36.27
MnO	0.75	1.02	0.90	0.97	0.57	0.59	0.99	1.25	1.39	0.85	0.43	1.65
MgO	0.73	0.91	1.60	2.29	3.50	3.36	1.56	1.79	3.20	2.00	1.89	1.07
NiO	0.08	0.04	0.05	0.08	0.06	0.00	nd	nd	nd	nd	nd	nd
CaO	0.17	0.05	0.06	0.15	0.03	0.04	0.00	0.00	0.03	0.08	0.00	0.02
Sum	100.60	99.80	99.35	99.74	99.18	99.71	100.62	99.51	100.12	101.08	100.65	99.68
	MT	MT	MT	MT	MT	MT	MT	IL	MT	MT	MT	IL
Ulv. (mole%)	43.57	53.12	55.47	55.27	50.60	46.21	67.11		51.52	68.16	74.77	
R_2O_3 (mole%)								4.83				8.48
T(°C)								805				1054
-lof fO_2								15.3				10.4

You have either reached a page that is unavailable for viewing or reached your viewing limit for this book.

You have either reached a page that is unavailable for viewing or reached your viewing limit for this book.

You have either reached a page that is unavailable for viewing or reached your viewing limit for this book.

Table 2.4 (continuation).

	98	103		123	142	152	154	161	181	193		197
	PS236	PS237	PS237	3395	PS30	PS56	PS58	PS86	3090	3164	3164	3346
	L	E	L	L	L	L	E	L	E	E	L	E
SiO_2	36.33	38.59	34.93	38.22	38.26	39.08	40.29	37.51	39.12	35.05	35.91	37.75
TiO_2	7.36	7.96	5.03	7.42	7.18	6.78	7.83	7.06	4.64	7.31	4.59	7.36
Al_2O_3	13.65	12.41	13.17	14.46	14.55	13.72	13.21	14.66	13.76	15.22	15.45	14.00
Cr_2O_3	0.02	0.00	0.00			0.00	0.00	0.00		0.07	0.00	0.00
MgO	14.34	15.50	12.64	14.84	15.16	16.27	19.26	13.84	15.52	11.98	14.22	15.78
CaO	0.00	0.00	0.05	0.00	0.00	0.00	0.06	0.10	0.00	0.04	0.10	0.00
MnO	0.16	0.11	0.26	0.14	0.17	0.16	0.13	0.19	0.18	0.42	0.35	0.11
FeO_{tot}	13.08	12.35	17.46	13.22	13.06	12.07	4.95	13.02	15.54	17.76	16.73	11.70
SrO	0.00	0.00	0.00									
BaO	0.34	0.39	0.06									
Na_2O	0.45	0.35	0.54	0.00	0.00	0.00	0.27	0.21	0.00	0.10	0.06	0.11
K_2O	9.41	9.41	9.47	8.92	8.95	8.98	9.75	8.96	8.49	9.92	10.18	10.20
NiO	0.04	0.04	0.00				0.06			0.00	0.00	0.00
F	0.77											
Sum	95.96	97.11	93.61	97.22	97.33	97.06	95.81	95.55	97.25	97.87	97.59	97.01
O=F,Cl	0.33	0.00	0.00	0.00	0.00	0.00	0.00	0.00	0.00	0.00	0.00	0.00
Sum	95.63	97.11	93.61	97.22	97.33	97.06	95.81	95.55	97.25	97.87	97.59	97.01
H_2Ocalc	3.64	4.12	3.84	4.15	4.15	4.17	4.23	4.07	4.12	4.02	4.04	4.12
Sum	99.60	101.23	97.45	101.37	101.48	101.23	100.04	99.62	101.37	101.89	101.63	101.13
Si^{IV}	5.439	5.617	5.450	5.526	5.522	5.626	5.709	5.529	5.690	5.224	5.331	5.488
Al^{IV}	2.409	2.129	2.422	2.464	2.475	2.328	2.206	2.471	2.310	2.673	2.669	2.399
Ti^{IV}	0.152	0.254	0.129	0.009	0.002	0.046	0.085	0.000	0.000	0.103	0.000	0.114
Sum (Z)	8.000	8.000	8.000	8.000	8.000	8.000	8.000	8.000	8.000	8.000	8.000	8.000
Al^{VI}	0.000	0.000	0.000	0.000	0.000	0.000	0.000	0.075	0.049	0.000	0.035	0.000
Ti^{VI}	0.677	0.617	0.461	0.797	0.777	0.688	0.749	0.783	0.508	0.716	0.512	0.691
Cr	0.002	0.000	0.000	0.000	0.000	0.000	0.000	0.000	0.000	0.008	0.000	0.000
Mg	3.201	3.363	2.940	3.199	3.262	3.492	4.068	3.041	3.365	2.662	3.147	3.420
Mn	0.020	0.014	0.034	0.017	0.021	0.020	0.016	0.024	0.022	0.053	0.044	0.014
Fe''	1.637	1.503	2.278	1.599	1.576	1.453	0.587	1.605	1.890	2.214	2.077	1.422
Ni	0.005	0.005	0.000	0.000	0.000	0.000	0.007	0.000	0.000	0.000	0.000	0.000
Sum (Y)	5.542	5.502	5.713	5.612	5.636	5.652	5.426	5.527	5.835	5.653	5.816	5.547
Ca	0.000	0.000	0.008	0.000	0.000	0.000	0.009	0.016	0.000	0.006	0.016	0.000
Sr	0.000	0.000	0.000	0.000	0.000	0.000	0.000	0.000	0.000	0.000	0.000	0.000
Na	0.132	0.099	0.163	0.000	0.000	0.000	0.074	0.060	0.000	0.029	0.017	0.031
K	1.798	1.747	1.885	1.645	1.648	1.649	1.762	1.685	1.575	1.886	1.928	1.892
Ba	0.020	0.022	0.004	0.000	0.000	0.000	0.000	0.000	0.000	0.000	0.000	0.000
Sum (X)	1.950	1.868	2.060	1.645	1.648	1.649	1.846	1.761	1.575	1.921	1.961	1.923
F	0.366	0.000	0.000	0.000	0.000	0.000	0.000	0.000	0.000	0.000	0.000	0.000
OH	3.634	4.000	4.000	4.000	4.000	4.000	4.000	4.000	4.000	4.000	4.000	4.000
Sum	4.000	4.000	4.000	4.000	4.000	4.000	4.000	4.000	4.000	4.000	4.000	4.000
mg#	0.66	0.69	0.56	0.67	0.67	0.71	0.87	0.65	0.64	0.55	0.60	0.71

You have either reached a page that is unavailable for viewing or reached your viewing limit for this book.

You have either reached a page that is unavailable for viewing or reached your viewing limit for this book.

You have either reached a page that is unavailable for viewing or reached your viewing limit for this book.

Table 2.6 - Microprobe analyses of feldspars.

	47	50	51		52	57	67	68		78			86		96
	PS263	3153	3152	3152	PS264	PS269	3149	3150	PS243	PS243	PS243	PS242	PS242	PS242	PS230E
SiO_2	63.64	65.44	64.90	64.98	64.96	64.23	60.77	66.23	65.60	65.00	64.42	60.60	64.15	63.08	58.07
Al_2O_3	18.39	18.53	18.36	18.38	19.33	19.38	24.48	18.74	18.42	18.48	17.65	19.15	19.10	19.73	23.97
CaO	0.20	0.00	0.00	0.00	0.38	0.40	6.01	0.00	0.11	0.16	0.00	0.00	0.47	0.70	6.54
Fe_2O_3	0.80	0.00	0.00	0.00	0.00	0.19	0.00	0.00	0.63	0.25	0.87	0.49	0.33	0.30	0.26
SrO	0.04				0.31	0.33			0.11	0.00	0.02	0.99	0.32	0.34	0.59
BaO	1.46				0.64	0.67			0.16	0.00	0.16	0.64	0.09	0.00	0.43
Na_2O	1.73	1.83	0.25	0.57	4.29	1.59	7.41	4.49	4.85	2.91	1.86	0.16	3.56	4.63	6.50
K_2O	13.57	14.32	16.60	16.22	10.26	14.06	1.26	10.49	9.64	12.76	14.17	15.92	11.13	8.83	1.68
Sum	99.83	100.12	100.11	100.15	100.17	100.85	99.93	99.95	99.52	99.55	99.15	97.95	99.16	97.61	98.04
Si	11.851	11.997	11.998	11.995	11.836	11.790	10.849	11.999	11.956	11.949	11.990	11.630	11.816	11.705	10.698
Al	4.036	4.004	4.000	3.999	4.151	4.193	5.151	4.001	3.957	4.003	3.871	4.331	4.147	4.315	5.205
Ca	0.040	0.000	0.000	0.000	0.074	0.079	1.150	0.000	0.021	0.031	0.000	0.000	0.093	0.139	1.291
Fe^{+++}	0.168	0.000	0.000	0.000	0.000	0.039	0.000	0.000	0.130	0.052	0.183	0.106	0.069	0.063	0.053
Sr	0.004	0.000	0.000	0.000	0.033	0.035	0.000	0.000	0.012	0.000	0.003	0.110	0.035	0.037	0.063
Ba	0.107	0.000	0.000	0.000	0.046	0.048	0.000	0.000	0.011	0.000	0.012	0.048	0.007	0.000	0.031
Na	0.625	0.650	0.090	0.204	1.515	0.566	2.565	1.577	1.714	1.037	0.671	0.060	1.272	1.665	2.322
K	3.224	3.349	3.915	3.820	2.385	3.293	0.287	2.424	2.241	2.992	3.364	3.898	2.616	2.091	0.395
Sum	20.055	20.001	20.004	20.018	20.039	20.043	20.001	20.002	20.043	20.064	20.092	20.183	20.055	20.015	20.058
Z	16.056	16.001	15.999	15.994	15.986	16.022	16.000	16.000	16.043	16.004	16.043	16.067	16.032	16.083	15.956
X	3.999	4.000	4.005	4.024	4.053	4.020	4.001	4.002	4.000	4.060	4.049	4.116	4.023	3.932	4.102

	96									98				103	
	PS230 E	PS230 L	PS230 L	PS230 L	PS230 L	PS230 L	PS236 E	PS236 L	PS236 L	PS236 L	PS236 L	PS236 L	PS236 L	PS237 E	PS237 L
SiO_2	54.19	64.28	64.31	64.37	64.15	64.37	54.92	63.25	64.53	63.76	60.86	60.65	59.89	52.80	58.62
Al_2O_3	27.28	18.64	18.55	18.63	18.76	18.63	27.11	20.47	18.68	18.51	20.84	20.55	21.43	28.67	25.31
CaO	10.51	0.69	0.67	0.68	0.72	0.68	9.32	2.00	0.32	0.19	0.27	0.38	2.45	10.90	6.78
Fe_2O_3	0.22	0.21	0.19	0.20	0.24	0.20	0.46	0.38	0.13	0.10	0.10	0.26	0.25	0.24	0.27
SrO	0.69	0.22	0.27	0.22	0.16	0.22	0.79	0.26	0.07	0.05	0.12	0.01	0.41	0.68	0.43
BaO	0.25	0.15	0.13	0.22	0.09	0.22	0.13	0.46	0.00	0.03	0.09	0.00	0.33	0.49	0.28
Na_2O	5.15	4.66	4.82	4.42	4.74	4.42	4.98	6.95	0.81	0.51	0.32	1.82	0.72	4.22	6.95
K_2O	0.38	9.54	9.24	9.88	9.49	9.88	1.29	4.67	15.43	16.16	15.76	12.91	13.71	0.97	1.03
Sum	98.77	98.39	98.18	98.61	98.36	98.61	99.00	98.44	99.97	99.31	98.35	96.57	99.20	98.97	99.67
Si	9.966	11.871	11.887	11.877	11.837	11.877	10.076	11.546	11.919	11.892	11.485	11.527	11.248	9.736	10.580
Al	5.912	4.057	4.040	4.051	4.079	4.051	5.862	4.404	4.067	4.068	4.636	4.602	4.743	6.231	5.384
Ca	2.071	0.137	0.133	0.134	0.143	0.134	1.832	0.391	0.063	0.039	0.054	0.077	0.493	2.154	1.311
Fe^{+++}	0.045	0.044	0.041	0.042	0.049	0.042	0.094	0.078	0.028	0.021	0.021	0.056	0.053	0.051	0.054
Sr	0.074	0.024	0.029	0.024	0.018	0.024	0.084	0.028	0.007	0.005	0.014	0.001	0.045	0.073	0.045
Ba	0.018	0.011	0.009	0.016	0.007	0.016	0.009	0.033	0.000	0.002	0.006	0.000	0.024	0.035	0.020
Na	1.836	1.669	1.727	1.581	1.697	1.581	1.771	2.460	0.290	0.184	0.117	0.671	0.264	1.509	2.432
K	0.088	2.248	2.179	2.325	2.235	2.325	0.302	1.088	3.636	3.844	3.794	3.130	3.285	0.228	0.237
Sum	20.025	20.059	20.045	20.050	20.064	20.050	20.030	20.026	20.010	20.056	20.127	20.064	20.155	20.017	20.063
Z	15.938	15.972	15.967	15.971	15.966	15.971	16.032	16.027	16.014	15.981	16.142	16.185	16.043	16.018	16.018
X	4.087	4.087	4.077	4.079	4.098	4.079	3.999	3.999	3.997	4.075	3.985	3.879	4.110	3.999	4.045

You have either reached a page that is unavailable for viewing or reached your viewing limit for this book.

You have either reached a page that is unavailable for viewing or reached your viewing limit for this book.

You have either reached a page that is unavailable for viewing or reached your viewing limit for this book.

Table 2.7 - Microprobe analyses of feldspathoids.

	39	50	51		57		68		77		78	86	98	123
	PS530	3153	3152	PS269	PS269	PS269	3150	PS245	PS245	PS245	PS243	PS242	PS236	3395
	E	L	L	L	L	L	L	L	L	L	L	L	L	L
	lc	anc	ne	ne	ne	ne	ne	ne	ne	ne	anc	anc	anc	ne
SiO_2	55.86	53.96	43.51	44.22	43.45	42.72	49.01	41.32	41.49	41.46	54.32	57.36	53.14	44.08
Al_2O_3	23.57	25.88	32.52	32.09	33.30	33.62	30.61	32.61	32.80	32.82	22.72	23.77	25.60	33.73
CaO	0.00	1.46	1.85	1.73	0.59	1.10	1.58	0.00	0.03	0.05	0.58	0.67	1.27	0.00
Fe_2O_3	0.20	0.00	0.00	0.69	0.24	1.04	0.00	1.72	0.03	0.01	0.50	0.90	0.54	0.00
SrO	0.00	0.22		0.15	0.06	0.11		0.00	0.00	0.03		0.07	0.09	
BaO	0.06	0.04		0.04	0.07	0.05		0.00	1.38	1.27		0.09	0.08	
Na_2O	1.30	11.98	15.88	12.19	15.26	13.98	13.09	14.53	14.51	14.67	12.07	14.45	11.12	17.22
K_2O	19.88	3.02	3.83	3.92	6.17	5.78	5.71	8.47	8.70	8.44	1.97	0.57	2.80	4.97
Sum	101.05	96.56	97.59	95.65	99.15	98.41	100.00	100.20	99.00	98.83	92.61	98.69	95.13	100.00
Cats=	6 Ox	7 Ox	32 Ox	32 Ox	32 Ox	32 Ox	32 Ox	32 Ox	32 Ox	32 Ox	7 Ox	7 Ox	7 Ox	32 Ox
Si	2.000	2.236	8.473	8.723	8.403	8.307	9.217	8.176	8.238	8.233	2.333	2.322	2.239	8.414
Al	0.995	1.264	7.463	7.460	7.590	7.706	6.784	7.605	7.673	7.683	1.150	1.134	1.271	7.588
Ca	0.000	0.065	0.386	0.366	0.123	0.229	0.318	0.000	0.007	0.011	0.027	0.029	0.057	0.000
$Fe^{'''}$	0.008	0.000	0.000	0.153	0.053	0.229	0.000	0.385	0.006	0.003	0.024	0.041	0.026	0.000
Sr	0.000	0.005		0.017	0.006	0.013		0.000	0.000	0.004	0.000	0.002	0.002	0.000
Ba	0.001	0.001		0.003	0.005	0.004		0.000	0.107	0.099	0.000	0.001	0.001	0.000
Na	0.090	0.963	5.996	4.662	5.722	5.273	4.773	5.574	5.586	5.648	1.005	1.134	0.908	6.373
K	0.908	0.160	0.951	0.986	1.522	1.435	1.370	2.138	2.203	2.139	0.108	0.029	0.150	1.210
Sum	4.002	4.693	23.269	22.371	23.424	23.194	22.462	23.878	23.820	23.819	4.648	4.693	4.655	23.584
Na/K	0.1	6.0	6.3	4.7	3.8	3.7	3.5	2.6	2.5	2.6	9.3	38.5	6.0	5.3
(Si+Al+$Fe^{'''}$)	3.00	3.50	15.94	16.34	16.05	16.24	16.00	16.17	15.92	15.92	3.51	3.50	3.54	16.00
(Al+$Fe^{'''}$)	1.00	1.26	7.46	7.61	7.64	7.93	6.78	7.99	7.68	7.69	1.17	1.18	1.30	7.59
(Na+K+Ba+2Ca)	1.00	1.12	6.95	5.65	7.25	6.71	6.14	7.71	7.90	7.89	1.11	1.16	1.06	7.58

	137	161		193	197		200		208	224	225	228	230	235
	PS96	PS86	PS86	3164	3346	3346	3327	3327	3341	3160	3339	3335	3354	3159
	L	L	L	L	E	L	E	L	L	L	L	L	L	L
	ne	ne	ne	ne	ne	ne	ne	ne	ne	ne	ne	ne	ne	ne
SiO_2	43.95	46.09	46.09	42.33	41.26	41.58	41.60	41.54	48.24	41.19	46.44	41.82	42.25	44.49
Al_2O_3	34.10	30.97	30.97	34.41	35.07	35.34	35.36	35.31	30.80	33.49	31.10	35.55	32.89	31.78
CaO	1.98	0.00	0.00	0.00	1.78	2.48	1.13	1.19	0.18	0.00	0.24	2.55	1.39	1.11
Fe_2O_3	0.04	0.00	0.00	0.00	0.00	0.00	0.53	0.77	0.00	0.00	0.00	0.32	0.00	0.00
SrO														
BaO														
Na_2O	13.97	16.17	16.17	16.19	15.25	15.75	17.52	16.94	15.85	15.79	16.04	15.31	15.84	14.86
K_2O	5.30	4.04	4.04	7.15	6.16	4.39	4.02	3.95	4.07	6.96	3.96	4.89	3.98	4.90
Sum	99.38	97.27	97.27	100.08	99.52	99.54	100.64	100.39	99.14	97.43	97.78	100.73	96.35	97.14
Cats=	32 Ox	32 Ox	32 Ox	32 Ox	32 Ox	32 Ox	32 Ox	32 Ox	32 Ox	32 Ox	32 Ox	32 Ox	32 Ox	32 Ox
Si	8.407	8.929	8.929	8.172	7.995	7.998	7.968	7.980	9.130	8.170	8.942	7.987	8.344	8.687
Al	7.688	7.071	7.071	7.830	8.009	8.012	7.982	7.994	6.870	7.829	7.058	8.002	7.656	7.314
Ca	0.406	0.000	0.000	0.000	0.370	0.511	0.232	0.245	0.036	0.000	0.050	0.522	0.294	0.232
$Fe^{'''}$	0.010	0.000	0.000	0.000	0.000	0.000	0.115	0.166	0.000	0.000	0.000	0.069	0.000	0.000
Sr														
Ba														
Na	5.181	6.074	6.074	6.060	5.730	5.874	6.506	6.309	5.816	6.072	5.988	5.669	6.065	5.626
K	1.293	0.998	0.998	1.761	1.523	1.077	0.982	0.968	0.983	1.761	0.973	1.191	1.003	1.221
Sum	22.986	23.072	23.072	23.823	23.626	23.472	23.785	23.662	22.835	23.832	23.010	23.442	23.362	23.079
Na/K	4.0	6.1	6.1	3.4	3.8	5.5	6.6	6.5	5.9	3.4	6.2	4.8	6.0	4.6
(Si+Al+$Fe^{'''}$)	16.11	16.00	16.00	16.00	16.00	16.01	16.07	16.14	16.00	16.00	16.00	16.06	16.00	16.00
(Al+$Fe^{'''}$)	7.70	7.07	7.07	7.83	8.01	8.01	8.10	8.16	6.87	7.83	7.06	8.07	7.66	7.31
(Na+K+Ba+2Ca)	6.47	7.07	7.07	7.82	7.25	6.95	7.49	7.28	6.80	7.83	6.96	6.86	7.07	6.85

You have either reached a page that is unavailable for viewing or reached your viewing limit for this book.

You have either reached a page that is unavailable for viewing or reached your viewing limit for this book.

You have either reached a page that is unavailable for viewing or reached your viewing limit for this book.

Table 3.5 - Microprobe analyses of feldspars.

	69		100			107		108		109					
	3151	3151	PS233	PS233	PS233	PS252	PS252	ADG	ADG	PS226	PS226	PS226	PS226	PS226	PS226
	P	gm	P	gm	gm	gm	gm	gm	gm	P	gm	gm	gm	gm	gm
SiO_2	54.56	65.30	57.43	59.18	65.47	63.83	64.97	53.69	64.62	48.20	54.37	53.81	47.07	65.08	63.57
Al_2O_3	28.86	18.47	25.75	24.86	19.42	18.05	18.78	27.85	18.88	32.95	28.34	27.47	31.86	19.53	18.25
CaO	11.08	0.00	7.47	6.65	0.69	0.32	0.69	10.28	0.05	16.16	10.78	10.60	16.30	0.96	0.11
Fe_2O_3	0.00	0.00	0.18	0.26	0.21	0.18	0.19	0.28	0.66	0.70	0.78	0.63	0.59	0.31	0.00
SrO			0.13	0.12	0.15	0.08	0.09	0.31	0.00	0.63	0.51	0.58	0.53	0.00	0.14
BaO			0.11	0.29	0.21	0.13	0.08	0.08	0.00	0.07	0.15	0.01	0.00	0.37	0.11
Na_2O	5.08	1.32	6.09	6.81	4.66	2.98	4.65	5.30	2.84	2.04	4.72	4.91	1.93	6.17	0.93
K_2O	0.33	15.06	1.35	1.26	9.54	12.45	9.79	0.10	12.28	0.23	0.81	0.64	0.20	7.10	15.07
Sum	99.91	100.15	98.51	99.43	100.35	98.02	99.24	97.89	99.33	100.98	100.46	98.65	98.65	99.52	98.18
Si	9.856	12.000	10.473	10.680	11.835	11.930	11.874	9.911	11.884	8.800	9.845	9.909	8.803	11.784	11.955
Al	6.144	4.000	5.535	5.288	4.137	3.975	4.044	6.059	4.092	7.090	6.048	5.962	7.023	4.168	4.045
Ca	2.144	0.000	1.460	1.286	0.134	0.065	0.135	2.033	0.010	3.161	2.091	2.091	3.267	0.186	0.022
Fe'''	0.000	0.000	0.037	0.052	0.043	0.039	0.040	0.058	0.136	0.144	0.159	0.132	0.124	0.064	0.000
Sr			0.014	0.013	0.016	0.008	0.009	0.033	0.000	0.067	0.054	0.062	0.057	0.000	0.015
Ba			0.008	0.021	0.015	0.010	0.006	0.006	0.000	0.005	0.011	0.001	0.000	0.026	0.008
Na	1.779	0.470	2.153	2.383	1.633	1.081	1.648	1.897	1.013	0.722	1.657	1.754	0.701	2.166	0.339
K	0.076	3.531	0.314	0.290	2.200	2.968	2.282	0.024	2.881	0.054	0.187	0.151	0.048	1.640	3.616
Sum	20.000	20.001	19.993	20.012	20.013	20.076	20.039	20.020	20.016	20.043	20.053	20.062	20.023	20.035	20.000
Z	16.000	16.000	16.044	16.020	16.015	15.945	15.959	16.028	16.113	16.034	16.053	16.003	15.961	16.016	16.000
X	4.000	4.001	3.949	3.992	3.998	4.131	4.080	3.993	3.904	4.009	4.000	4.059	4.088	4.019	4.000

	109			139						143			145		
	PS226	PS226	PS226	PS3	PS3	PS3	PS3	PS3	PS31	PS31	PS31	3382	3382	3382	3382
	gm	gm	gm	X	P	P	gm	gm	P	gm	gm	P	gm	gm	gm
SiO_2	62.63	65.07	65.07	50.92	62.56	65.56	63.57	67.50	52.17	62.75	64.56	53.73	57.94	66.69	64.72
Al_2O_3	18.76	18.36	19.40	30.65	22.45	19.86	18.74	19.80	30.52	22.94	19.97	29.04	25.43	20.79	18.87
CaO	0.00	0.17	1.14	13.09	4.19	1.23	0.60	0.49	12.96	4.25	1.38	11.36	8.25	1.59	0.55
Fe_2O_3	0.03	0.09	0.30	0.27	0.98	0.92	0.00	0.04	0.00	0.00	0.00	0.28	0.22	0.00	0.34
SrO	0.09	0.00	0.00	0.77	0.21	0.11	0.00	0.00				0.29	0.13	0.00	0.00
BaO	0.20	0.04	0.03	0.12	0.39	0.76	0.00	0.00				0.06	0.20	0.00	0.23
Na_2O	0.06	3.50	6.23	3.33	8.11	5.95	3.24	9.10	3.93	8.22	4.67	4.81	6.75	10.64	4.06
K_2O	16.64	11.65	7.03	0.65	1.53	7.21	11.35	3.54	0.11	1.55	9.01	0.29	0.17	0.36	10.18
Sum	98.42	98.87	99.19	99.80	100.42	101.60	97.50	100.47	99.69	99.71	99.59	99.86	99.09	100.07	98.95
Si	11.839	11.984	11.778	9.338	11.152	11.699	11.876	11.890	9.482	11.183	11.726	9.751	10.491	11.701	11.882
Al	4.179	3.985	4.138	6.625	4.717	4.177	4.126	4.111	6.538	4.818	4.275	6.211	5.427	4.299	4.083
Ca	0.000	0.034	0.221	2.572	0.800	0.235	0.120	0.092	2.524	0.811	0.269	2.209	1.600	0.299	0.108
Fe'''	0.007	0.018	0.060	0.055	0.197	0.186	0.000	0.009	0.000	0.000	0.000	0.057	0.045	0.000	0.071
Sr	0.010	0.000	0.000	0.082	0.022	0.011	0.000	0.000				0.031	0.014	0.000	0.000
Ba	0.015	0.003	0.002	0.009	0.027	0.053	0.000	0.000				0.004	0.014	0.000	0.017
Na	0.023	1.251	2.185	1.184	2.803	2.059	1.174	3.108	1.385	2.840	1.645	1.693	2.370	3.620	1.445
K	4.012	2.736	1.623	0.152	0.348	1.641	2.705	0.796	0.026	0.352	2.088	0.067	0.039	0.081	2.384
Sum	20.085	20.011	20.007	20.017	20.065	20.062	20.000	20.006	19.954	20.005	20.002	20.023	20.000	19.999	19.991
Z	16.025	15.987	15.976	16.018	16.065	16.062	16.002	16.010	16.020	16.001	16.001	16.020	15.963	16.000	16.037
X	4.060	4.024	4.030	3.999	4.000	4.000	3.999	3.996	3.934	4.004	4.001	4.003	4.037	3.999	3.954

You have either reached a page that is unavailable for viewing or reached your viewing limit for this book.

You have either reached a page that is unavailable for viewing or reached your viewing limit for this book.

You have either reached a page that is unavailable for viewing or reached your viewing limit for this book.

*Table 4.1 - Microprobe analyses of clinopyroxenes. (*) : Fe^{+++} and Fe^{++} calculated according to Papike et al. (1974); Fe**: $Fe^{++}+Fe^{+++}+Mn$; Mg# = Mg /(Mg+Fe^{++}).*

		D18			D19			D76			D82	
	PS503 PC	PS503 PR	PS503 mP	PS503A PC	PS503A PR	PS503A gm	PS259 P	PS259 mP	3317 XC	3317 XR	3317 PC	3317 PR
SiO_2	51.68	51.17	51.50	52.67	52.08	54.53	48.70	45.58	53.58	50.58	51.54	50.28
TiO_2	0.95	0.86	0.39	0.61	0.58	0.19	1.38	2.42	0.13	0.87	0.50	0.88
Al_2O_3	1.70	2.18	1.48	1.90	1.90	0.34	3.83	5.88	0.01	3.12	2.98	3.23
Cr_2O_3	0.01	0.00	0.00	0.13	0.07	0.16	0.08	0.02	0.01	0.06	0.86	0.06
Fe_2O_3*	1.23	1.75	4.84	1.01	1.49	1.32	4.16	5.40	0.72	2.23	1.36	2.21
FeO*	6.48	7.29	9.48	5.54	5.60	3.77	3.54	3.45	7.92	4.79	3.40	4.84
MnO	0.22	0.30	0.61	0.17	0.18	0.22	0.17	0.13	0.27	0.19	0.12	0.21
MgO	13.26	12.06	9.17	14.63	13.85	15.90	13.85	12.09	14.11	14.64	15.78	14.52
NiO	0.04	0.00	0.00	0.01	0.00	0.01	0.02	0.00				
CaO	23.09	22.87	21.33	23.04	22.99	24.17	23.09	22.85	22.70	22.73	22.38	22.35
Na_2O	0.59	0.77	1.76	0.48	0.62	0.52	0.39	0.49	0.38	0.23	0.38	0.29
Sum	99.20	99.26	100.57	100.18	99.36	101.12	99.20	98.31	99.83	99.44	99.30	98.87
Si	1.940	1.930	1.951	1.943	1.942	1.982	1.827	1.739	2.000	1.883	1.903	1.882
Al^{IV}	0.060	0.070	0.049	0.057	0.058	0.015	0.169	0.261	0.000	0.117	0.097	0.118
Sum	2.000	2.000	2.000	2.000	2.000	1.997	1.997	2.000	2.000	2.000	2.000	1.995
Al^{VI}	0.015	0.027	0.018	0.026	0.026	0.000	0.000	0.003	0.000	0.020	0.033	0.025
Fe^{++}	0.203	0.230	0.300	0.171	0.175	0.115	0.111	0.110	0.247	0.149	0.105	0.152
Mn	0.007	0.010	0.020	0.005	0.006	0.007	0.005	0.004	0.009	0.006	0.004	0.007
Mg	0.742	0.678	0.518	0.804	0.770	0.861	0.774	0.687	0.785	0.912	0.869	0.810
Ni	0.001	0.000	0.000	0.000	0.000	0.000	0.000	0.000				
Fe^{+++}	0.035	0.050	0.138	0.028	0.042	0.036	0.118	0.155	0.020	0.063	0.038	0.062
Cr	0.000	0.000	0.000	0.004	0.002	0.005	0.002	0.000	0.000	0.002	0.025	0.002
Ti	0.027	0.024	0.011	0.017	0.016	0.005	0.039	0.069	0.004	0.024	0.014	0.025
Ca	0.929	0.924	0.866	0.911	0.919	0.941	0.928	0.934	0.908	0.907	0.886	0.897
Na	0.043	0.056	0.129	0.034	0.045	0.037	0.028	0.036	0.027	0.017	0.027	0.021
Sum	2.000	2.000	2.000	2.000	2.000	2.007	2.007	2.000	2.000	2.000	2.000	2.000
Ca	48.49	48.84	47.02	47.47	48.06	48.01	47.93	49.42	46.11	46.82	44.84	46.53
Mg	38.72	35.83	28.12	41.90	40.28	43.93	39.98	36.35	39.87	41.92	47.18	42.01
Fe**	12.79	15.33	24.86	10.63	11.66	8.06	12.09	14.23	14.02	11.26	7.98	11.46
mg#	0.79	0.75	0.63	0.99	0.82	0.89	0.89	0.86	0.76	0.85	0.89	0.84

	D82		D84			D87					D88	
	3317 mP	3317 gm	PS126 P	PS126 P	PS126 gm	PS216 PC	PS216 PR	PS216 mP	PS216 gm	PS129 PC	PS129 PR	PS129 P
SiO_2	50.77	50.57	49.35	48.43	45.59	49.44	49.30	47.24	46.89	53.24	46.75	50.32
TiO_2	0.74	0.97	1.47	1.45	3.61	1.09	1.21	1.52	1.84	0.56	1.69	0.93
Al_2O_3	2.92	5.60	5.59	5.53	6.95	3.48	3.87	5.34	5.45	1.18	6.97	4.52
Cr_2O_3	0.21	0.02	0.16	0.17	0.00	0.02	0.02	0.09	0.04	0.41	0.07	0.08
Fe_2O_3*	2.14	4.69	0.98	2.72	4.37	3.00	2.48	4.38	3.50	0.00	3.80	0.95
FeO*	4.43	4.86	6.81	5.99	3.62	4.95	5.66	4.07	5.64	5.57	6.13	7.17
MnO	0.16	0.32	0.26	0.35	0.30	0.19	0.19	0.15	0.19	0.11	0.16	0.22
MgO	14.83	11.55	14.44	13.56	11.94	14.08	13.70	12.98	12.28	17.15	13.01	14.37
NiO						0.04	0.02	0.01				
CaO	22.53	21.00	20.87	21.97	23.71	21.79	21.68	22.18	21.68	21.77	21.81	21.42
Na_2O	0.32	1.87	0.17	0.12	0.47	0.42	0.43	0.45	0.48	0.00	0.00	0.12
Sum	99.06	101.45	100.10	100.29	100.56	98.46	98.54	98.40	97.99	99.99	100.39	100.11
Si	1.893	1.854	1.827	1.802	1.701	1.864	1.860	1.790	1.791	1.953	1.745	1.869
Al^{IV}	0.107	0.146	0.173	0.198	0.299	0.136	0.140	0.210	0.209	0.047	0.255	0.135
Sum	2.000	2.000	2.000	2.000	2.000	2.000	2.000	2.000	2.000	2.000	2.000	2.000
Al^{VI}	0.022	0.096	0.071	0.044	0.007	0.019	0.032	0.029	0.037	0.004	0.051	0.063
Fe^{++}	0.138	0.149	0.211	0.186	0.113	0.156	0.179	0.129	0.180	0.171	0.191	0.222
Mn	0.005	0.010	0.008	0.011	0.009	0.006	0.006	0.005	0.006	0.003	0.005	0.007
Mg	0.824	0.631	0.797	0.752	0.664	0.790	0.770	0.733	0.699	0.938	0.724	0.794
Ni						0.001	0.000	0.000				
Fe^{+++}	0.060	0.129	0.027	0.076	0.123	0.035	0.070	0.125	0.101	0.000	0.107	0.027
Cr	0.006	0.000	0.005	0.005	0.000	0.000	0.000	0.003	0.001	0.012	0.002	0.002
Ti	0.021	0.027	0.041	0.041	0.101	0.031	0.034	0.043	0.053	0.015	0.047	0.026
Ca	0.900	0.825	0.828	0.876	0.948	0.880	0.876	0.901	0.887	0.856	0.872	0.851
Na	0.023	0.133	0.012	0.009	0.034	0.031	0.031	0.033	0.036	0.000	0.000	0.009
Sum	2.000	2.000	2.000	2.000	2.000	2.000	2.000	2.000	2.000	2.000	2.000	2.000
Ca	46.70	47.31	44.25	46.82	51.05	45.88	46.08	47.60	47.36	43.50	45.92	44.76
Mg	42.76	36.18	42.60	40.19	35.76	41.24	40.51	36.72	37.32	47.66	38.13	41.77
Fe**	10.54	16.51	13.15	14.59	13.19	12.88	13.41	13.68	15.32	8.84	15.95	13.47
mg#	086	0.81	0.79	0.80	0.85	0.84	0.81	0.85	0.80	0.85	0.79	0.78

You have either reached a page that is unavailable for viewing or reached your viewing limit for this book.

You have either reached a page that is unavailable for viewing or reached your viewing limit for this book.

You have either reached a page that is unavailable for viewing or reached your viewing limit for this book.

Table 4.2 - Microprobe analyses of olivines.

	D76	D84	D87				D88			D89		D106
	PS259	PS126	PS216	PS216	PS129	PS129	PS129	PS129	PS129	PS130	PS130	PS104
	P	mP	PC	PR	PC	PR	mPC	mPR	gm	P	gm	gm
SiO_2	39.71	38.00	38.26	37.69	39.51	36.77	37.35	35.50	34.55	39.15	37.74	37.33
FeO	16.82	23.56	20.03	23.20	16.47	30.73	26.80	35.50	41.37	17.53	27.21	27.43
MnO	0.24	0.71	0.38	0.46	0.31	0.71	0.60	1.11	1.02	0.38	0.62	0.58
MgO	43.64	36.87	39.81	37.05	43.20	31.22	34.37	26.62	22.12	42.19	34.57	33.88
NiO	0.19	0.00	0.16	0.11						0.21	0.16	0.15
CaO	0.31	0.54	0.23	0.27	0.46	0.66	0.51	0.66	0.63	0.26	0.52	0.58
Sum	100.91	99.68	98.90	98.78	99.95	100.09	99.72	99.12	99.73	99.72	100.82	99.95
Si	0.998	1.001	0.998	1.000	1.000	1.000	1.000	1.000	1.000	1.000	1.000	1.000
Fe	0.353	0.519	0.437	0.515	0.349	0.699	0.600	0.836	1.001	0.375	0.603	0.614
Mn	0.005	0.016	0.008	0.010	0.007	0.016	0.013	0.026	0.025	0.008	0.016	0.015
Mg	1.634	1.448	1.548	1.465	1.631	1.265	1.372	1.117	0.954	1.606	1.365	1.353
Ni	0.004	0.000	0.003	0.002						0.004	0.003	0.003
Ca	0.008	0.015	0.007	0.008	0.013	0.019	0.015	0.020	0.020	0.007	0.015	0.017
Sum	3.002	2.999	3.001	3.000	3.000	2.999	3.000	2.999	3.000	3.000	3.000	3.000
Fo	81.66	72.46	77.41	73.33	81.59	63.27	68.58	55.87	47.70	80.47	68.36	67.73
Fa	17.66	25.99	21.85	25.77	17.46	34.95	30.01	41.81	50.07	18.76	30.20	30.78
Tph	0.26	0.79	0.42	0.52	0.33	0.82	0.68	1.32	1.25	0.41	0.70	0.66
Lar	0.42	0.76	0.32	0.38	0.62	0.96	0.73	1.00	0.98	0.36	0.74	0.83

	D110	D111	D113	D114		D142	D148	D149	D151	D159	D176	
	PS102	PS103	PS97	PS98	PS98	PS24	PS18	PS19	PS28	PS9	PS43	PS43
	mP	mP	P	P	gm	mP	gm	mP	mP	mP	P	gm
SiO_2	38.21	38.92	39.40	37.82	38.77	37.81	37.78	38.41	38.63	37.97	38.42	37.80
FeO	21.34	20.38	18.49	20.25	19.15	25.04	24.81	21.79	20.78	24.03	21.77	25.19
MnO	0.80	0.78	0.79	1.32	0.83	0.68	0.60	0.99	0.92	1.26	0.34	0.68
MgO	38.31	39.79	41.59	38.09	40.53	35.78	35.87	38.40	39.35	36.56	38.90	35.68
NiO	0.08	0.16	0.31	0.14	0.29	0.17	0.16	0.18	0.14	0.08	0.07	0.03
CaO	0.63	0.66	0.40	0.66	0.17	0.59	0.67	0.35	0.32	0.21	0.29	0.70
Sum	99.37	100.69	100.98	98.28	99.74	100.07	99.89	100.12	100.14	100.11	99.79	100.08
Si	1.000	1.000	1.000	0.996	1.000	1.000	1.000	1.000	1.000	1.000	1.000	1.000
Fe	0.467	0.438	0.393	0.448	0.413	0.554	0.549	0.474	0.450	0.529	0.474	0.557
Mn	0.008	0.016	0.031	0.014	0.029	0.015	0.013	0.022	0.020	0.028	0.007	0.015
Mg	1.495	1.524	1.573	1.500	1.558	1.410	1.415	1.490	1.518	1.435	1.509	1.407
Ni	0.002	0.003	0.006	0.003	0.006	0.004	0.004	0.004	0.003	0.002	0.002	0.001
Ca	0.018	0.018	0.011	0.019	0.005	0.017	0.019	0.010	0.009	0.006	0.008	0.020
Sum	3.000	3.000	3.000	3.000	3.000	3.000	3.000	3.000	3.000	3.000	3.000	3.000
Fo	74.83	76.31	78.91	75.16	78.14	70.65	70.87	74.65	76.02	71.81	75.51	70.37
Fa	23.39	21.93	19.69	22.42	20.72	27.75	27.51	23.77	22.53	26.49	23.71	27.88
Tph	0.89	0.85	0.85	1.48	0.91	0.76	0.67	1.09	1.01	1.41	0.38	0.76
Lar	0.89	0.91	0.55	0.94	0.23	0.84	0.95	0.49	0.44	0.29	0.40	0.99

	D190	D201	D216	
	PS66	PS79	3161	3161
	mP	gm	mP	gm
SiO_2	37.58	36.92	38.85	39.28
FeO	26.21	29.42	17.52	17.91
MnO	0.51	0.74	1.02	0.65
MgO	35.09	32.09	41.13	42.04
NiO	0.06		0.04	0.07
CaO	0.44	0.53	0.37	0.05
Sum	99.89	99.70	99.29	100.00
Si	1.000	1.001	1.003	1.002
Fe	0.583	0.667	0.378	0.382
Mn	0.011	0.017	0.022	0.014
Mg	1.392	1.297	1.582	1.598
Ni	0.001		0.001	0.002
Ca	0.013	0.015	0.010	0.001
Sum	3.000	2.997	2.996	2.999
Fo	69.62	64.96	79.39	80.08
Fa	29.18	33.42	18.98	19.14
Tph	0.57	0.35	1.12	0.70
Lar	0.63	0.77	0.51	0.68

You have either reached a page that is unavailable for viewing or reached your viewing limit for this book.

You have either reached a page that is unavailable for viewing or reached your viewing limit for this book.

You have either reached a page that is unavailable for viewing or reached your viewing limit for this book.

Table 4.5 - Microprobe analyses of amphiboles, garnets and sphene.

	D119				D149			D173				D216
	PS36	PS36	PS36	PS36	PS19	PS19	PS19	PS59	PS59	PS59	PS59	3161
	PC	PR	mP	gm	PC	PR	gm	PC	PR	mP	gm	gm
SiO_2	38.19	37.99	37.67	37.57	43.28	43.73	44.34	38.36	38.41	39.04	39.11	40.29
TiO_2	1.42	2.67	2.37	1.98	4.07	4.64	3.79	3.89	4.12	4.03	4.02	3.80
Al_2O_3	12.45	13.02	12.92	12.81	9.87	9.88	8.78	14.24	13.79	13.37	13.27	11.07
MgO	6.64	8.44	7.28	6.32	15.38	14.87	15.84	10.27	10.73	10.65	11.58	11.60
CaO	10.97	11.46	11.37	11.13	12.32	11.86	11.46	11.86	11.73	11.89	11.80	11.55
MnO	0.70	0.67	0.89	0.99	0.28	0.30	0.09	0.36	0.32	0.35	0.28	0.38
FeOtot	22.90	19.61	21.42	23.02	9.90	10.62	9.64	15.04	14.57	14.85	13.84	15.25
Na_2O	2.40	2.15	2.08	2.10	2.40	2.45	2.48	2.19	2.22	2.18	2.16	2.48
K_2O	2.49	2.43	2.49	2.52	1.63	1.70	1.68	2.10	2.08	2.11	2.12	1.52
Sum	98.16	98.44	98.49	98.44	99.13	100.05	98.10	98.31	97.97	98.47	98.18	97.94
H_2O_{calc}	1.90	1.94	1.92	1.90	2.06	2.08	2.05	1.98	1.98	1.99	1.99	1.98
Sum	100.06	100.38	100.41	100.34	101.19	102.13	100.15	100.29	99.95	100.46	100.17	99.92
Si	6.023	5.885	5.892	5.925	6.295	6.311	6.479	5.800	5.816	5.885	5.884	6.097
Al^{IV}	2.314	2.377	2.382	2.381	1.692	1.680	1.512	2.538	2.461	2.375	2.353	1.974
Ti^{IV}	0.000	0.000	0.000	0.000	0.014	0.009	0.009	0.000	0.000	0.000	0.000	0.000
Sum	8.000	8.000	8.000	8.000	8.000	8.000	8.000	8.000	8.000	8.000	8.000	8.000
Ti^{VI}	0.168	0.311	0.279	0.235	0.432	0.495	0.407	0.442	0.469	0.457	0.455	0.432
Al^{VI}	0.337	0.262	0.273	0.306	0.000	0.000	0.000	0.338	0.277	0.261	0.236	0.072
Mg	1.561	1.949	1.697	1.486	3.335	3.199	3.450	2.315	2.422	2.393	2.597	2.617
Mn	0.094	0.088	0.118	0.132	0.034	0.037	0.011	0.046	0.041	0.045	0.036	0.049
Fe"	3.020	2.540	2.802	3.036	1.204	1.282	1.178	1.902	1.845	1.872	1.741	1.930
Sum	5.180	5.150	5.169	5.195	5.005	5.012	5.047	5.043	5.054	5.028	5.065	5.100
Ca	1.854	1.902	1.905	1.881	1.920	1.834	1.794	1.921	1.903	1.920	1.902	1.873
Na_B	0.146	0.098	0.095	0.119	0.080	0.166	0.206	0.079	0.097	0.080	0.098	0.127
Sum	2.000	2.000	2.000	2.000	2.000	2.000	2.000	2.000	2.000	2.000	2.000	2.000
Na_A	0.588	0.548	0.536	0.523	0.597	0.519	0.497	0.563	0.555	0.558	0.532	0.600
K	0.501	0.480	0.497	0.507	0.302	0.313	0.313	0.405	0.402	0.406	0.407	0.293
Sum	1.089	1.028	1.033	1.030	0.899	0.832	0.810	0.969	0.957	0.963	0.939	0.894
OH	2.000	2.000	2.000	2.000	2.000	2.000	2.000	2.000	2.000	2.000	2.000	2.000
Sum_{cats}	16.606	16.440	16.476	16.530	15.904	15.845	15.857	16.350	16.288	16.252	16.240	16.065
mg#	0.33	0.43	0.37	0.32	0.73	0.71	0.74	0.54	0.56	0.56	0.59	0.57

You have either reached a page that is unavailable for viewing or reached your viewing limit for this book.

You have either reached a page that is unavailable for viewing or reached your viewing limit for this book.

You have either reached a page that is unavailable for viewing or reached your viewing limit for this book.

APPENDIX III.2 - MINERAL CHEMISTRY: Na-ALKALINE ROCK-TYPES

Table 5 - Na-alkaline lavas and dykes: synopsis of the analyzed samples. (x): analyzed minerals. Form: LD, lava dome; LF, lava flow; D, dyke; P, plug. Order and field numbers, as well nomenclature, as in Comin-Chiaramonti et al. (this volume, Appendix I).

Locality	Form	Cpx	Ol	Op	Am	Af	Foids	Sph	Gar	Sample	Rock-type
Cerro Medina	LD	x		x	x	x	x			**118**-PS221	Peralkaline phonolite
	LD				x	x				**119**-PS218	Peralkaline phonolite
Sapucai	D	x		x	x	x	x	x	x	**D101**-PS106	Peralkaline phonolite
	D	x		x	x	x	x	x	x	**D143** -PS25	Peralkaline phonolite
	D	x					x			**D147**-PS17	Peralkaline phonolite
Cerro Gimenez	LD	x			x		x			**178**-PS214	Peralkaline phonolite
	LD	x				x		x		PS**179**- 213B	Peralkaline phonolite
Limpio	LF	x	x	x			x			**263**-3082	Nephelinite
Cerro Verde	P	x	x	x			x			**265**-3080	Ankaratrite
Ñemby	P	x	x	x			x			**267**-3092	Nephelinite
	P	x	x							**271**-3207	Nephelinite
	P	x								**276**-3222	Nephelinite
	P	x								**284**-3270	Nephelinite
	P	x	x	x			x			**287**-3281	Nephelinite
	P	x	x	x						**289**-3284	Nephelinite
Cerro Confuso	LD	x					x			**302**-3081	Peralkaline phonolite
Nueva Tablada	LF	x	x	x		x				**304**-3103	Nephelinite
Lambaré	P	x	x	x			x			**305**-3097	Nephelinite
Tacumbú	P	x	x	x			x			**307**-3068	Nephelinite

You have either reached a page that is unavailable for viewing or reached your viewing limit for this book.

You have either reached a page that is unavailable for viewing or reached your viewing limit for this book.

Table 5.4 - Microprobe analyses of amphiboles.

	118								119			
	PS221 P	PS221 gm	PS221 gm	PS221 gm	PS221 gm	PS221 PC	PS221 PR	PS221 gm	PS218 gm	PS218 gm	PS218 gm	PS218 mP
SiO_2	40.23	40.05	38.36	37.73	37.61	37.25	37.77	44.93	46.56	47.32	45.96	49.35
TiO_2	3.29	2.92	3.94	3.57	4.32	4.10	3.82	0.93	0.85	0.81	0.79	0.93
Al_2O_3	10.21	10.01	13.23	12.78	13.85	12.37	12.25	3.61	2.53	1.68	1.80	2.16
Cr_2O_3			0.02	0.00	0.00	0.04	0.02	0.01		0.00	0.03	0.00
MgO	9.18	8.25	11.62	9.35	11.81	9.24	8.40	4.69	5.36	6.67	5.19	8.21
CaO	15.41	14.66	11.73	11.64	11.72	11.71	11.64	21.43	17.33	20.65	21.04	5.65
MnO	0.51	0.65	0.23	0.31	0.13	0.36	0.48	1.34	1.64	1.14	1.60	1.81
FeOtot	14.86	16.76	12.86	16.46	13.01	16.76	17.82	18.27	19.25	16.61	17.88	21.00
SrO			0.05	0.03	0.08	0.01	0.03	0.00		0.00	0.00	0.00
BaO			0.02	0.02	0.05	0.02	0.05	0.09		0.02	0.00	0.00
Na_2O	2.20	2.19	2.82	2.49	2.51	2.70	2.64	1.50	2.69	1.52	1.55	5.74
K_2O	0.92	1.12	1.40	1.61	1.42	1.46	1.69	0.04	0.38	0.00	0.03	1.63
NiO			0.01	0.00	0.02	0.01	0.01	0.00		0.01	0.03	0.00
F	0.13	0.17	0.45	0.16	0.22	0.08	0.06	0.08	0.58	0.00	0.20	2.43
Sum	96.94	96.78	96.73	96.14	96.75	96.09	96.65	96.92	97.17	96.42	96.09	98.91
O=F,Cl	0.05	0.07	0.19	0.07	0.09	0.03	0.03	0.03	0.24	0.00	0.09	1.02
H_2O_{calc}	1.88	1.84	1.75	1.85	1.86	1.88	1.88	1.86	1.63	1.92	1.79	0.78
Sum	98.82	98.62	98.48	97.98	98.61	97.97	98.54	98.78	98.80	98.34	97.88	99.69
Si	6.200	6.241	5.859	5.891	5.737	5.837	5.912	7.100	7.346	7.391	7.318	7.674
Al^{IV}	1.800	1.759	2.141	2.109	2.263	2.163	2.088	0.673	0.470	0.310	0.337	0.326
Ti^{IV}	0.000	0.000	0.000	0.000	0.000	0.000	0.000	0.110	0.101	0.095	0.095	0.000
Fe	0.000	0.000	0.000	0.000	0.000	0.000	0.000	0.116	0.082	0.204	0.250	0.000
Sum	8.000	8.000	8.000	8.000	8.000	8.000	8.000	8.000	8.000	8.000	8.000	8.000
Ti^{VI}	0.381	0.342	0.453	0.419	0.496	0.483	0.449	0.110	0.000	0.000	0.000	0.109
Al^{VI}	0.055	0.079	0.242	0.242	0.226	0.122	0.172	0.000	0.000	0.000	0.000	0.070
Cr	0.000	0.000	0.002	0.000	0.000	0.005	0.002	0.001		0.000	0.003	0.000
Mg	2.109	1.917	2.647	2.175	2.685	2.159	1.959	1.105	1.261	1.554	1.233	1.903
Mn	0.067	0.086	0.029	0.041	0.017	0.048	0.063	0.179	0.219	0.151	0.215	0.238
Fe"	1.915	2.184	1.643	2.150	1.660	2.196	2.333	2.299	2.458	1.966	2.131	2.731
Ni	0.000	0.000	0.002	0.000	0.002	0.001	0.001	0.000		0.001	0.003	0.000
Sum C	4.527	4.608	5.017	5.027	5.086	5.012	4.980	3.695	3.938	3.671	3.585	5.051
Ca	2.545	2.448	1.920	1.946	1.916	1.966	1.953	3.628	2.930	3.457	3.590	0.941
Sr			0.004	0.003	0.007	0.001	0.002	0.000	0.000	0.000	0.000	0.000
Na_B			0.076	0.051	0.077	0.033	0.045		0.000	0.000	0.000	0.000
Sum B	2.545	2.448	2.000	2.000	2.000	2.000	2.000	3.628	2.930	3.457	3.590	0.941
Na_A	0.657	0.662	0.758	0.703	0.667	0.788	0.755	0.461	0.823	0.461	0.478	0.672
Ba			0.001	0.001	0.003	0.001	0.003		0.000	0.001	0.000	0.000
K	0.181	0.223	0.273	0.321	0.275	0.291	0.338	0.007	0.076	0.000	0.006	0.323
Sum A	0.838	0.884	1.032	1.025	0.945	1.080	1.096	0.474	0.899	0.461	0.484	0.995
F	0.063	0.084	0.216	0.078	0.106	0.037	0.032	0.039	0.289	0.000	0.102	1.195
OH	1.937	1.916	1.784	1.922	1.894	1.963	1.968	1.961	1.711	2.000	1.898	0.805
	2.000	2.000	2.000	2.000	2.000	2.000	2.000	2.000	2.000	2.000	2.000	2.000
Sum_{cats}	15.910	15.940	16.049	16.052	16.031	16.092	16.076	15.797	15.767	15.589	15.659	14.987
mg#	0.52	0.47	0.62	0.50	0.62	0.50	0..46	0.31	0.33	0.42	0.34	0.41

Table 5.4 (conclusion).

			D101			D173		178
	PS106	PS106	PS106	PS106	PS106	PS25	PS25	PS214
	PC	PR	mPC	mPR	gm	PC	PR	P
SiO_2	36.06	33.88	36.59	36.46	36.27	36.55	37.00	41.77
TiO_2	2.21	1.84	2.17	1.87	3.20	2.54	2.42	2.33
Al_2O_3	14.13	20.13	13.47	15.64	13.82	13.28	12.92	7.49
MgO	5.38	4.82	5.77	5.71	6.12	5.32	5.46	7.51
CaO	11.23	10.33	10.99	10.83	11.38	11.00	10.93	15.61
MnO	1.04	0.92	0.96	0.92	0.83	1.14	1.07	0.92
FeOtot	23.80	21.77	23.34	22.67	22.35	23.26	23.37	16.75
Na_2O	2.10	1.79	2.26	2.14	2.16	2.24	2.26	2.33
K_2O	2.60	2.34	2.49	2.4	2.37	2.62	2.61	0.80
Sum	98.55	97.82	98.04	98.64	98.50	97.95	98.04	95.51
H_2O_{calc}	1.89	1.91	1.89	1.91	1.90	1.88	1.89	1.90
Sum	100.44	99.73	99.93	100.55	100.40	99.83	99.93	97.41
Si	5.722	5.316	5.814	5.711	5.710	5.823	5.884	6.591
Al^{IV}	2.278	2.684	2.186	2.289	2.290	2.177	2.116	1.393
Ti^{IV}	0.000	0.000	0.000	0.000	0.000	0.000	0.000	0.016
Sum	8.000	8.000	8.000	8.000	8.000	8.000	8.000	8.000
Ti^{VI}	0.264	0.217	0.259	0.220	0.379	0.304	0.289	0.260
Al^{VI}	0.364	1.039	0.337	0.598	0.274	0.316	0.305	0.000
Mg	1.273	1.127	1.367	1.333	1.436	1.263	1.294	1.767
Mn	0.140	0.122	0.129	0.122	0.111	0.154	0.144	0.123
Fe^{++}	3.158	2.857	3.102	2.970	2.942	3.099	3.108	2.210
Sum C	5.198	5.362	5.194	5.243	5.142	5.137	5.141	4.360
Ca	1.909	1.737	1.871	1.817	1.919	1.878	1.862	2.639
Na_B	0.091	0.263	0.129	0.183	0.081	0.122	0.138	0.000
Sum B	2.000	2.000	2.000	2.000	2.000	2.000	2.000	2.639
Na_A	0.555	0.281	0.567	0.467	0.579	0.569	0.559	0.713
K	0.526	0.468	0.505	0.480	0.476	0.532	0.529	0.161
Sum A	1.081	0.750	1.072	0.947	1.055	1.102	1.088	0.870
OH	2.000	2.000	2.000	2.000	2.000	2.000	2.000	2.000
Sum_{cats}	16.279	16.112	16.266	16.190	16.197	16.239	16.229	15.869
mg#	0.29	0.28	0.31	0.31	0.33	0.29	0.29	0.44

You have either reached a page that is unavailable for viewing or reached your viewing limit for this book.

You have either reached a page that is unavailable for viewing or reached your viewing limit for this book.

You have either reached a page that is unavailable for viewing or reached your viewing limit for this book.

ISBN 85-314-0362-6